Frontispiece

Apparatus for the Emission Intensity Studies of Characteristic Radiations excited by Electrons.

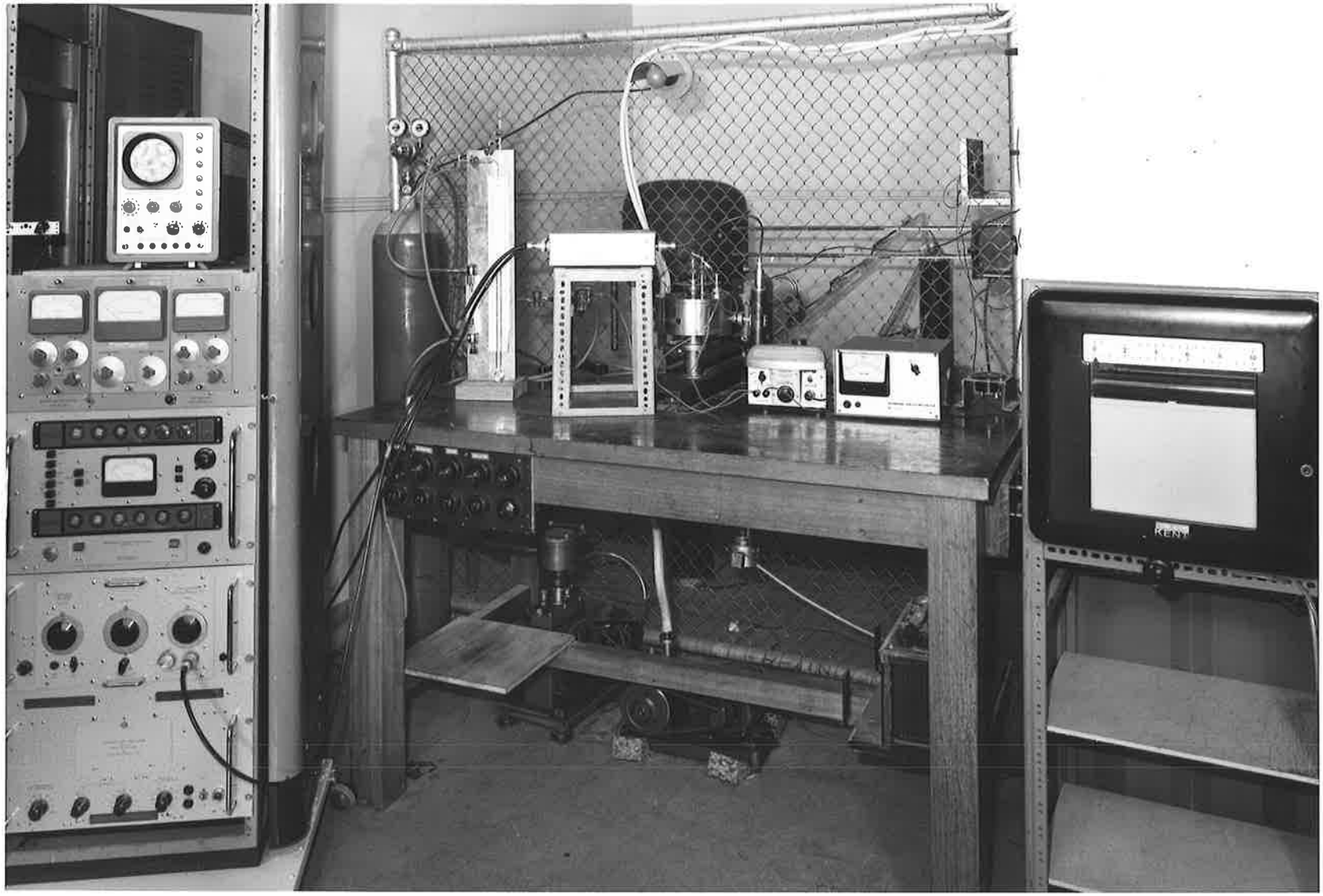
KENT

INTENSITY OF EMISSION OF CHARACTERISTIC X-RADIATIONS

by

L.H. Fong, B.Sc.

A Thesis

Submitted for the Degree of

Doctor of Philosophy

in the

Physics Department

University of Adelaide

MAY 1967

CONTENTS

SUMMARY

A description of the absolute emission intensities of characteristic X-radiations excited in thick metal targets is given in this thesis, which is divided into two parts. Part A refers to the study of soft characteristic radiations excited in metal elements by electrons of energies up to 60 keV. Part B refers to the preliminary study of the excitation of characteristic radiations by protons of energies up to about 40 keV.

Investigations on the absolute emission intensities of the K radiations of Cu, Cr, Ti, Al, and C, the L radiations of Ag, Cu, Ti, and Cr and the M radiations of Pt, Au, and W as a function of the incident electron energy are described in Part A. The quantum yields are given for various angles of emission to the target surface in order to investigate the validity of the theoretical expression for the target absorption factor.

A review of experimental and theoretical studies on the electron excitation of characteristic radiations is given. The Tomlin intensity formula, which is based on the average electron behaviour in its interaction with matter, is adopted for comparison with the present experimental results. Some aspects of the theory are discussed. An approximate form of the theory, which does not involve any complex integration and can be easily computed, is given.

The apparatus used for the absolute intensity measurements of characteristic radiations is described. Particular attention is

given to the experimental investigations on the characteristics of the two gas flow proportional counters constructed by the author.

Although the Tomlin intensity formula is applicable for the computation of L and M radiation intensities, there is a lack of information on the ionization cross section, the atomic fluorescence yield and the mass absorption coefficient of the element for its own characteristic radiations. A simple expression for the total L ionization cross section for silver is given in a form similar to the Worthington - Tomlin formula for the K ionization cross sections. The resultant calculated AgL radiation intensities are compared with experimental data.

A method is given for evaluating the total L or M ionization cross sections from experimental thick target intensity data. This procedure is tested for the total L ionization cross section of silver. Lack of relevant data prevents the extension of this procedure for finding other L and M ionization cross sections.

The proton source constructed by the author is described in Part B. No previous experimental study has been made at such low energies.

This thesis contains no material which has been accepted for the award of any other degree or diploma in any University, and to the best of the candidate's knowledge and belief, the thesis contains no material previously published or written by another person, except where due reference is made in the text of the thesis.

L.H. Fong

PREFACE

The research work described in this thesis was carried out in the Physics Department of The University of Adelaide during the period from February, 1962 to February, 1967 under the supervision of Dr. S.G. Tomlin.

The author wishes to express his sincere gratitude to Dr. Tomlin for his unfailing encouragement and patient guidance throughout the progress of the work, and is greatly indebted to him for the many long hours he has spent in reading through the first draft of this manuscript.

The author also wishes to acknowledge help and suggestions from various members of the Physics Department.

Special thanks are due to Mr. K. Merry of the Physics Department Work shop, who constructed the proton source and associated apparatus, to Mr. A. Ewart for technical assistance, to Miss Heather Barrow, who prepared the diagrams, and to Mrs. Phillips, who typed this thesis.

The candidate wishes to record his thanks for a "University Research Grant" (1962) and for a "Commonwealth Postgraduate Award" (1963-66).

***

PART A

Absolute Intensities of Soft Characteristic Radiations excited by Electrons

CHAPTER 1.

REVIEW OF LITERATURE.

1.1 Introduction.

Apart from its intrinsic interest, an understanding of the absolute intensity of emission of characteristic radiations is important for several practical applications. It is essential for the quantitative X-ray micro-analysis of the elements (Castaing, 1960; Duncumb and Shields, 1963; Archard and Mulvey, 1963), which is a widely used technique in industries connected with metallurgy, mineralogy, and petrography. It is required in determining the optimum conditions for the efficient operation of X-ray sources.

Indirectly, experimental yield values provide a means of testing the degree of validity of current theories describing the various physical phenomena involved in the excitation of characteristic X-radiations, as any satisfactory theory on the absolute yield must include expressions describing these phenomena.

For convenience, the theoretical expression for the absolute yield, in its basic form, is stated at this point in order to clarify the notations used later in this thesis. Following the procedure of Metchnik and Tomlin (1963), the expression for the quantum efficiency of K characteristic photon production may be stated as follows,

$$N_{\phi}(T_o, Z) = kN \int_{T_o}^{T_K} Q_K \frac{ds}{dT} g(x, \mu_T, \theta, \phi) dT \qquad \ldots (1.1)$$

where N_{ϕ} is 4π times the number of K photons emitted at the anode surface per unit solid angle per incident electron at an angle of emergency ϕ to the target surface with the electron beam striking the target at an angle θ to its surface. T_o and T_K are the initial and the excitation energy of the electrons respectively. N is the number of atoms per unit volume of the target element of atomic number Z. Q_K is the total K ionization cross-section. dT/ds is the rate of energy loss suffered by the electron along its path s. The function $g(x, \mu_T, \theta, \phi)$ expresses the target absorption of the characteristic photons produced at a depth x within the anode, which has a mass absorption coefficient μ_T for its own K radiations. Consideration has to be given to the deflections and the energy losses suffered by the electron along its track as a result of elastic and inelastic collisions with the target atoms.

The factor k, where $k = \omega_K \left(\frac{P+1}{P}\right) Rp$, includes correction terms for:

(a) the fluorescence yield, ω_K;

(b) the indirect production of K photons by high energy bremmstrahlung radiations, $\frac{P+1}{P}$;

(c) the backscattered electrons which have not made a full ionizing contribution within the target, R;

(d) the ratio of the number of the particular K radiation component under investigation to the total number of photons in the K spectrum, p.

If N_{ϕ} refers to the total K intensity, the correction (d) should be omitted.

Similar considerations apply to the L and M radiations.

Unless otherwise stated, the significance of the above notations applies throughout this volume.

1.1.1 Review of Existing Theories.

Early analytical expressions for X-ray emission intensities were derived empirically from experimental data, which were mainly confined to characteristic K radiations from heavy elements. Formulation of the intensity function from fundamental theories was not attempted owing to insufficient knowledge of the physical processes involved. These early formulae were expressed in arbitrary units and dealt only with their relative variation with the incident electron energy.

Thick and thin target intensity functions were included in an article by Webster, Clark, and Hansen (1931). For thick target emissions, the most commonly used expression has the form

$$I(U) = K(U-1)^{n} \qquad \ldots \quad (1.2)$$

where I is the characteristic K intensity,

$U = T_e/T_K$,

K and n are constants.

For a particular radiation, agreement with experimental results holds only over a limited range of U, as n is dependent on U (Webster, Hansen and Duveneck, Fig. 6, 1933b). Separate determinations of the constants K and n were necessary for each set of conditions defined by θ, ϕ, and Z.

It is interesting to note that the form of the expression (1.2) for I(U) was later derived by Green and Cosslett (1961) by theoretical means for conditions where the target absorption can be neglected.

A theoretical study of the thick target emission intensity problem was first attempted by Kirkpatrick and Baez (1947), who computed the AgK_α intensities generated at the point of excitation within the target. The absence of the target absorption problem greatly simplified their calculations, as no description of the complicated electron trajectories within the target was necessary. Experimental values of Clark (1935) and Webster et al (1933a) for the AgK cross-section were used. A modified form of Williams' (1931) empirical formula was employed to describe the rate of energy loss of electrons in silver. On recalculating the intensities based on Bethe's theoretical formula (Livingstone and Bethe, 1937) for the electron stopping power, no significant change in the results was observed. All four corrections (a), (b), (c), and (d) in the k factor were considered. These were assumed to be independent of the electron energy and their values were obtained from Stephenson (1937), Webster

(1928), Webster et al (1933b), and Williams (1933), respectively.

Kirkpatrick and Baez's calculated intensities cannot be directly compared with experimental data which refer to the intensities emitted at the target surface. Kirkpatrick and Baez adopted Kulenkampff's (1922) approximate procedure, as outlined in Webster et al (1933b), for correcting the target absorption in the relative experimental results of Webster et al (1933b), which were standardized by their own absolute measurement. The corrected experimental intensities exhibited good agreement with the theoretical intensities.

A theory on the K radiation intensities excited in thick targets was given by Tomlin and his co-workers (Worthington and Tomlin, 1956; Metchnik and Tomlin, 1963; and Tomlin, 1964). Equation (1.1) represents their basic formula. The quantum yield, N_{ϕ}, was considered to be a function of $T_{o,\theta}$, ϕ, and Z. Their theory was restricted to these values of T_o below approximately 60 keV, where the relativistic effects were not important. The absolute yield defined in this way proved to be more expedient than that of Kirkpatrick and Baez, as the theoretical results can be directly compared with experimental data. Although the theory did involve an added complexity in the target absorption problem, it represents a more complete description of the radiation production mechanism.

Bethe's (1930) non-relativistic formula for the average electron stopping power was chosen to represent the depth-energy

relationship. In an endeavour to test its validity, Worthington and Tomlin derived from the Bethe function, an expression involving an arbitrary end point to represent the total range of electrons in matters. Direct comparison with experimental ranges was complicated by the fact that the Bethe range, R_B, referred to the actual path followed by the electrons.

Cosslett and Thomas (1964b) classified and defined the various experimental electron ranges determined from both electron transmission and electron energy loss measurements. They considered that the mean range was the most appropriate of the experimental ranges to be compared with R_B, as both referred to the mean energy of the transmitted electrons. Within the range of incident electron energies from 9 keV to 18 keV, their investigations on Al, Cu, Ag, and Au foils indicate that in all cases, the mean range lies below R_B (about 25% on the average) and that the discrepancy increases with an increase in the atomic number of the absorber element. This was attributed to the fact that the experimental range refers to the depth of penetration of the electron and that the actual path followed by the electron must exceed its depth of penetration owing to the various deflections suffered by it along its track. As the mean angle of scattering increases with Z, the difference between the two ranges also increases with Z.

Bethe's (1930) non-relativistic expression for the K ionization cross-section was used. Its derivation involved the use of the

first Born approximation and screened hydrogenic wave functions. To reduce mathematical complexity, the change in momentum of the incident electron was assumed to be small. A simple function resulted from these assumptions, which unfortunately, also introduced serious discrepancies at low energies. Worthington and Tomlin (1956) replaced the constant B in the Bethe formula with an arbitrary function of energy. The resultant expression for the K cross-section gave a better agreement with the experimental data (section 2.2).

In the preliminary theory of Worthington and Tomlin, the k factor values used were doubtful. The values for ω_K were taken from Compton and Allison (1935) whose values for light elements were uncertain. The other correction terms in the k factor were taken from the data supplied by Kirkpatrick and Baez (1947). These referred only to the AgK_α radiations and no account was taken of their dependence on the electron energy. Although the studies of Green and Cosslett (1961) and Tomlin (1964) indicate that the error caused by the latter assumption was not serious, it was found that the indirect excitation term in the k factor was strongly dependent on Z (Green and Cosslett, 1961). The use of the silver data to describe this term would overestimate the AlK results by half as much again. This accounts for much of the discrepancy encountered by experimenters (Dyson, 1959, Dolby, 1960, Campbell, 1963) who compared their data with the theoretical intensities of Worthington and Tomlin. The comparison between the results of

Dyson, and Worthington and Tomlin was not strictly valid, as the conditions were not identical. Dyson's results referred to the radiations measured in the forward direction of the electron beam, whereas the theoretical results were based on the radiations emitted from a massive target in the backward direction. Consequently, there was a difference in the lengths of the absorption path within the target.

Green and Cosslett's data for the indirect excitation of characteristic radiations by high energy bremmstrahlung radiations were later included in the calculations of Metchnik and Tomlin (1963) and Tomlin (1964).

From a comparison with the experimental studies of Castaing and Descamp (1955), Archard (1960) pointed out an omission in Worthington and Tomlin's theory, that is, their neglect of the electron scattering processes which occur within the target. Worthington and Tomlin themselves indicated that their straight electron path model oversimplified the problem. The higher target absorption resulting from their assumption would underestimate the computed intensities. To remedy this, Archard introduced a combination of two model electron paths. However, his analysis was based only on a comparison with the relative experimental values of Mulvey and Alford (1959).

The electron penetration problem was reconsidered by Metchnik and Tomlin (1963) who obtained an expression for the mean depth of electron penetration, $\langle x \rangle$, adapted from Lewis' (1950) multiple scatter-

ing theory. Their expression was not completely satisfactory. Lewis' theory was derived on the basis of the electron scattering process in an infinite medium, whereas the actual target could only be considered as semi-infinite in extent. The use of the Tomlin-Lewis formula for $\langle x \rangle$ had the effect of reducing the estimated mean depth of penetration of the electrons thus leading to an overestimation of the computed intensities.

Using experimental scattering data, Monte Carlo calculations of $\langle x \rangle$ and $\langle x^2 \rangle$, the second moment of distribution in x, were made by Bishop (1965) for 29 keV electrons incident on a copper target. His results for an infinite medium were found to be consistent with the corresponding quantities derived from the Tomlin-Lewis formula for an infinite medium. The latter expression quoted by Bishop is a simpler form of the approximation stated by Tomlin (1966) to represent $\langle x \rangle$. Tomlin found a similar agreement in the cases of 10 keV electrons incident on copper and aluminium. For a semi-infinite medium, Bishop found that by modifying a constant term in the simpler version of the Tomlin-Lewis formula for $\langle x \rangle$, there was a satisfactory agreement between the two results.

From the Tomlin-Lewis expression for $\langle x \rangle$, Tomlin (1963) derived an expression representing the theoretical diffusion depth, x_d of electrons in an infinite medium. In the case of a semi-infinite medium, x_d was experimentally determined by Cosslett and Thomas (1964a) for several metal elements. They found that the values of the diffusion

depths were dependent on their definition. On averaging the results from applying the several definitions, Cosslett and Thomas arrived at values for x_d in good agreement with Tomlin's (1963) theoretical values, after these had been modified by Cosslett (1964) for a semi-infinite target. An empirical factor of 1.5 was introduced into Tomlin's expression for x_d.

The above recent studies seem to suggest that in instances where the target absorption is important, such as at low angles of emergence and for light target elements, the use of the Tomlin-Lewis formula for $\langle x \rangle$ would cause a significant overestimation of the theoretical intensities. Metchnik and Tomlin considered that the effect of this error was reduced by the occurrence of another error which tends to underestimate the computed intensities. This was the omission of the statistical spread in the depth of penetration for the electrons. The overall error was given as a few per cent.

Experimental data for the NiK ionization cross-section were used by Metchnik and Tomlin to estimate the CuK and the CrK cross-sections. Recognizing that this procedure was not entirely satisfactory, as it assumed that $Q_K V_K^2$ was independent of Z, they considered that the atomic numbers of the three elements were sufficiently close together as not to introduce too serious an error through this assumption.

There was a good agreement between their measured and calculated intensities for the K_α radiations of Ag, Cu, and Cr. The largest

discrepancies occur in the CrK_α results, and at low angles of emergence for the CuK_α and the AgK_α radiations. The former discrepancy is the direct result of their use of the backscatter term in the k factor which is applicable only to the AgK_α radiations. The k factor values used in the calculations of Metchnik and Tomlin are more accurate than those used by Worthington and Tomlin, as Green and Cosslett's (1961) data for indirect excitation were used. The discrepancies at low angles of emissions could be attributed to the errors associated with the Tomlin-Lewis expression for $\langle x \rangle$, as the correction for the target absorption increases in importance at low angles of emergence, where the radiation paths within the target are longer.

Tomlin (1964) recalculated the K_α intensities for copper and chromium on the basis of a more rigorous investigation on the various terms in the k factor. New data for the correction factor for the loss of ionization due to backscattered electrons were given. The resultant theoretical intensities were in good agreement with the measured results of Metchnik and Tomlin.

Calculations of the total K radiation yield from light elements, namely, beryllium, carbon, boron, and aluminium were also made for high angles of radiation emission. These were compared with the measured data of Campbell (1963). In general, larger discrepancies occurred between the calculated and experimental intensities for the soft radiations as compared with the characteristic radiations emitted

from elements of higher atomic number. An exception was the AlK intensities, for which there was good agreement. However, if Dolby's (1960) experimental AlK results were used for comparison, then apart from the BeK results, the measured data would be significantly lower than the calculated values. The discrepancies could be caused by the values used for ω_K and by the expression used to allow for the target absorption in the intensity formula. The experimental values for ω_K compiled by Fink et al (1966) indicate that there is considerable uncertainty in these values for elements of low atomic number. Tomlin used Burhop's (1952) formula to evaluate ω_K. For elements of higher Z, Burhop's results are lower than the existing experimental values. A discussion is given in section (2.3). Comparison of Worthington and Tomlin's cross-section formula with the experimental data compiled by Kieffer and Dunn (1966) for the K ionization of the helium atom (Figure 2.3) indicates that the large discrepancy between the theoretical and measured intensities for soft radiations could not be wholly attributed to any error in the K ionization cross-section formula. Any error in the target absorption expression is more significant in the intensity calculations for soft radiations than for the harder radiations. This is due to the increase of μ_T as the atomic number of the target element decreases.

The unique behaviour observed in the comparison of the BeK results could have been caused by the experimental errors discussed by Campbell. Their effect was to underestimate the intensities.

An approximate discussion of the quantum yield was given by Cosslett (1961), who, in particular, investigated its variation with Z. The yield, assumed to be proportional to the product of the total number of K ionizations per incident electron and ω_K, was found to vary as Z^2, as compared to the $Z^{3/2}$ variation predicted by Archard's (1961) modified version of Worthington and Tomlin's theory. Cosslett's observations were found to be in qualitative agreement with the experimental data of Dolby (1960) for Copper K and carbon K radiations.

Green and Cosslett (1961) derived a simple formula for the K characteristic intensity. It was expressed as a function of Z and U. They considered that if the product ZU satisfied the conditions $ZU < 100$, then the correction for the target absorption could be neglected. The problem was then greatly simplied.

The Thomson-Widdington formula,

$$T_o - T_p^2 = c\rho x$$

where T_p is the most probable energy of the transmitted electrons at a depth x in a medium of density ρ, was used to derive the formula for the electron stopping power in matter. Their values for c in the stopping power expression were not entirely satisfactory. Cosslett and Thomas (1964b) found that the "constant" c is dependent on x for thin foils, even for a given absorber element and at the same incident electron energy. In addition, the values of c were experimentally determined in relation to x and not to s, the actual electron path,

the quantity used in the electron stopping power formula. This had the effect of increasing the effective stopping power.

The constant b in Bethe's (1930) non-relativistic formula for Q_K was modified on the basis of a comparison with the experimental AgK and NiK data of Kirkpatrick and Baez (1947) and Pockman et al (1947) respectively. The resultant semi-empirical expression is in satisfactory agreement with the measured results. Q_K for light elements was evaluated by Worthington and Tomlin's extrapolation technique.

All the relevant corrections in the k factor were considered. In particular Green and Cosslett calculated the correction term associated with the indirect excitation of characteristic radiations. They observed that for light elements this correction term could be neglected. This conclusion is consistent with that of Brown and Ogilvie (1964). The semi-empirical formula of Laberrique-Frolow and Radvanyi (1956) was used to evaluate ω_K. The use of this expression is not entirely satisfactory for computing ω_K values for light elements as the values of the empirical constants contained in it vary over different ranges of Z.

In view of the uncertainties in the values of Q_K and ω_K for light elements and in the experimental values used for c in the electron stopping power formula, they arrived at results which were in fair agreement with the measured data, provided that the experimental conditions satisfied the restriction which they imposed.

Allowing for the different values used in the k factor, Green

and Cosslett's (1961) calculated intensities are generally higher than Tomlin's (1964) theoretical results. As the expressions used for Q_K in the two theories are approximately similar, the difference could be attributed to the neglect of target absorption and to the overestimation of the electron stopping power in Green and Cosslett's theory.

A simple function was derived by Brown and Ogilvie (1964) in their theoretical treatment of the K characteristic emission problem. Their basic formula was adopted from Worthington and Tomlin. Mathematical complexity associated with the evaluation of the intensity formula was much reduced by the averaging technique which they applied to the expressions for Q_K and the depth of X-ray production.

On the basis of their theoretical studies, calculations were made for the correction term to account for the indirect excitation of characteristic radiations. They found that for target elements of $Z \leq 22$, the correction amounts to less than 1%.

Their estimation of Q_K by averaging Q_K over the electron energies is not entirely satisfactory at low energies, as Q_K varies rapidly with the energy up to $3T_K$.

To account for target absorption, they first assumed a simple straight path model for the electron trajectory. Electron scattering effects were then allowed for by the inclusion of an empirical parameter in the target absorption term. This parameter was chosen on the basis of a comparison with the experimental data with reference only to the atomic number of the target element. For low values of

ϕ, the take-off angle, where the correction for target absorption is important, their assumption of a correction factor for electron scattering to be constant over the whole range of electron energies appears not to be valid at low incident energies and for target elements other than the lightest elements. For TiK and NiK, although a satisfactory agreement exists between theoretical and experimental results in the upper region of the energy range considered (25-35 keV), in the lower energy region, the theoretical values exceed the measured data by as much as 50% up to 2.5 T_K. (The values of T_K implied in figures 6 and 7 of Brown and Ogilvie (1964) for the NiK and the TiK results indicate that the captions beneath the diagrams should be interchanged.)

A disadvantage of Brown and Ogilvie's theory is that a preliminary experiment has to be made to determine the parameter associated with electron scattering. The theory cannot be used independently to predict the characteristic intensities.

Brown and Ogilvie's correction method for electron scattering is somewhat similar to the technique discussed by Duncumb and Shields (1963), who used the following relation to compute the characteristic intensity, I,

$$I = f(\chi)\, I_s \qquad \ldots (1.3)$$

where I_s is the calculated intensity based on a straight path model for the electron penetration, $f(\chi)$ is the experimentally determined

quantity dependent on $\chi = \mu_T \rho \operatorname{cosec} \phi$ and ρ is the target density. Experimental data for $f(\chi)$ for several target elements and at various incident electron energies were tabulated by Green (1962). This method of allowing for electron scattering appears to be more satisfactory than that of Brown and Ogilvie, as all the variables affecting the scattering process were considered in the determination of $f(\chi)$.

Evaluation of $f(\chi)$ by Monte Carlo techniques has been carried out by Archard and Mulvey (1963) and Bishop (1965). Archard and Mulvey adopted Archard's (1961) diffusion model to construct hypothetical electron paths within the medium. Within the limitations of this model, which is not entirely valid for light elements, the calculated results were shown to be consistent with the experimental data of Castaing and Descamp (1955) and with those of Green (1962). The discrepancies encountered with the results for heavy elements, were attributed to the large fraction of indirectly excited characteristic radiations produced within the target.

Bishop based his calculations on the Monte Carlo technique developed by Green (1963), who used experimental scattering data for thin films. There was good agreement with the measured results of Castaing and Descamp and Green. Worthington and Tomlin's formula for Q_K was used. Bishop reported that his calculated values of the quantum yield were approximately 30% lower than the experimental data of Metchnik and Tomlin, and Green. The magnitude of this discrepancy was considered to be satisfactory in view of the uncertainties in Q_K and ω_K.

When individual electron paths were considered, Archard and Mulvey (1963) pointed out that the Bethe (1930) formula, which was used in both Monte Carlo calculations, represented only an approximate description of the energy loss of electrons in matter, as the Bethe formula was associated with the average electron behaviour.

Suominen (1964) derived a formula for the characteristic quantum yield with the basic features of Worthington and Tomlin's intensity formula including their expression for Q_K. Makhov's (1960) semi-empirical functions were used to describe the electron penetration characteristics. These functions gave the actual number of electrons at a given depth and their energy distribution, hence, no correction was necessary to account for the effect of those backscattered.

Although Makhov's expression for η, the relative number of electrons transmitted, is consistent with Cosslett and Thomas' (1964b) experimental data, the energy distribution of the transmitted electrons does not follow the general behaviour of Cosslett and Thomas' experimental curves.

As Makhov's formula referred to the depth of electron penetration, Suominen allowed for the scattering process by including a mean angle of scattering, θ_m, in his calculations. The value of θ_m used, which was assumed to be independent of Z and T, was based on Dyson's (1959) work on the diffusion depth associated with 10 keV electrons incident on an aluminium target. Hence, the value for θ_m refers to

that at the diffusion depth. The experimental studies of Cosslett and Thomas (1964a) suggest that at the diffusion depth, Suoninen's assumption is basically sound. But for the initial scattering process, Cosslett and Thomas' results (1964a) indicate that θ_m varies rapidly with T and to a less extent with Z. For these initial conditions, Suoninen considered that the error involved was not serious, in view of the smallness of the integrand in the intensity formula. The actual value of θ_m used by Suoninen was 60° as compared to 38° given by Cosslett and Thomas (1964a) for the most probable angle of scattering. The distribution curves of figure 4(b) (Cosslett and Thomas, 1964a) indicate that at the diffusion depth, θ_m, approximates to the most probable angle of scattering. Assuming the correct value of θ_m to be 40°, Suoninen's calculations for the characteristic intensities would represent an overestimation of 50%.

Suoninen defined an "average depth of excitation", $\langle x \rangle_s$, as that depth up to which the radiation intensity produced, as detected at the target surface, is half the total intensity emitted. The results for $\langle x \rangle_s$ are significantly lower than those from the Tomlin-Lewis formula for $\langle x \rangle$ in the form as stated by Bishop (1965) for a semi-infinite medium. If the plateaux of the $\langle x \rangle$ curves are considered, then $\langle x \rangle$ exceeds $\langle x \rangle_s$ by a factor of two. Owing to the differences in definition of the two quantities, the comparison has only a qualitative significance.

For the CuK intensities, Suoninen's computed intensities are in good agreement with the measured data of Metchnik and Tomlin (1963). For the AlK intensities, Suoninen's results exceed Dolby's (1960) measurements by about 20% and those of Campbell (1963) by a factor of two. Absolute calculations of the CK intensities were not attempted owing to uncertainties in some of the parameters in Makhov's equations. However, it was shown that the relative CK intensities were consistent with Dolby's (1960) measurements.

Examination of the various theories in this topic indicates that most adopt the basic features of equation (1.1). The main difference lies in the correction for target absorption. Archard (1960), Brown and Ogilvie (1964), and Suoninen (1964) used approximate methods. Green and Cosslett (1961) ignored the target absorption completely. In recent years, Monte Carlo techniques have come into prominence. These are used to simulate mathematically the actual electron trajectories in detail. These include Archard and Mulvey's (1963) diffusion model and the technique based on experimental scattering data (Green, 1963; Bishop, 1965). To the present time, the latter method is probably the most accurate. The accuracy depends mainly on the detail with which the measured scattering data are collected and the number of electron paths considered. Even with the facility of fast digital computers, the large number of paths necessary involves very high costs in computing times. Otherwise, calculations of characteristic intensities based on equation (1.3) using tabulated values of $f(\chi)$ depend

on the availability of these values.

The theory of Tomlin et al (Metchnik and Tomlin, 1963, Tomlin, 1964) which is based on the average electron behaviour, in view of recent investigations on certain simplifications in the theory, is probably the most suitable, with regards to accuracy and the computation time involved. Cosslett (1964) and Bishop (1965) have successfully converted an approximate form of the Tomlin-Lewis expression for $\langle x \rangle$ to that appropriate for a semi-infinite medium in the case of a copper target. Tomlin (1966) has derived an analytical form for the distribution function, $f(x,s)$, in depth for an electron of a given energy. For an infinite medium, there is a satisfactory agreement between Tomlin's (1966) distribution function and Bishop's Monte Carlo calculations for 29 keV electrons incident on copper. There is a similar agreement for a semi-infinite medium in the case where the path length, s, approaches R_B, the Bethe range. These distribution functions are semi-empirical expressions with restricted applicability. Until a more general function is found, the approximations in their intensity formula discussed by Metchnik and Tomlin (1963) cannot be remedied. Except for low angles of radiation emission, comparison of the intensity theory in its less complete form with experimental data indicates that the approximations in the theory are secondary effects. For soft characteristic K radiations there is a greater uncertainty in the ω_K values.

1.1.2 Past Experimental studies.

Early experimental studies were hampered by the lack of suitable detection techniques. The photographic-photometric detector and the ionization chamber were commonly used. As the exact response of these detectors to the incident radiations was not known, only relative intensity measurements were attempted. Early work was mainly concerned with the measurement of moderately hard radiations as the available detection techniques were not sufficiently sensitive to low energy radiations. Among the pioneers engaged in characteristic intensity measurements were Duane and Stenstrom (1920), Zacek and Sieghbahn (1923), Allison and Armstrong (1925), Woo (1926), Jonsön (1926), Meyer (1929), Hicks (1930, 1931) and Williams (1931). Their studies were mainly concerned with the relative line intensities in the K and L spectra.

With the increase in use of X-ray sources, it was found useful to examine the variation of the emission intensity with the accelerating potential, V, of the incident electrons. Relative intensity measurements of the AgK_α doublet emitted from a thick target were made by Webster et al (1933b) for values of V up to 180 kV and with ϕ varying from 1° to 25° for a normal electron beam incidence. These relative curves were later standardized by the single absolute measurement of Kirkpatrick and Baez (1947), whose result refers to the intensity excited within the target. An absolute intensity measurement was also made by Braxton et al (1945) for the CuK_α doublet

excited from a thick target.

In an endeavour to ascertain the K ionization probability of the target atoms, thin target emission intensities were also investigated. These targets were made sufficiently thin to ensure no appreciable energy loss by electrons as well as to minimize the target absorption. Relative intensities of the AgK_{α} doublet (Webster et al, 1933a) and of the NiK_{α} doublet (Pockman, Webster and Kirkpatrick, 1947) were determined. These data were standardized by a comparison with the absolute measurements of Clark (1935) and Smick and Kirkpatrick (1945) respectively.

The practical techniques used in the above measurements were similar. For the relative measurements, the incident heterogeneous radiations were monochromatized with a crystal spectrometer, and for the absolute intensity determinations, a pair of Ross filters was used. A common detector used was the ionization chamber. Its operation at that time involved the collection of the total charge produced by the ionizing radiations. Its calibration for use as an absolute intensity detector requires accurate data for the average number of ion pairs produced in the gas filling per electron volt of the energy lost by the ionizing radiations. According to a review article by Binks(1936), the results for air, which was a common gas filling, varied considerably. Electron recombination and attachment processes (Fulbright, 1958) could reduce the total charge collected. Error introduced by the former effect was probably not serious, as it could be minimized by a

sufficient electric field between the electrodes. However, no action was taken to suppress the electron attachment processes. Another possible source of experimental error was the use of differential filters in isolating the characteristic lines of interest. The absorption functions of the elements are complex and the way in which they vary with the wavelength of the incident radiations, λ, are not identical for the two absorbers used. A satisfactory balance can only be made over a limited range in λ.

A preliminary measurement of the CuK_α intensity was made by Worthington and Tomlin (1956) at a low angle of emergence. Absolute intensities of CuK_α radiations were measured by Dyson (1959) for low incident electron energies in the range between 9 and 15 keV. The anodes he used were sufficiently thick to stop the incident electron beam but not thick enough to seriously attenuate the characteristic radiations produced. The measurements were made in the forward direction of the electron beam. The detection system consisted of a proportional counter and a single channel pulse height analyzer.

Soft characteristic radiations were investigated by Dolby (1960). For incident electron energies below 10 keV, absolute intensities of the total K radiations emitted from massive anodes of aluminium and carbon were measured. The detection system was similar to that employed by Dyson (1959). The window of the proportional counter consisted of an aluminized 6 μ melinex sheet, the measured transmission of which for CK was given as 10%. To obtain a satisfactory counting

rate, a large counter window subtending a solid angle of 0.47 steradians was used. This solid angle was too large to ensure that all the radiations detected were emitted at a given angle to the target surface. It involved the angular range from 11° to 55°. This causes some difficulty in the use of Dolby's data for comparison purposes with theoretical results.

Apart from a retarding potential of 1740 volts on the window, no attempt was made to deflect electrons backscattered from the target away from the window. The excitation of CK radiations in the melinex by these electrons would have caused some spurious counts in the CK measurements. In view of the thick window used, there was also the possibility of indirect excitation of CK radiations by high energy bremmstrahlung radiations in the melinex. There was some evidence of the above effects in Dolby's recorder trace for the Alk radiations, where a definite peak appeared in a position corresponding to the CK radiations. This was inccnclusive, however. Apart from the fact that the backscattered ratio for carbon is less than that for aluminium, the secondary peak could have originated in the carbonaceous deposit on the aluminium anode. The value of the vacuum pressure quoted (10^{-4} mm Hg) indicates that this was a distinct possibility, as an insufficient baffle system for the oil diffusion pump would have caused an undesirably high percentage of oil vapour in the vacuum chamber. If this were the case, then only Dolby's Alk results would have been affected as the surface coating would have reduced the

energy of the electrons incident on the anode.

Secondary excitation of Alk radiations in the counter window was less serious than the corresponding excitation of CK radiations owing to the thinness of the aluminium coating (200Å). Spurious counts arising from photo-excitation by bremmstrahlung radiations could be neglected. As the counter window is normally placed with the conducting layer facing the inside of the counter, attenuation of the back-scattered electrons by the 6μ melinex together with the retarding potential was sufficient to suppress the excitation of the unwanted Alk radiations in the coating, in view of the low incident electron energies considered.

An estimate of the fraction of bremmstrahlung radiations lying under the characteristic peak was made by Dolby by an experimental determination of the continuous quantum intensity per energy interval at a point situated on the high energy side of the peak and well separated from it. No account was given of the variation of this value with the continuous quantum energy. For the Ck intensities, a low value of 1% was given as the correction factor for the bremmstrahlung radiations. This was attributed to the monochromatizing effect of the melinex window. It appears that all of the continuous radiations whose energies correspond to the low energy side of the pulse distribution curve were considered to have been absorbed by the window and the correction came from the high energy tail of the pulse distribution curve only. This would have accounted for the low value

of the correction factor.

Absolute intensities of total AgK and CuK radiations were measured by Green and Cosslett (1961) at high angles of emergence. Only a single measurement was made for each radiation. No account was given of their experimental procedure.

Up to this time, no extensive absolute intensity measurement had been made. Of the existing data that were available, only a few correspond to emission from a massive target. As the limited amount of experimental information was insufficient to provide an adequate check for their theoretical studies, Metchnik and Tomlin (1963) made absolute determinations of the K_α radiations emitted from massive targets of copper, chromium and silver. These measurements covered a wide range of V and ϕ and were made with a variety of detectors - the Geiger tube, the proportional counter and the scintillation counter. Comparison of the measurements from each detector served as mutual checks for each other. The CuK_α lines were isolated with a pair of balanced Ni-Fe filters and monochromatization of the other radiations was achieved with a double crystal monochromator. Further monochromatization was achieved with a pulse height analyzer. Counting losses in the detectors were all accounted for. As commercial proportional and Geiger tubes were used, the accuracy of their results relies to some extent on the construction details of these detectors supplied to them by the manufacturer. Apart from the measurements made with the Geiger tube, there was good agreement in the results obtained with the

other two detectors (Metchnik, thesis, 1961). Effects due to back-scattered electrons were eliminated by a thick piece of aluminium foil used to seal off the X-ray tube window. A combination of pulse height discrimination and the high absorption losses suffered by any secondary AlK radiations produced in the foil was sufficient to suppress any spurious effects.

1.1.3 Experimental Studies published since the start of the present project.

Absolute intensities of soft characteristic K radiations excited in massive targets were measured by Campbell (1963) for incident electron energies from 0.5 keV to 30 keV. Characteristic emissions from several target elements of atomic numbers within the range 4 (Be) to 13 (Al) were investigated. These measurements refer to the radiations emitted at right angles to the electron beam, which was inclined at 45° to the target surface. For CK, additional measurements were made with an angle of emergence of 10°. A small gas flow proportional counter was used. To increase its detection efficiency for soft radiations, the counter window was made of a thin film of nitrocellulose and the detector itself was mounted within the vacuum chamber. The transmission ratio of the window for the softest radiation, BeK, was 50% of the incident intensity. The relatively high detection efficiency enabled Campbell to use a small counter window.

Spurious radiations due to the excitation of the window material by backscattered electrons were minimized by means of a small deflecting magnet. The window absorption was considered to be sufficiently small to reduce any undesirable photoexcitation effects in the nitrocellulose. As his target specimens were mounted directly above the throat of the oil diffusion pump, where the concentration of oil vapour could have been considerable, Campbell found it necessary to heat the target to reduce the formation of carbonaceous deposits.

The amount of continuous radiation lying within the characteristic peak was estimated by an analysis of the shape of the pulse distribution curve. Fuchs and Kulenkampff's (1954) relationship was used to compute the intensity variation of the bremmstrahlung radiations near the characteristic peak. The statistical spread in output pulse heights resulting from the multiplication processes in the detector gas was determined from Feller's (1957) distribution function. The effects on the shape of the pulse distribution curve due to statistical fluctuations in the number of primary ionizations produced in the gas filling and the window absorption were allowed for empirically. A parameter in the computed distribution function was chosen to fit the computed function with the observed pen recorder trace of the output pulse heights. The bremmstrahlung correction for CK was much higher than Dolby's (1960) value. Dolby attributed his low value to the monochromatizing effect of the thick counter window. Campbell's procedure, which included the effects of the variation of the continuous

radiation intensity with its energy and the statistical processes in the gas, had a sounder basis than that of Dolby.

Campbell's AlK and CK results were approximately half those determined by Dolby. Although the geometrical arrangements of the target with respect to the detector and the electron beam were not identical, present theoretical and experimental studies show that the intensities based on these two experimental arrangements should be comparable in magnitude. For a normal electron-beam incidence, the variation of the intensity with ϕ is small for a given electron energy for large values of ϕ. The spread in ϕ, which extends down to 11° in Dolby's experiment, could only have reduced the intensities below those obtained for high angles of emergence. In fact, Green (1962) who repeated some of Dolby's AlK results, found that improved collimation of the emerging radiation beam did not have much effect on the results. Hence the difference in the experimental arrangement could not have caused the large discrepancy between the two sets of results.

The high absorption of the melinex window used by Dolby could have been a source of discrepancy. With thick windows, the computed unattenuated intensity is sensitive to the degree of accuracy with which the window absorption is determined. Also, the probability of photoexcitation of the window material increases with thickness. These effects are only applicable to Dolby's CK intensities. As discussed before, it was unlikely that secondary excitation of the AlK radiations in the aluminium coating by backscattered electrons could have occurred,

as these electrons first had to penetrate the 6μ melinex to reach the aluminium. No attempt was made by Dolby to remove the deposition of extraneous matter on the targets. The deposit could only have affected the intensity in that the effective electron energy was reduced at the target surface. In the case of the aluminium target, spurious radiations excited in the carbonaceous deposit could have been removed by pulse height discrimination. Green (1962) indicated that the formation of a thin carbonaceous deposit on aluminium had no noticeable effect on the AlK results. Indirect excitation of the aluminium coating was probably negligible owing to the thickness of the coating. It is difficult to estimate to what extent Dolby's CK intensities were affected by indirect excitation. The experimental studies of Sternglass (1954) and Campbell (1963) indicate that the number of backscattered electrons with sufficient energy to excite the CK radiations is small. The probability of photoexcitation of soft characteristic radiations is also small (Green and Cosslett, 1961). However, the counter must have had a high detection efficiency for radiations excited in its window. The porous nature of carbon and the high absorption it has for its own characteristic radiations result in the CK intensities being dependent on the condition of the target surface. This factor could also contribute to the discrepancy.

Isolated absolute measurements of AlK, TiK, and NiK intensities were reported by Brown and Ogilvie (1964). These were determined for angles of emergence of 15.5° and -90° for a normal electron beam

incidence. The target absorption in these experimental arrangements was higher than in those of Dolby and Campbell. No apparent effort was made to prevent the occurrence of secondary excitations in the counter window.

Absolute K intensity measurements of radiations emitted from target elements of high and medium atomic numbers were made by Birks et al (1964, 1965). For all their measurements, the detector was placed to receive radiations emitted at right angles to the electron beam for various orientations of the target. They found that the TiK results of Brown and Ogilvie (1964) were some 30% to 50% higher than their own after reversing the captions of figures (6) and (7) in Brown and Ogilvie's article.

Their definition of the quantum yield differs from that of the other authors; the number of electrons incident on the target refers to the "specimen current-to-ground" and not to the total number. By neglecting the correction for the backscattered fraction, they considered that their definition was equivalent to that of the others. However, they failed to account for those electrons, which after having made some ionizations in the target, rediffused out of it. For the elements considered, the experimental studies of Sternglass (1954) indicate that, except for elements of high Z, the backscattered electrons, which have lost more than the K ionization energy, represent a significant fraction of the total. The effect of this

omission is to overestimate the quantum yield.

1.2 Review of Experimental work on L and M radiation intensities.

Experimental studies of outer shell characteristic emissions were mainly restricted to relative line measurements for a particular shell and to radiations of short wavelengths. Results of previous work, nearly all of which had been carried out more than thirty years ago were discussed by Compton and Allison (p642, 1935). Some of these data referred to the intensity directly registered by the detector; wavelength dependent quantities, such as the coefficient of reflection of the monochromatizing crystal, detection efficiency of the counter, attenuation by the target and by other absorbers, were either neglected or only approximately corrected.

Only recently, investigations of L and M shell emissions were resumed. Using a lead stearate pseudo-grating and a gas flow proportional counter, Wykoff and Davidson (1965) made relative yield measurements for soft L - shell radiations emitted from elements of atomic number ranging from 17 to 51. These were all directly observed quantities; no allowance was made for any of the effects mentioned above.

The only reports on the absolute determination of the L and M radiation intensities were those given by Birks et al (1964, 1965), who confined their investigations to L-lines of heavy elements.

CHAPTER II

THEORETICAL CALCULATIONS OF K CHARACTERISTIC RADIATION INTENSITIES

2.1 Introduction.

The theoretical intensities used in this project for comparison with experimental data have been calculated from the expressions of Metchnik and Tomlin (1963) and Tomlin (1966). In this chapter, the component functions in the intensity formula describing the physical processes associated with the production of characteristic radiations are reviewed and their validity examined. Some of these terms have been altered. Calculations of the absolute intensities based on Bishop's (1965) expression for the mean depth of electron penetration, $\langle x \rangle$, for a semi-infinite medium have been carried out. An approximate intensity formula in a non-integral form has been derived and its validity discussed.

2.2 The Total K Ionization Cross-section.

An approximate, non-relativistic expression for fast incident electrons was derived by Bethe (1930). It has the form

$$Q_K = \frac{2\pi e^4}{TT_K} \, b \ln\left(\frac{4T}{B}\right) \qquad \ldots (2.1)$$

where e is the electronic charge. The other symbols have been defined in section (1.1). The values of b, which depend on Z and the electronic

shell, were tabulated by Bethe (Table 4, p582, 1930), and B was estimated by Mott and Massey (1949) to be $4T_K$ for low incident electron energies and $1.65\ T_K$ for high energies.

Worthington and Tomlin (1956) constructed an empirical function for B in an attempt to satisfy the conditions for both high and low energies. B was given as

$$B = (1.65 + 2.35\ \exp(1-U))\ T_K \qquad \ldots \quad (2.2)$$

where $U = T/T_K$

Figures (2.1) and (2.2) indicate that there is a fair agreement between Worthington and Tomlin's modified formula and the experimental K cross-sections for silver and nickel with the theoretical curves falling below the measured data. The resultant curve derived from equations (2.1) and (2.2) is denoted as WT in the figures (2.1) to (2.8). The resultant cross-section is to be referred to as the WT cross-section.

To allow for relativistic effects, Mott and Massey (1949) arrived at the expression,

$$Q_K = \frac{2\pi e^4}{TT_K}\, b \quad \left(\ln \frac{4T}{B} - \ln \left(1-\frac{v^2}{c^2}\right) - \frac{v^2}{c^2} \right) \qquad \ldots \quad (2.3)$$

where v is the electron velocity and c is the velocity of light. Q_K derived from equation (2.3) is shown in figure (2.1). B is given by equation (2.2). The resultant curve is denoted as WT (relativistic) in the figure. The figure shows that the effect of the relativistic terms is negligible. Similarly, Perlman's (1965) relativistic studies

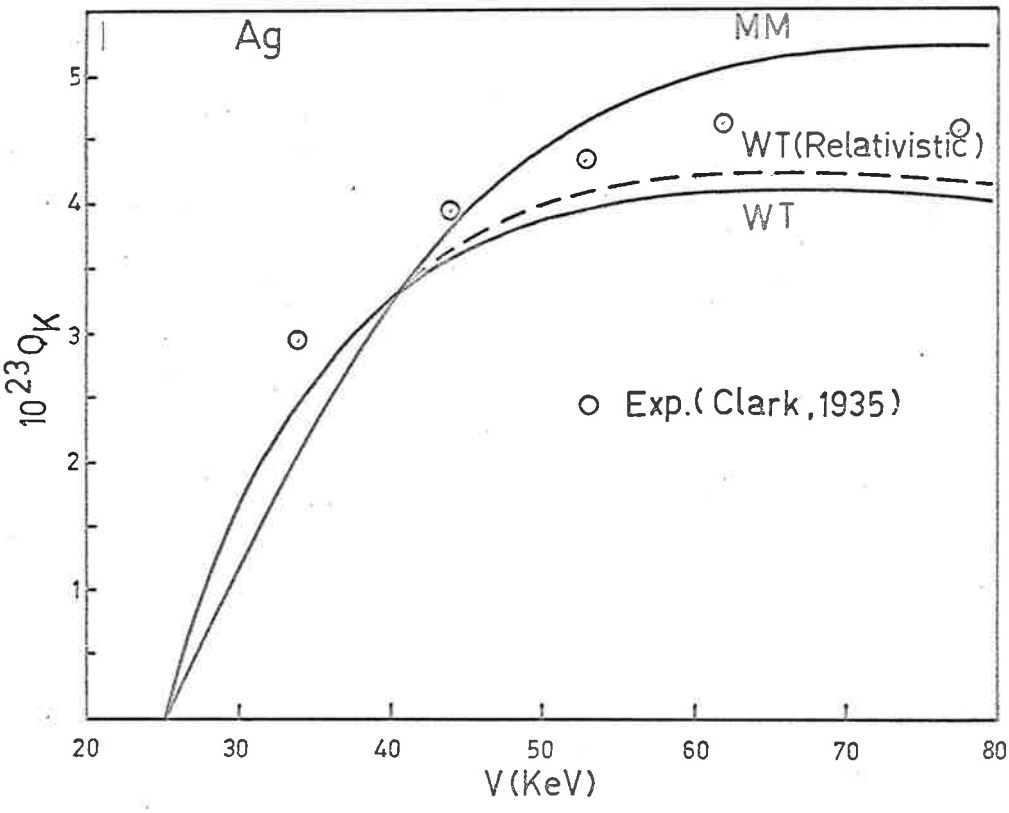

Figure 2.1 Total K ionization cross-sections for Silver.

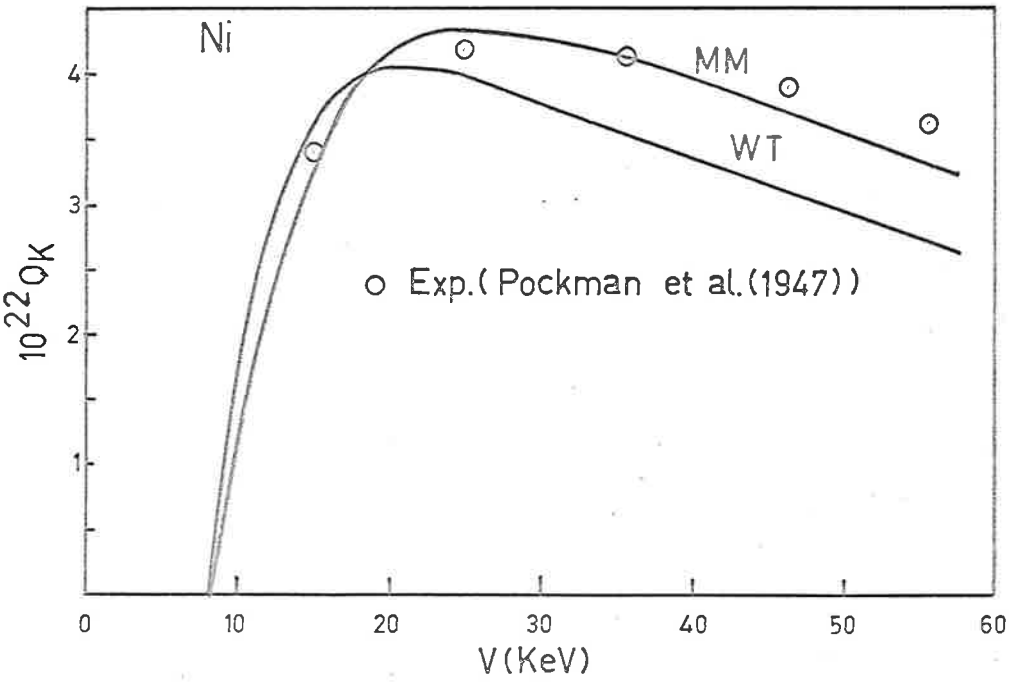

Figure 2.2 Total K ionization cross-sections for Nickel.

indicate that the relativistic effect may be neglected within the range of electron energies up to 60 keV.

In the absence of suitable experimental data for light elements, it is difficult to verify the validity of equation (2.1) for soft radiation calculations.

A non-relativistic treatment of the K shell ionization problem was discussed by Mott and Massey (1949, 1965). The solution was based on several approximations. These include the Born approximation, the neglect of electron exchange and the use of the hydrogenic wave functions. The effective nuclear charge was given as (Z - s), where Z is the actual nuclear charge and s, the screening constant as defined by Slater (1930).

The formula reduced to a form suitable for integration is set out below.

$$Q_K = \int_0^{K_{max}} \int_{K'_{min}}^{K'_{max}} I(K',K)\, dK'\, dK \qquad \ldots (2.4)$$

$$I(\theta,\phi)\, d\omega\, dK = \frac{2^{10} K K'}{a_o^2 k K'} \mu^6 f(K',K)\, d\omega\, dK \qquad \ldots (2.5)$$

$$f(K',K) = \frac{\left(K'^2 + \frac{1}{3}(\mu^2 + K^2)\right)}{\left(\mu^4 + 2\mu^2 (K^2 + K'^2) + (K^2 - K'^2)^2\right)^3}$$

$$\times \exp\left(-\frac{2\mu}{K} \arctan \frac{2\mu K}{K'^2 - K^2 + \mu^2}\right) \left(1 - \exp\left(\frac{-2\pi\mu}{K}\right)\right)^{-1} \qquad \ldots (2.6)$$

where the incident electron is scattered in the direction (θ,ϕ) into a solid angle $d\omega$ with the reference axis of the polar co-ordinate system along $\underset{\sim}{K'}$, the change in momentum of the incident electron,

and $\frac{K^2\hbar^2}{2m} = E_e$, the energy of the ejected electron,

$\frac{k'^2\hbar^2}{2m} = E_s$, the energy of the scattered electron,

$\frac{k^2\hbar^2}{2m} = E_o$, the energy of the incident electron,

$a_o = \hbar^2/me^2$, the Bohr radius,

m = electron mass

$\mu = Z_K/a_o$

$Z_K e$ = effective nuclear charge of the K shell,

$\underset{\sim}{K'} = \underset{\sim}{k} - \underset{\sim}{k'}$

$|\underset{\sim}{K'}| = K' = (k^2 + k'^2 - 2kk' \cos\theta)^{\frac{1}{2}}$

$K'dK' = kk' \sin\theta \, d\theta$ ... (2.7)

$2\pi \sin\theta \, d\theta = d\omega$ ... (2.8)

from (2.7) and (2.8)

$$d\omega = \frac{2\pi K \, dK}{k\,k'} \quad \text{... (2.9)}$$

from (2.5) and (2.9)

$$I(K',K)\, dK'\, dK = \frac{2^{11}\pi m^2 e^4 \mu^6 K}{\hbar^4 k^2 K'} f(K',K)\, dK'dK \quad \text{... (2.10)}$$

Equation (2.10) is identical to Burhop's (1940) integrand, apart from a term in the function $f(K',K)$, where a multiplying fraction $\frac{1}{2}$ appeared

instead of $\frac{1}{3}$ before the term $(\mu^2 + K^2)$. An examination of Burhop's results for the AgK cross-sections indicates that the factor $\frac{1}{2}$ was a typographical error.

The integration limits of the double integral (2.4) may be derived from the laws of conservation of energy and momentum. If E_K is the K excitation energy,

$$E_o = E_s + E_e + E_K$$

$$\text{or} \qquad k^2 = k'^2 + \frac{2m\,(E_K + E_e)}{\hbar^2}$$

$$k'^2 = (k^2 - K^2 - \frac{2mE_K}{\hbar^2})^{\frac{1}{2}}$$

The limits of the inner integral is given by

$$K'_{max} = k + k'$$

$$K'_{min} = k - k'$$

and for the outer integral, the limits are o and K_{max}, where

$$K^2_{max} = \frac{2m\,(E_o - E_K)}{\hbar^2}$$

Owing to the complex nature of the integrand, (2.4) can only be evaluated numerically. This was achieved with the assistance of the 3200 Control Data digital computer to within an accuracy of better than 1%.

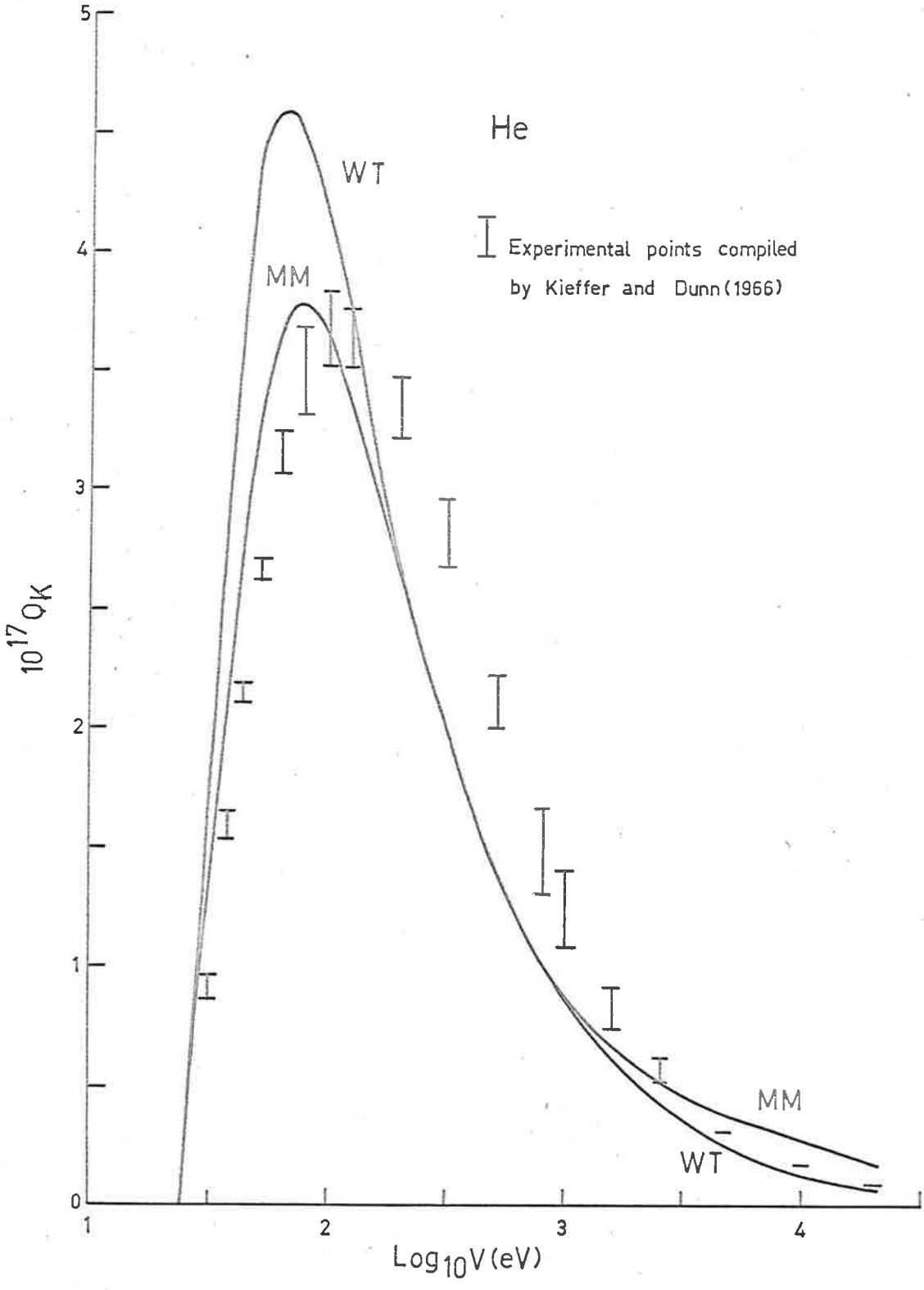

Figure 2.3 Total K ionization cross-sections for Helium.

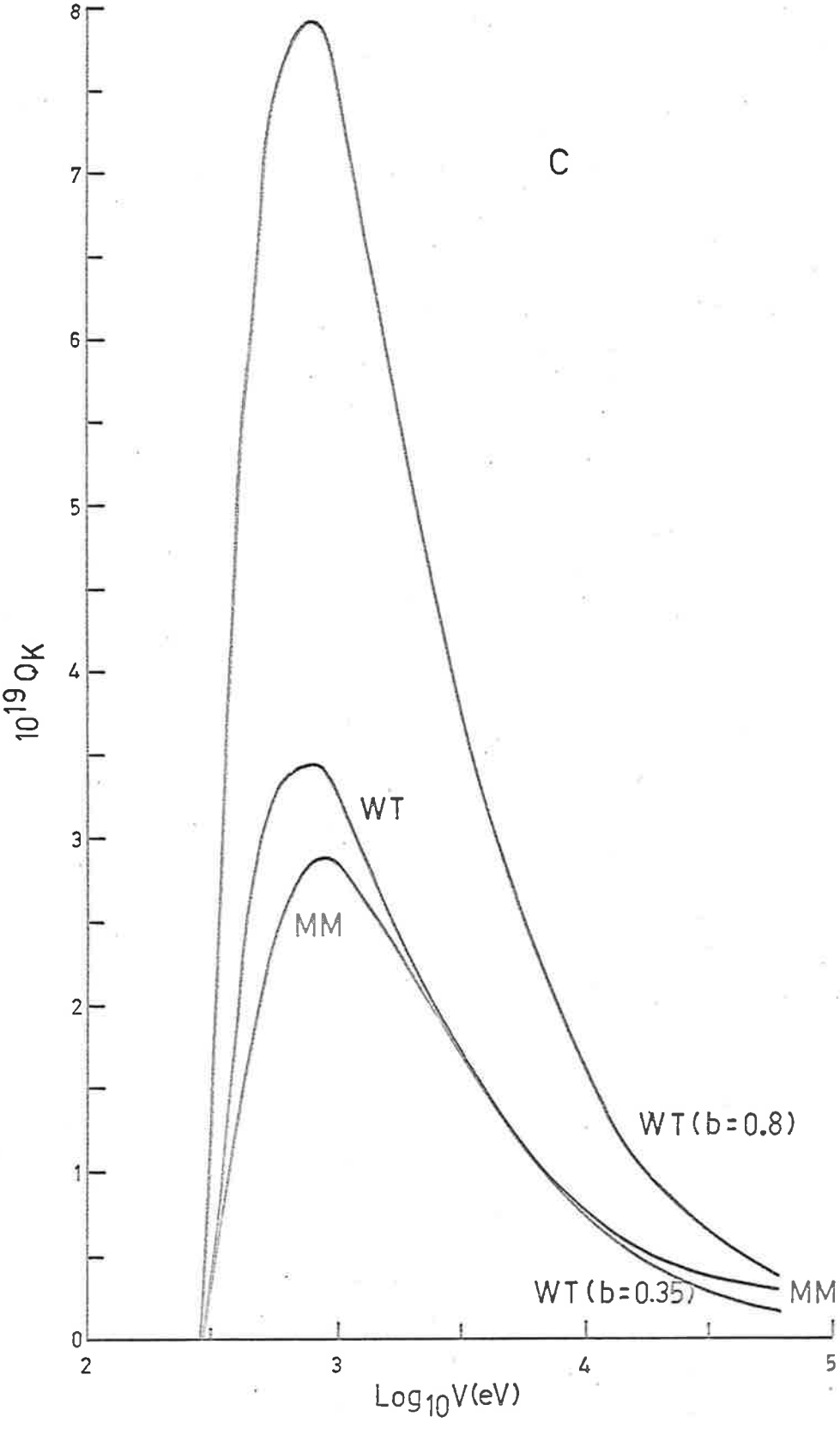

Figure 2.4 Total K ionization cross-sections for Carbon.

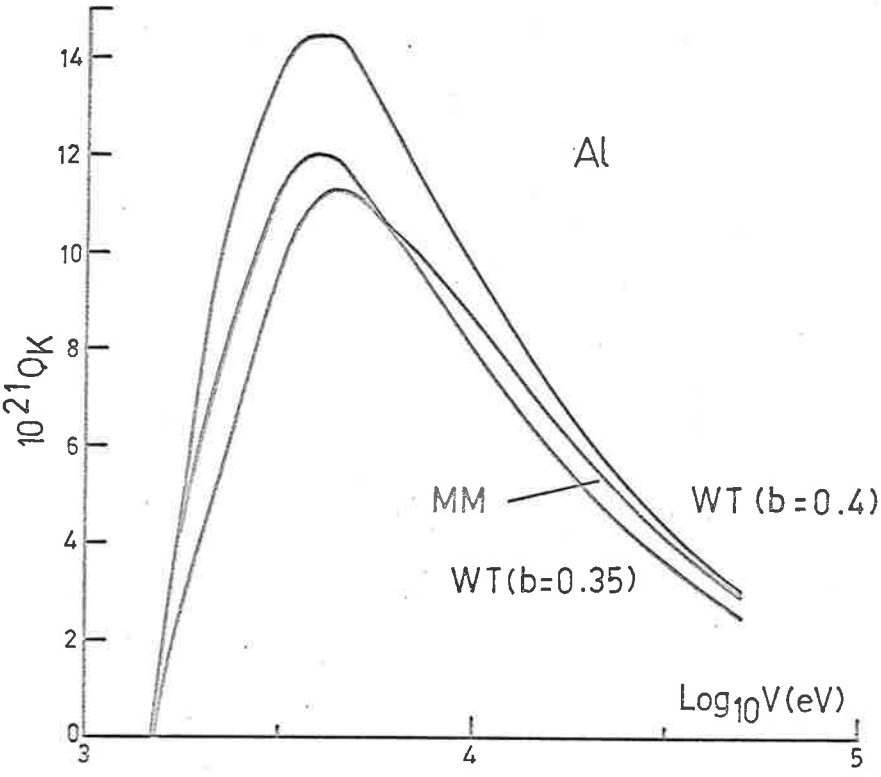

Figure 2.5 Total K ionization cross-sections for Aluminium.

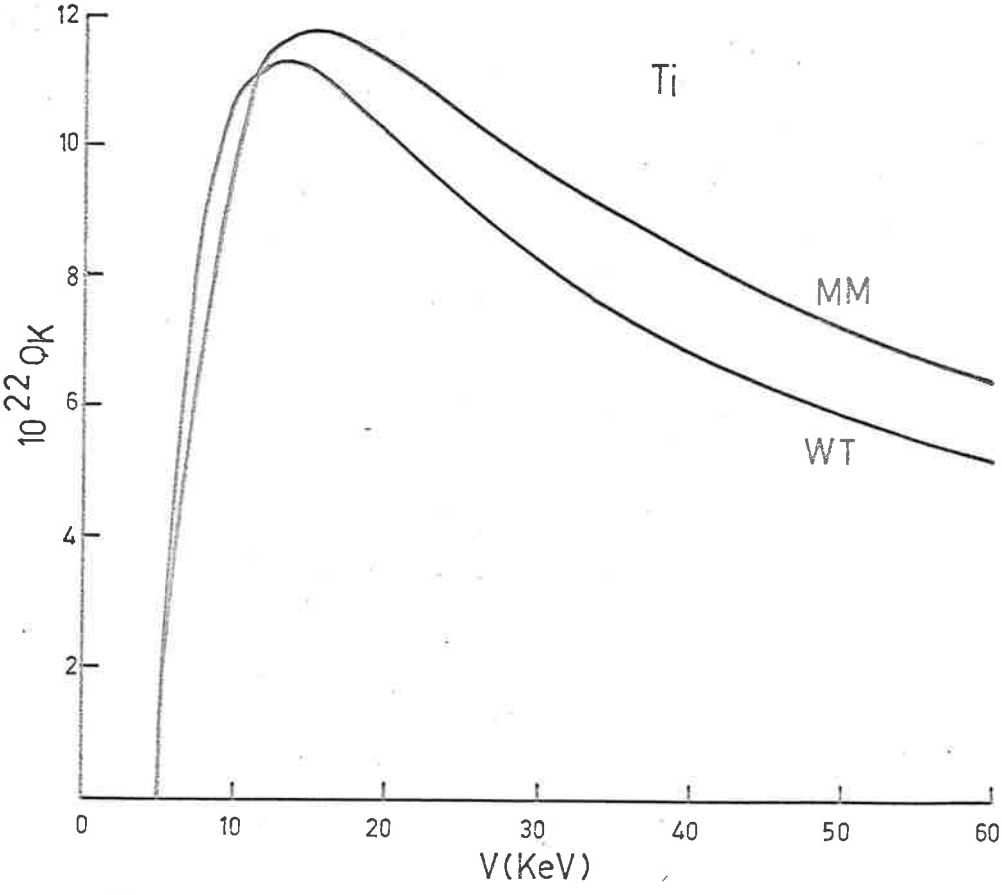

Figure 2.6 Total ionization cross-sections for Titanium.

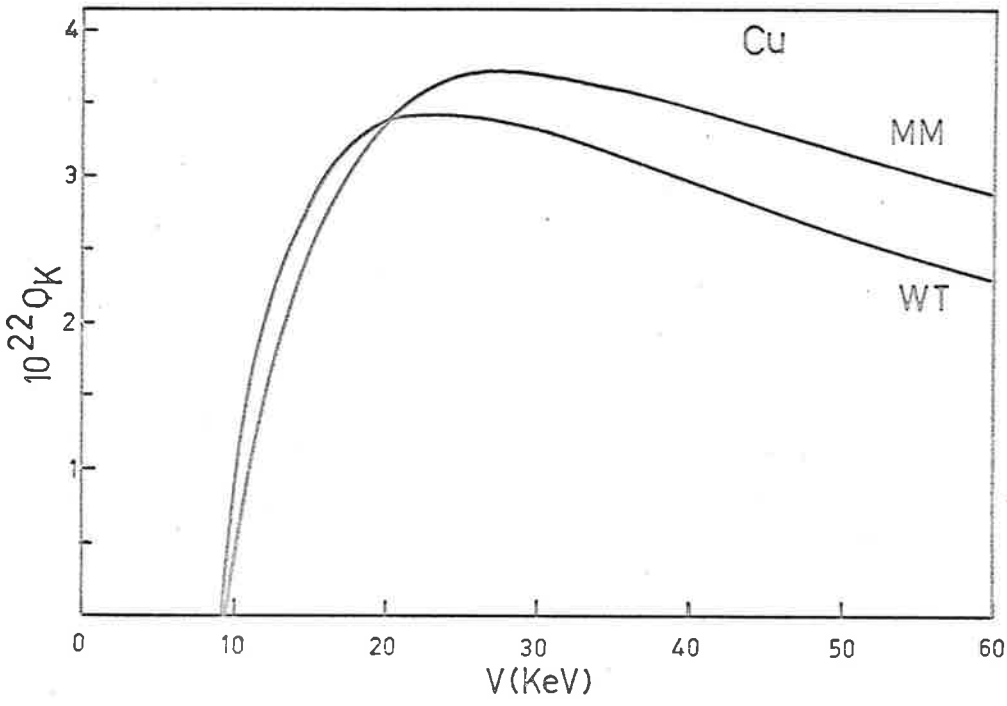

Figure 2.7 Total K ionization cross-sections for Copper.

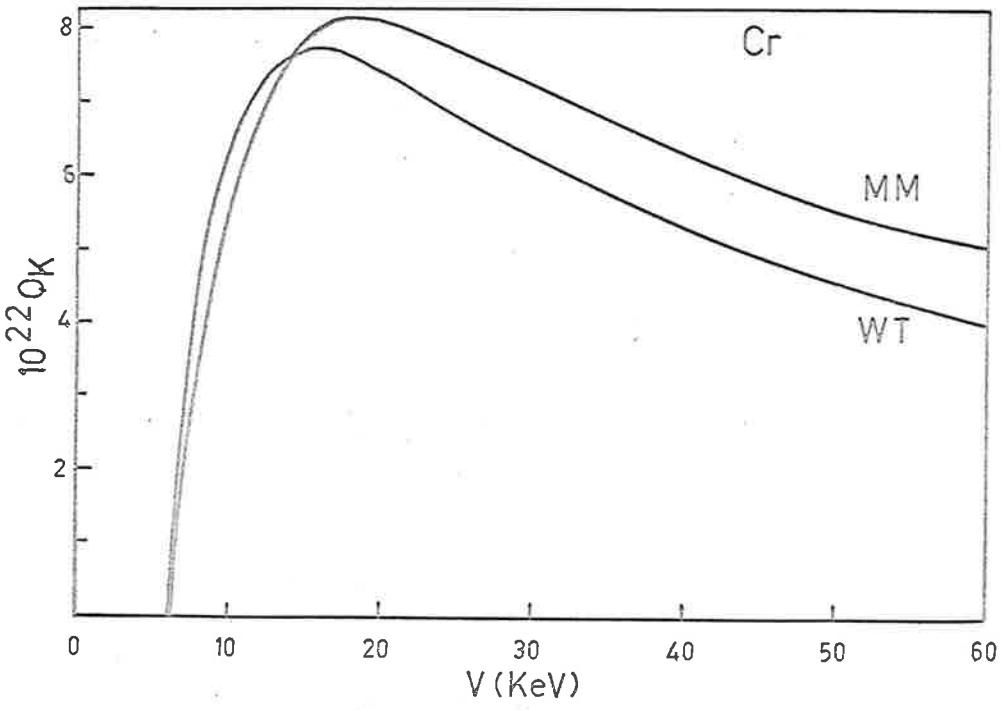

Figure 2.8 Total K ionization cross-sections for Chromium.

2.2.1 Discussion.

Computations were made for the total K ionization cross-sections for helium, carbon, aluminium, titanium, chromium, copper, nickel, and silver. These are shown graphically in figures (2.1) to (2.8) together with experimental data where available. The curves derived from equation (2.4) are denoted as MM in the diagrams. Some of the cross-sections had previously been calculated - HeK by Massey and Mohr (1933), NiK and AgK by Burhop (1940), whose results are approximately 5% lower than the present calculations. The difference may be attributed to the higher accuracy attained through the use of the digital computer.

Figures (2.1), (2.2), and (2.3) show that the theoretical AgK, NiK, and the HeK ionization cross-sections compare favourably with the experimental data, and that the relativistic effect is unimportant within the range of the incident electron energies considered. The effects of the Born approximation and the neglect of electron exchange were discussed by Mott and Massey (1965). These were considered to be important only at incident energies less than three times the excitation energy. The overestimation of the theoretical cross-sections within this energy range was attributed to these effects. Figures (2.1), (2.2), and (2.3) indicate that these sources of discrepancy are not serious.

The WT curves are consistently higher than the MM curves at electron energies below $2T_K$, and above this energy, they lie below the

MM curves. Below $3T_K$, the simple WT formula applies equally as well as the more complicated equation (2.4). However, above $3T_K$, the latter equation becomes more valid, if the experimental results are to be taken as correct.

For these calculations, the constant b in equation (2.1) is taken as 0.35, a value suggested by Mott and Massey (1949). The figures indicate that it is close to the optimum value for b. For the very light atoms, Bethe's (1930) calculated values for b are too large. Figure (2.4) shows the WT curves calculated for b = 0.35 and for Bethe's value of 0.8 for the carbon atom. The use of the latter value appears to be valid only close to the upper region of the electron energies considered.

Figure (2.3) compares the theoretical MM K ionization cross-sections with the experimental data compiled by Kieffer and Dunn (1966) for the helium atom. The good agreement between the different sets of measured results obtained by several independent observers verifies the reliability of these results. The figure shows that in the electron energy range below 100 eV, the MM curve is approximately 20% higher than the measured data. A discrepancy of approximately the same magnitude but of reversed sign occurs in the range 100 eV to 1000 eV. At higher energies, the theoretical cross-sections again exceed the experimental results. The variation in sign of the discrepancies in the formula for Q_K has the effect of reducing the resultant error in the radiation intensity formula. Assuming that a similar situation

applies to the other light atoms, the use of equation (2.4) for Q_K in the intensity calculations for soft K radiations is not unsatisfactory.

2.3 The K Fluorescence Yield.

The fluorescence yield, ω_K, expresses the probability that a K shell ionization results in the emission of a K characteristic photon. There are several theories which adequately treat atoms of medium and high atomic numbers but their validity in the low Z region remains suspect. Experimental information for the lightest atoms is scanty. The uncertainty in the values for ω_K is probably a contributing factor in the discrepancy between calculated and experimental intensities encountered by Tomlin (1964) in his paper on soft characteristic K emissions.

A theoretical discussion was given by Burhop (1952), who arrived at the formula,

$$\omega_K = (1 + a_K Z^{-4})^{-1} \qquad \ldots \quad (2.11)$$

where $a_K = 9 \times 10^5$ for $Z < 10$

$a_K = 1.19 \times 10^6$ for $10 \leq Z \leq 18$

$a_K = 1.27 \times 10^6$ for $Z > 18$

The formula has the same form as that first derived by Wentzel (1927). Burhop improved Wentzel's solution by including M and N shell transitions. According to Campbell (1963), Burhop's description of the

atomic electrons as having screened hydrogenic wave functions with discrete energy states as in free atoms is not entirely valid for very light atoms, where the wave functions are affected by the solid structure.

A comprehensive review of the atomic fluorescence yield was given by Fink et al (1966). They discussed the theories of Burhop (1952), Rubinstein and Snyder (1955), Listengarten (1962), and Callan (1963). Values of ω_K for only a few atoms were calculated by Rubinstein and Snyder, who used the Hartree self-consistent field method to compute the initial wave functions. Their procedure is unsuitable for calculating ω_K for light atoms for which the inherent approximations were considered to be seriously in error. Callan's calculations extend from Z = 16 to Z = 80 and those of Listengarten are restricted to heavy atoms.

A semi-empirical function of the form

$$\omega_K = (1 + a(Z-b-cZ^3)^{-4})^{-1}$$

is commonly quoted (Burhop (1955), Laberrique-Frolow, and Radvanyi (1956)). The constants a, b, and c, are selected by comparison with experimental data. Owing to the fact that electronic transitions involved in the K shell ionization are not similar for all atoms, the values of the above constants are dependent on the particular interval in Z considered. Evaluation of ω_K for light atoms by extrapolation is likely to introduce errors.

A list of experimental data for ω_K published up to as recently as May, 1966, was compiled by Fink et al. It reveals a considerable scatter among the measured data and the relative spread increases with a decrease in Z. Where no recent data were available, as in the case of the lightest atoms, Fink et al tabulated the average of the older data summarized by Broyles et al (1953), neglecting those based on the approximate cloud chamber method. The wide scatter of the experimental values for ω_K in the low Z region casts a doubt on their validity.

On comparison of the theories of Rubinstein and Snyder, Callan and Listengarten, Fink et al found that they are consistent with each other and with the experimental data. Callan's theoretical results exhibited good agreement with the best fit curve drawn by Fink et al through the experimental points (Fig. 8, Fink et al, 1966) and his results correspond closely with the experimental data obtained from the more accurate methods of measurement such as those of Taylor and Merritt (1963). Figure (2.9) is a reproduction of Fink et al's graph in the low to medium Z region. The ω_K values computed from Burhop's formula are also included. Burhop's curve runs approximately parallel to Callan's results but lies below it by 0.05 units on the ω_K scale. The discrepancy increases with a decrease in Z.

For light atoms, the ω_K values of direct interest in the present project are those of aluminium and carbon. For the aluminium atom, the experimental values tabulated by Fink et al (1966) spread

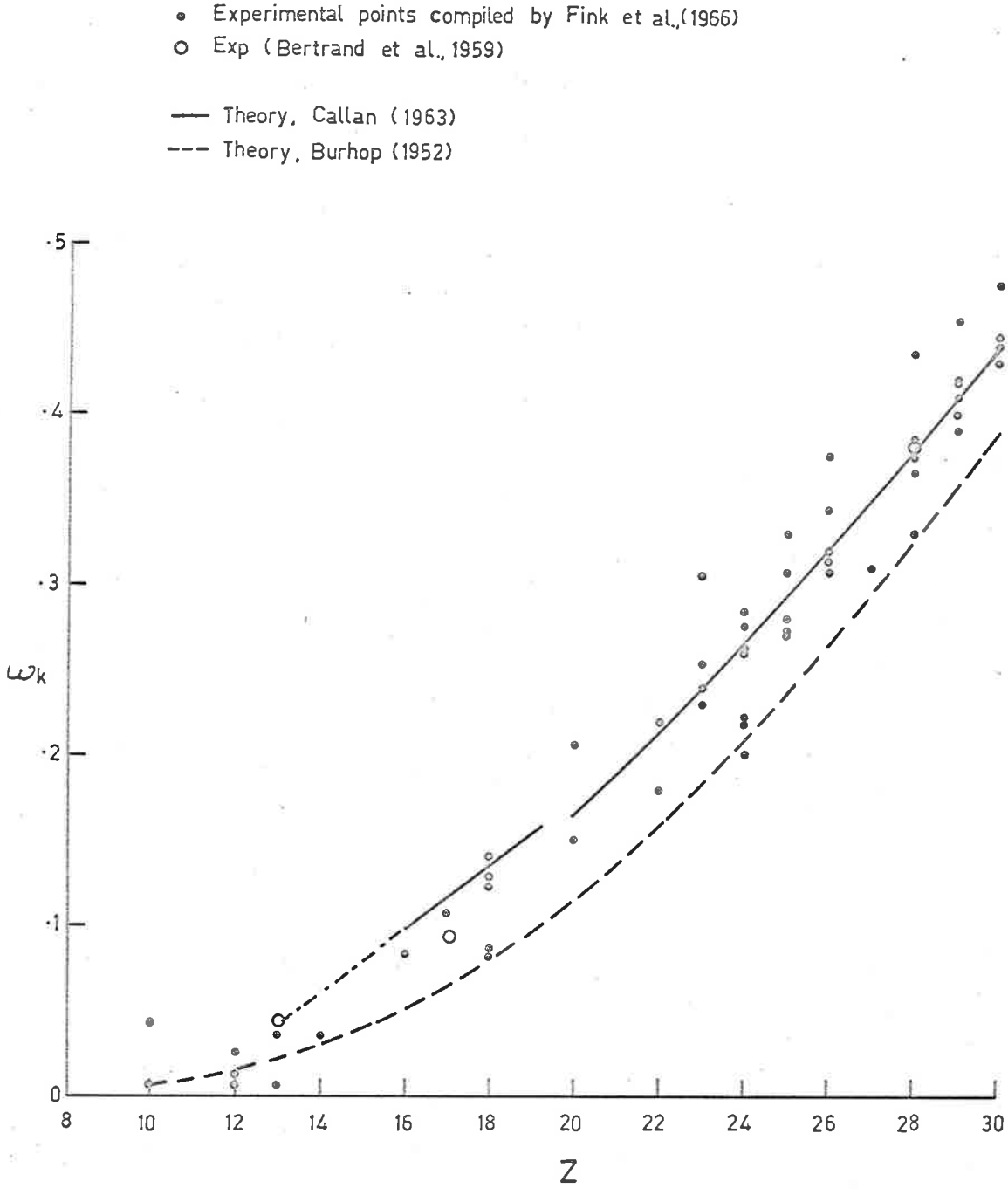

The K-shell fluorescence yields are shown as a function of the atomic number. Callan's theoretical curve is extrapolated to Z=13.

Figure 2.9

from a value of 0.008 to 0.045. No value was given from Callan's theory. An estimate may be obtained by extrapolating those data calculated by Callan for atoms whose atomic number lies within the range $10 \leq Z \leq 18$, i.e. the group of atoms whose interactions only involve L and M electrons when a vacancy occurs in the K shell. This results in a value of 0.04 for the aluminium atom which is significantly greater than Burhop's value of 0.0234. The extrapolation of Callan's curve to $Z = 13$ is shown in figure (2.9). The sign of the discrepancy is consistent with that observed in the higher Z values. The closest experimental result to this extrapolated value is that of Bertrand et al (1959) whose value is 0.045. A survey of the other measured data of Bertrand et al indicates that they are in good agreement with the experimental results from other sources and with Callan's calculated values. The present measured intensities for AlK radiations are in better agreement with the theoretical results when Betrand et al's value of 0.045 for ω_K is used (section 4.5).

An estimate of the ω_K value for carbon by extrapolation of the Callan results is likely to be uncertain. Firstly, the interval in Z between carbon and the lightest atom, whose ω_K value is known, is large. Secondly, a K shell ionization of the carbon atom results in interactions involving only the L shell electrons, whereas L and M electronic transitions are possible in the case of atoms where atomic numbers exceed 9. It appears that more experimental information is needed on the fluorescence yield of carbon. If the observed trend of

the Burhop curve in the medium Z region extends to the lightest atoms, then the use of its value for ω_K would result in an underestimation of the computed CK radiation intensities. The present measured intensities for CK do in fact lie above the computed intensities. If an ω_K value of 2.06×10^{-3} is used for carbon, a better correspondence between theory and experiment is obtained.

On the basis of the experimental evidence compiled by Fink et al, Callan's values for ω_K, where available, are used for the theoretical calculations. The ω_K values used in this thesis are tabulated in Table (2.1) together with their sources.

	Z	K	Source
C	6	2.06×10^{-3}	*
Al	13	0.045	Bertrand et al (1959)
Ti	22	0.213	Callan (Fink et al, 1966)
Cr	24	0.272	Callan
Cu	29	0.407	Callan

Table (2.1)

* Value obtained by a comparison of the theoretical CK intensities with the present experimental data (section 4.6).

Tomlin (1964) in his calculations of characteristic intensities used the ω_K values supplied by Davidson and Wyckoff (1962). Their values are similar to those derived from the Burhop formula. On the basis of the ω_K values in Table (2.1), his CuK_α, CrK_α, and AlK

intensities were underestimated by 10%, 22%, and 40% respectively.

2.4 The Correction Factor, R, for the Backscattered Electrons.

In calculating the X-ray emission intensity allowance has to be made for the loss of electrons from the target. Some are backscattered with a little loss in energy. Some leave the target after making some ionizations in the target. In the procedure of Webster et al (1931), the backscattered electrons were allowed to excite a second target without further backscatter. The secondary radiations were then subtracted from the primary radiations. Tomlin (1964) modified this method. He reasoned that if all the backscattered electrons were to suffer energy losses less than the ionization energy then the exact solution would be to subtract this number from the incident beam, ignoring the distribution in energy of the backscattered electrons. For the remaining backscattered electrons, Tomlin followed the Webster procedure by calculating the number of photons excited by these electrons in a second target without backscatter. The results tabulated by Tomlin (Table 1, 1964) have been used in the present calculations. These results were based on his (1963) empirical formula for the backscattered ratio b (section 2.4.1) except for the lightest elements for which experimental data were used. The energy distribution function of the backscattered electrons used by Tomlin is discussed in section (2.4.2).

For light elements, the effect of any error in R on the

absolute intensity calculations is likely to be small as the back-scattered ratio for light target elements is small and there is a good correspondence between the theoretical energy distribution function and the experimental distribution function.

2.4.1 The Number of Backscattered Electrons, b.

In calculating R, the actual number of electrons backscattered is required. The backscattered fraction, b, was investigated experimentally by Becker (1925), Schonland (1925), Stehberger (1928) and more recently by Palluel (1947), Sternglass (1954), Holliday and Sternglass (1957), Kanter (1957), Matskevich (1957), Campbell (1963), and Burkhalter (1965).

The earlier works were reviewed by Webster et al (1931) who pointed out that the apparent inconsistency in some of the results originated in the difference in definition of the reflection ratio. This arose from the practical impossibility in separating the low energy reflected electrons from the true secondaries. Fortunately there are two factors which justify the introduction of an artificial separation potential. According to Sternglass (1954), the proportion of true secondary electrons whose energy is below 30 eV exceeds 95% of the total number. It was qualitatively shown by Webster et al (1931) and Archard (1961) that low energy backscattered electrons have a small probability of escaping from the target surface. Further-

more, the choice of a separation potential is not critical as was revealed in Campbell's results, which showed that for targets of low atomic numbers, b is nearly independent of the separation potential over a range of up to 100 eV provided the incident potential is sufficiently large. This led to the current convention which introduces an arbitrary cut-off potential at 50 eV to isolate the true secondaries from the backscattered electrons. Any error caused by the presence of reflected electrons, whose energies lie below the cut-off potential is probably reduced to some extent by the occurrence of high energy secondaries, whose existence is attributed by Sternglass (1954) to close electron-electron collisions.

From a graphical compilation of past data and those of his own work, Sternglass confirmed the earlier observations of Palluel and Schonland that b was essentially independent of the primary energy except in the low energy region. His results further revealed that for elements of low and medium atomic numbers, this constancy extended down to a primary energy of a few eV. For elements whose atomic numbers exceeded 30, the constancy in b terminated at a few keV, where b then decreased rapidly with a reduction in the incident energy.

There remain two variables which could affect the backscattered ratio, namely, the atomic number of the target material and the angle of incidence of the electron beam. Brand (1936) indicated that the backscattered ratio was not seriously affected by the latter. However, Campbell's results for light elements show a noticeable

difference in the values at normal incidence and at 45° incidence for the electron beam.

This problem was treated theoretically by Everhart (1960) and Archard (1961) from two entirely different approaches. Each considered only one facet of the interactions involved. Everhart based his theory solely on a single, large angle scattering of the incident electrons utilizing the Rutherford formula. Whereas, Archard regarded the phenomenon as a small angle scattering process following Bethe's (1940) concept of the depth of complete diffusion within the target. Both theories arrived at relationships which were independent of the incident energy, as was observed experimentally. These theories were acknowledged by the respective authors to be over-simplified. Both types of interactions should have been considered. This fact was illustrated in Archard's review of the Everhart formula, which in its original form fell well below the experimental data. By including the possibility of an additional small angle deflection in the Everhart theory, Archard arrived at an expression which approached the empirical expression introduced by Everhart to fit the experimental points.

In the Archard theory, the electrons were assumed to follow an idealized straight path in the target down to a depth of complete diffusion, at which point, all angles of electron deflection were considered to have an equal probability of occurrence. The resultant curve appears to be significant only for elements of high atomic numbers. Serious discrepancies occurred for light elements. Archard's

model was adopted by Tomlin (1963), who arrived at an improved expression by modifying the expression for the depth of complete diffusion, which was derived from Lewis' (1950) formula. Tomlin found that the experimental data for b lay fairly closely to his empirical formula

$$b = \frac{1}{6} \ln Z - \frac{1}{4}$$

Good agreement between Tomlin's empirical formula and experimental data was also reported by Burkhalter (1965).

2.4.2 The Energy Distribution of the Backscattered Electrons.

Webster et al (1931) constructed two alternative empirical distribution functions for the energies of the redifussed electrons as functions of dimensionless parameters. These functions were derived from the knowledge of a few end points associated with the energy distribution and its general curve shape deduced from the approximate results of Wagner (1930) and Wisshak (1930). Adopting one of the normalized functions, Tomlin (1964) determined the value of the dimensionless parameter by comparison with the improved experimental data of Sternglass (1954). Comparison with the intermediate energy distribution of Brand (1936) and the high energy distribution of Bothe (1949) indicates that an increase in the incident energy is accompanied by a progressive shift of the peak of the distribution towards the high energy region. For elements of low atomic numbers, this shift

is not serious and the curve shapes remain nearly independent of the incident energy. But for elements of atomic numbers ~ 30, Brand's (1936) curve differed significantly in shape from that of Sternglass which was obtained at a much lower incident electron energy. This was attributed by Sternglass to backscattering involving inelastic collisions at energies comparable to the ionization energy of the target element. A discrepancy in the curve shape was also found by Tomlin (1964) between his empirical distribution function and Sternglass' (1954) experimental data for iron. For the other target elements, Tomlin found that there was a good agreement between his distribution function and the experimental data.

In his calculation of R, Tomlin (1964) did not allow for the dependence of the energy distribution function on the angle of incidence of the primary electrons at the target. Brand (1936) indicated, however, that this dependence was not great.

2.5 Indirect Excitation.

The correction factor in the intensity formula, $\frac{P+1}{P}$, to allow for the fraction of K radiations excited by high energy continuous radiations was obtained from Green and Cosslett (1961), who calculated values for $\frac{1}{P}$, the ratio of the indirectly excited to the directly excited K radiations. Although their theoretical treatment involved a number of approximations, one of which was the omission of

target absorption, there was good agreement between their results and the experimental data for $Z > 30$, which were available. The approximations involved probably affected each characteristic component nearly equally. For target elements of atomic numbers less than 30, the value of $(\frac{P+1}{P})$ approaches unity. For the characteristic K intensities investigated in this project, a correction for the indirect excitation was found necessary only for the calculations of the CuK_α intensities, for which a value of 1.06 was used. The indirectly excited ratio was also studied by Brown and Ogilvie (1964), whose theoretical treatment included a correction for the target absorption. They found that for elements with $Z \leq 28$ the indirect contributions were negligible for thick targets.

2.6 The Ratio of the Number of K_α Photons to the Total Number of K Photons.

For the copper and the chromium radiations, the intensities of the K_α component were calculated. The ratio of the number of K_α photons to the total number of K photons, p, was computed from the experimental data of Williams (1933), who determined the ratios of the energy intensities of the component K lines to that of the $K_{\alpha 1}$ line for a number of target elements. The corrections for CuK_α and CrK_α radiations were 0.89 and 0.93 respectively. A value of 0.88 for CuK_α was used by Metchnik (1961).

2.7 The Absolute Intensity Formula.

The formula used for computing N_ϕ followed that of Metchnik and Tomlin (1963). It included the modifications made by Tomlin (1966), namely, the expression for $\langle x \rangle$ included a correction for scattering by atomic electrons, and the experimental data of Bakker and Segrè (1951) were used for B, a term in the expression for J, the mean excitation energy of the target atoms. The intensity formula is set out below.

$$N_\phi = k \int_{T_\bullet}^{T_K} N Q_K \frac{ds}{dT} \exp\left(-\mu_T \rho \langle x \rangle \operatorname{cosec} \phi \cos\theta\right) dT \quad \ldots (2.12)$$

where $k = Rp \left(\frac{P+1}{P}\right) \omega_K$

$$N = \frac{L\rho}{A}$$

$$\frac{ds}{dT} = -\frac{T}{2\pi e^4 NZ} \cdot \frac{1}{\ln \frac{2T}{J}}$$

$$\langle x \rangle = \frac{J^2}{8\pi NZe^4} \cdot \frac{\exp\left(-\gamma_o (Z+1)/(Z+9)\right)}{\gamma_o^{\frac{1}{4}\alpha(Z+1)}} \left(F(\gamma_o) - F(\gamma)\right) \quad \ldots (2.13)$$

$F(\gamma)$ is given by the asymptotic expansion

$$F(\gamma) = e^{\gamma} \gamma^{\frac{1}{4}\alpha(Z+1)-1} \left(1 - \frac{\frac{1}{4}\alpha(Z+1)-1}{\gamma} + \frac{\left(\frac{1}{4}\alpha(Z+1)-1\right)\left(\frac{1}{4}\alpha(Z+1)-2\right)}{\gamma^2} - \ldots\right)$$

$$\gamma = \frac{Z + 9}{4} \ln \frac{2T}{J}$$

$$\alpha = \frac{1}{3} \ln Z + \ln B - 2.917$$

$J = 1.602 \times 10^{-12}$ BZ erg

L = Avogadro's number

ρ = density of the target elements

A = atomic weight of the target element.

The other notations used have already been referred to in Chapter I and in this chapter.

It was found that the intensities computed with the modified expression for $\langle x \rangle$ differed very little from those computed with the original expression of Metcfhnik and Tomlin (1963).

In the intensity calculations of the characteristic K radiations, μ_T is assumed to be identical to the mass absorption of the target element for the K_α component. Owing to the high proportion of K_α radiations in the K spectrum, the consideration of the K_β component makes very little difference to the results (Tomlin, 1964).

Calculations of N_ϕ were made using both the formula of Worthington and Tomlin (1956) for Q_K (these intensity curves are to be referred to as WT) and the expression (2.4) for Q_K (the resultant intensity curves are to be referred to as MM). These curves are contained in Chapter IV together with the corresponding experimental points.

These calculations were made with the assistance of the

Control Data 3200 digital computer. The integral for the intensity function was numerically evaluated by means of Simpson's Rule with the integrand equally divided into 50 intervals. The sub-program for this integration operation was tested with simple functions which had definite integrals. The accuracy was found to be much better than 1%. Evaluation of the MM curves would have required prohibitively long computing times if the full expression for Q_K was incorporated directly in the expression (2.12) for N_ϕ. Instead, Q_K was first evaluated at a number of selected values of T. The interval in T between the successive values evaluated was chosen according to the degree of variation of Q_K with T. A sub-program was written which enabled Q_K to be evaluated for all T within the range defined by the integration limits of N_ϕ on the basis of those values of Q_K already computed from the full expression. This was achieved by fitting a quadratic equation to three successive evaluated values of Q_K, whose range in T contained the point for which the value for Q_K was required by the main program. This sub-program for the curve fitting process was tested by comparing the values of Q_K obtained from it with the corresponding values computed directly from the equation (2.4) for Q_K. The agreement was better than 1%. Using this technique, the total computing time required to evaluate a typical set of 60 intensity results was approximately 5 minutes. The time taken was comparable to that for evaluating the simpler intensity formula

using equations (2.1) and (2.2) for Q_K. The theoretical intensities for TiK and AlK radiations are shown in figures (2.10) and (2.11) respectively. Equation (2.4) was used for Q_K and the ω_K values were 0.213 and 0.045 for titanium and aluminium respectively.

Calculations for N_ϕ have also been made using the Bishop-Tomlin expression for $\langle x \rangle$ for an infinite and semi-infinite target (Bishop, 1965). The expression, which has been modified here to allow for the scattering by atomic electrons, has the form

$$\langle x \rangle = a \frac{8}{(Z+9)} R_B \left(1 - \exp -\left(\frac{1}{a} \frac{(Z+9)}{4} \left(1 - \frac{T}{T_o}\right)\right)\right) \quad \ldots (2.14)$$

where the Bethe range, R_B, is given by (Worthington and Tomlin, 1956)

$$R_B = \frac{J^2}{8\pi NZe^4} E_i \frac{(8\gamma_o)}{Z+9} \quad \ldots (2.15)$$

where $E_i(y)$ is the exponential integral. For large y, $E_i(y)$ may be represented by the asymptotic series

$$E_i(y) = \frac{e^y}{y} \left(1 + \frac{1}{y} + \frac{2!}{y^2} + \ldots\right) \quad \ldots (2.16)$$

a = 1 for an infinite medium and

a = 1.5 for a semi-infinite medium.

Although equation (2.14) has only been shown by Bishop to agree with his Monte Carlo results for a semi-infinite copper target, Cosslett and Thomas (1964a) indicated that the expression for the

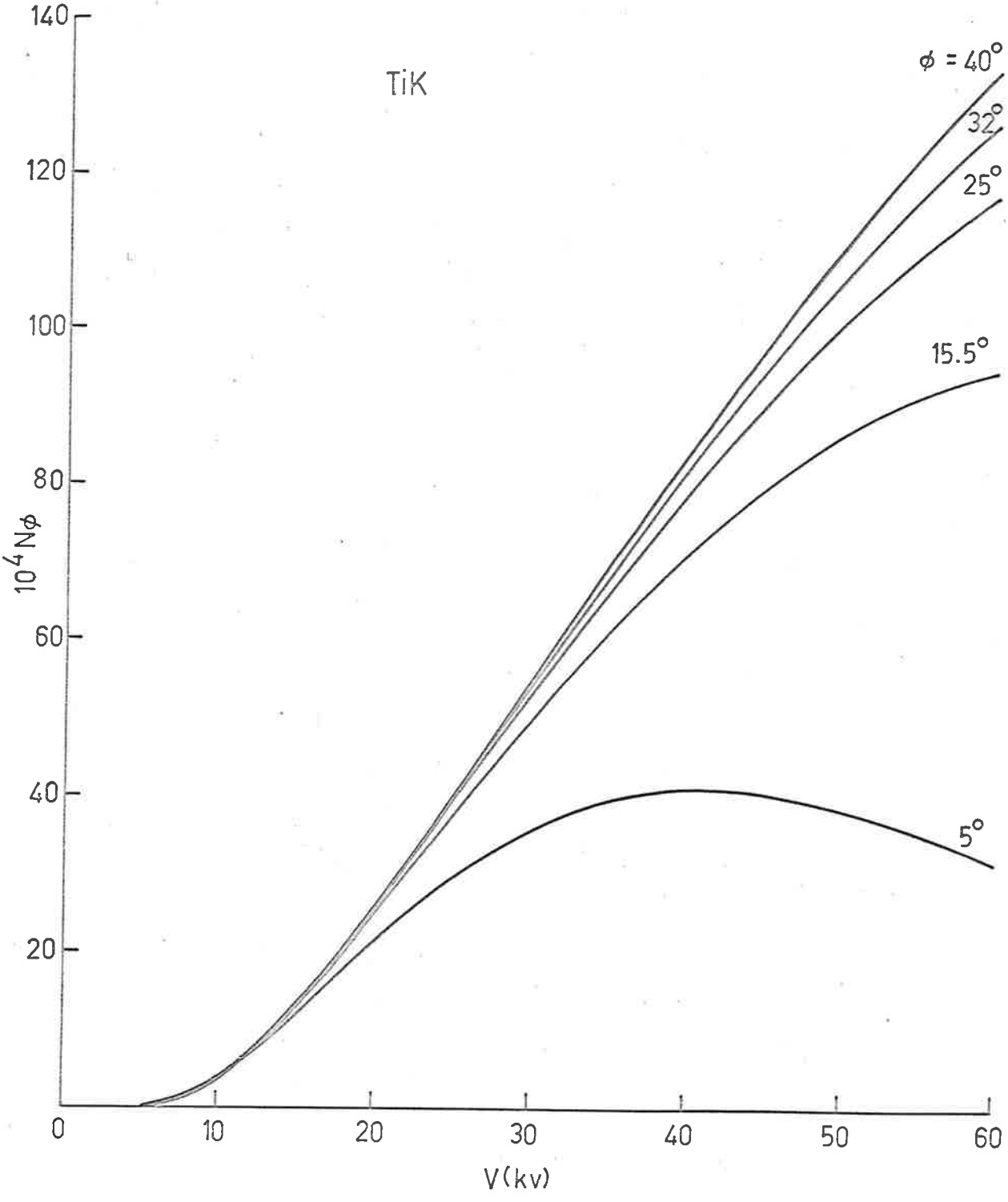

Figure 2.10 Theoretical results for TiK radiation intensities.

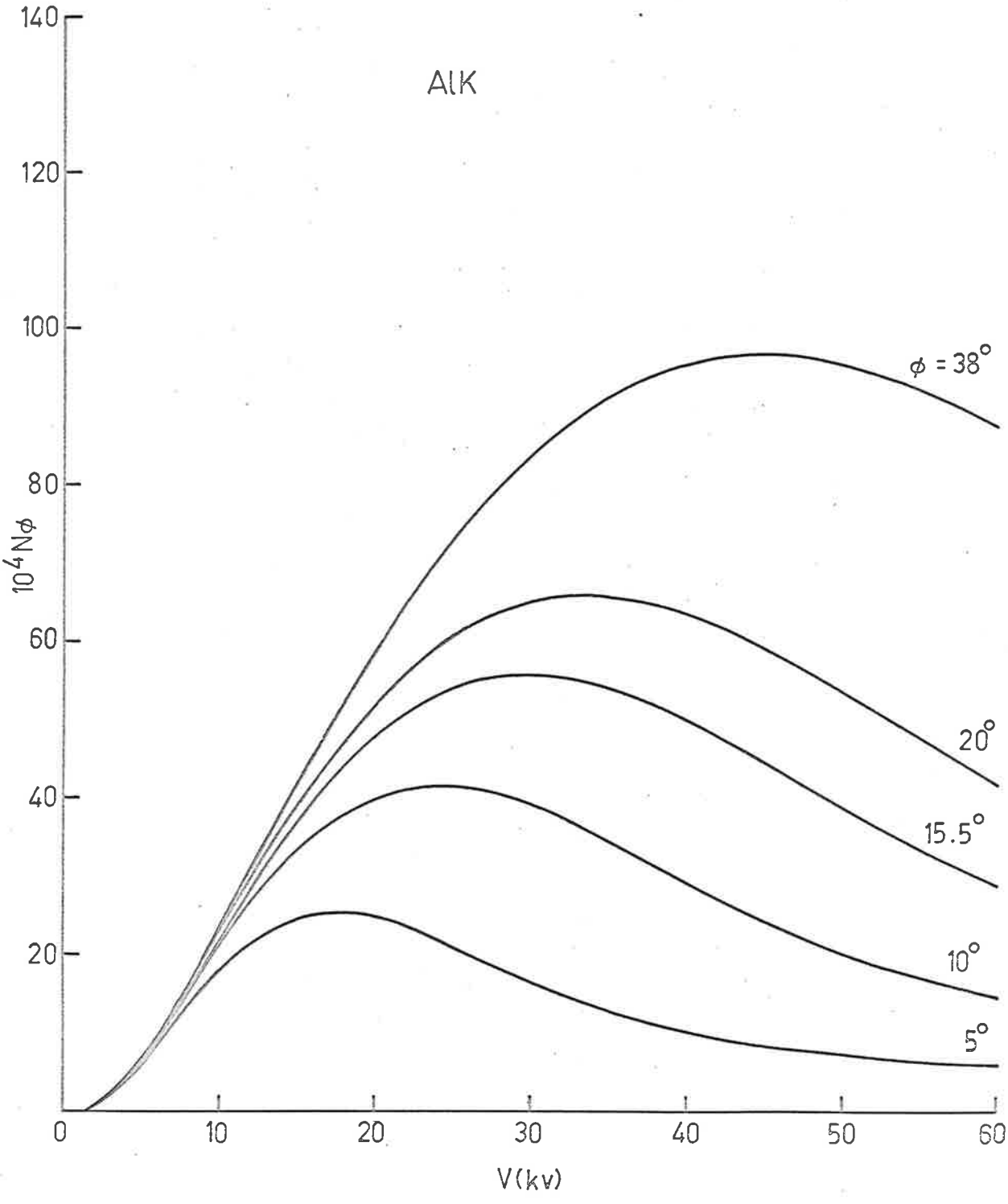

Figure 2.11 Theoretical results for AlK radiation intensities.

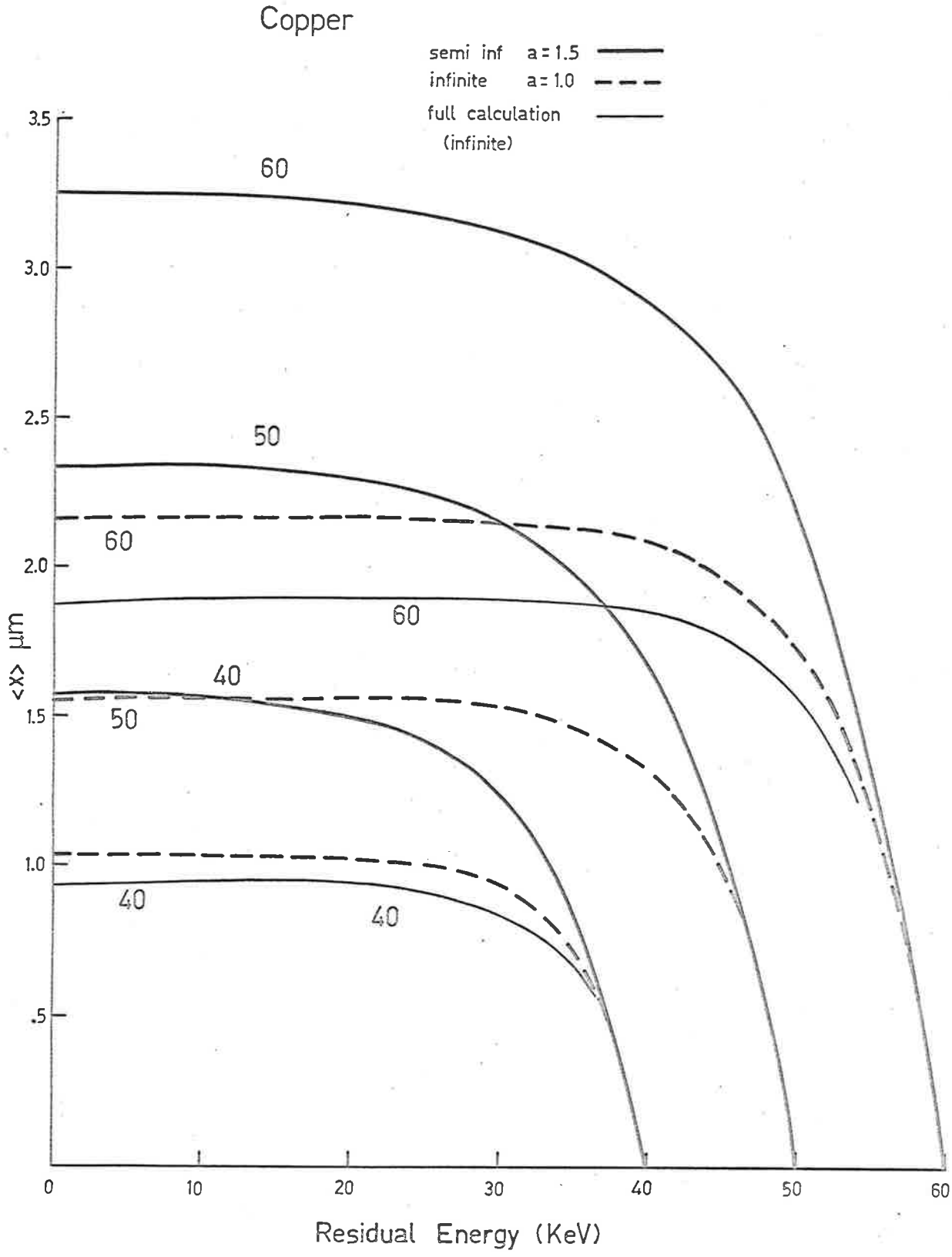

Depth of electron penetration into a copper target.

Figure 2.12

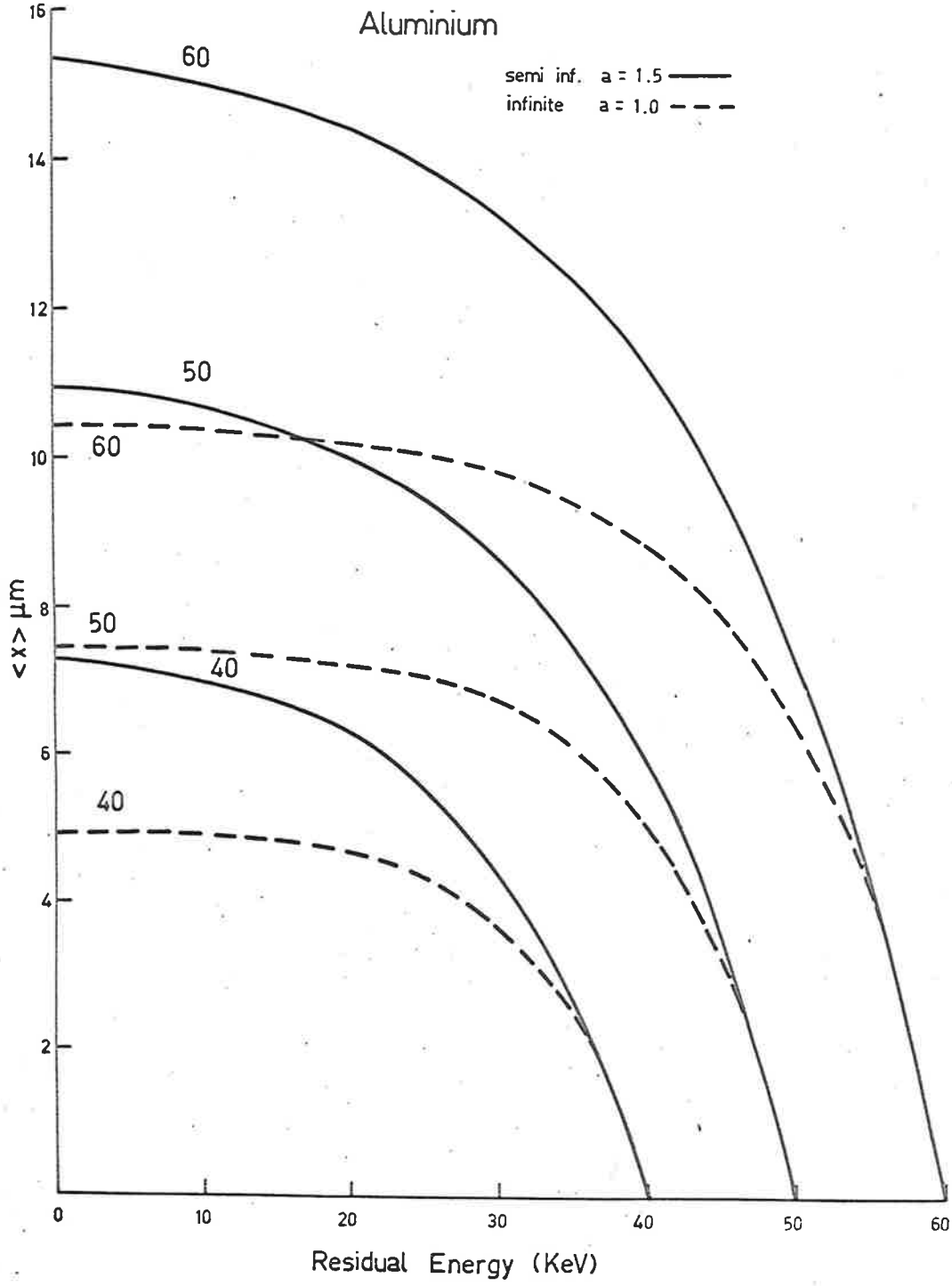

Figure 2.13 Depth of electron penetration into an aluminium target.

depth of complete diffusion derived from (2.14) for a semi-infinite medium was consistent with his experimental data for aluminium, copper and silver targets with 20 keV electrons (section 1.1.1).

The equation (2.15) for $\langle x \rangle$ was evaluated for both semi-infinite and infinite media. Figures (2.12) and (2.13) and the curves for copper and aluminium respectively for various incident electron energies. Except in the range where the residual electron energy approaches the incident energy, the figures indicate that the curves for $\langle x \rangle$ computed for a semi-infinite target exceed the corresponding curves computed for an infinite target by 50%. The effects on the intensity functions due to the use of the semi-infinite formula (2.14) for $\langle x \rangle$ are shown in figures (2.14) and (2.15), which are the theoretical intensity curves for CuK_α and AlK radiations respectively. As expected, in the case of the semi-infinite target, the larger values of $\langle x \rangle$ result in theoretical intensities which are less than the corresponding intensities computed for an infinite medium. For both radiations at low incident electron energies, the intensities computed for a semi-infinite target differ very little from those computed for an infinite target. This difference between the corresponding curves for AlK is generally much more pronounced than that of the CuK_α radiations. This is due to the higher absorption of aluminium for its own K radiations. At the lower angle of incidence, where the radiation absorption path in the target is longer, the difference in the values of $\langle x \rangle$ becomes more impor-

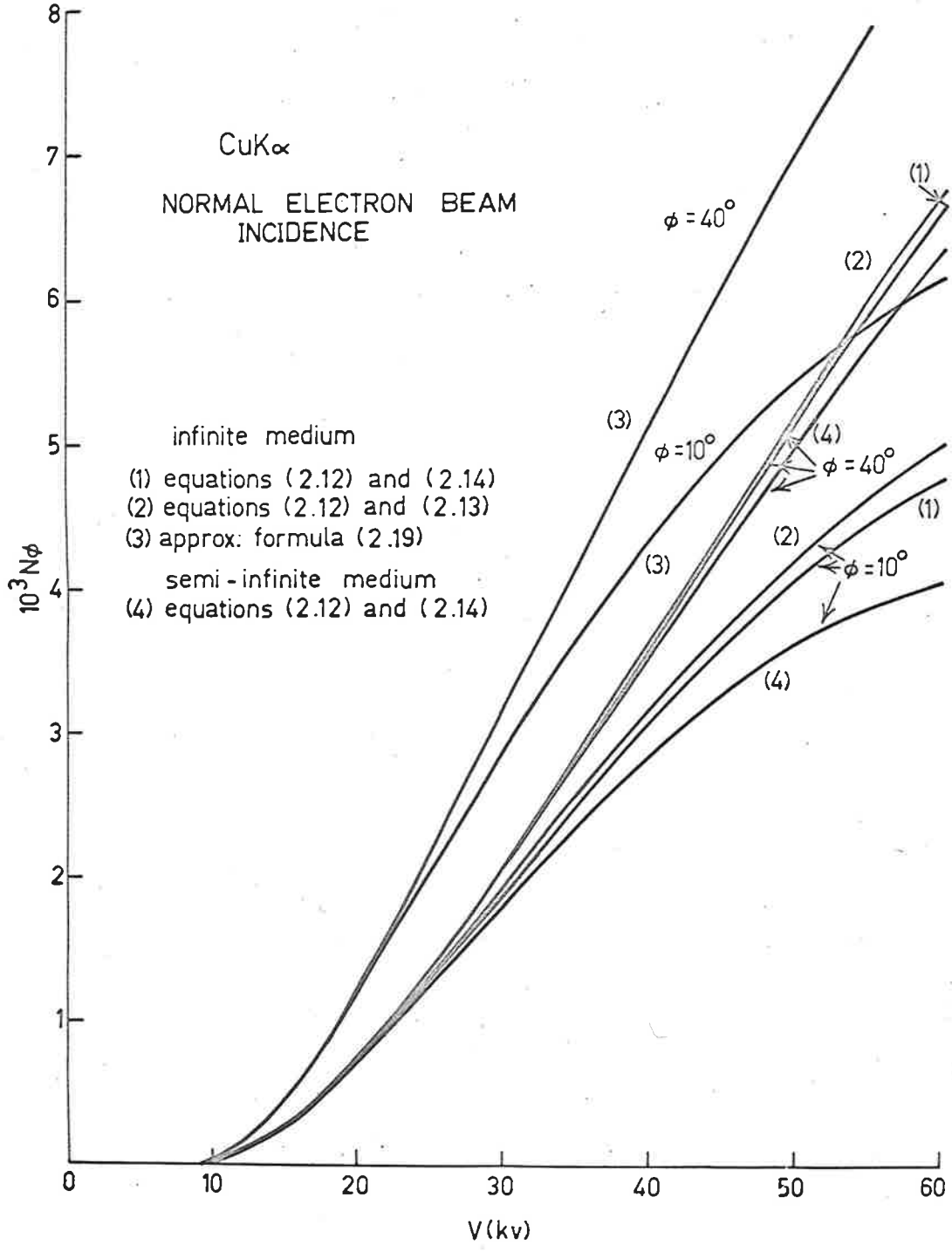

Figure 2.14 Theoretical results for CuKα radiation intensities.

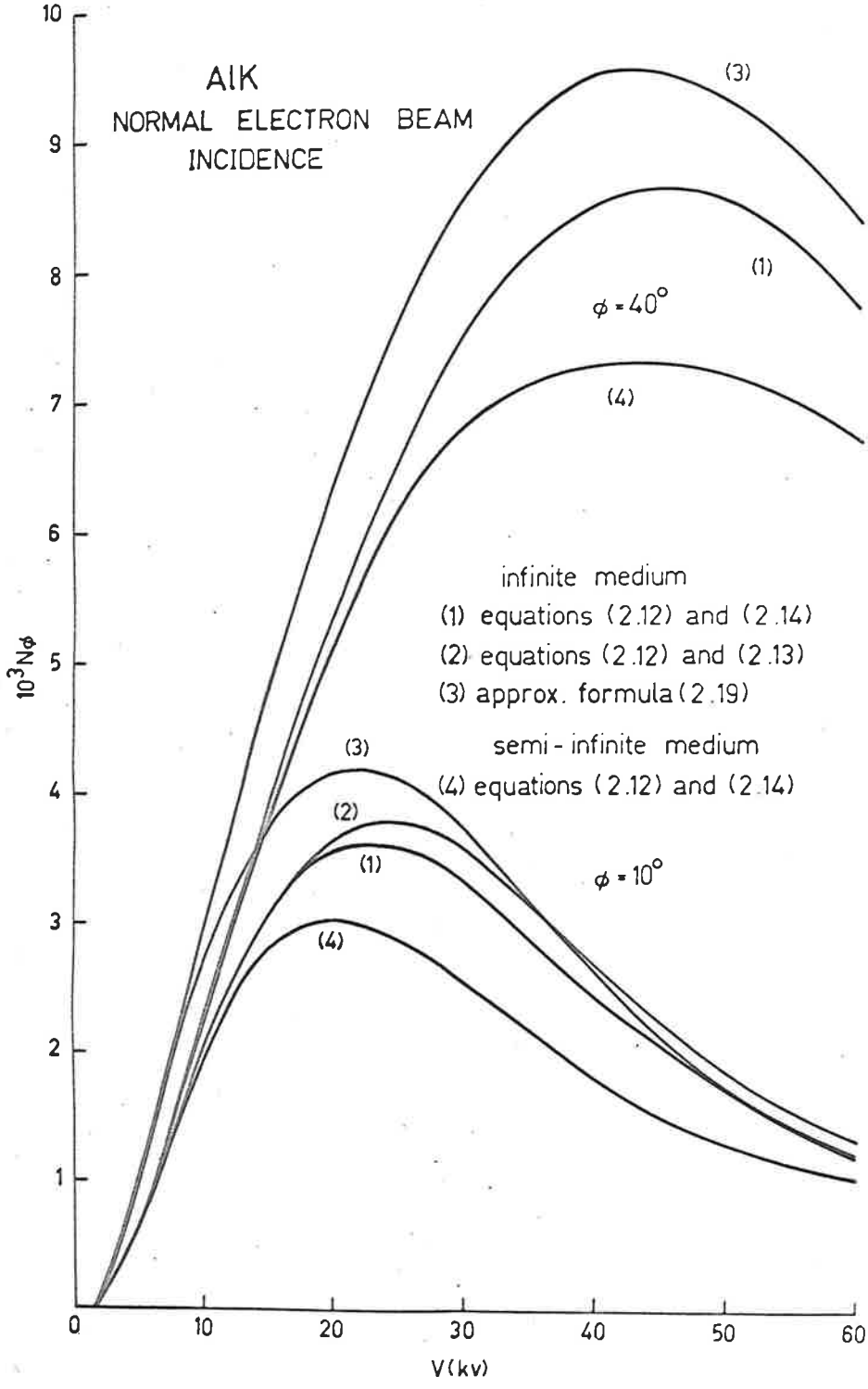

Figure 2.15 Theoretical results for AlK radiation intensities

tant. This is reflected in the intensity curves (figures (2.14) and (2.15)), which show that the difference between the corresponding curves is greater at the lower emergence angle.

For an infinite copper target, the curves obtained by evaluating the complete expression (2.13) for $\langle x \rangle$ have been included in figure (2.12) for comparison with the approximate expression. The figure shows that the approximation is a good one. For 40 keV and 60 keV electrons incident on an infinite copper target, figure (2.12) shows that the approximate curves obtained from equation (2.14) are about 10% higherthan the curves derived from the complete expression (2.13). The effect of this discrepancy on the intensity function is negligible. This is shown in figures (2.14) and (2.15) which include curves for N_ϕ using the full expression (2.13) for $\langle x \rangle$.

2.8 A Simple Intensity Formula.

Without the assistance of a digital computer, the evaluation of the intensity formula (2.12), even using the simpler expression (2.14) for $\langle x \rangle$ is a time consuming process. The derivation of a much simpler expression, which can be evaluated readily with a desk calculation is set out below. Starting with the basic formula,

$$N_\phi = kN \int_{T_o}^{T_K} Q_K \; e^{-\mu_T \rho \langle x \rangle \operatorname{cosec} \phi \cos \Theta} \frac{ds}{dT} \, dT$$

and using equations (2.1) and (2.2) for Q_K

$$Q_K \frac{ds}{dT} = -\frac{b}{NZT_K} \frac{\ln \frac{4T}{B}}{\ln \frac{2T}{J}}$$

$$= -\frac{b}{NZT_K} \left(1 + \frac{\ln \frac{2J}{B}}{\ln \frac{2T}{J}} \right) \quad \ldots \quad (2.17)$$

For $T \gg J$

$\ln \frac{2T}{J}$ varies very slowly with T

assume $Q_K \frac{ds}{dT}$ = constant and is equal to its value at $T = T_\bullet$.

From (2.14), for an infinite medium,

let a = 1

$$\langle x \rangle = \frac{8}{Z + 9} R_B \left(1 - \exp \left(- \left(\frac{Z + 9}{4} \right) \frac{\delta}{T_\bullet} \right) \right)$$

where R_B = Bethe range and is given by the equation (2.15)

$$x_d = \frac{8R_B}{Z + 9}$$

$$\delta = T_\bullet - T$$

Let $A = \mu \rho \operatorname{cosec} \phi \cos \theta$. x_d

$$N_\phi = \frac{kb}{ZT_K} \left(1 - \frac{\ln B_\diagup 2J}{\ln 2T_\diagup J} \right) e^{-A} X$$

$$\int_{T_K}^{T_\bullet} e^{-A \exp \left(- \frac{Z + 9}{4} \left(1 - \frac{T}{T_\bullet} \right) \right)} dT$$

now $$e^x = \sum_{n=0}^{\infty} \frac{x^n}{n!}$$

The integral may be written as

$$I = \int_{T_K}^{T_o} \left(1 + Ae^{-\frac{Z+9}{4}\left(1 - T/T_o\right)} + \frac{A^2}{2!} e^{-\frac{2(Z+9)}{4}\left(1 - T/T_o\right)} + \ldots + \frac{A^n}{n!} e^{\frac{n(Z+9)}{4}\left(1 - T/T_o\right)} + \ldots \right) dT$$

$$= (T_o - T_K) + \sum_{n=1}^{\infty} \frac{A^n}{n!} \int_{T_K}^{T_o} e^{\frac{-n(Z+9)(T_o - T)}{4T_o}} dT$$

changing the variable to z

where $$z = \frac{n(Z+9)}{4}\left(\frac{T_o - T}{T_o}\right)$$

or $$T/T_o = 1 - \frac{4z}{n(Z+9)}$$

$$dT = \frac{-4T_o}{n(Z+9)}\, dz$$

$$I = (T_o - T_K) + \sum_{n=1}^{\infty} \frac{A^n}{n!} \int_{\frac{n(Z+9)(T_o - T_K)}{4T_o}}^{0} -e^{-z} \frac{4T_o}{n(Z+9)}\, dz$$

$$= (T_o - T_K) + \frac{4T_o}{(Z+9)} \sum_{n=1}^{\infty} \frac{A^n}{n!n} \int_{0}^{\frac{n(Z+9)(T_o - T_K)}{4T_o}} e^{-z}\, dz$$

$$= (T_o - T_K) + \frac{4T_o}{(Z + 9)} \sum_{n=1}^{\infty} \frac{A^n}{n!n} \left(1 - \exp\left(-\frac{(Z + 9)(T_o - T_K)}{4T_o}\right)\right) \quad \ldots (2.18)$$

$$N_\phi = \frac{k\,b}{ZT_K} \left(1 - \frac{\ln B_o/2J}{\ln 2T_o/J}\right) e^{-A}\, I \quad \ldots (2.19)$$

If $T_K \ll T_o$ and $Z \geq 4$, equation (2.18) may be simplified further

$$I = (T_o - T_K) + \frac{4T_o}{(Z + 9)} \sum_{n=1}^{\infty} \frac{A^n}{n!n} \quad \ldots (2.20)$$

The results calculated from the approximate expression (2.19) are shown in figures (2.14) and (2.15). These curves are denoted as (3) in the figures. There is generally a better agreement between the approximate formula and the full expression (2.12) for the AlK radiation than for the harder CuK_α radiations and the agreement between the two formulae improves with increasing electron energy for both cases. For the AlK radiation intensities, the discrepancy between the curves (3) and (2) is negligible for incident electron energies exceeding 25 keV, whereas for the CuK_α intensities, the approximate results exceed the full calculations by about 40% even at 50 keV electron energy. The reason for this is apparent in figures (2.16) and (2.17) in which the magnitude of the produce $Q_K \frac{ds}{dT}$ is shown as a function of the electron energy for copper and aluminium respectively. The basic assumption in the derivation of the

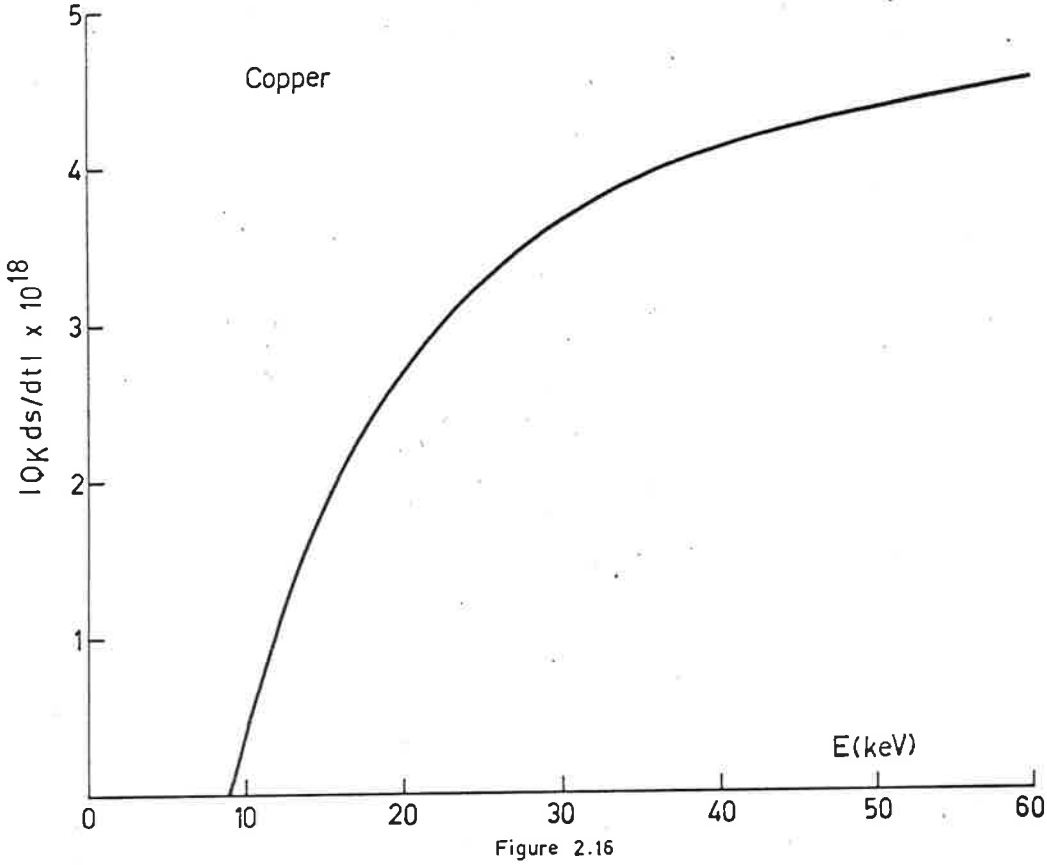

Figure 2.16

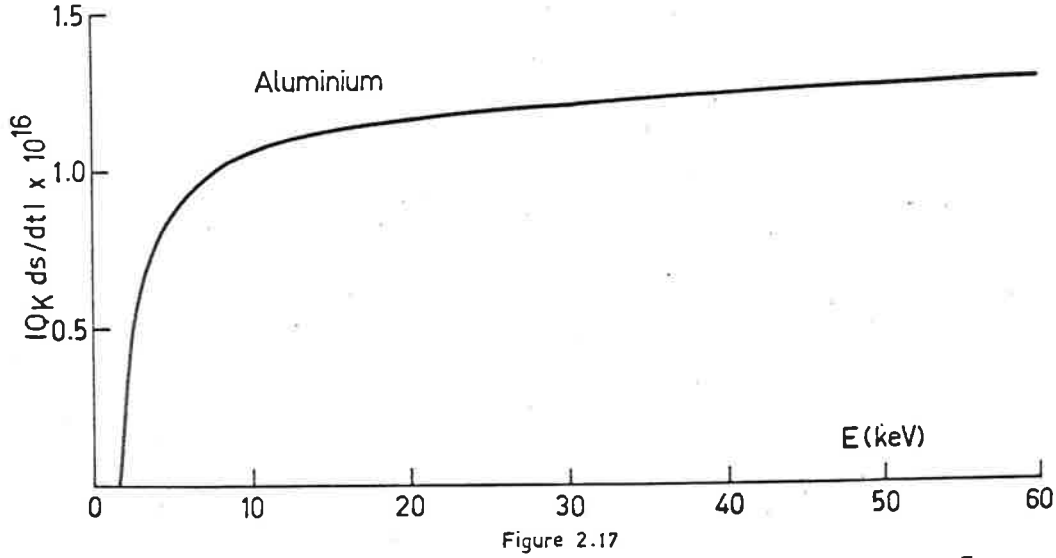

Figure 2.17

Variation of the magnitude of the product $Q_K \, ds/dt$ with the electron energy E.

approximate formula (2.19) is that $Q_K \frac{ds}{dT}$ is constant and is equal to its value at T_o. For aluminium, figure (2.17) shows that this assumption is sound except at low electron energies, where the product $Q_K \frac{ds}{dT}$ varies rapidly with the electron energy. For copper, the $Q_K \frac{ds}{dT}$ curve is still increasing with energy even at 60 keV electron energy. It appears that the approximate formula (2.19) is valid from an incident electron energy of about 10 T_K onwards. Within an electron energy range up to 60 keV, the approximation is a very good one for soft radiations.

CHAPTER III

DESCRIPTION OF APPARATUS.

3. The Gas Flow Proportion Counters.

3.1 Introduction.

The wavelengths of characteristic radiations investigated in this project varied from 1.54Å (CuK_α) to 44Å (CK). Isolation of the characteristic lines of interest by means of balanced differential filters or the crystal monochromator is impractical except for the shortest wavelengths in the above region. The proportional counter is the most suitable detector for the above radiations. It has a reasonable resolving power as well as a sufficient internal amplification so that the additional amplification needed to produce sufficient output pulse sizes for soft incident radiations is not excessive. In order to achieve a suitable transmission for soft radiations, an ultra thin window, which was semi-porous, had to be used. This required a continuous flow of the counter gas mixture to flush out any impurities which might impair the counting characteristics.

For precise measurements, special considerations have to be paid to the construction of the proportional counter. Common window arrangements are the end window and the side window geometries. Although the end window tubes with their long absorption path are best suited for hard radiation measurements, distortions due to end effects introduce zones of ineffectual counting action, as the output

pulse sizes are sensitive to changes in the field intensity. It is necessary to confine the multiplication processes to regions of distortion free fields, otherwise a deterioration of the energy resolution of the counter results. This is particularly serious in its application as a spectrometer. This may be avoided with a side window entry and a collimated incident radiation beam, as the avalanche formation processes in the proportional counting action are localized (Fulbright, 1958). A minimum ratio of four is recommended for the counter length to its diameter to reduce end effects (Dowling et al, 1956; Lang, 1956). Cockroft and Curran (1951) reported the use of field tubes to minimize field distortions near the end supports in instances where long detectors prove unwieldy. Tests on the present counters indicated that their resolutions were comparable to those fitted with field tubes. To prevent fluorescent excitations in the chamber walls, which could result in spurious pulses, a thin exit window was placed diametrically opposite the entry window to permit any unabsorbed incident radiations to pass.

Two gas flow counters of the side window type and with different physical dimensions were constructed and tested. They provided mutual checks for each other's measurements and will be referred to as Counters A and B.

Owing to a lack of a suitable soft monochromatic radiation source, investigations of the characteristics of the counters were confined to incident monochromatic radiations of moderate energies.

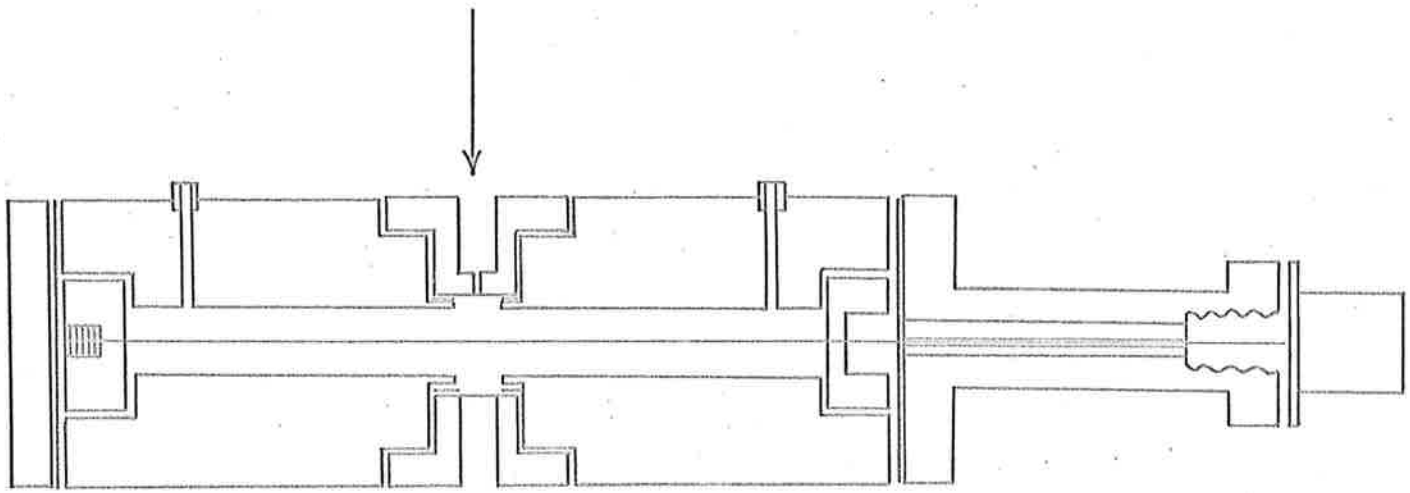

Figure 3.1 Gas flow proportional counter A.

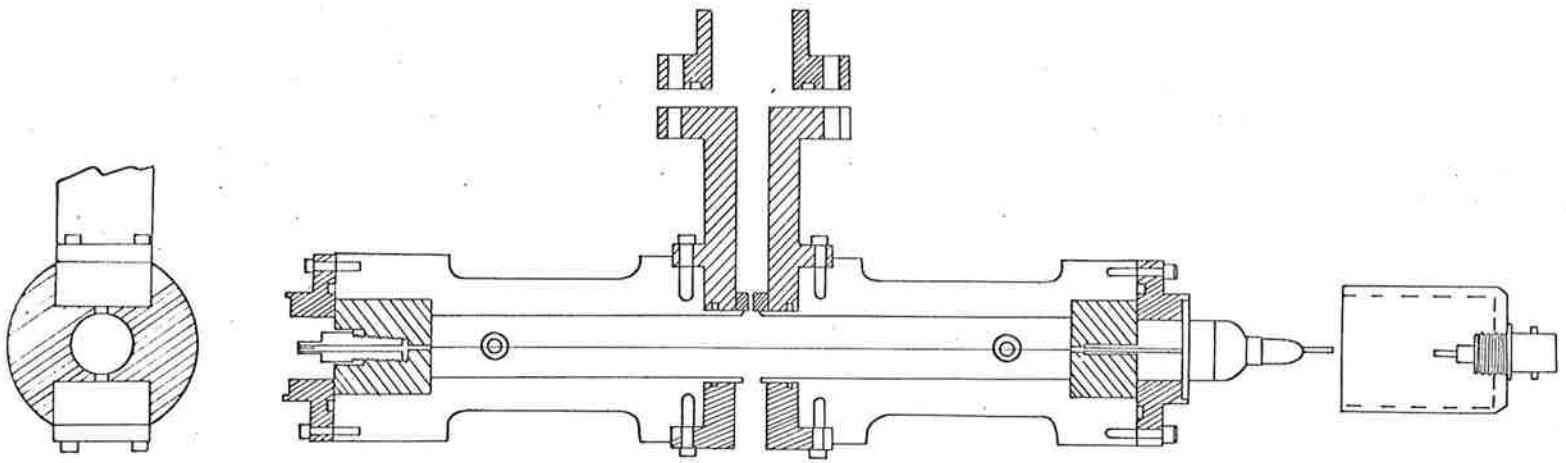

Figure 3.2 Gas flow proportional counter B.

3.1.1 Construction Details.

Counter A (figure 3.1) had a cylindrical active volume 0.264" in diameter and 0.882" in length. The gas chamber was accurately drilled along the axis of a brass rod. To reduce field distortions in the active volume, the chamber walls were first reamed and then polished with a fine emery paper to produce the final dimensions. The walls were then finished with a metal polish and thoroughly cleaned with methanol. A 0.0005" diameter tungsten wire was centrally supported in the chamber by means of capillary holes drilled in the PVC (polyvinyl chloride) end spacers. A suitable tension was maintained in the anode wire by means of a screw set in one of the spacers. External electrical connection was made via a coaxial socket attached to a Kovar seal. Before assembly, the anode wire was allowed to glow in vacuum to remove microscopic specks of dust and any sharp projections along the wire, as these would result in localized regions of high field. Seals were achieved with rubber washers. Fine machine-finished grooves were left on the end surfaces of the centralizing bushes to increase their surface resistivity. To test the system for leakage currents across the PVC spacers, a potential in excess of its normal operating value was applied to the central wire. No leakage was observed.

The constructional details of counter B (figure 3.2) were basically similar to counter A. Certain improvements were included. The body was constructed of copper as brass sometimes has a tendency

to adsorb gases to its surface due to porosity. The anode consists of a 0.002" diameter platinum wire, as platinum may be heated in air. An annealed mu-metal sleeve was fitted over the counter body to protect the active volume from external magnetic interference. Rubber O-rings were used instead of rubber washers for seals. The copper chamber was gently heated to enable a uniform oxide film to form on its surface. This ensured stability on its counting characteristics with time. The centralizing bushes for the anode wire were machined from PTFE (polytetrafluoroethylene). Counter B had a cylindrical active volume of $\frac{1}{2}$" in diameter and 5" in length. This gave a length to diameter ratio of 10, which is in excess of the minimum ratio recommended. Before the final assembly, the components of both counters were rinsed with pure methanol and examined for the deposition of extraneous matter. Examination of the counter wire near the entry window was carried out before each series of measurements.

Counter A was mounted inside the vacuum chamber. By means of a system of pulleys and a rotary vacuum seal, the angle of emission ϕ may be varied.

By means of vacuum screw unions, the larger counter B was attached externally to the circular vacuum chamber containing the target assembly at one of a number of fixed ports spaced around the chamber to enable a variation of ϕ to be made. The ports all lay in the plane containing the center of the target and normal to the target surface.

In both cases, the length of the absorption path in the gas for the incident radiations was independent of ϕ, as the radiation beam was normal to the axis of the counter at all times. This ensured that the detector had a constant quantum counting efficiency for radiations of a given wavelength irrespective of the angle of emission. In both arrangements, absorption losses were minimized, as the incident radiations encountered only the counter window in its path to the detector. To measure the attenuation of the counter window, a duplicate window was supported on a disc attached to a movable rod, such that the duplicate window foil could be lowered into the path of the incident radiations while the chamber was still under vacuum.

Spurious radiations could result from the incidence of backscattered electrons on the counter window. These electrons were deflected from the window by means of a transverse magnetic field. It was found that a magnetic field of 700 oersted was sufficient for this purpose. Small permanent magnets were used. The primary electron beam was shielded from the effects of the magnets.

3.1.2 The Gas Mixture.

The choice of the gas filling is dictated by considerations associated with the efficient operation of the counters. It is important that a majority of the incident photons be absorbed in

the gas. For soft radiations, this requirement poses no problem. The inert gases are commonly used because of their chemical stability. An important factor governing the choice of the gas filling is the occurrence of the "escape peak" phenomenon in the pulse distribution curve (section 3.4). As this phenomenon reduces the effective resolving power of the detector, it is desirable that the excitation energies of the gas filling for fluorescent radiations should be higher than the energy of the incident radiations, or failing this, the fluorescence yields of the gas filling should be low. Argon was chosen because it was readily available and its ω_K values were lower than those of the heavier inert gases. Its critical K absorption edge, 3.2 keV, is higher than the energies of the characteristic lines of interest in this project, excepting those of CuK, TiK, and CrK radiations. Although there is a probability for the excitation of the argon L lines, the combination of the low L fluorescence yields and the high absorption of these soft radiations by the argon gas is probably sufficient to prevent any significant number of L quanta escaping from the active counting volume. The experimental pulse distribution curves did not reveal any escape peak corresponding to the argon L radiations. Its effect was assumed to be negligible.

An effect which could lead to the reduction of output pulse sizes and distortion of the pulse distribution curve is that of electron attachment. The presence of impurities, even in small

quantities, such as water vapour and oxygen, which have high affinities for electrons, will prevent the efficient collection of the electrons originated in the multiplication processes. Wilson et al (1950) recommended an addition of a small percentage of CO_2 to the gas filling to suppress the negative ion formation. The action of the CO_2 is to reduce the mean energy of the electrons through inelastic collisions and hence, the mean free path of the electrons in argon is increased. The use of a mixture of gases also assists in the de-excitation of meta-stable atoms which could give rise to spurious pulses (Fulbright, 1958).

The counters were filled with 3% CO_2 in argon. Both gases were of high purity and were supplied ready mixed.

3.1.3 The Gas Flow System.

The gas mixture was dried over phosphorus pentoxide and the gas flow rate was regulated by a flow-meter. A mercury manometer attached to the system measured the counter pressure. Figure (3.3) shows the arrangement. Before each experiment, the whole system was outgassed for half an hour by evacuation. It was then thoroughly flushed with the gas mixture before use.

It is desirable that the characteristics of the proportional counters should remain independent of small variations of the flow rate. As the gain and the quantum counting efficiency of the

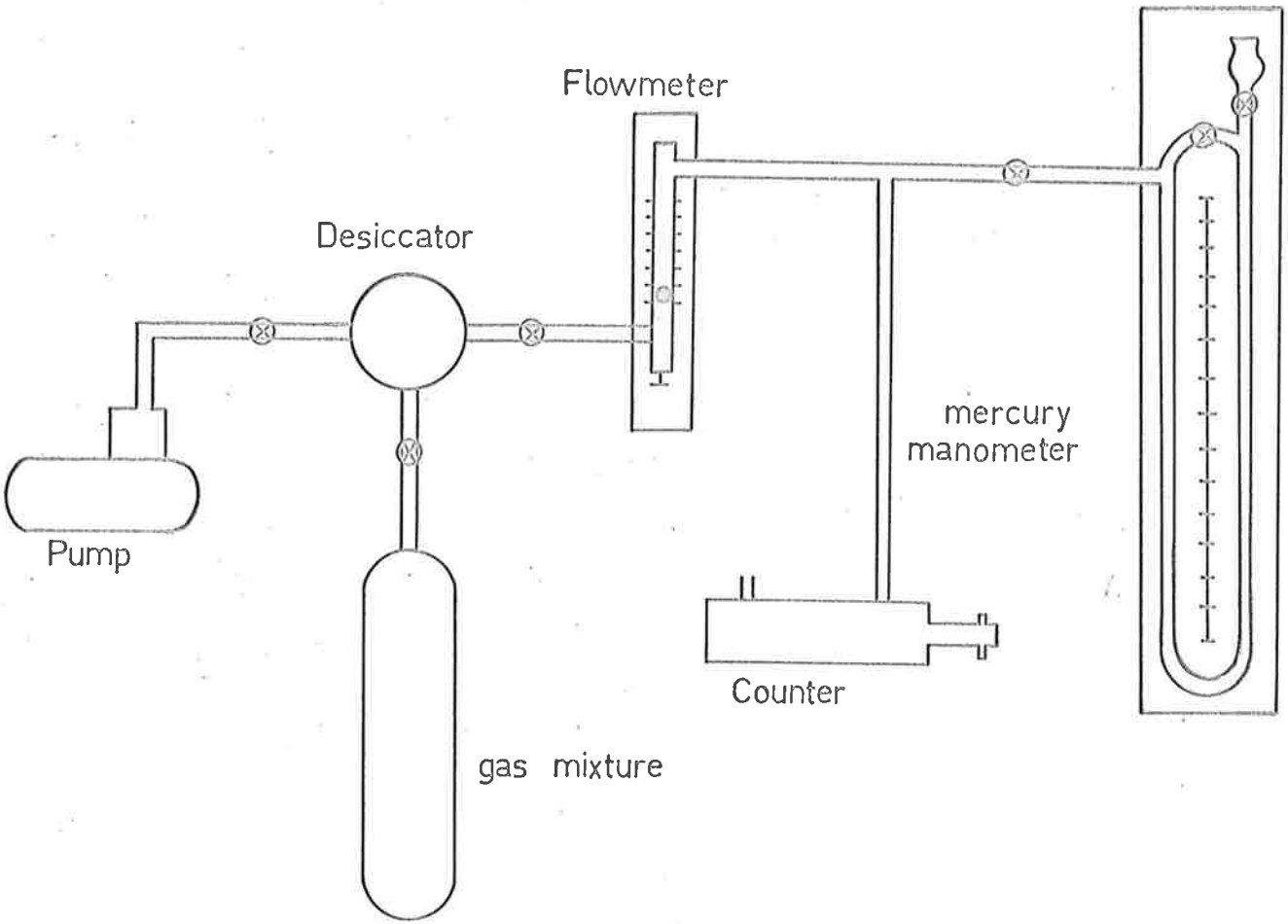

Figure 3.3 Schematic diagram of the gas flow system.

counter are both dependent on the gas pressure, it is necessary to keep the pressure constant and independent of the flow rate. If the inlet and the outlet gas ports are too narrow, the counter gas pressure would be sensitive to changes in the flow rate. It was found that inlet and outlet ports of 0.08" diameter were sufficiently large for the counter pressure to remain at atmospheric pressure for flow rates up to 4 c.ft/hr. Over this range, no change in either the mean position of the pulse height distribution curve or the counting rate was detected. With the gas flow shut-off and the counter sealed off from the atmosphere, the characteristics of both counters were found to be the same as those obtained with a slow continuous gas flow through the system, indicating that the mylar window used was sufficiently non-porous to prevent contamination of the counter atmosphere. During the actual intensity measurements, a gas flow of 1 to 1.5 c.ft/hr was maintained as a precaution against outgassing of the counter walls. The gas flow was essential for ultra-soft radiation measurements where a semi-porous parlodion window was used.

As the gas flow counter was open to the atmosphere, the counter pressure was susceptible to changes in the atmospheric pressure. The mean position of the pulse height distribution was found to decrease slightly with an increase in atmospheric pressure. This did not affect the intensity measurements however, as prior to each measurement, a differential curve of the incident radiations was traced on a pen recorder to locate the position of the characteristic

peak. To check the variations in the counting rate with changes in the atmospheric pressure, the window of the discriminator was first adjusted to a sufficient width to accommodate any variations in the mean position of the pulse distribution curve. The counter pressure was increased by restricting the gas flow to simulate the variations in the atmospheric pressure. It was found that within the range of pressure variations encountered in the atmosphere (approximately 750 - 770 mm Hg), there was no change in the counting rate.

3.1.4 The Counter Windows.

It was found that a counter window made of mylar, nominally 0.00025" thick and aluminized on one side, was sufficiently transparent to radiations of wavelengths up to that of AlK (8.3Å), for which the measured transmission ratio was 0.42. The mylar was placed in a recess in the counter with its aluminized side facing the inside of the counter. The window block with a rubber O-ring pressed on the mylar. In counter A, a pinhole 0.68 mm in diameter was drilled in the brass window block. In counter B, a 0.84 mm hole was drilled in a lead plug set in the window block. Measurements of the window diameters were made along several directions with a travelling microscope and the mean value taken. The solid angles subtended at the center of the target by the windows of A and B were 2.86×10^{-5} and 1.89×10^{-5} ster-radians respectively.

For radiations of wavelengths longer than AlK, a thin film of parlodion (cellulose nitrate) was used for the counter windows. Only counter B was used for these ultra-soft radiation measurements. As the counter was attached directly to the radiation source, a suitable counter window had to be thin enough to transmit a major fraction of the incident beam of the softest radiation (CK), and at the same time, be sufficiently thick to enable it to withstand atmospheric pressure, and sufficiently non-porous that an adequate vacuum could be maintained in the chamber. It was found that the window made by dissolving 2% parlodion in amyl acetate satisfied the above requirements. A clean glass slide was dipped in the solution and slowly withdrawn from it. It was held vertically and allowed to dry. Corresponding sections of film on the front and the back of the slide were scribed with a needle and floated off by immersing the glass slide in distilled water, the surface of which was kept clean. One section was deposited over the counter window. On drying, the film formed a vacuum tight adhesion to the window block, which had 6 pinholes of average diameter 3.44×10^{-2} cm. The total solid angle subtended at the target was 1.89×10^{-5} ster-radians. The parlodion window was found to last for several days. The other section, which was deposited on a brass washer was used to find the transmission ratio of the window film, assuming that both sections had the same thickness. Owing to the way in which the films were made, the film thickness along the length of the slide was not uniform. However

small corresponding sections on the front and back of the film should have the same thickness. The samples chosen were from sections from which the diffracted light had a similarity in colour. As a check, the transmission ratio of a number of corresponding pairs of films were measured. Good agreement in thicknesses was found.

Since the counter window was subjected to a pressure difference of one atmosphere, there was a bowing effect in the window. The effect appeared to a less extent in the mylar window. The duplicate film, on which the measurement for the transmission ratio was made, did not experience this. This effect could overestimate the measured intensities. Owing to the high transmission of the parlodion window for the ultra soft radiations (a typical film had a transmission ratio of 0.85 for CK radiations), the resultant error in the intensity measurements due to the above effect was not serious.

3.2 Ancillary Electronic Apparatus.

The output pulses from the detector were shaped and amplified by an EKCO N568B linear amplifier, whose total voltage gain was 10^6. It was found that the magnitude of the output pulses was increased by reducing the effective input capacity. This was done by shortening the coaxial cable connecting the detector to the preamplifier. The amplified pulses were then fed into an EKCO N600 unit consisting of a single channel pulse height analyzer and a ratemeter. The output

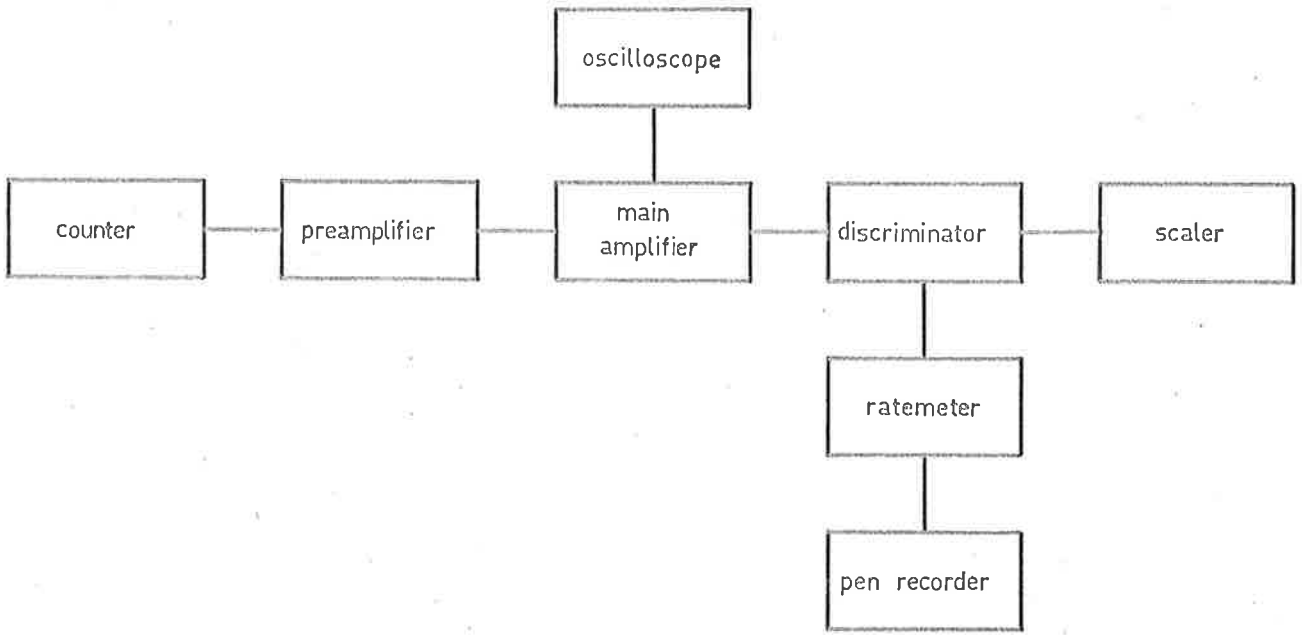

Figure 3.4 Schematic block diagram for measuring radiation intensities.

pulses from the amplifier were also displayed visually on an oscilloscope screen. Pulses of magnitudes defined by the analyzer settings were then recorded by an EKCO N530D scaler unit. The anode wire of the detector was polarized by an EKCO N570B power unit, whose output voltage was highly stabilized. There was a facility on the analyzer unit to analyze the energy distribution of the incident radiations. An automatic scanning device enabled a narrow discriminator window of fixed width to traverse the pulse height range of the input pulses. The frequency of the input pulses as a function of the pulse height was then recorded with a pen recorder. Figure (3.4) is a schematic diagram of the arrangement.

3.3 The Monochromatic Radiation Sources for the Calibration of the Detectors.

In the following investigations on the proper functioning of the gas flow proportion counters, monochromatic radiations were used. The heterogeneous radiations from a Hilger Microfocus Tube with copper or chromium targets were monochromatized with a double crystal monochromator. The radiation path from the source to the detector was suitably collimated. Lead shielding was used to prevent the detection of any spurious fluorescent radiations produced in the surroundings. It was found that if the X-ray source was switched on

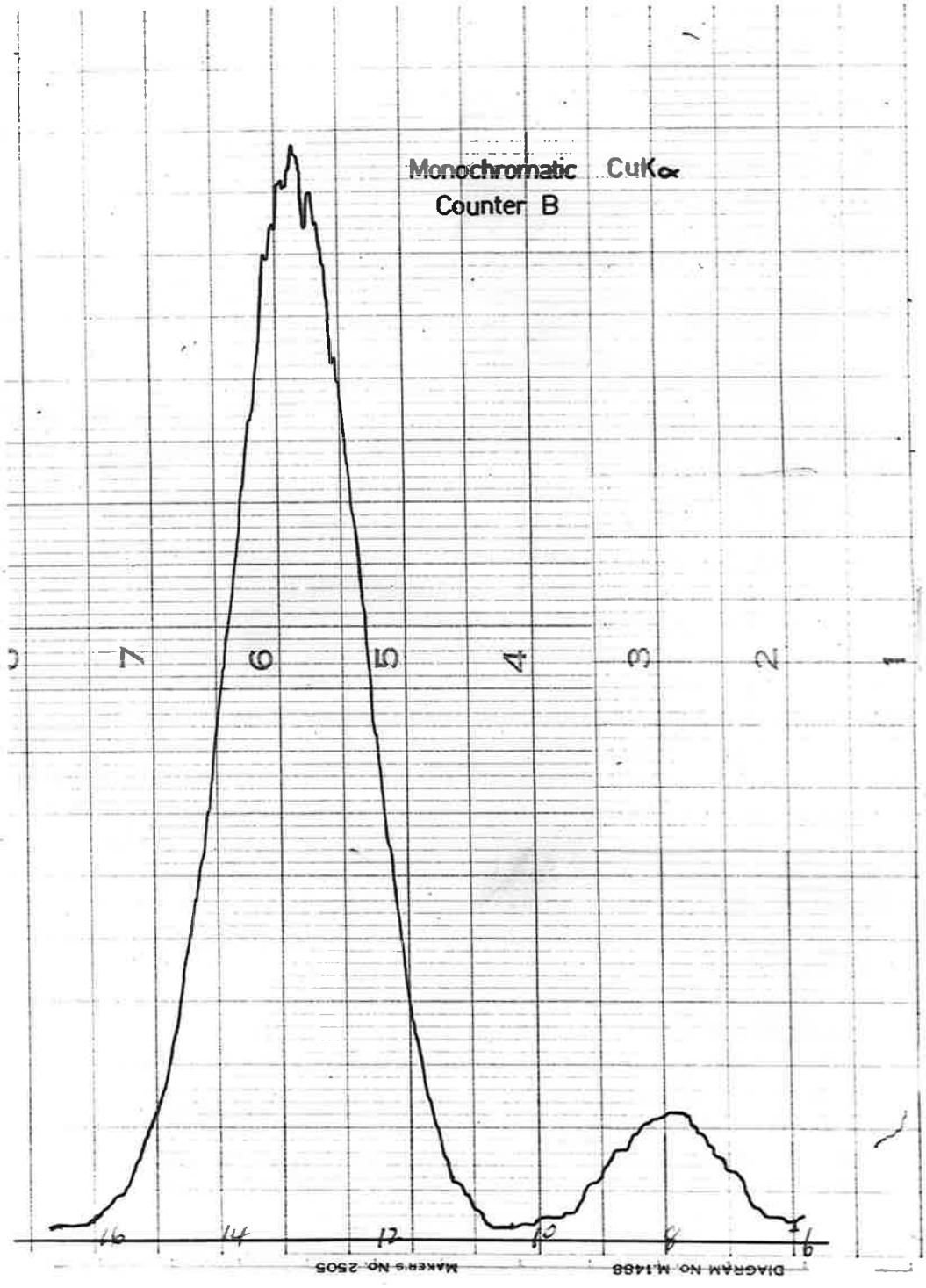

Figure 3.5 Pulse height distribution from monochromatic CuK_{α} radiations.

for half an hour before measurements were taken, the emitted intensity remained fairly constant. The maximum deviation from the mean of a number of readings was about 2%.

To test the purity of the monochromatic beam, a differential curve was traced. Figure (3.5) shows a typical recorder trace of the CuK_{α} radiations. The curve indicates a negligible background. With the discriminator window set to receive the incident monochromatic radiations only, a measurement was made. This measurement was compared with that obtained when the discriminator window was opened wide to receive incident radiations of all energies. No significant difference was detected.

3.4 The Escape Peak.

If the energy, E_o, of the incident monochromatic radiations exceeds the excitation energy of one of the characteristic lines of the counter gas, fluorescent radiations are produced. Some of the fluorescent quanta may not be absorbed by the counter gas and escape from the active counting volume. These will not contribute to the pulse formation processes in the gas, resulting in output pulses of reduced amplitude. Hence corresponding to every critical absorption edge in the gas filling, there is a possibility of an escape peak appearing in the differential curve of the incident monochromatic radiations.

Its energy E_{ep} is given by

$$E_{ep} = E_o - E_N \qquad \ldots \quad (3.1)$$

where E_N is the energy of the fluorescent quanta.

The relative size of the escape peak to the primary peak is dependent on the value of the corresponding fluorescence yield and the absorption efficiency of the gas filling for the fluorescent radiations concerned (Lang, 1956). With the argon gas filling, whose critical K absorption edge was 3.2 keV, an escape peak appeared when monochromatic CuK_α or CrK_α radiations were incident on the counter (figure 3.5). From equation (3.1), the position of the escape peak in the differential curves indicates that it was formed as a result of the escape of fluorescent AK radiations from the active counter volume. Theoretically, two peaks corresponding to the AK_α and AK_β component of the fluorescent radiations should have appeared. But the limited resolution of the detector did not permit their separation. No secondary peak corresponding to the escape of AL radiations was detected. This was probably due to the low value of ω_L for argon and the high absorption of the gas filling for the soft AL lines. Burhop (1952) and Fink et al (1966) indicated that the values of ω_L were more than an order of magnitude less than the corresponding ω_K values.

Of the characteristic radiations investigated in this project, those whose energy exceeded the critical K absorption edge

of argon were CuK_α, CrK_α, and TiK_α radiations. Under the actual conditions in the absolute intensity measurements of these radiations, the incident radiations were heterogeneous. It was very difficult to estimate the relative size of the escape peak, owing to its small size and the high bremmstrahlung background at low energies. It was first necessary to determine the relative number of characteristic photons, which appeared under the escape peak for a monochromatic beam.

Differential curves were traced for incident CuK_α, CuK_β, and CrK_α radiations. Different values of the counter potential V_c and attenuation setting A_T (decibels) of the linear amplifier were used for each radiation to investigate their effect on the relative size of the escape peak. The area of the escape peak, A_2, was compared with that of the primary peak, A_1, for each differential curve. Some of the results are summarized in Table (3.1).

Counter	Radiation	(Å)	V_c	A_T	A_2/A_1
A	CuK_α	1.54	900	14	0.124
A	CuK_α	1.54	1050	32	0.123
A	CuK_β	1.39	1050	32	0.124
A	CrK_α	2.29	900	8	0.121
B	CuK_α	1.54	1350	16	0.094
B	CuK_α	1.54	1300	12	0.093

TABLE (3.1)

Table (3.1) indicates that the ratio A_2/A_1 depends on the geometry of the detector and appears to depend only slightly on the wavelength of the incident radiations within the range from 1.39Å to 2.29Å. The latter was probably due to the fact that the majority of the fluorescent radiations which escaped absorption were excited very close to the boundary of the active counter volume, and over the small absorption path between the point of excitation and the boundary, the dependence of the fraction absorbed on the wavelength of the fluorescent radiations was slight.

As a monochromatic beam of TiK radiations was not available, an estimate was made of the relative size of the escape peak for the TiK radiations. Values of 0.12 and 0.09 were used for counters A and B respectively. The slow variation of the values for A_2/A_1 for radiations of wavelength close to the wavelength of TiK (2.74Å) indicates that the estimates were quite reasonable.

3.5 The Linearity of the Detectors.

For accurate absolute intensity measurements, it is imperative that the response of the detector to the incident radiation intensities be linear. Following the entry of the incident photons into the counter, there is a localized conglomeration of positive and negative charges originated from the multiplication processes near the anode wire in the vicinity of the window. Owing to their higher

mobility, electrons in the charged cloud are rapidly collected leaving behind a positive ion sheath surrounding the anode, which lowers the electric field intensity in this region. This has the effect of either terminating the multiplication processes completely or causing a reduction in the output pulse size. A period of ineffectual pulse forming action follows until the positive ion sheath has drifted sufficiently far from the anode wire. If the incident radiation intensity is excessively high, photons may enter the detector during this period, resulting in non-linearity in the counter response.

The experimental technique of Lonsdale (1948) and Alexander et al (1949) was used to determine the resolving time, τ, of the gas flow proportional counters. It is the minimum time interval required between the incidence of successive photons to ensure a proper linear response in a detector. A progressively increasing number of nickel foils of identical thickness was inserted in the path of an incident beam of pure CuK_{α} radiations. The intensity was recorded before and after each addition of a foil. To reduce the effects of fluctuations in the source intensity and counting statistics, for each measurement, the total number of counts were recorded several times over an interval of 100 seconds and the average value was taken. In addition the counting rates were not reduced to unsuitably low values where counting statistical errors became important. To ensure a reasonable uniformity in the foil thickness, the foils were taken from the same

sheet and the thickness of each was measured at several places with a micrometer screw gauge. The results were not affected by the spectral dependence of the mass absorption coefficient of nickel for the radiations, as a pure monochromatic beam was used. To prevent the detection of spurious radiations, the window of the pulse height analyzer was set to receive CuK_α radiations only.

The transmission ratio, I/I_o, for n foils of uniform thickness x cm is given by

$$I/I_o = e^{-\mu\rho nx}$$

$$\log_e I = \log_e I_o - \mu\rho nx \qquad \ldots (3.2)$$

For a detector with a linear response and with a constant source intensity, a graphical plot of the detected intensity I against n, the number of foils, should result in a linear graph. The graphs are shown in figure (3.6) and indicate that non-linearity in the counter response does not become apparent until the respective counting rates exceed about 5×10^3 counts per second and 10^4 counts per second.

The relationship between the actual counting rate N_A and the observed counting rate N_o is

$$N_A = \frac{N_o}{1-N_o\tau} \qquad \ldots (3.3)$$

or

$$\tau = \frac{N_A - N_o}{N_A N_o} \qquad \ldots (3.4)$$

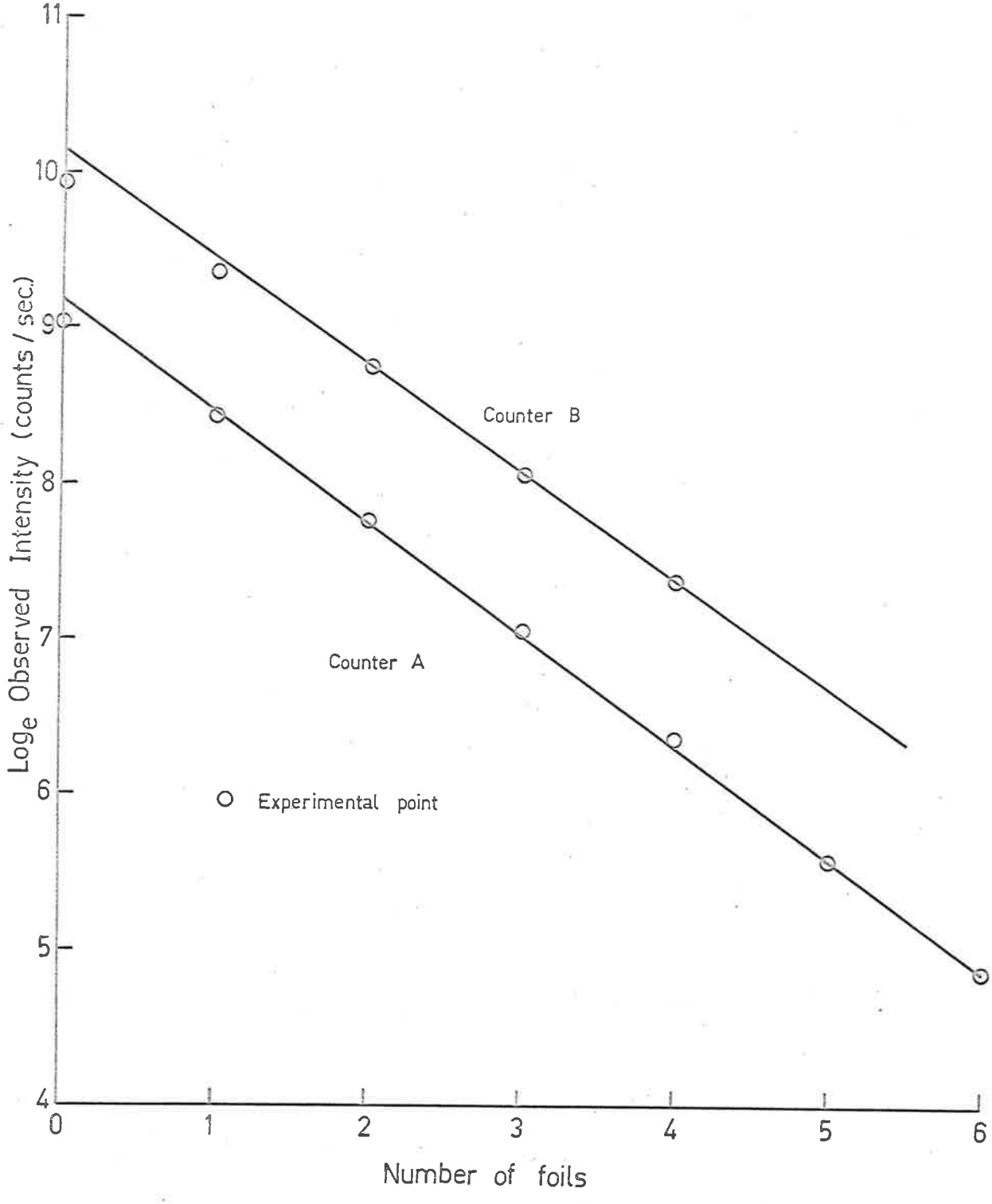

Figure 3.6 The multiple foil test for linearity.

Figure (3.6) indicates that at low incident radiation intensities, the observed values for $\log_e I$ vary linearly with n. Values for N_A at high counting rates, where non-linearity in the counter response occurs, were obtained by extrapolation of the linear section of the graphs. By reference to figure (3.6) and equation (3.4), the respective values of τ for counters A and B were found to be 10μ seconds and 5μ seconds. There was a slight dependence of τ on the counting rate at which τ was computed. This was attributed to the fact that there was a fluctuation in the radiation source intensity and that the thickness of the attenuating foils were not exactly identical. For measurements of excessively high radiation intensities, it is probably more accurate to estimate the actual intensity by a direct reference to figure (3.6) rather than by deriving N_A based on the computed value for τ.

Experimental investigations of the linearity in response to incident radiation intensities were carried out for the gas flow counters A and B according to the method of Short (1960). An advantage of this method was that only a single attenuating foil was required, hence the difficulty associated with the former technique in requiring a number of identical foils was avoided. This method involved the determination of the "apparent absorption factor", $e^{-\mu\rho x}$, for various values of the unattenuated radiation intensity, I_o. I_o was varied by adjusting the tube current of the radiation source. The apparent absorption factor was given by the measured

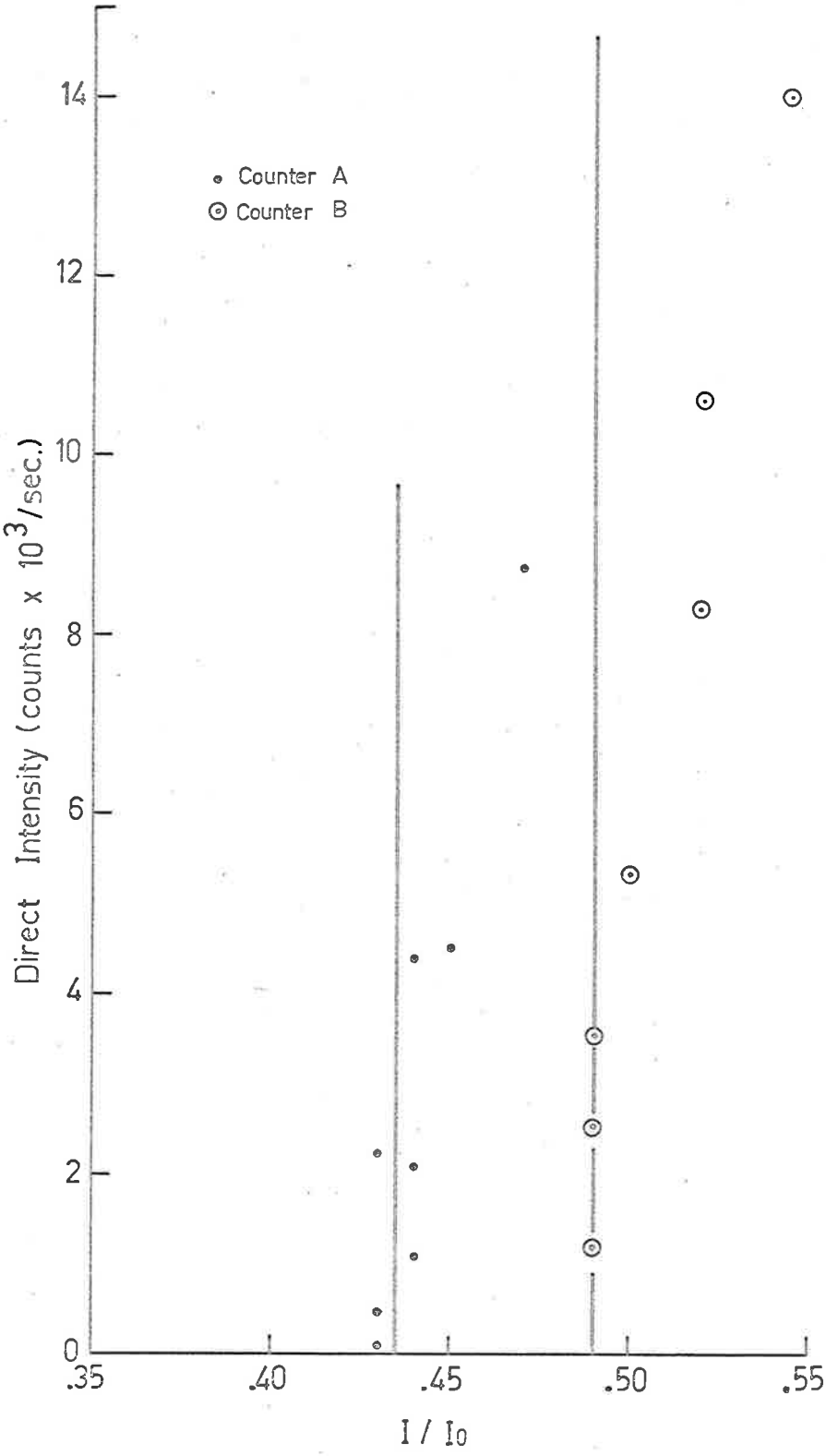

Figure 3.7 The single foil test for linearity.

transmission ratio of the foil. Within the range of intensities for which a detector has a linear response, a graphical plot of the observed unattenuated intensities against the apparent absorption factor should result in a vertical linear graph, any departure from which is an indication of non-linearity.

The nickel foil used in this experiment was checked with a micrometer screw gauge to ensure a uniformity in thickness over its extent. In order that any non-linearity in the counter response was readily detectable, a sufficiently thick foil was used to absorb a significant fraction of the incident intensity. Foils with transmission ratios of 0.435 and 0.49 for CuK_{α} radiations were used. This was to ensure that the counting losses connected with the detection of the unattenuated intensity were substantially greater than those connected with the detection of the attenuated intensity. Figure (3.7) indicates that the counters A and B were linear for counting rates up to 3000 counts/second and 3500 counts/second respectively. The upper limits of the range of linearity of the detectors A and B are lower than those determined with the less sensitive multiple foil method.

In the absolute intensity measurements, all the counting rates were within the linear range. No correction was required for counting losses due to non-linearity in the counter response.

3.6 Proportionality.

For an ideal proportional counter, the ratio of the output pulse amplitudes should be equal to the corresponding ratio of the incident photon energies. In practice, owing to statistical effects associated with the electron-ion multiplication processes in the counter, there is a distribution in the output pulse sizes corresponding to photons of a given energy. For low energy photons, this distribution is asymmetric (Snell, 1962). However, for incident photons of moderate energies, the pulse height distribution as represented by the differential curve approximates to a Gaussian curve (figure 3.5). For these radiations, the mean value of the pulse height distribution is given by the peak of the differential curve. The proportionality in the positions of these peaks for the gas flow counters A and B were examined.

For a valid comparison of the mean heights of the pulse height distributions for incident radiations of different energies, the same values of the polarizing anode potential and the external amplifications were used in recording the differential curve for each characteristic radiation. It was also found necessary for the differential curve to be traced under the same conditions of atmospheric pressure and the counting rate. An increase in atmospheric pressure reduced the mean height of the output pulse height distribution (section 3.1.3) and a reduction in the counting rate increased the mean height. The latter effect was only noticeable when the total

detected counting rate was well above 5000 counts per second, a limit which was not exceeded in the intensity measurements. The reduction in the mean value of the output pulse heights at high counting rates was probably due to the formation of a positive ion sheath around the anode wire (section 3.5). Burkhalter et al (1966) found that this effect was less in sealed proportional detectors. It is uncertain why this is so.

In tracing out the differential curves, the same values of the discriminator window width, the scanning speed and the ratemeter time constant were used. The output pulses from the ratemeter lagged behind the input pulses by approximately the time constant of the ratemeter (Parrish, 1956). This resulted in a slight shift of the peak of the differential curve towards the high energy side. This shift was reduced by a reduction of the ratemeter time constant but it was found that the "jitter" of the pen recorder trace increased, causing some difficulty in determining the position of the peak accurately. By having identical ratemeter and discriminator settings, it was hoped that any instrumental shift of the peak of the differential curve would have affected the differential curves for the monochromatic radiations used, CuK_{α} and CrK_{α}, equally. The discrepancy in the proportionality based on the comparison of the positions of the peaks of the differential curves for the above radiations was about 7%. This was attributed to the error involved in estimating the positions of the peaks and the long interval between the recording of the two

differential curves, during which time there was a variation in the atmospheric pressure. The time lapse between the two measurements was unavoidable as the anode of the radiation source had to be changed and this meant waiting for the diffusion pump to cool.

It was found more convenient to compare the relative positions of the main peak and the escape peak in the differential curve for a given monochromatic radiation. An advantage of this method was that only one differential curve was required. The time involved in recording this curve was relatively short, hence the two peaks were traced under identical atmospheric conditions. The equivalent energy of the escape peak, E_{ep} is given by

$$E_{ep} = E_o - E_N \qquad \text{(section 3.4)}$$

The values of E_{ep} for incident CuK_α and CrK_α radiations were 5.09 keV and 2.46 keV respectively. For a proportional counter, since

$\bar{P} \propto E$

$$\frac{\bar{P}_o}{E_o} = \frac{\bar{P}_{ep}}{E_{ep}} \qquad \ldots (3.5)$$

where $\bar{P}_o$ and $\bar{P}_{ep}$ are the positions of the pulse height of the primary peak and the escape peak respectively. The value of $\bar{P}_{ep}$ was first calculated from equation (3.5) for an ideal proportional counter. This was then compared with the measured value for $\bar{P}_{ep}$ for various values of the counter anode potential required for the absolute intensity

measurements. The total integrated detected counting rate for these measurements was up to 4000 counts per second, a value which was in excess of the counting rates encountered in the absolute intensity measurements of the characteristic radiations. The reason for this was to test the proportionality of the counters under the most unfavourable condition to be encountered in the actual measurements of characteristic radiations.

A summary of these results is tabulated in Table (3.2) and Table (3.3).

Counter A. Source: CuK_α

Counter pot (Volts)	Attenuation (dB)	$\bar{P}_o$	$\bar{P}_{ep}$ (measured)	$\bar{P}_{ep}$ (calc.)
750	0	16	10.3	10.1
800	6	13.4	8.6	8.5
850	12	11.7	7.6	7.4
900	14	17.1	11	10.8
1000	30	10	6.7	6.3
1050	32	16.3	10.5	10.3
1100	38	17.9	12.9	11.3

TABLE (3.2)

Counter B. Source: CuK_α

Counter Pot (Volts)	Attenuation dB	Peak differential counting rate (c/sec)	gas flow (c.ft/hr)	Resolution $W_{\frac{1}{2}}/\bar{P}\%$	$\bar{P}_o$	$\bar{P}_{ep}$ (measured)	$\bar{P}_{ep}$ (calculated)
1200	6	1000	$1\frac{1}{2}$	23.8	10.3	-	-
1250	6	1000	$1\frac{1}{2}$	21	16.7	10.5	10.3
1300	6	1000	$1\frac{1}{2}$	17.2	26.7	16.8	16.8
1300	12	1000	$1\frac{1}{2}$	16.7	12	7.6	7.4
1300	12	100	$1\frac{1}{2}$	17.7	12.8	8.1	8.0
1300	12	1000	2	17.3	12.7	8.0	7.8
1300	12	1000	1	18.5	12.8	8.1	7.8
1350	16	1000	1	17.3	12.8	8.1	7.8
1400	20	1000	1	16.5	13.0	8.2	8.0

TABLE (3.3)

The positions of the peaks of the primary and the escape peaks are in relative units and owing to the jitter of the differential curves the accuracy in the determination of the positions of the peaks was about 0.25 relative units. Within this experimental error, (Table 3.3) indicates that the counter was proportional over the ranges of the counter potential, gas flow rate, external amplification and differential counting rates used. Table (3.2) are the corresponding results for counter A. For A, which had an anode wire of smaller diameter than B, departures from proportionality began to show at a counter potential of 1100 volts.

3.7 Resolution.

The energy resolution, R, of a detector for a given radiation is commonly defined as $R = W/\bar{P}$, where W is the width of the differential curve at half height and $\bar{P}$ is the mean value of the output pulse sizes. For a Gaussian distribution of the form, $y = Ae^{-x^2/2\sigma_P^2}$, to which the shape of differential curves for hard and moderately hard radiations approximates (Hanna et al, 1949), the relationship between R and the relative standard deviation $\frac{\sigma_P}{P}$ is

$$R = 2.355\ \sigma_P/P \qquad \ldots \quad (3.6)$$

The variation of R with the external amplification, and with the counter anode potential, is included in Table (3.3) for a beam of

CuK_α radiations incident on the counter B. Table (3.4) shows the results for counter A.

Counter A. Source CuK_α

	Resolution (%)			
Counter pot (volts)	800	900	1000	1050
attenuation (dB)				
2	15	13.6		
8		14.5		
14		14.0	15.5	
18			15.0	
26			15.2	16.1
32				16
34				16.9

TABLE (3.4)

The tables indicate that the resolution is independent of the external amplification and for values of the anode potential within the range for which the detector is proportional, R, depends very little on the potential. It was found that for a given radiation, the resolution of the detectors deteriorated a little for values of the counter potential close to the lower limit of the proportionality range (Table 3.3) and for values of the anode potential close to the upper limit (Table 3.4).

Resolution, $\frac{W}{p}(\%)$

Counter Pot (V)			900			1000
atten	CrK_α	CuK_α	CuK_β	CrK_α	CuK_α	CuK_β
8	18	14.5				
14	17.3	14	13.4			
26				20.5	15.2	15

TABLE (3.5)

Table (3.5) shows the variation of R of counter A with the energy, E, of the incident radiations for various values of the counter potential and of the external amplification. The results indicate that $R \propto \frac{1}{\sqrt{E}}$, a proportionality which is consistent with the result of Mulvey and Campbell (1958), who derived theoretically that

$$\frac{\sigma_P}{P} = \frac{0.19}{\sqrt{E}} \qquad \ldots (3.7)$$

which represents the ultimate resolution of the proportion counter. However, they found that the resolution of the actual detector was better than that given by equation (3.7), which they modified to

$$\frac{\sigma_P}{P} = \frac{0.15}{\sqrt{E}} \qquad \ldots (3.8)$$

	Percentage relative standard deviation $\sigma_P/\bar{P}$	
Incident radiation	theoretical	best exp. value
CrK_α	6.45	7.4
CuK_α	5.28	5.8
CuK_β	5.02	5.7

TABLE (3.6)

The resolutions of counter A were compared with those computed from equation (3.8) for various incident radiations. These results are tabulated in Table (3.6), which indicates that the performance of counter A compares favourably with the "ideal" detector of Mulvey and Campbell (1958). The resolution of counter B is slightly worse than that of A, its value for CuK_α radiations being 7%.

3.8 The Gas Flow Proportional Counters as Absolute Intensity Detectors.

Normally, the intensity of an incident radiation beam registered by a detector does not represent the full beam intensity. A fraction of the incident intensity is absorbed by the window, and

of the transmitted fraction, f_T, only a fraction f_A is absorbed in the counter gas. The quantum counting efficiency of a counter (to be referred to as QCE) is given by

$$QCE = f_T \times f_A$$

The total number of incident photons, N_o, is given by

$$N_o = N/QCE$$

where N is the number detected.

The values for f_T were determined experimentally for each characteristic radiation. F_A may be evaluated from either the measured length of the gas absorption path, L, in the counter, or from an experimental determination of the transmission ratio of the gas for a monochromatic beam. L is the distance between the entry and the exit windows. The distance was measured for each counter by means of a micrometer screw gauge with its posts touching the ledges on which the windows were placed. Values of 0.795 cm and 1.41 cm were obtained for the counters A and B respectively. Owing to the low percentage of CO_2 in the argon-CO_2 gas filling, the transmission characteristics of the gas mixture were assumed to be identical with those of pure argon. The density of argon at NTP is 1.784 gm/liter. At room temperature and pressure, an average density of 1.67 gm/liter was used. Within the variations of the atmospheric conditions encountered in the experiments, there was a negligible

departure in the values for the QCE from that calculated from the above average value for the argon density.

The transmission ratio, T, is given by the formula

$$T = \frac{I}{I_o} = e^{-\mu \rho L} \qquad \ldots \quad (3.9)$$

where I_o and I are the incident and the transmitted intensity, respectively, ρ is the density of argon and μ, the mass absorption coefficient of argon for the incident radiations. Values for μ were either taken from tables compiled by Allen (1947) or from the empirical formula of Henke, White, and Lundberg (1957). From the relative intensity measurements of Williams (1933) and Wyckoff and Davidson (1965), calculations indicate that only the α component need be considered for calculating T for K and L radiations. Similarly for the M radiations, only the M_α component was considered. Characteristic radiations investigated in this project, of wavelengths longer than that of AlK, were completely absorbed in the gas. For AlK, the values of T were 0.22 and 0.065 for the counters A and B respectively, and for CuK_α, the corresponding values were 0.86 and 0.765. The resultant QCE's for CuK_α were low. However, the CuK_α measurements only served as introductory experimental techniques for the soft radiation measurements, which were the main concern in this project.

The operation of the gas flow counters as absolute

intensity detectors was tested with a commercial sealed proportional counter and a scintillation counter. Using the latter two detectors, the absolute intensities measured for the same incident beam of CuK_α radiations were found to differ by 5%. This discrepancy could be attributed to the fluctuations in the incident beam intensity and the use of the manufacturer's data for computing the QCE for the commercial proportional tube. The QCE for the scintillation counter was taken from Metéhnik (1961, thesis). The absolute intensities determined with the flow counter A and the sealed proportional tube were found to agree to within 4%. A corresponding agreement was found between the absolute measurements of the scintillation counter and the gas flow counters A and B. For incident CuK_α and CrK_α radiations, the transmission ratios of the gas absorption path in the flow counters were experimentally determined. These agree with the calculated values using the measured value for L within the error caused by the fluctuations in the beam intensity. For all the radiations in this project, the transmission ratio of the detectors was computed from the measured value for L. This is justified by the good agreement between the results determined with the different detectors. The discrepancy involved, if any, does not affect the results for characteristic radiations of wavelengths longer than AlK investigated in this project, as their value for T was definitely zero.

3.9 The Radiation Source for Absolute Intensity Measurements.

Apart from a few slight modifications, the radiation source was essentially that described by Metchnik (1961, thesis). A continuously variable 100 kV DC supply was obtained from a 50 kV transformer and a Cockroft-Walton voltage doubler, the primary of the transformer being controlled by a variable autotransformer. In practice, the design of the X-ray tube and the high voltage system did not permit a potential of more than 65 KV drop across the tube. The voltage was measured by a micro-ammeter connected to a resistance chain. Before the present series of measurements, both the resistance chain and the micro-ammeter were calibrated. The electron gun consisted of a tungsten filament energized by a 6 volt accumulator, which when fully charged, supplied quite a steady emission current. The electron beam was focussed onto the target by a magnetic lens. The target and the fluorescent screen were set in a metal block supported by a rotary seal which could bring either of the two into the path of the electron beam. Also the orientation of the target with respect to the incident beam could be varied. A brass target with a hole 3 mm in diameter drilled through its center was placed in the target holder. When the target face was normal to the incident electron beam, no current was registered by the galvanometer connected to the target. This ensured that the anode current measured represented the electrons striking the target within the focal spot as seen on the fluorescent screen.

CHAPTER IV Experimental Results

4.1 Method of Measurements.

For each experimental point, the differential curve of the incident radiations was first recorded. From the curve obtained, the base level and the window width of the pulse height analyzer were adjusted to accommodate the characteristic peak of interest. With the selected analyzer settings, several readings for the total number of counts were taken with the scaler over 50 or 100 second periods. The time interval was chosen according to the incident radiation intensity so that the number of counts registered in each reading was well above 10^4. As a result of statistical counting errors, the relative percentage error in the detection of N counts is $100/\sqrt{N}$. Consequently, the statistical counting error involved was less than 1%. The frequency of the noise counts was frequently checked throughout the course of each experiment. As the signal to noise ratio exceeded 100, the effect of the noise counts was negligible. To minimize the resolution time losses, the incident radiation intensity was adjusted to a value such that the resultant counting rate did not exceed the experimentally determined limits at which the resolution time losses became apparent (section 3.5). It was found that when the total electron current falling on the target was of the order of 10^{-7} ampere, a satisfactory counting rate was obtained.

The quantum yield is given by

$$N_{\phi} = \frac{4\pi NcA}{\Omega I \times QCE}$$

where N is the number of detected counts/sec, A is the correction for the attenuation of the radiations in its path to the counter, Ω is the solid angle subtended by the counter window at the target, I is the incident electron current expressed as electrons per second, QCE is the quantum counting efficiency of the counter and c is the correction for the continuous background (section 4.2).

For these measurements, the discriminator window was adjusted to accommodate the main characteristic peak only. If the incident radiations were sufficiently energetic that an escape peak appeared, then the quantum yield was given by

$$N'_{\phi} = N_{\phi}(1 + r)$$

where r is the ratio of the areas of the escape peak and the main peak. Values for r were predetermined using monochromatic radiations (section 3.4).

The target surface was smoothed with a carborundum lapping compound, polished with a metal polish and then rinsed in methanol. The target surface was frequently cleaned during the course of the experiment. There was no noticeable contamination of the surface even after a lengthy period of operation of the radiation source. This was attributed to the fact that the target was located well away from the

throat of the diffusion pump. With the exception of the TiL radiations, there was no significant variation in the counting rate with the time length of operation of the radiation source. This seems to suggest that the reduction in the TiL intensities with time was primarily caused by the attenuation of the emitted TiL radiations by a surface deposit of carbon, a most likely contaminant (Ennos, 1953), rather than by the loss of energy suffered by the incident electrons in the carbon deposit. This is supported by the following facts,

(a) provided the incident electron energy is not too low, the electrons suffer little loss in energy after passing through a carbon layer less than a micron in thickness (equation (2.13), the graph is similar to figure (2.13)),

(b) of the radiations investigated, carbon has the highest mass absorption coefficient for the TiL radiations (Henke, White, and Lundberg, 1957).

4.2 Correction for the Continuous Background.

In the differential curve, the pulse distribution of the characteristic peak was superimposed on that of the bremmstrahlung radiations. For the AlK radiations and the other characteristic radiations of shorter wavelengths investigated, the resolution of the gas flow proportional counters used was sufficiently good to enable the characteristic peaks to stand out prominently from the bremmstrahlung distribu-

tion. From the trend of the differential curve due to bremmstrahlung radiations alone, a line was drawn under the peak to separate the characteristic distribution from the bremmstrahlung distribution. A planimeter was used to determine the ratio of the area of the peak to the total area under the differential curve within the limits defined by the pulse height analyzer settings used in the integrated counting measurements.

Typical differential curves obtained for AlK (8.32Å) and AgL (4.15Å) radiations are included in appendix (1). The line separating the characteristic distribution from the bremmstrahlung distribution for each differential curve is also shown.

An allowance was also made for the "tails" of the characteristic peak lying outside the limits of the discrimination window by estimating the areas under the tails of the characteristic peak. In most cases, the correction required was negligible.

For the characteristic radiations of wavelengths longer than that of AlK, i.e. from CuL (13.3Å) to CK (44Å), the resolution of the proportional counters did not permit an accurate separation of the characteristic distribution from the bremmstrahlung distribution. A knowledge of the theoretical curve shapes of the two component distributions was necessary.

The output pulse distribution for incident photons of a given energy results from the statistical variation in the number of primary electron-ion pairs produced per incident photon and in the size of the

subsequent avalanche produced by each in the counter gas. The statistical effect involved in the second process was investigated by Snyder (1947) and discussed by Snell (1962), who arrived at a probability function $P_\nu(x)$ for finding ν particles at a point x along the track where the duplication processes took place

$$P_\nu(x) = q_n \frac{(\nu-1)!}{(n-1)!(\nu-n)!} e^{-\gamma n x} (1 - e^{-\gamma x})^{\nu-n} \quad \ldots(4.1)$$

$$\bar{N} = e^{\gamma x} \quad \ldots(4.2)$$

where n is the number of primary particles at x = o,

$\nu = n + N$, is the total number of particles at x,

N is the number of particles produced at x by one initiating particle

and $\bar{N}$ is the mean number,

q_n is the probability of having n particles initially,

γ is the probability of electron duplication per unit potential interval.

From equations (4.1) and (4.2)

$$P_\nu(x) = q_n \frac{(\nu-1)!}{(n-1)!(\nu-n)!} \frac{1}{\bar{N}^n} (1 - \frac{1}{\bar{N}})^{(\nu-n)}$$

Using the following mathematical approximations (e.g. Price, P56, 1964),

$$(1 - \frac{1}{\bar{N}})^{\nu-n} \approx e^{-\nu/\bar{N}}$$

and $$\frac{(\nu-1)!}{(\nu-n)!} \approx \nu^{n-1}$$

$$\therefore \quad P_\nu(x) = q_n \left(\frac{\nu^{n-1}}{(n-1)!} \frac{1}{\bar{N}^n} e^{-\nu/\bar{N}}\right) \quad \ldots(4.3)$$

If the magnitude of the resultant pulse height is proportional to the number of particles produced in the multiplication process, and the fluctuation in n is ignored, then the probability distribution f(p) of a pulse height p produced by n primary particles is given by

$$f(p) = \frac{p^{n-1}}{(n-1)!} \quad \frac{1}{\bar{p}^n} \quad e^{-p/\bar{p}}$$

If $\frac{1}{\lambda} = \bar{p}$ is the mean size of the pulse height of a simple avalanche, then

$$f(p) = \frac{p^{n-1}}{(n-1)!} \quad \frac{1}{(1/\lambda)^n} \quad e^{-\lambda p}$$

$$= \frac{\lambda e^{-\lambda p} (\lambda p)^{n-1}}{(n-1)!} \qquad \ldots(4.4)$$

This is the probability function used by Campbell (1963) to describe the pulse height distribution for monochromatic radiations. For the bremmstrahlung radiations, Campbell used the following proportionality to describe the pulse height distribution

$$f(p) \propto \sum_{n=1}^{N} \frac{\lambda e^{-\lambda p} (\lambda p)^{n-1}}{(n+1) \quad (n-1)!} \qquad n \leq N \qquad \ldots(4.5)$$

Equation (4.5) was derived from the relationship of Fuchs and Kulenkampff (1954), which describes the variation of the energy intensity with energy of the bremmstrahlung radiations. A modification was also introduced to fit the theoretical distribution with the experimental bremmstrahlung distribution. This process made some allowance for the fact that the experimental bremmstrahlung pulse height distribution was

dependent on the variation in the attenuation of the incident radiations, by the counter window, with wavelength.

The distribution functions (4.4) and (4.5) were fitted point by point with the experimental differential curves by the method of least squares, as was found by Campbell (1963), a linear combination of the distribution function (4.4) for the characteristic peak with values of n, the number of primary ionizations produced per incident photon, distributed around its calculated value n_c, was required for a good fit. The necessity for having a composite curve for the characteristic peak was due to the neglect of the consideration of the statistical fluctuations in the number of primary ionizations in the derivation of equation (4.4). The operation for choosing the weights for the component distribution functions for the characteristic peak was combined in the same least squares method above.

The computer program for the whole operation was written. In the program, a corrective operation was included so that if the sum of the deviations squared of the calculated points from the experimental curve exceeded a certain value, two additional component distribution functions were used to describe the characteristic peak with $n = n_c \pm 1$. This process was continued until a good fit was obtained. For practically all cases, the CK radiations required 5 component characteristic distribution functions, TiL and CrL required 7, and CuL, 9. In all cases, the weight of the middle component, i.e. the function with the theoretical value for n, was the largest. The results for CuL

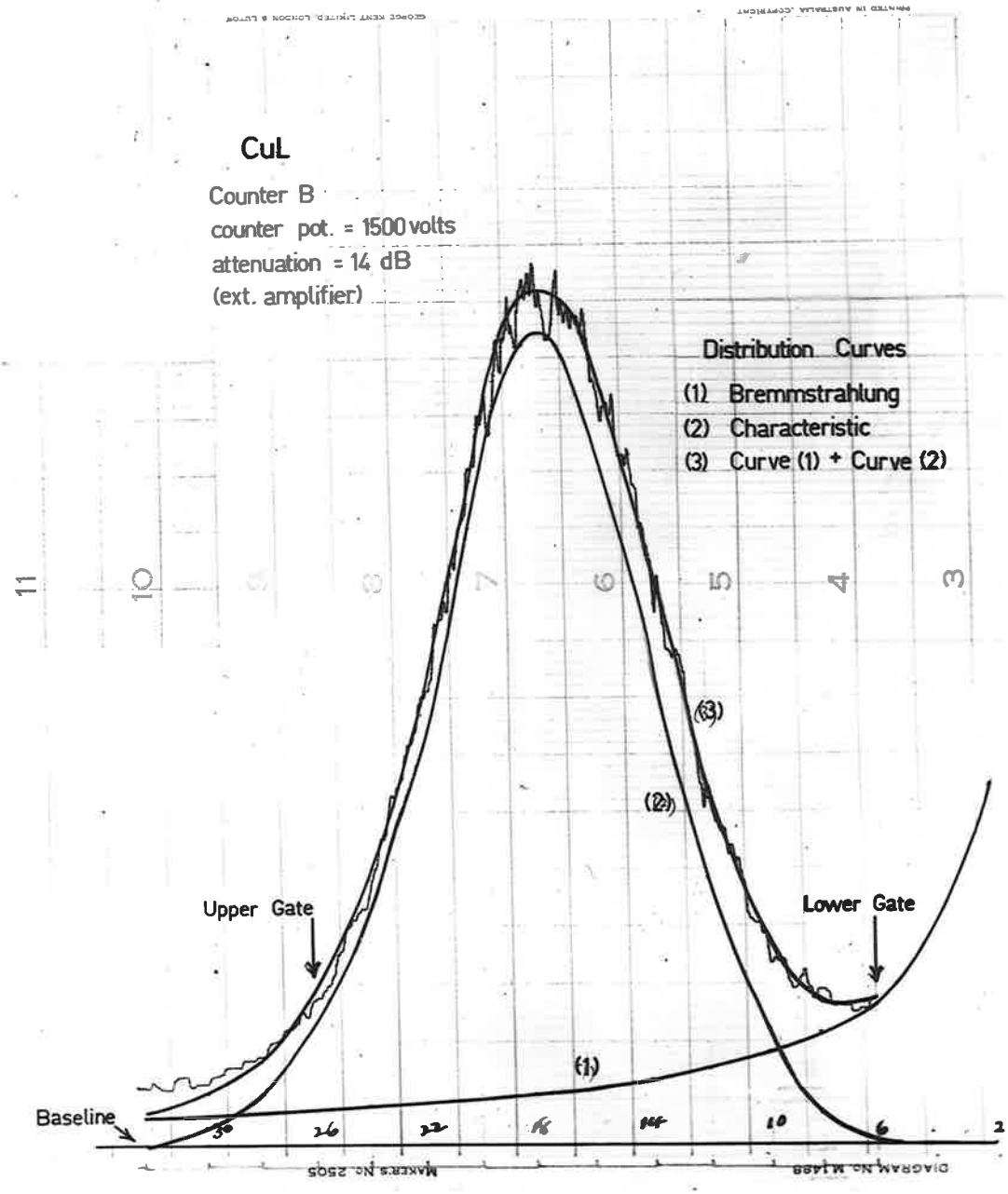

Figure 4.1 Pulse height distribution from CuL radiations.

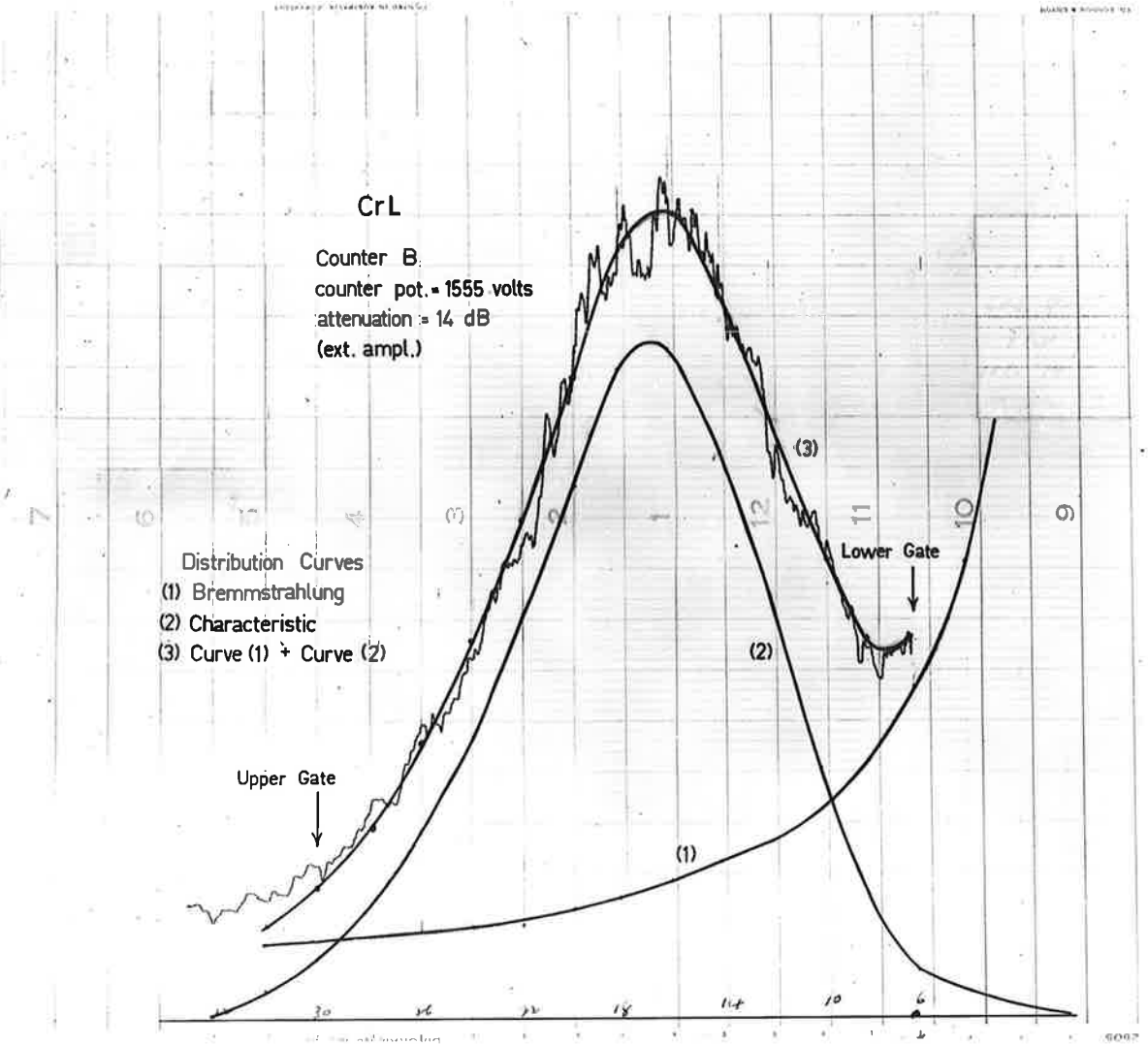

Figure 4.2 Pulse height distribution from CrL radiations.

and CrL radiations are shown in figures (4.1) and (4.2) respectively. The distribution curves for the bremmstrahlung radiations and the characteristic radiations are included. It must be remembered that the experimental differential curve represents the pulse height distribution of all the characteristic radiations in the K or L spectrum in addition to the bremmstrahlung radiations. No explicit allowance was made for the occurrence of several characteristic lines of similar energies nor for the variation in attenuation of the incident radiations by the counter window.

4.3 Absolute intensity measurements of CuK_α and CrK_α radiations.

In order to test pulse height discrimination as a method for isolating the characteristic radiations, several other techniques were also used to monochromatize the CuK_α and CrK_α radiations. As extensive absolute intensity measurements of these characteristic radiations have already been made (Metchnik, thesis, 1961; Metchnik and Tomlin, 1963), the measurements of these radiations served as a check on the performance of the gas flow proportional counters as absolute intensity detectors.

The CuK_α radiations were monochromatized by means of a pair of balanced differential filters and by means of a double LiF crystal monochromator. In addition to the two gas flow proportional counters, the radiations were detected by a Geiger counter, a sealed commercial proportional counter and a scintillation counter. The crystal mono-

chromator, the Geiger tube, the sealed proportional counter and the scintillation counter were the same as those described by Metchnik (1961, thesis).

The differential filters used consisted of a pair of nickel and iron filters of thicknesses 2.75×10^{-3} cm and 3.28×10^{-3} cm respectively. Theoretically, it is impossible to achieve a perfect balance for radiations of all wavelengths outside the pass band. The filter thicknesses were chosen to match the transmission ratios for radiations of wavelengths in the immediate neighbourhood of the pass band defined by the critical absorption edges of the two filters. Table (4.1) shows the degree of unbalance in the transmission ratios for radiations of wavelengths lying within and close to the pass band.

	Transmission ratio (%)			
	1Å	CuK_β	CuK_α	2Å
Ni	5.2	0.091	30	9.5
Fe	7.6	0.097	0.023	12.7

TABLE 4.1

The performance of this pair of differential filters was comparable to that used by Metchnik (1961). The effect of any unbalance in the transmission ratios for radiations of wavelengths far removed from the pass band was minimized by pulse height discrimination. It was found that with pulse height discrimination, the percentage transmission

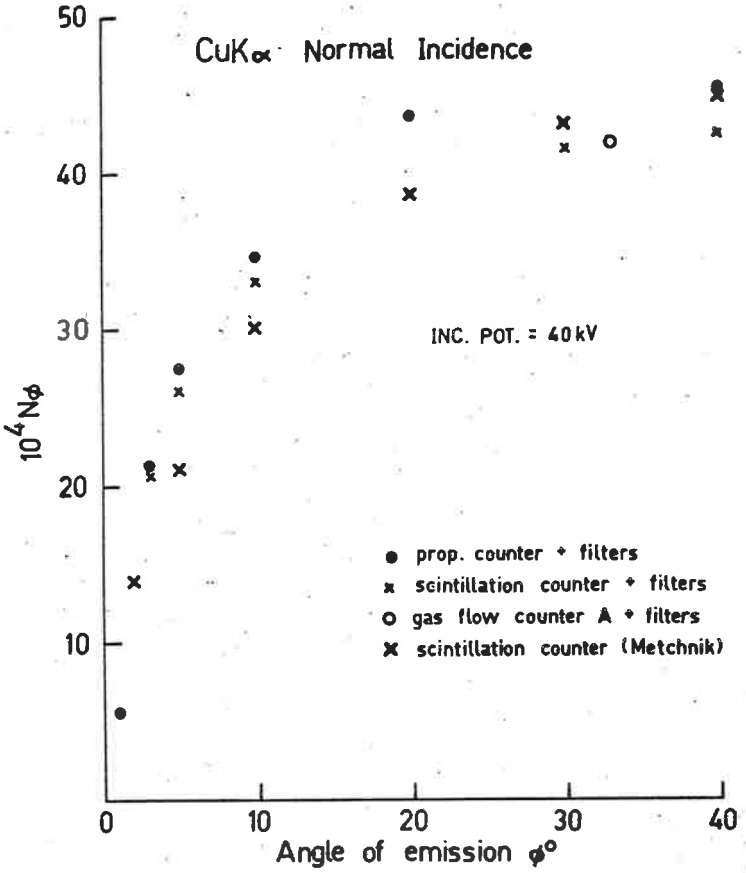

Figure 4.3

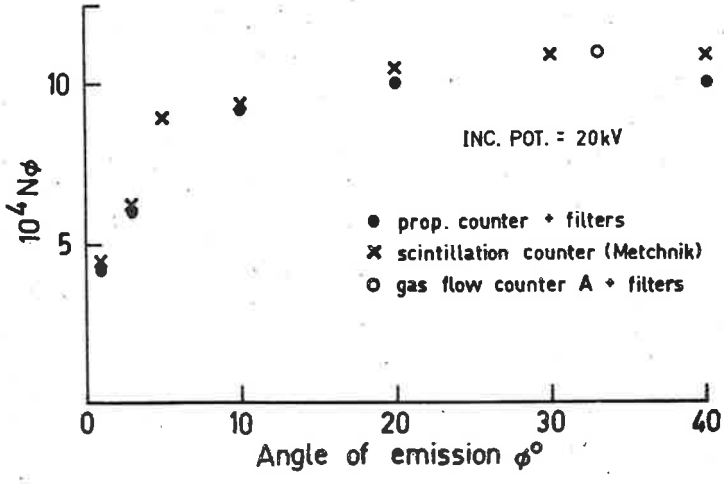

Figure 4.4

Experimental results for CuKα radiation intensities.

of MoK_α radiations (0.71Å) using the Ni-Fe filters was only 0.5%.

The QCE of the scintillation counter for the CuK_α radiations was taken from Metchnik (thesis, 1961). The QCEs of the sealed proportional counter and the Geiger tube were calculated from the manufacturer's data. Values of 0.813 and 0.71 were obtained respectively, as compared to Metchnik's values of 0.855 and 0.772. The discrepancy in the QCE for the proportional counter was due to a difference in the values used for the mass absorption coefficient for the beryllium window. Metchnik's value was 1.35 as compared with 1.6 given by Allen (1947) used in the present calculations. An experimental value of 0.72 was used for the transmission ratio of the aluminium window for the X-ray tube as compared with 0.698 used by Metchnik (1961).

In the measurements made with the scintillation counter, the base level of the discriminator had to be raised to eliminate low energy noise counts. This resulted in the low energy tail of the characteristic peak being cut off. An allowance was made for this in the calculations. Dead time and dead volume losses were considered in the results obtained with the Geiger tube.

Figures (4.3) and (4.4) show the present results obtained with the sealed proportional counter and the scintillation counter using balanced differential filters and pulse height discrimination to isolate the CuK_α radiations. The corresponding results of Metchnik (1961) are included for comparison. There is generally good agreement between all the results.

There was similar agreement in the measurements determined with the Geiger tube and the differential filters, and similarly in the measurements in which the double LiF crystal monochromator was used to isolate the CuK_α radiations.

Measurements of the CuK_α radiation intensities were also determined with the gas flow proportional counter A in conjunction with balanced differential filters and pulse height discrimination. These results are included in figures (4.5), (4.6), and (4.7) for $\phi = 10^\circ$, 20°, and 40° respectively for normal electron beam incidence. Metchnik's scintillation counter results are included for comparison.

Absolute intensities of CuK_α and CrK_α radiations were determined with the gas flow proportional counters A and B using pulse height discrimination alone to separate the continuous radiations from the characteristic radiations (section 4.2). The CuK_α results are included in figures (4.6) and (4.7), which indicate that the intensities determined by the two gas flow counters are in satisfactory agreement with each other and with Metchnik's results. The escape peak correction was included in the results (section 3.4).

The above series of experiments indicated that the gas flow proportional counters were accurate absolute intensity detectors and that pulse height discrimination was a satisfactory method for isolating the characteristic lines and estimating the continuous radiation correction. It should be pointed out that the resolution of proportional counters was insufficient to separate the K_α from the K_β radiations. Williams'

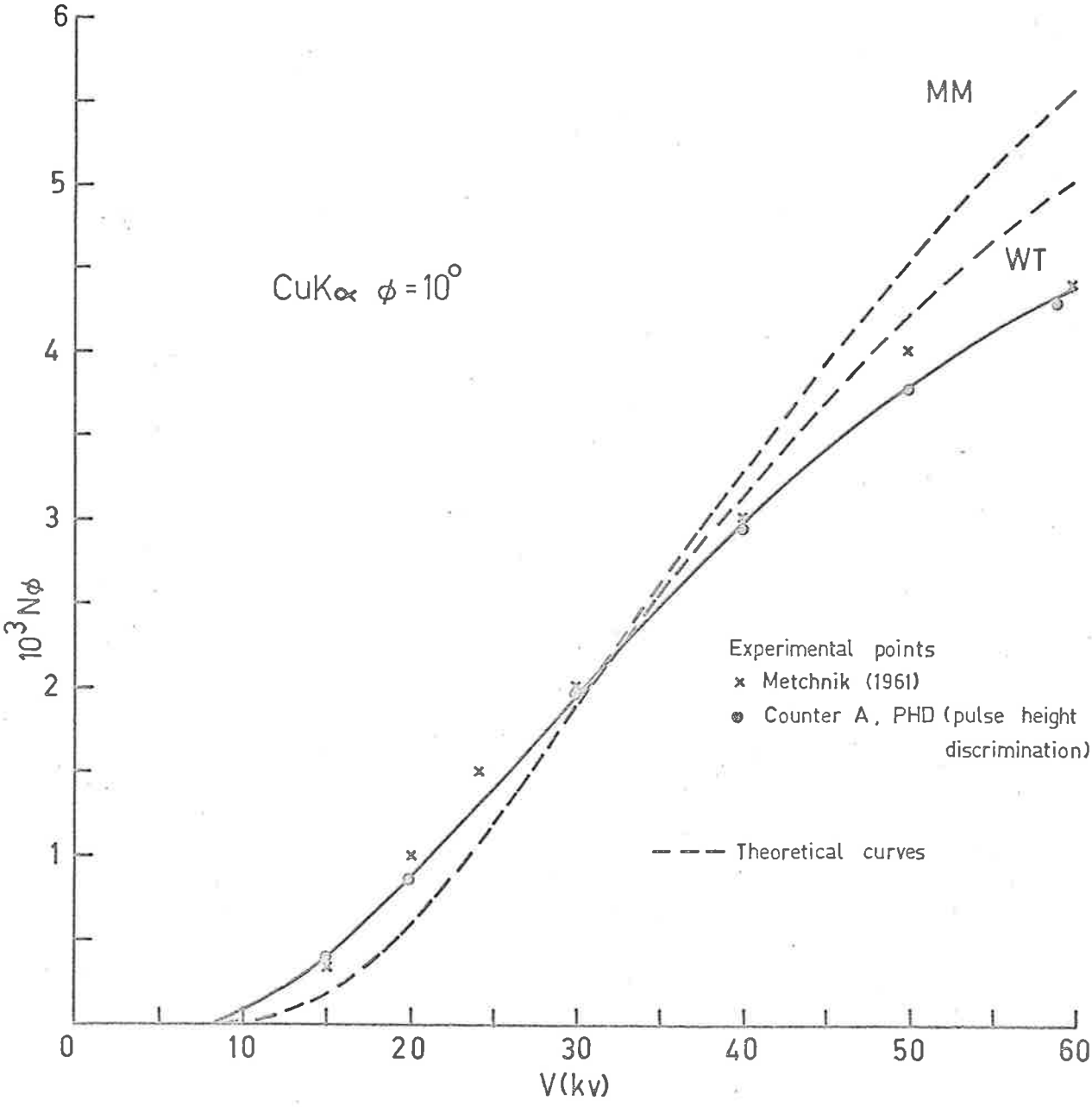

Figure 4.5 Experimental and theoretical results for CuKα radiation intensities.

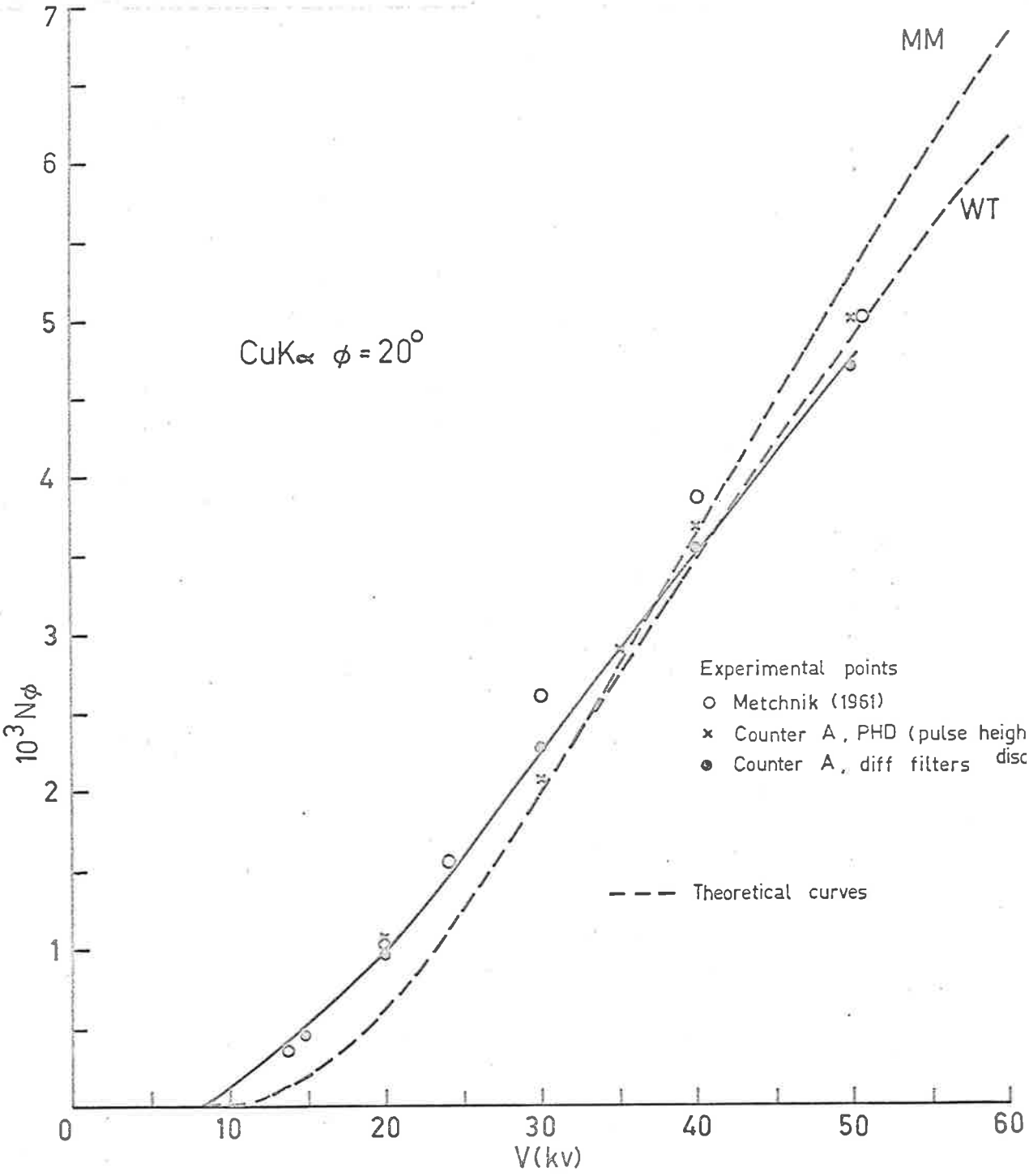

Figure 4.6 Experimental and theoretical results for CuKα radiation intensities.

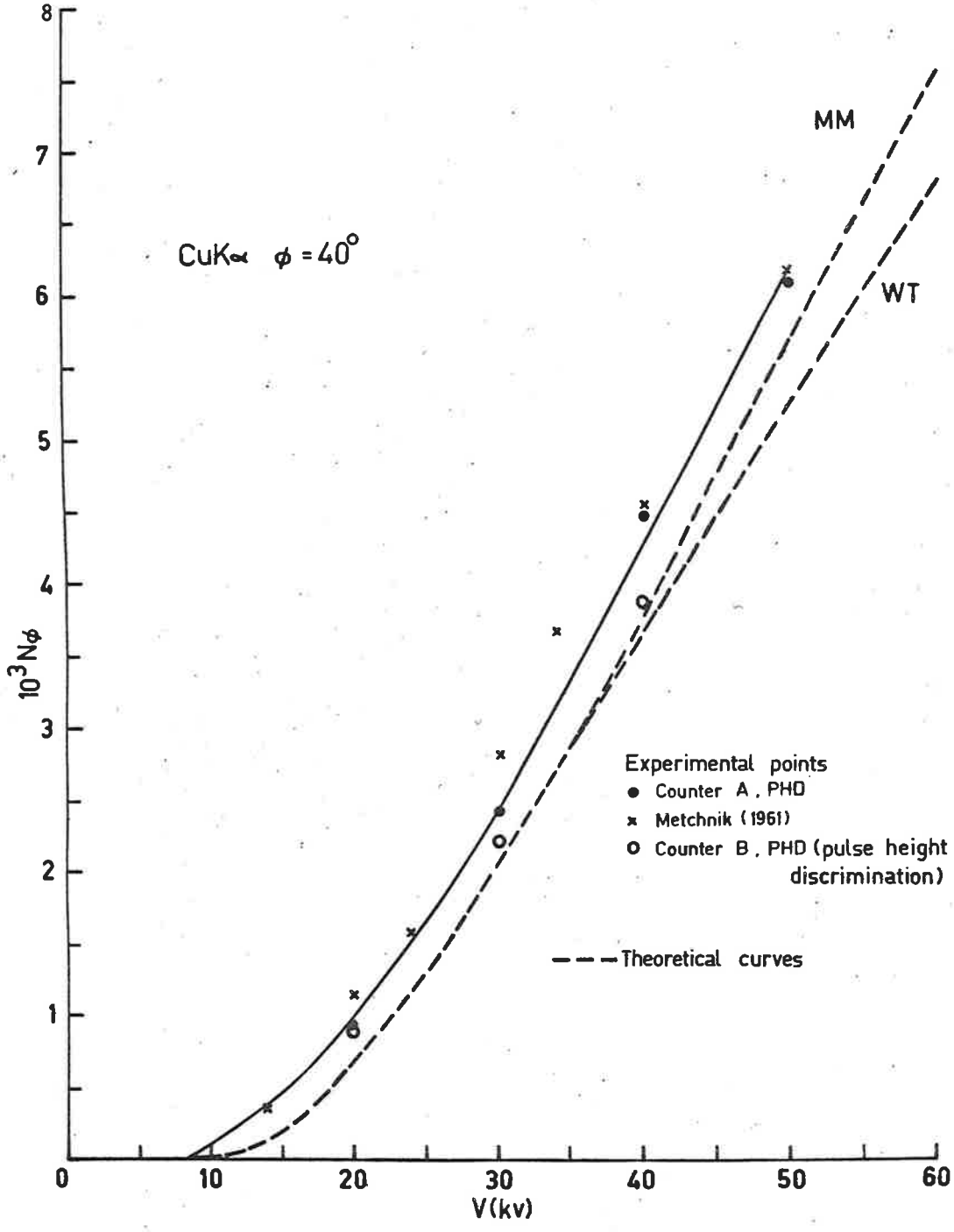

Figure 4.7 Experimental and theoretical results for CuKα radiation intensities.

(1933) data were used to estimate the fraction of K_α radiations in the K spectrum. For softer characteristic radiations, other than those of wavelengths longer than AlK (8.3Å), there was a much smaller low energy background. It was found quite easy to separate visually the characteristic peak from the continuous pulse distribution in the differential curve for these radiations.

The theoretical CuK_α intensities calculated from equation (2.12) are included in figures (4.5), (4.6), and (4.7). For the angle of emission ϕ^o in the range 10^o to 40^o and for the electron beam incident normally, there is little separating the theoretical curves calculated with the formula for Q_K as discussed by Mott and Massey (1965) (section 2.2; these intensity curves are denoted as MM in this and the following sections) from the curves calculated with Worthington and Tomlin's (1956) formula for Q_K (denoted as the WT intensity curves) up to $4T_K$, from which point, the MM curves lie above the WT curves, and this difference increases to about 10% at 60 keV incident electron energy. There is generally good agreement between the experimental points and the theoretical curves for the CuK_α radiation intensities. For all the angles of emission investigated and for electron energies below $3T_K$, the experimental results lie above the theoretical curves and the discrepancy increases with a reduction in the electron energy. Figure (2.2) indicates that there is a good agreement between the experimental result and both theoretical values for Q_K at approximately $2T_K$ for the nickel atom. Assuming that there is similar agreement for the copper atom, it appears

that the discrepancy does not lie in the expression used for Q_K. However, there is not enough experimental evidence to support the validity of the theoretical values for Q_K at low energies. The use of the Born approximation in the theories for Q_K should result in an overestimation of the theoretical intensities at low energies. The effect of any error in the correction for the target absorption at low electron energies should not be serious, especially at high angles of emission. In the intensity curves for $\phi = 10^{\circ}$ and at high electron energies (figure 4.5), where the target absorption is important, the experimental points lie below the theoretical curves. It is interesting to note that the discrepancy is about the same magnitude as that resulting from considering the target medium as infinite in extent in deriving $\langle x \rangle$, the average depth of electron penetration (see figure 2.14).

The experimental CrK_α intensities are shown in figure (4.8). These measurements were determined with the gas flow proportional counter B, and pulse height discrimination was used to separate the characteristic radiations from the continuous background. Williams' (1933) data was used to calculate the fraction of K_α radiations in the K spectrum. The measurements of Metchnik and Tomlin (1963) are included for comparison (denoted as MT in figure (4.8)). The theoretical MM intensity curves shown include both Burhop's (1952) value for ω_K (0.21) and Callan's value (0.272) (Fink et al, 1966). The continuous background was lower than that encountered in the CuK_α measurements, resulting in a better estimation for the continuous radiation correction. There is a close

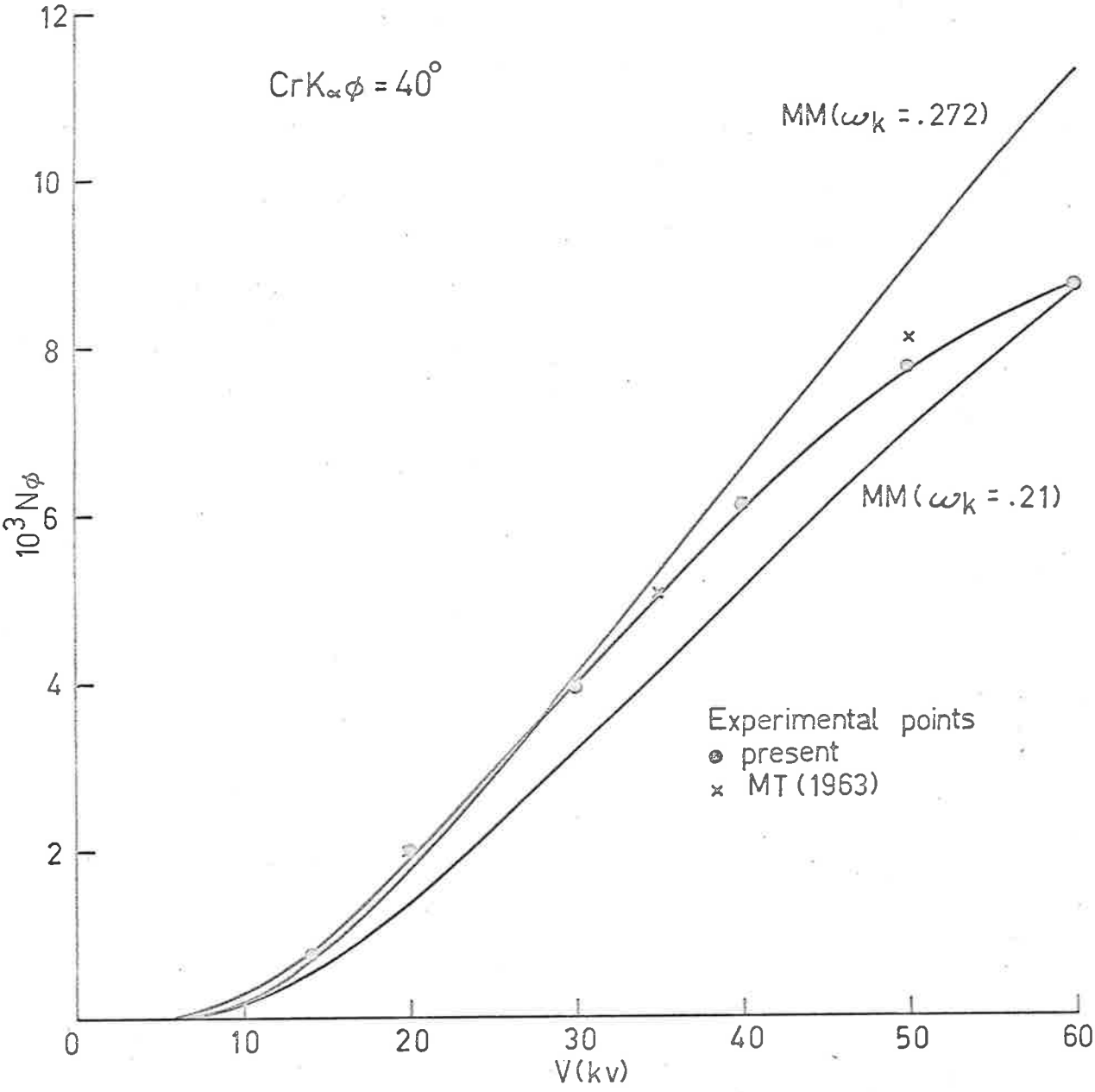

Experimental points and theoretical results for CrKα radiation intensities.

Figure 4.8

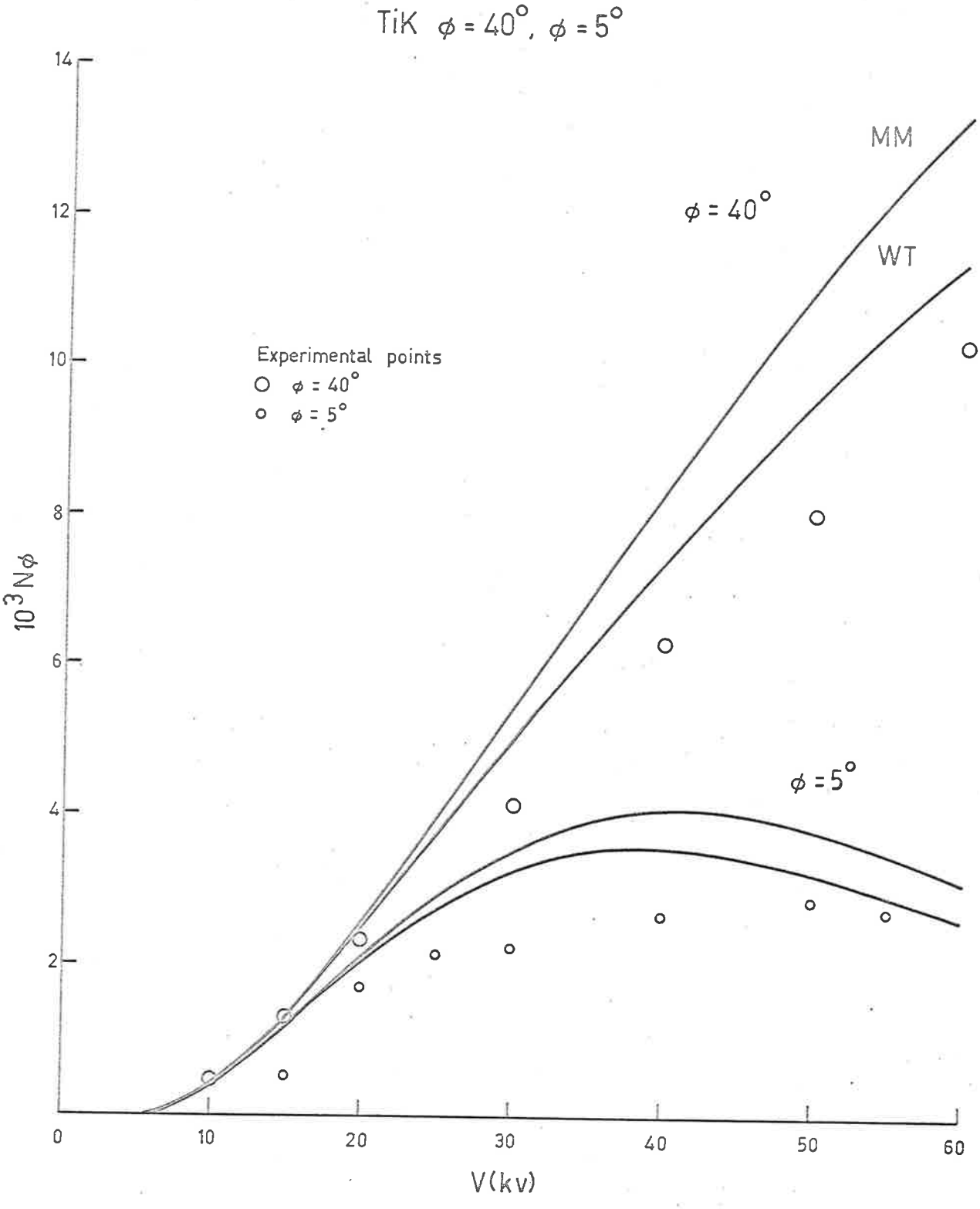

Experimental points and theoretical results for TiK radiation intensities.

Figure 4.9

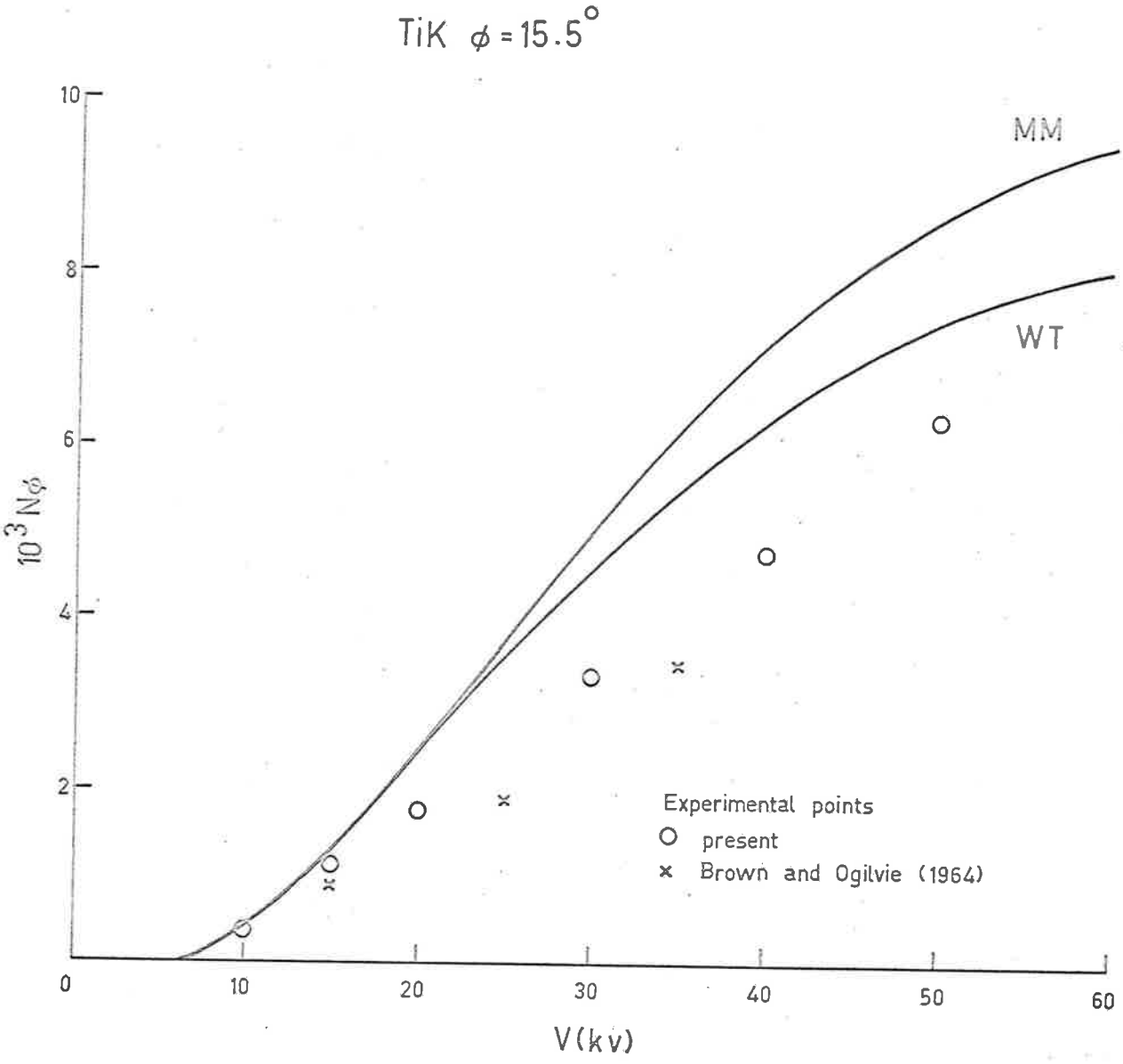

Experimental points and theoretical results for TiK radiation intensities.

Figure 4.10

agreement between the present CrK_α results and the MT's results. The experimental results lie between the theoretical curves calculated with the two ω_K values mentioned above. As in the case of the CuK_α results, the experimental points suggest that the correction in the theoretical formula for the target absorption is too low.

4.4 TiK results.

Total TiK radiation intensities were determined with the gas flow counter A. For a normal electron beam incidence, measurements were made for $\phi = 5^\circ$, 15.5°, 25°, 32°, and 40°. A series of measurements was also made for radiations emitted at 45° to the target surface with the electron beam inclined at 90° to the emitted radiations (this arrangement is denoted as oblique incidence). The results for $\phi = 5^\circ$, 40°, and 15.5° are shown in figures (4.9) and (4.10) and the other results are included in appendix (2). The experimental results fall below the WT theoretical curves by about 15% on the average and below the MM curves by about 25%. Assuming the intensity formula is satisfactory, the results suggest that Callan's value of (0.213) for ω_K used is too high. There is a better agreement if Burhop's (1952) value of 0.155 for ω_K is used. In fact the average of the available experimental values for ω_K for titanium lie between the two theoretical values (figure 2.9). Brown and Ogilvie's (1964) experimental data for $\phi = 15.5^\circ$ have been included in figure (4.10) for comparison. There is some doubt as to which of their values to use. The excitation energies implied in their

diagrams (figures 6 and 7), Brown and Ogilvie, 1964) suggest that the captions beneath the diagrams should be interchanged. If this is done, their experimental intensities become twice the present measurements. No mention was made of any attempt to allow for the backscattered and secondary electrons leaving the target. Judging from the schematic diagram of their experimental arrangement (figure 9, Brown and Ogilvie), only the target to ground current was considered. This would explain the discrepancy. If the original captions under their diagrams are assumed to be correct, there is much better agreement between the present results and those of Brown and Ogilvie (1964). These are the results included in Figure (4.10).

The measured intensities of Birks et al (1965) also exceed the present results by about 60% to 70%. Their results refer to target-to-ground currents. Even allowing for the backscattered electrons, a large discrepancy still occurs. It is probable that this was caused by secondary electrons escaping from the target in their experimental arrangement. Allowance for these electrons was not mentioned. A large discrepancy also exists between the present CuK_{α} results and those of Birks et al (1965).

4.5 AlK Results.

AlK intensities were measured with the gas flow counter A for $\phi = 5^{\circ}$, 10°, 20°, 32°, and 38° for normal incidence of electrons.

Measurements were also made for radiations emitted at 45° to the target surface with the emitted radiations inclined at 90° to the incident electron beam. Some of the measurements were redetermined with the gas flow counter B. there was no significant difference in the results determined with the two counters. The experimental points together with the theoretical curves are shown in figures (4.11) to (4.16). Using the experimental ω_K value of 0.045 of Bertrand et al (1959) (section 2.3), there is good agreement between both the WT and the MM curves with the present experimental data except at low angles of radiation emission, where a significant discrepancy exists between theory and experiment at high incident electron energies. At $\phi = 5^{\circ}$ (figure 4.12), the experimental points are twice the theoretical values for incident electron energies exceeding 40 keV. The discrepancies decrease with an increase in the angle of emission for corresponding electron energies.

Figure (4.11) shows that Campbell's (1963) experimental results are only about 65% of the present measurements. It was at first thought that the magnetic system used to deflect the backscattered electrons away from the counter window was unsatisfactory, so that spurious AlK radiations were produced in the aluminized mylar window. Some of the measurements were repated with a plain mylar counter window. However no significant change in the results was detected. These measurements

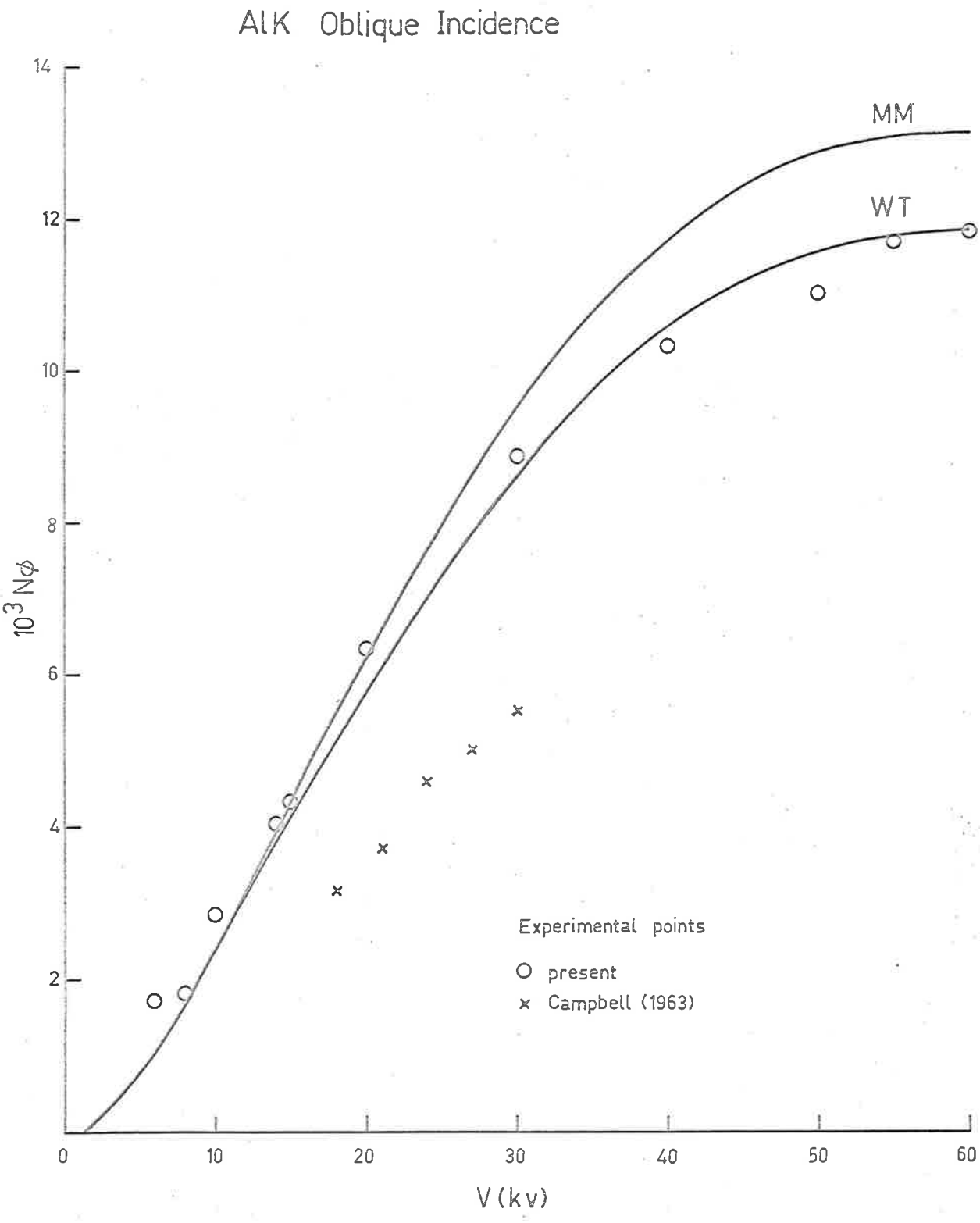

Figure 4.11 Experimental points and theoretical results for AlK radiation intensities.

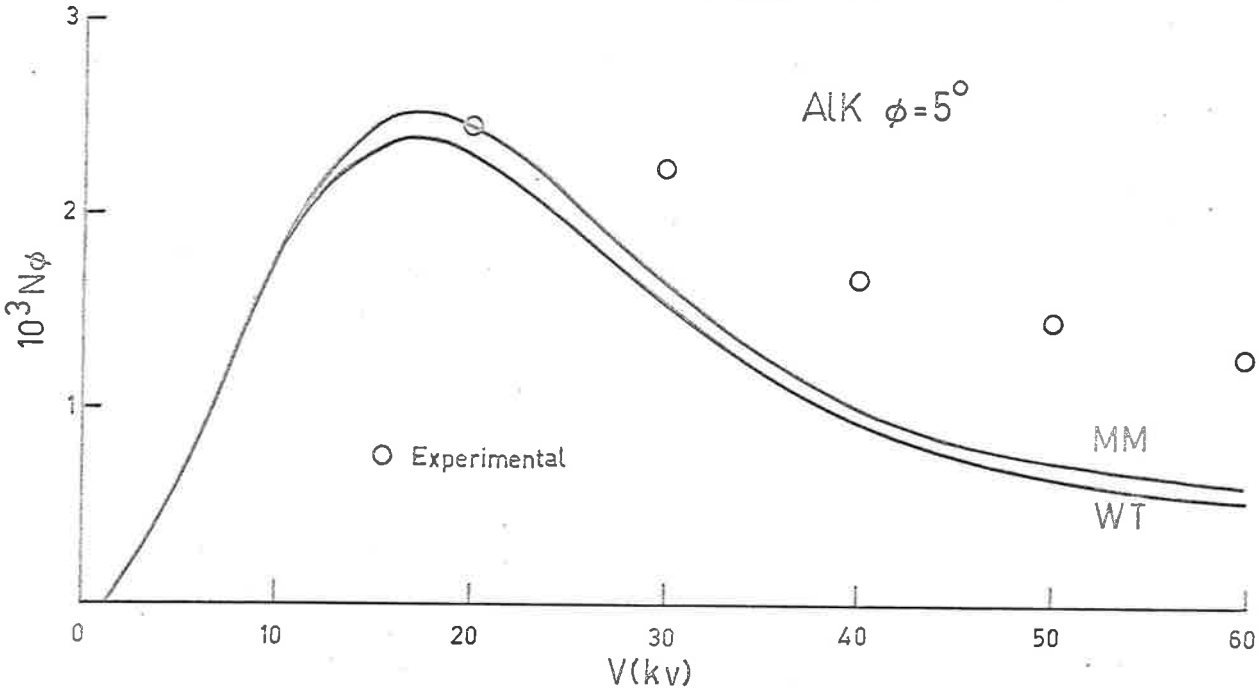

Figure 4.12

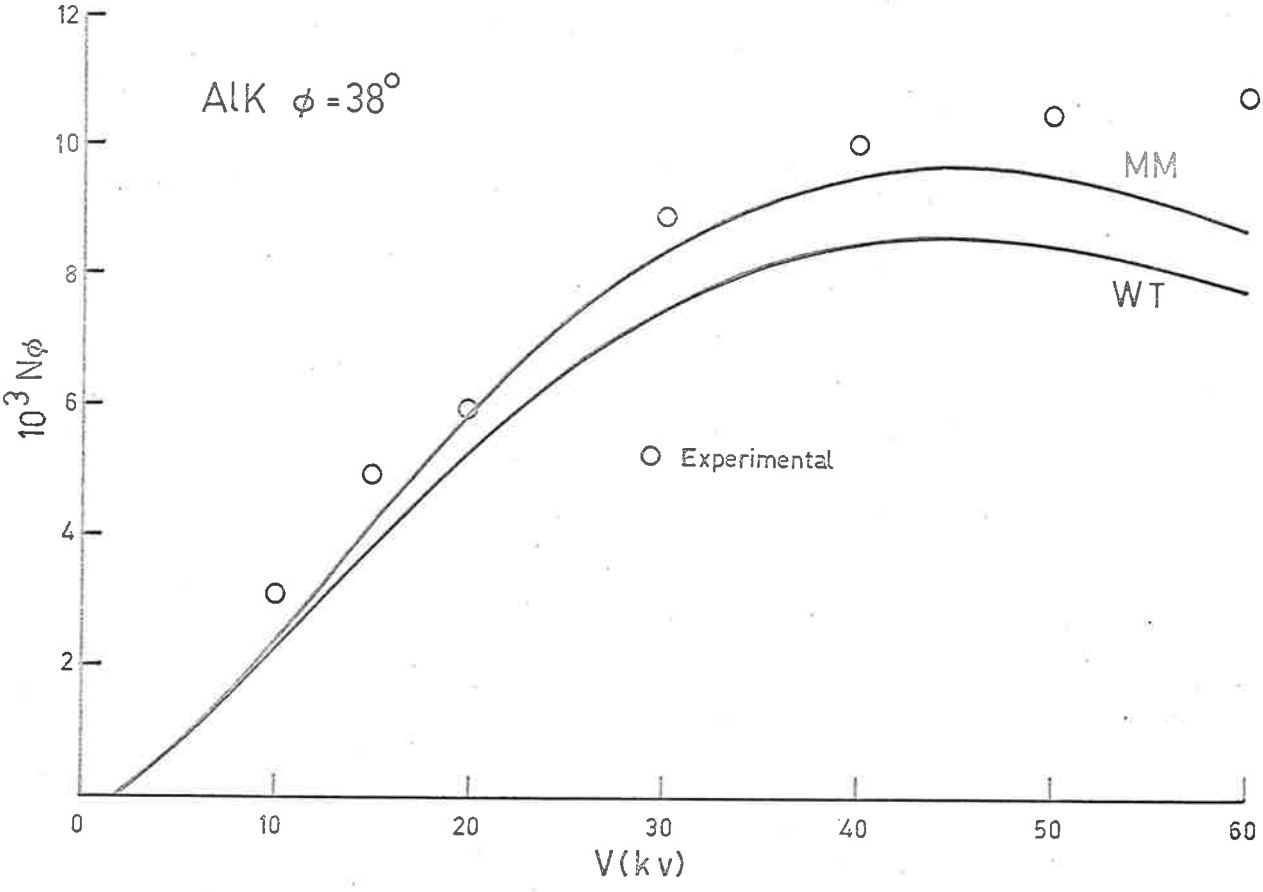

Figure 4.13

Experimental points and theoretical results for AlK radiation intensities.

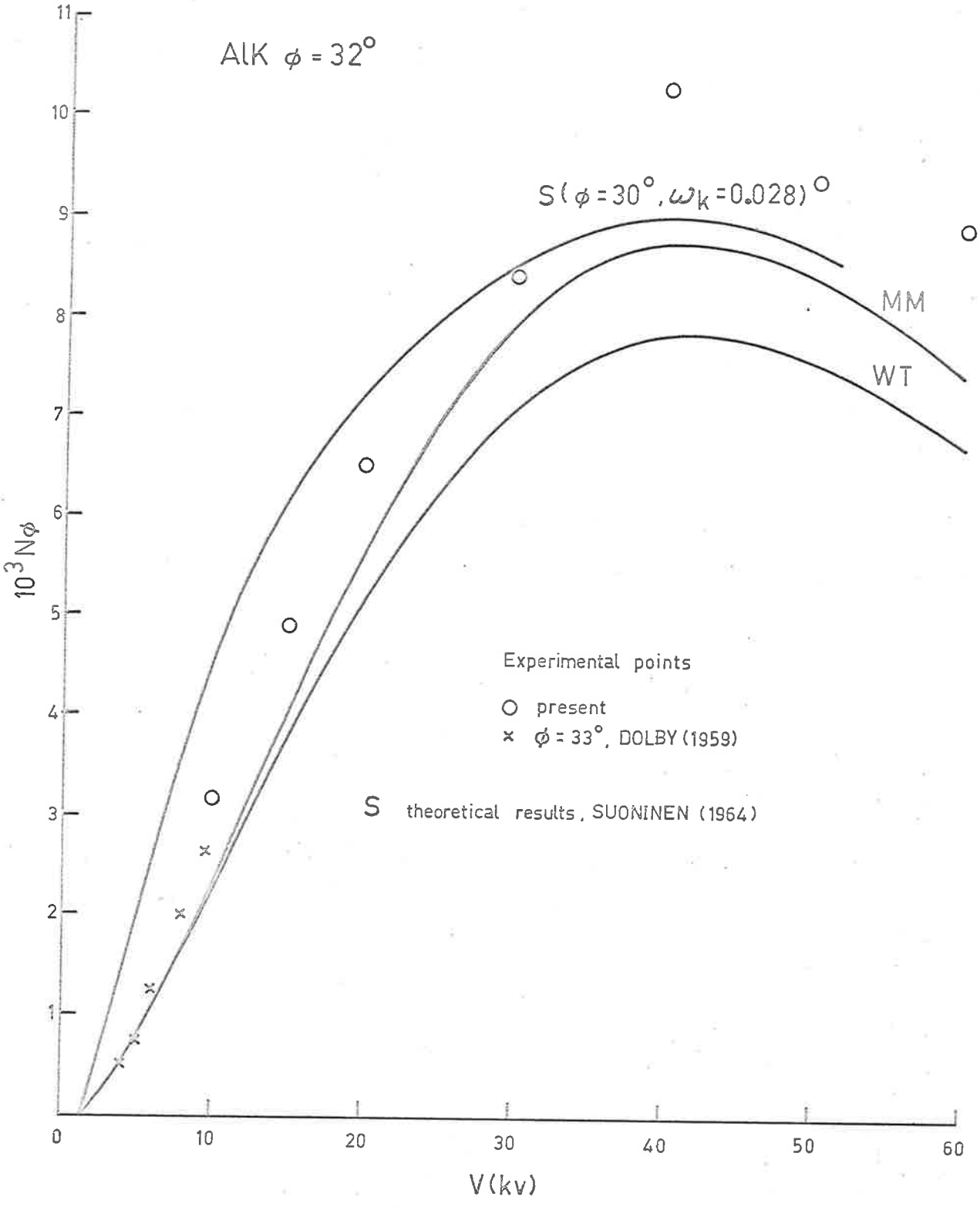

Experimental points and theoretical results for AlK radiation intensities.

Figure 4.14

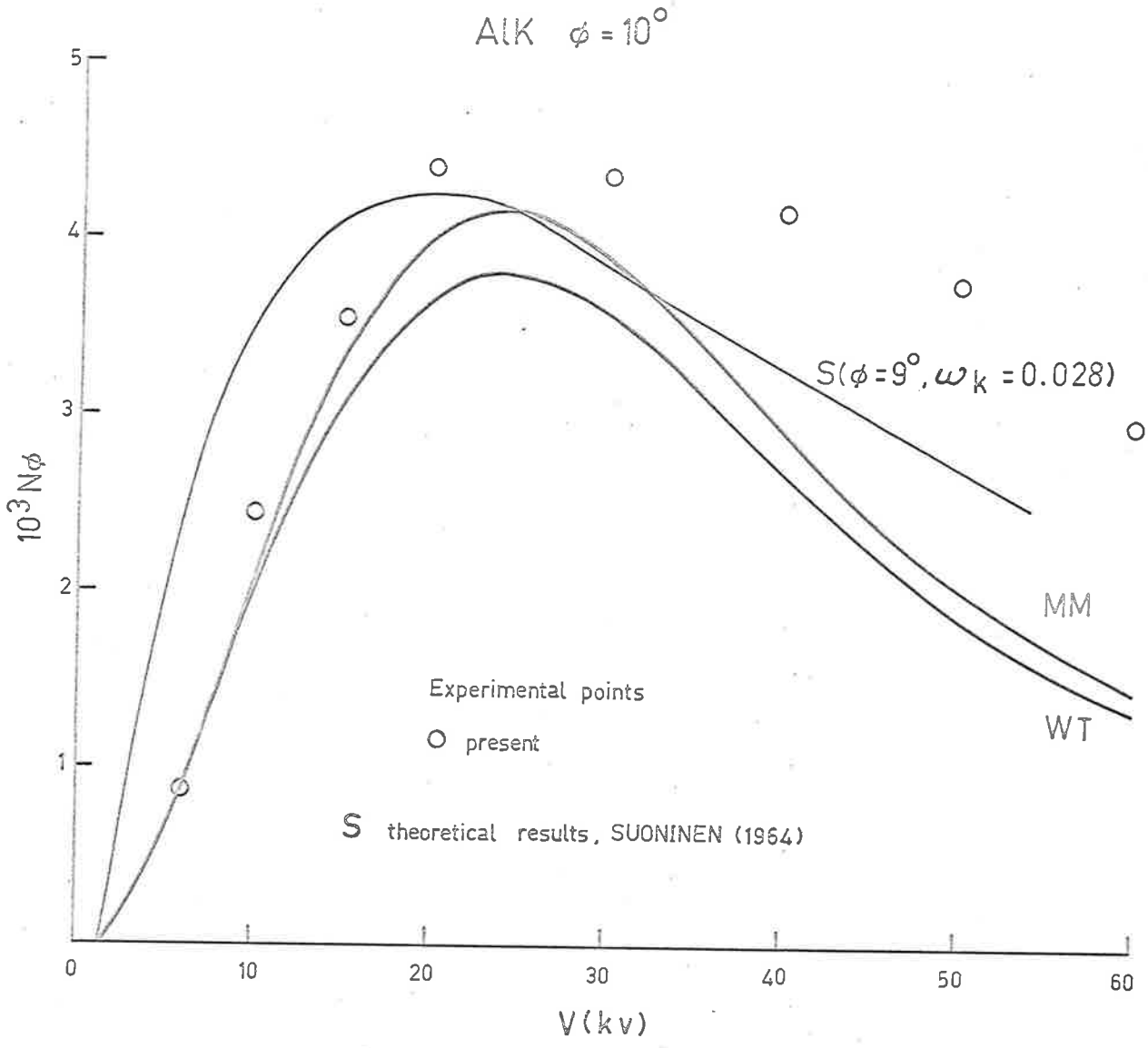

Experimental points and theoretical results for AlK radiation intensities.

Figure 4.15

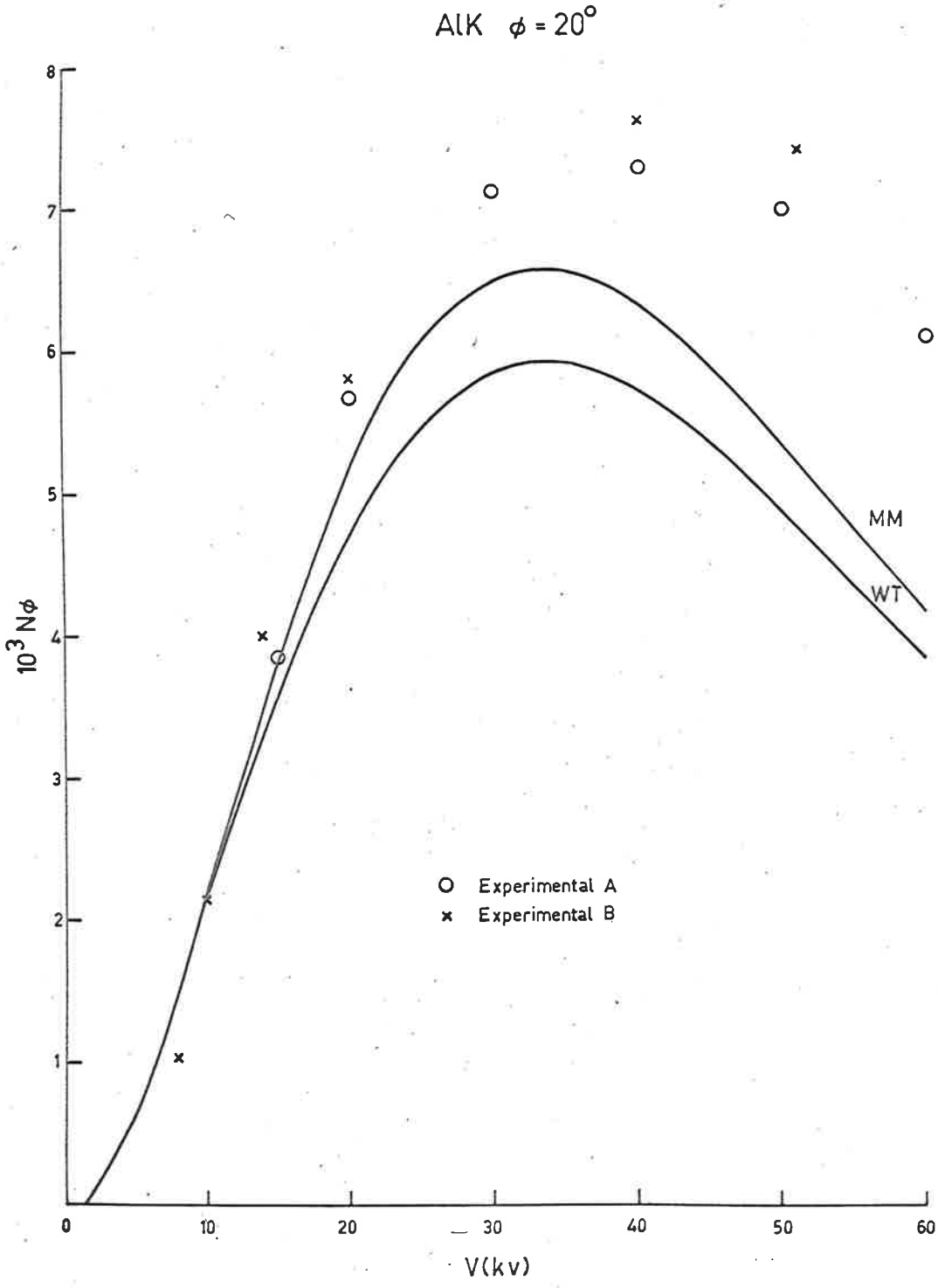

Figure 4.16 Experimental points and theoretical results for AlK radiation intensities.

are shown in figure (4.16) for $\phi = 20^{\circ}$. (The results determined with a plain mylar window are denoted as "experimental B" and those determined with an aluminized mylar window are denoted as "experimental A"). Figure (4.14) indicates that the present measurements are consistent with Dolby's (1960) experimental results. Although Dolby's experimental conditions were not ideal, it is unlikely that his results were seriously overestimated. A discussion of this is given in sections (1.1.2) and (1.1.3). Suoninen's (1964) theoretical results are included in figures (4.14) and (4.15). An ω_K value of 0.028 was used in these calculations.

4.6 CK Results.

Owing to the porosity of carbon, it is difficult to achieve a smooth surface finish for the carbon specimen. Dolby (1960) found that the CK intensities emitted from a carbon target were 70% of those from a polished diamond target and 7% higher than those from a roughly filed carbon surface. The target used in the present measurements was polished with a carborundum lapping compound. It is certain that this treatment is inadequate to produce a sufficiently smooth surface. It is assumed that the present measurements represent only 70% of the intensities emitted from an ideally smooth target. The resultant intensities are shown in figures (4.17), (4.18), and (4.19). Campbell's (1963) results are included in figure (4.17). Although there is good agreement between the two sets of experimental results up to 25 keV electron energy, from the trend of Campbell's results, it appears that the present intensities

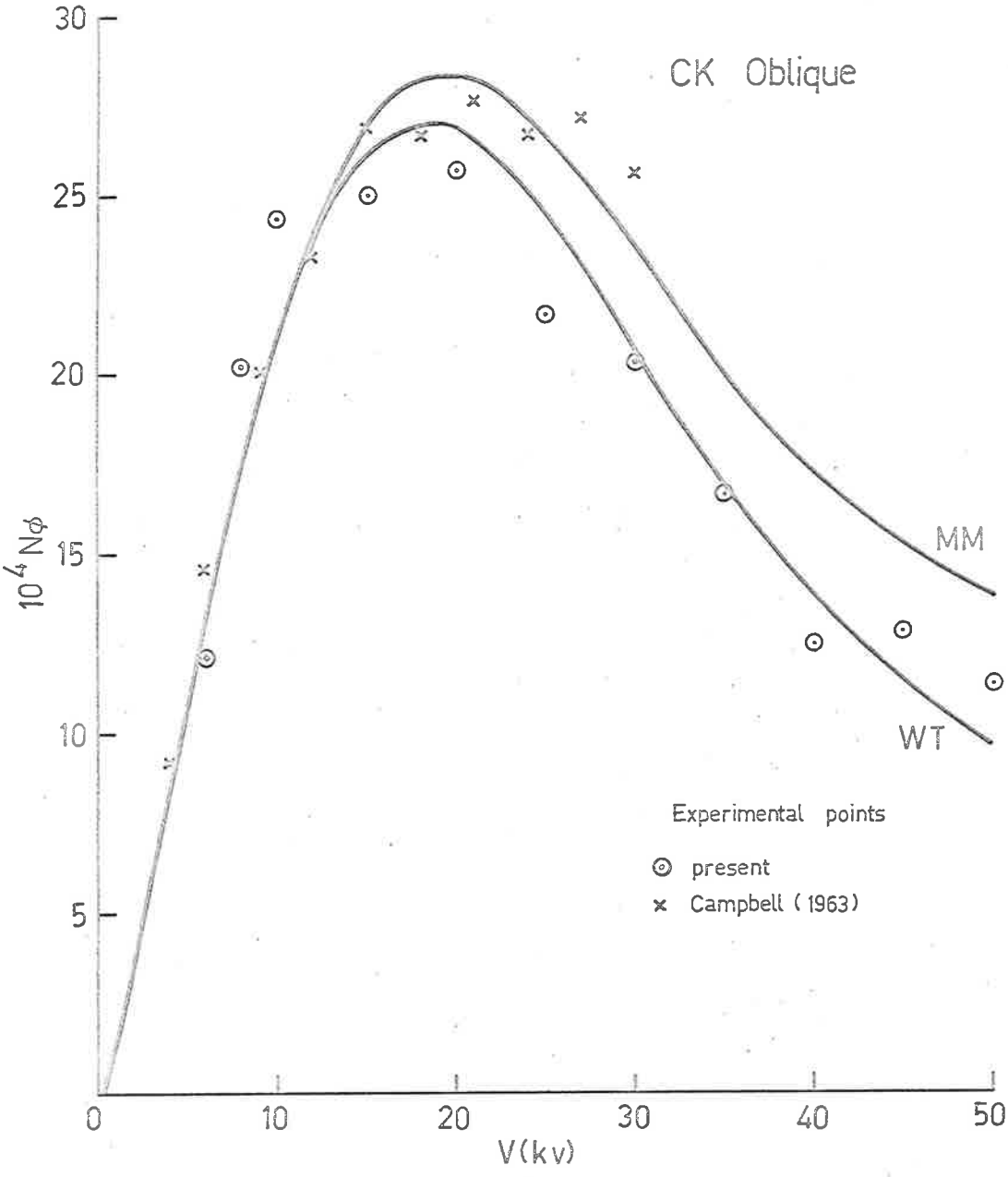

Figure 4.17 Experimental and theoretical results for total CK radiation intensities.

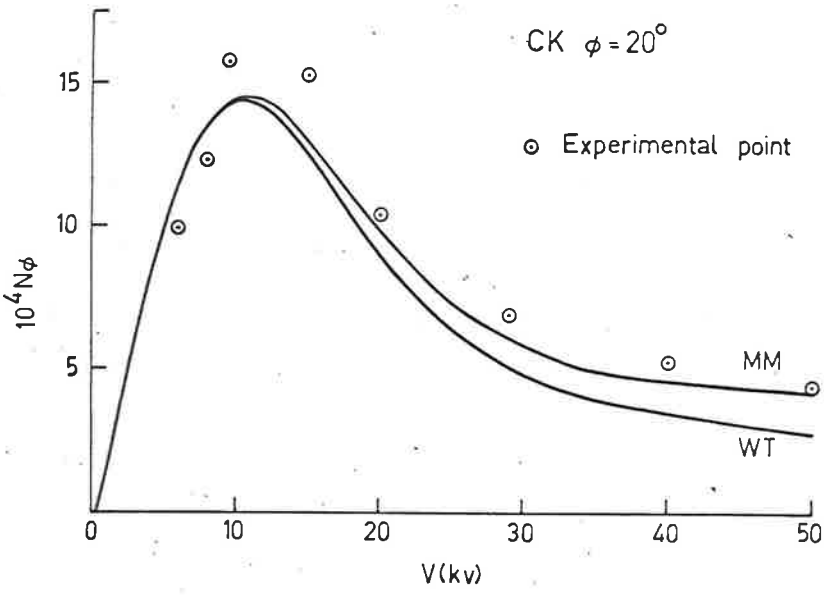

Figure 4.18

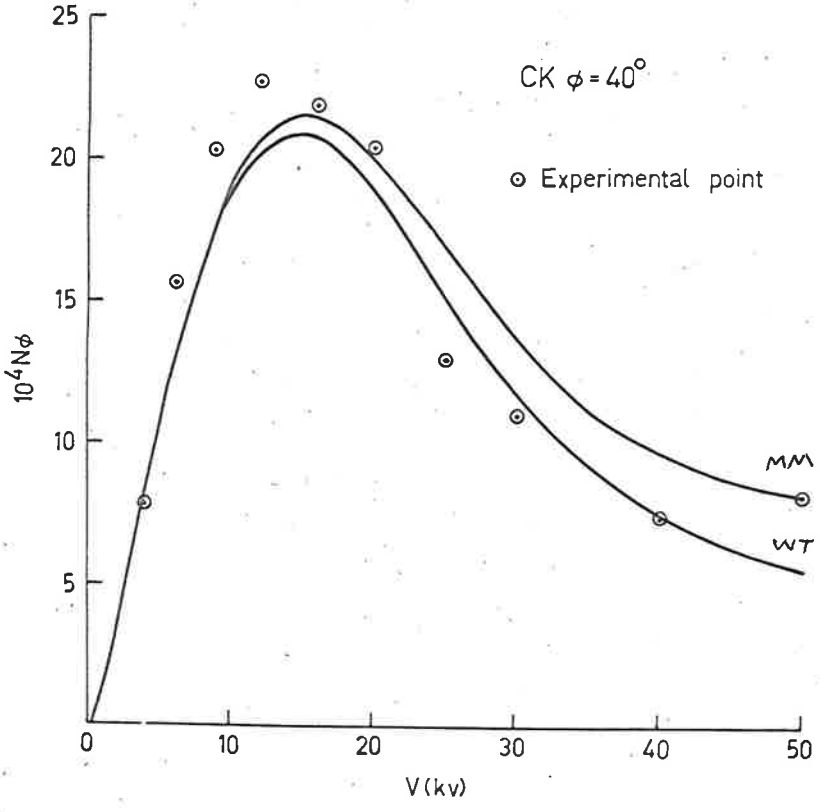

Figure 4.19

,Experimental and theoretical results for total CK radiation intensities.

decrease more rapidly with electron energy than Campbell's (1963) results. This is not certain, however, as Campbell's measurements extend only to 30 keV electron energy.

Dolby's (1960) experimental results for $\phi = 33^{\circ}$ are twice the present measurements for $\phi = 40^{\circ}$. Although there is a difference in the angle of emission, theoretical calculations indicate that there is very little difference in the intensities computed for the two experimental arrangements. It is certain that some secondary CK radiations were excited in the counter window in Dolby's experiment (section 1.1.2 and 1.1.3).

The theoretical MM and WT curves are included in figures (4.17), (4.18), and (4.19). An ω_K value of 2.06×10^{-3} was used in these calculations. This value was obtained from a comparison of the theoretical and experimental radiation intensity results. It appears that Burhop's (1952) ω_K value of 1.44×10^{-3} for carbon is too low.

4.7 Estimation of the Atomic Fluorescence Yield values from thick target Intensity Data.

Figure (2.9) shows that there is a wide spread in the experimental values for the fluorescence yield. This scatter in the ω_K values is particularly serious for light elements. Assuming that the theoretical MM intensity results are correct, the fluorescence yield may be estimated by a comparison between the experimental and theoretical intensity results.

The theoretical results which are most likely to be in error are those corresponding to low electron energies, due to the use of the Born approximation in the theory, and those corresponding to low angles of emission, where the target absorption term in the theory becomes important. The values obtained from a comparison between the theoretical and experimental intensity results from moderate to high electron energies and for high angles of radiation emission are listed in Table (4.2).

	Z	ω_K
C	6	2×10^{-3}
Al	13	.05
Ti	22	.16
Cr	24	.23
Cu	29	.37

TABLE (4.2)

For Cu and Cr, there is very little to choose between Burhop's (1952) values and Callan's (Fink et al, 1966) values for ω_K. For Ti, it appears that Burhop's value of 0.155 is the more appropriate one. For Al, the value obtained is similar to that of Bertrand et al (1959). The value for C is very much higher than that of Burhop (1952).

4.8 The L and M Radiation Intensities.

Absolute intensities were determined for AgL (4.15Å), CuL

(13.3Å), TiL (27.39Å), CrL (21.67Å), PtM (6.03Å), AuM (5.83Å), and WM (6.97Å) radiations (the wavelengths in brackets refer to the α_1 component). Some of these results are shown in figures (4.20) to (4.34). The rest are contained in appendix (3). There are no past experimental data available for comparison with the present results. The only absolute intensity data for L or M shell characteristic radiations are those of Birks et al (1964), who made a few isolated AuL and Zr L measurements. However, their results refer to the target-to-ground currents. In general, the shape of the experimental curves for the L radiations differs from that of the curves for the corresponding K radiations. Owing to the higher target absorption suffered by the softer L radiations, the experimental curves display a peak at a relatively low incident electron energy.

There are not sufficient data available to permit the calculation of the theoretical intensities of these L and M shell characteristic radiations. Data on the fluorescence yield, the ionization cross-section and the mass absorption coefficient of the target element for radiations of wavelengths longer than the L critical absorption wavelength of the target element are either lacking or are uncertain. Information in the fluorescence yield beyond the L-shell is scanty. A few isolated M shell fluorescence values were listed by Fink et al (1966). Except in the case of the AgL radiations, the mass absorption coefficient of the target element for its own L or M characteristic radiations is unknown. The paper of Henke, White, and Lundberg (1957) appears to be

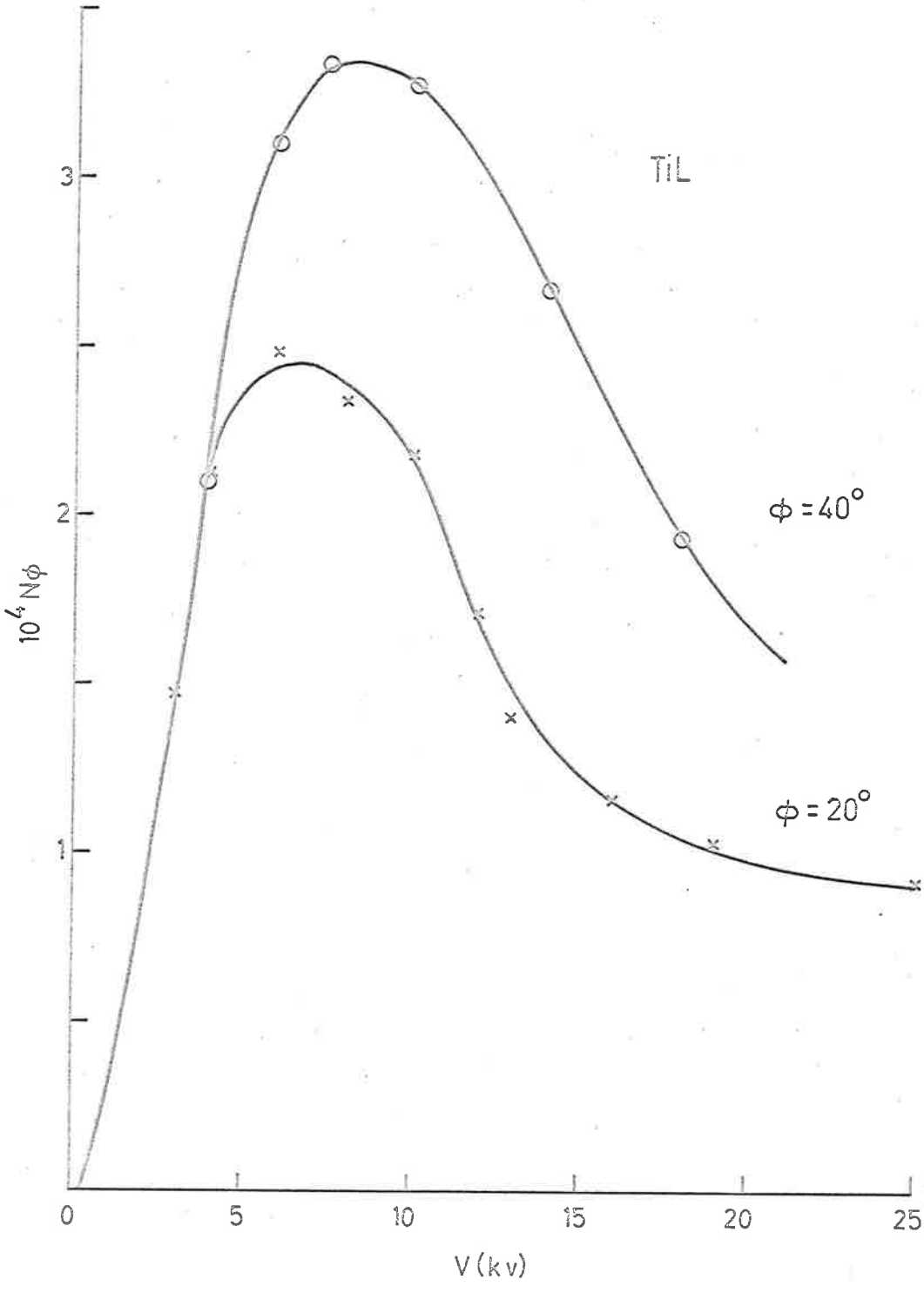

Experimental curves for total TiL radiation intensities.

Figure 4.20

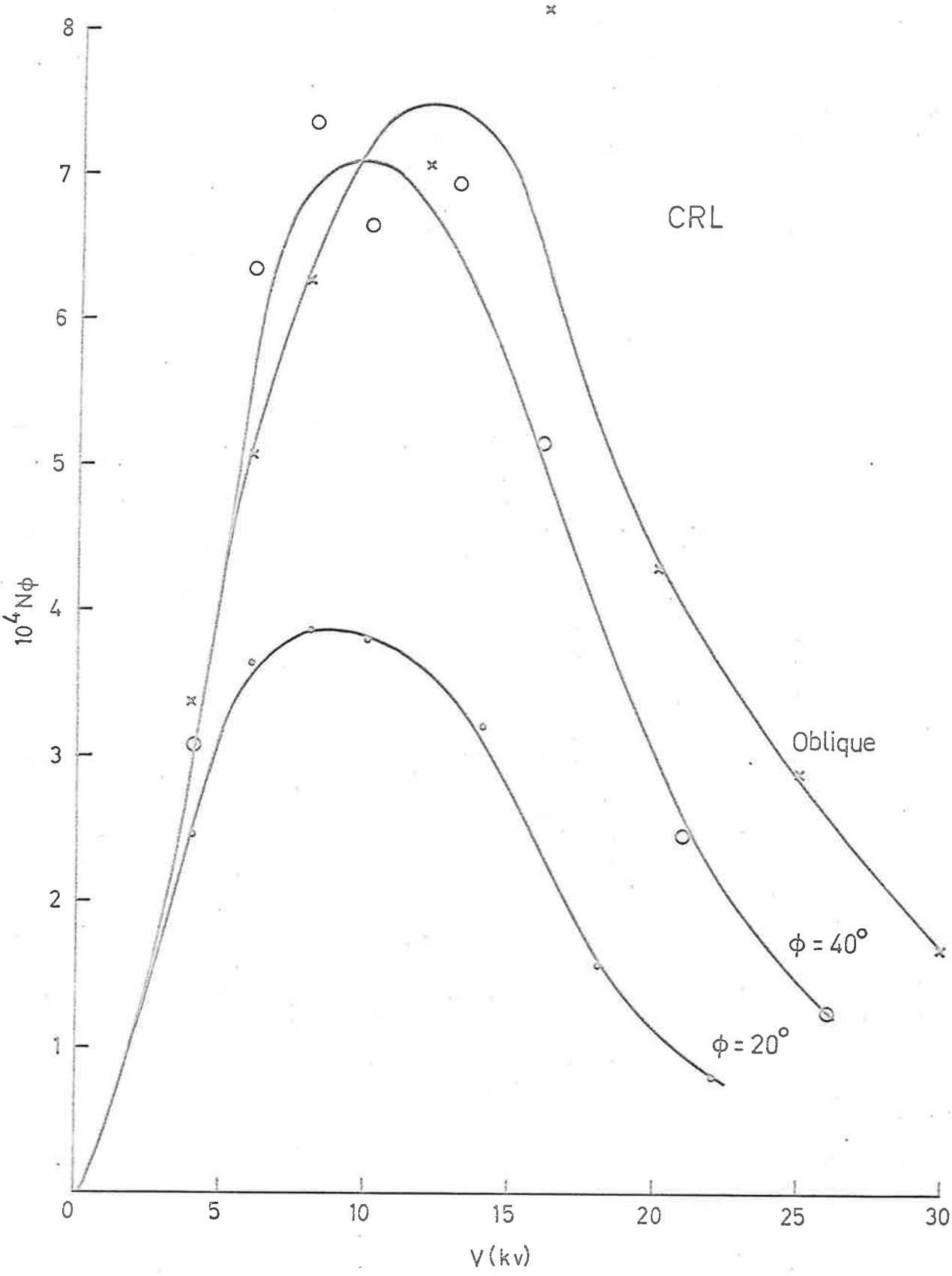

Experimental curves for total CRL radiation intensities.

Figure 4.21

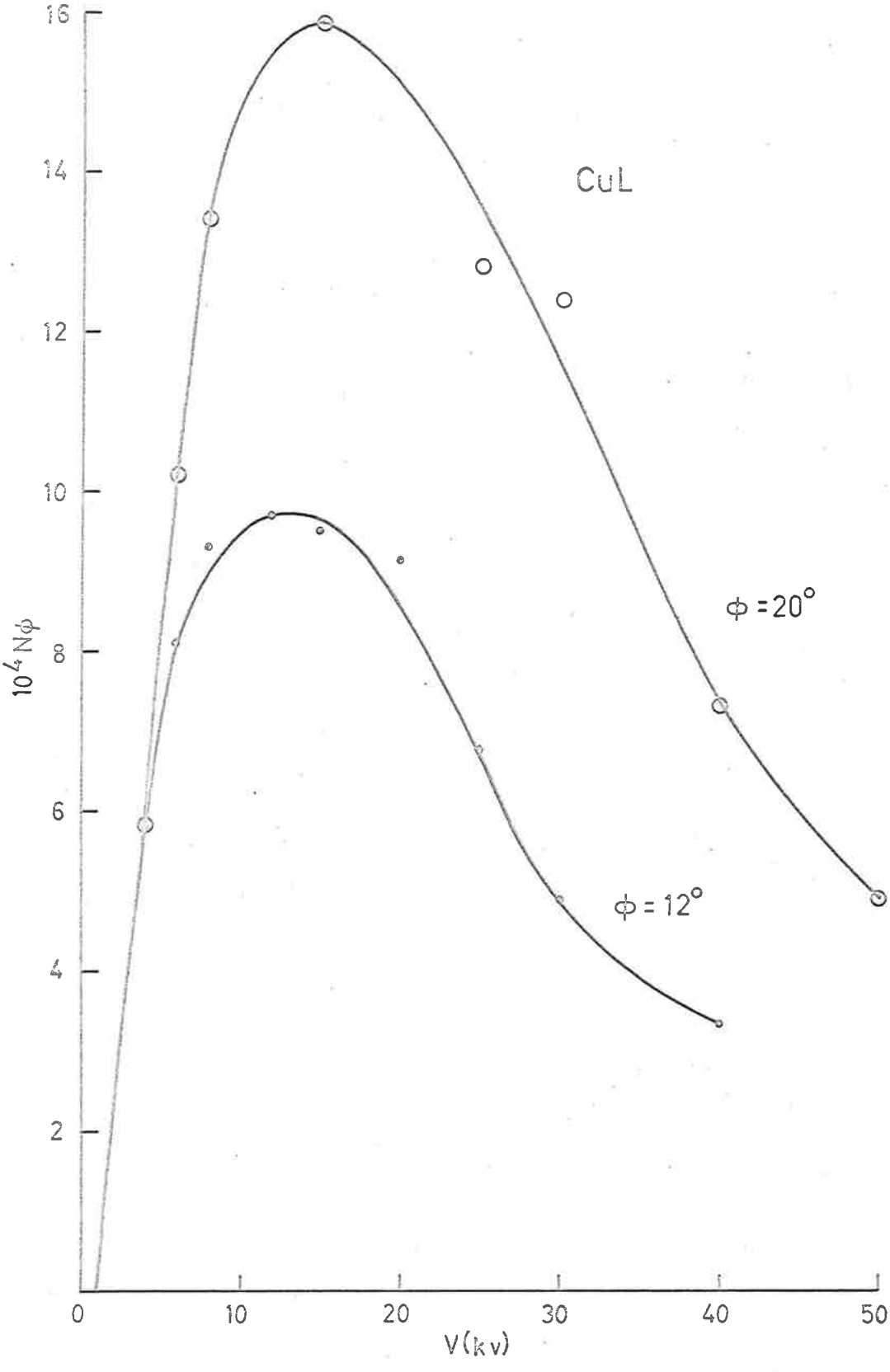

Experimental curves for total CuL radiation intensities.

Figure 4.22

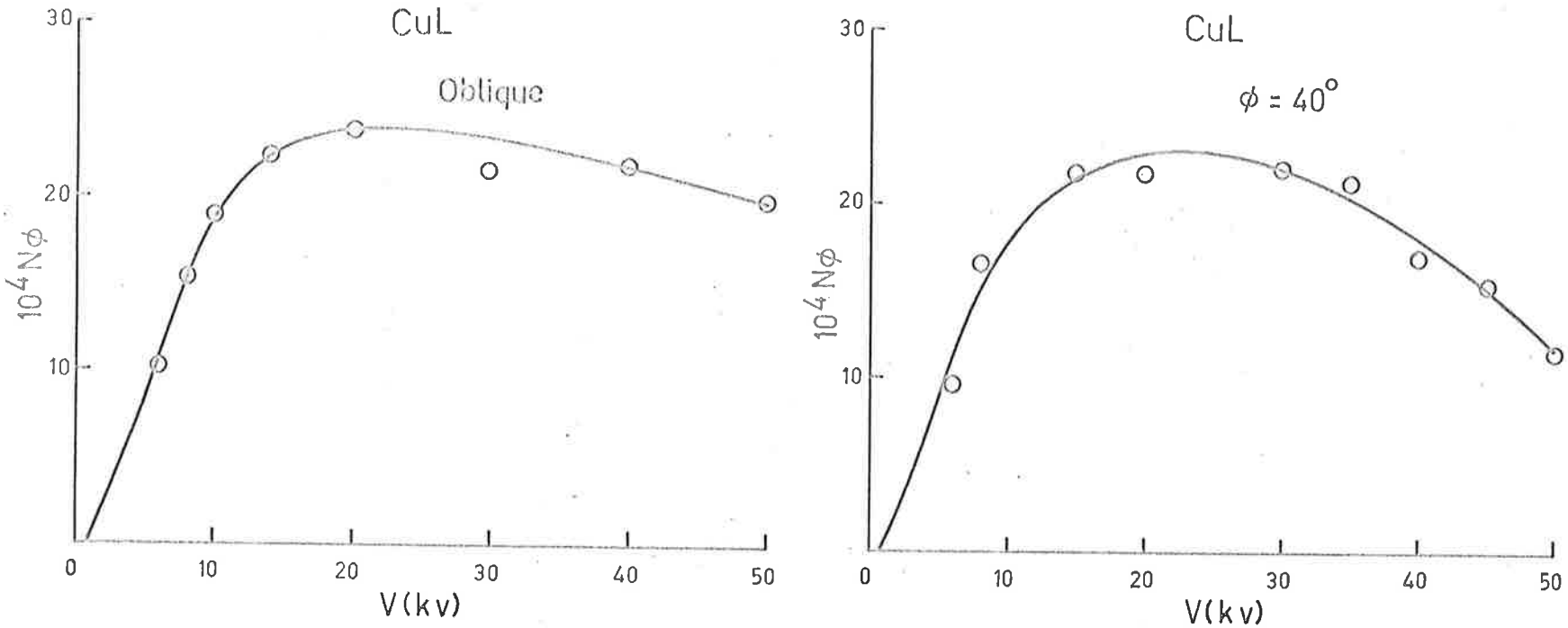

Figure 4.23 Experimental curves for total CuL radiation intensities.

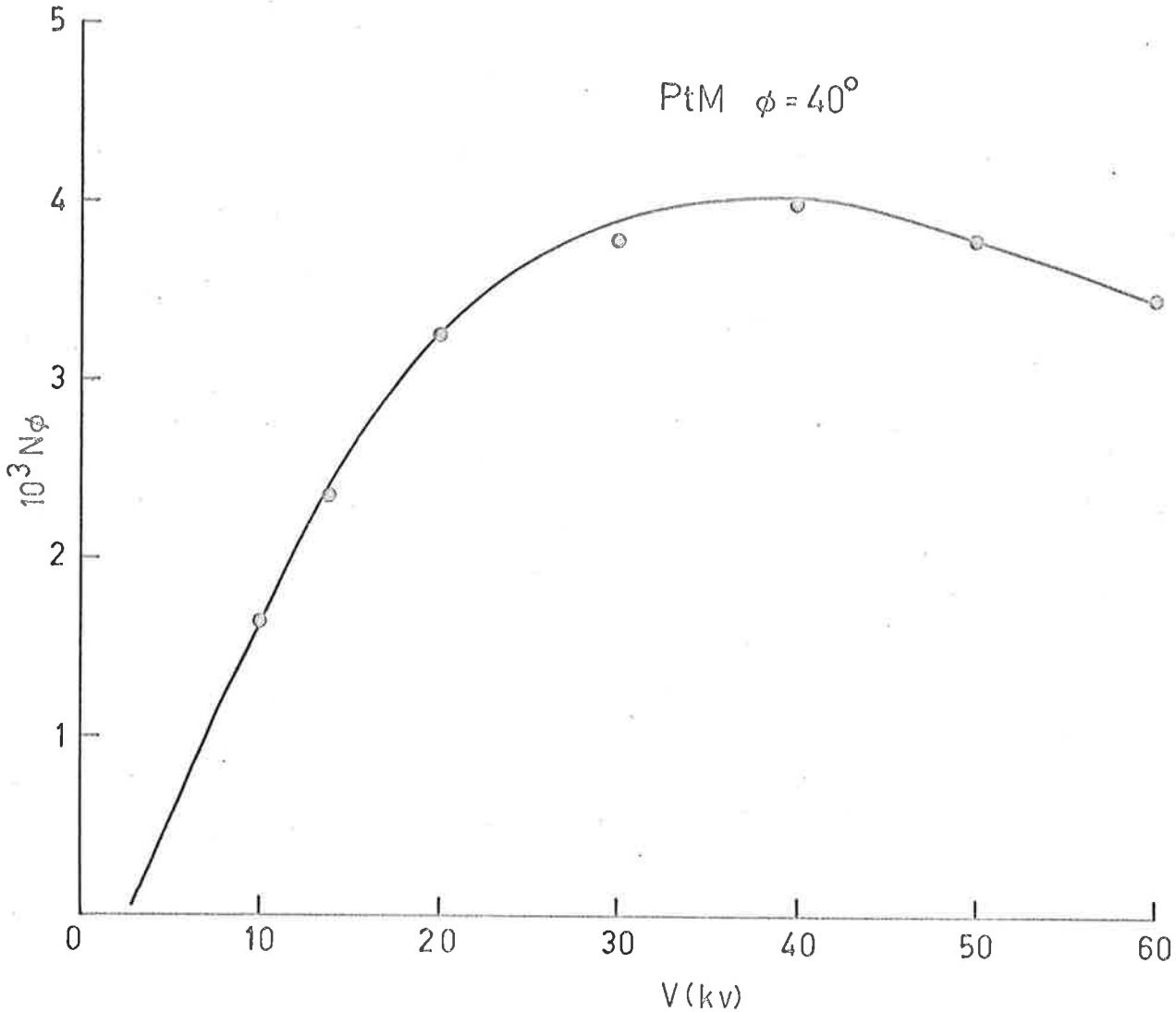

Experimental curve for total PtM radiation intensities.

Figure 4.24

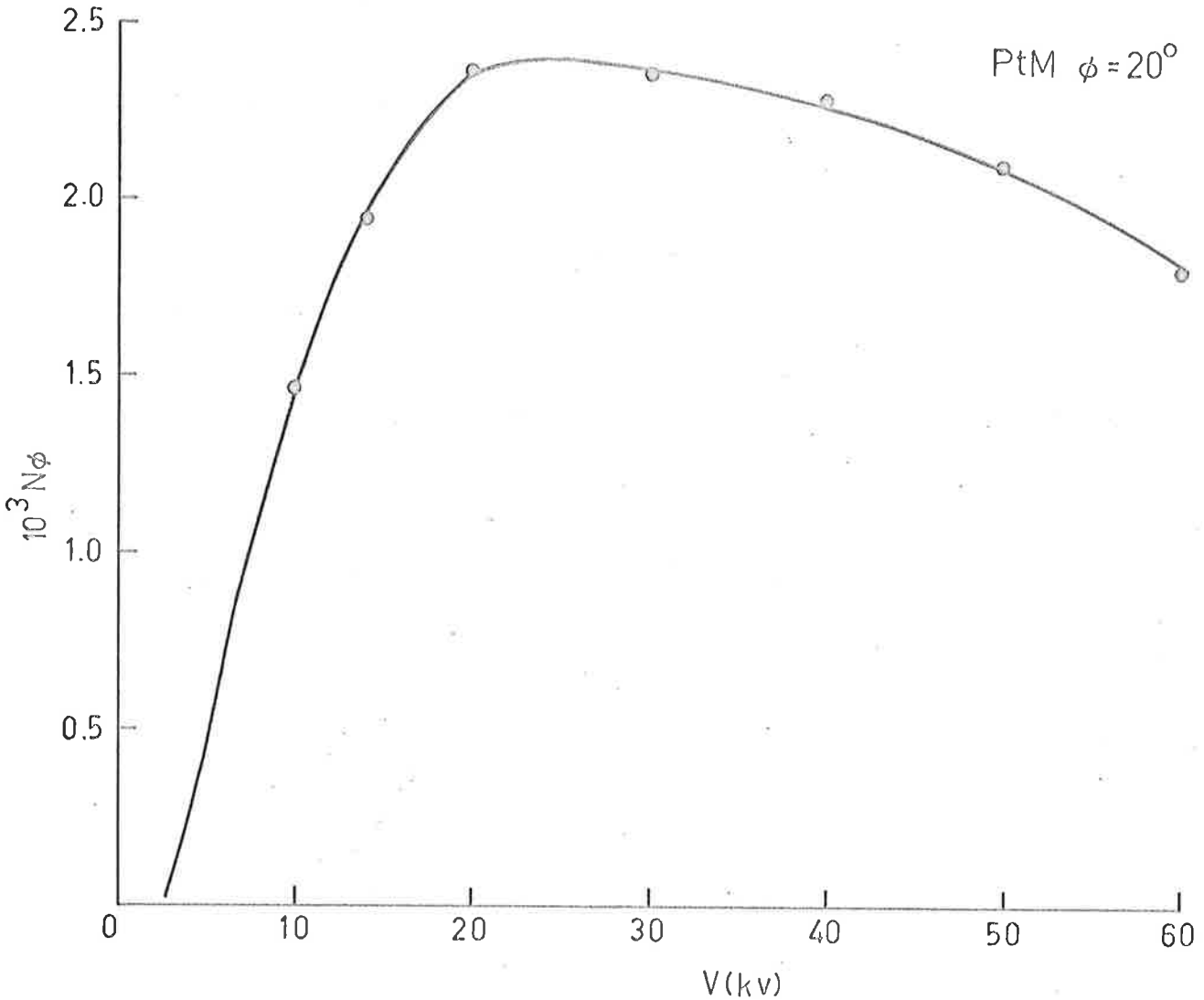

Experimental curve for total PtM radiation intensities.

Figure 4.25

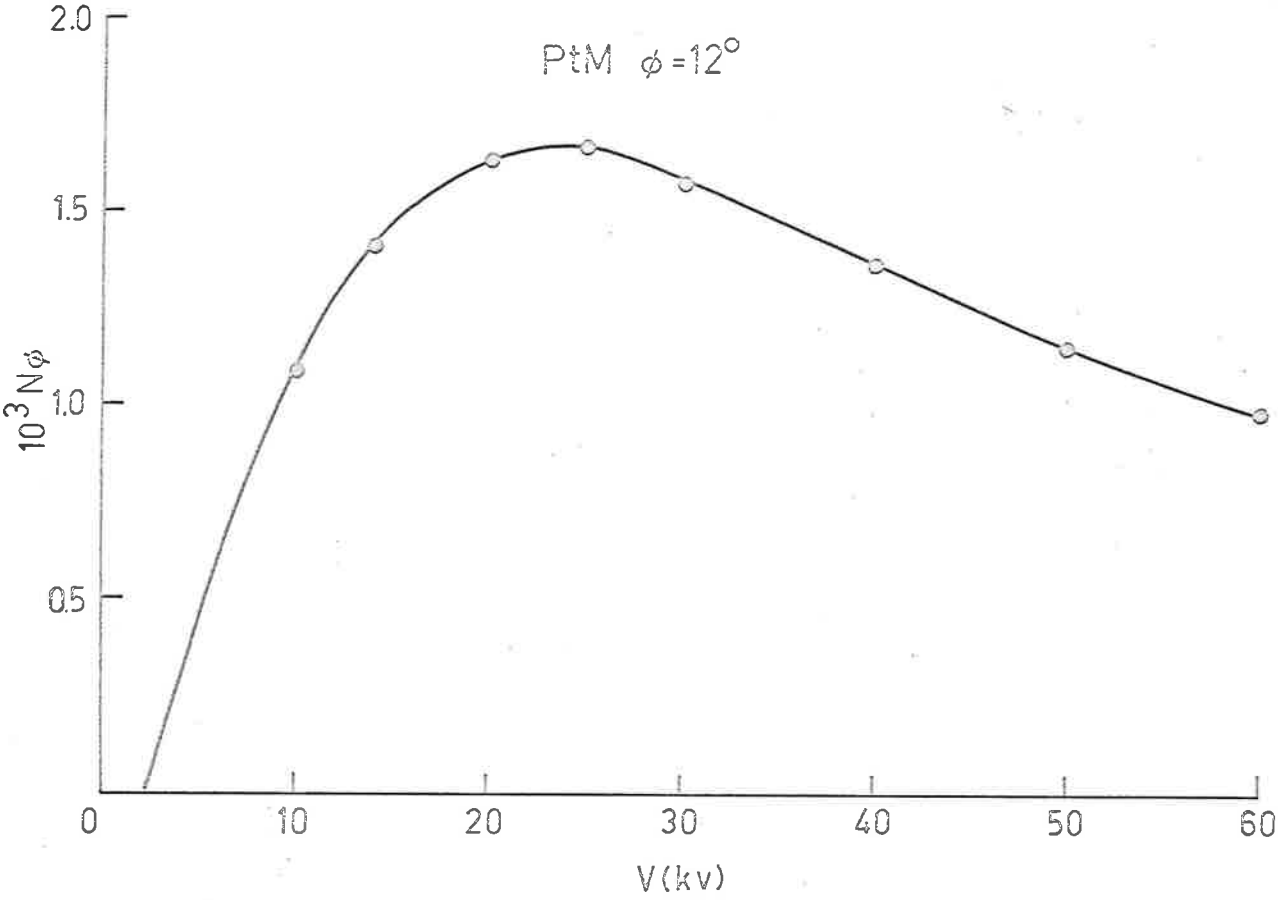

Experimental curve for total PtM radiation intensities.

Figure 4.26

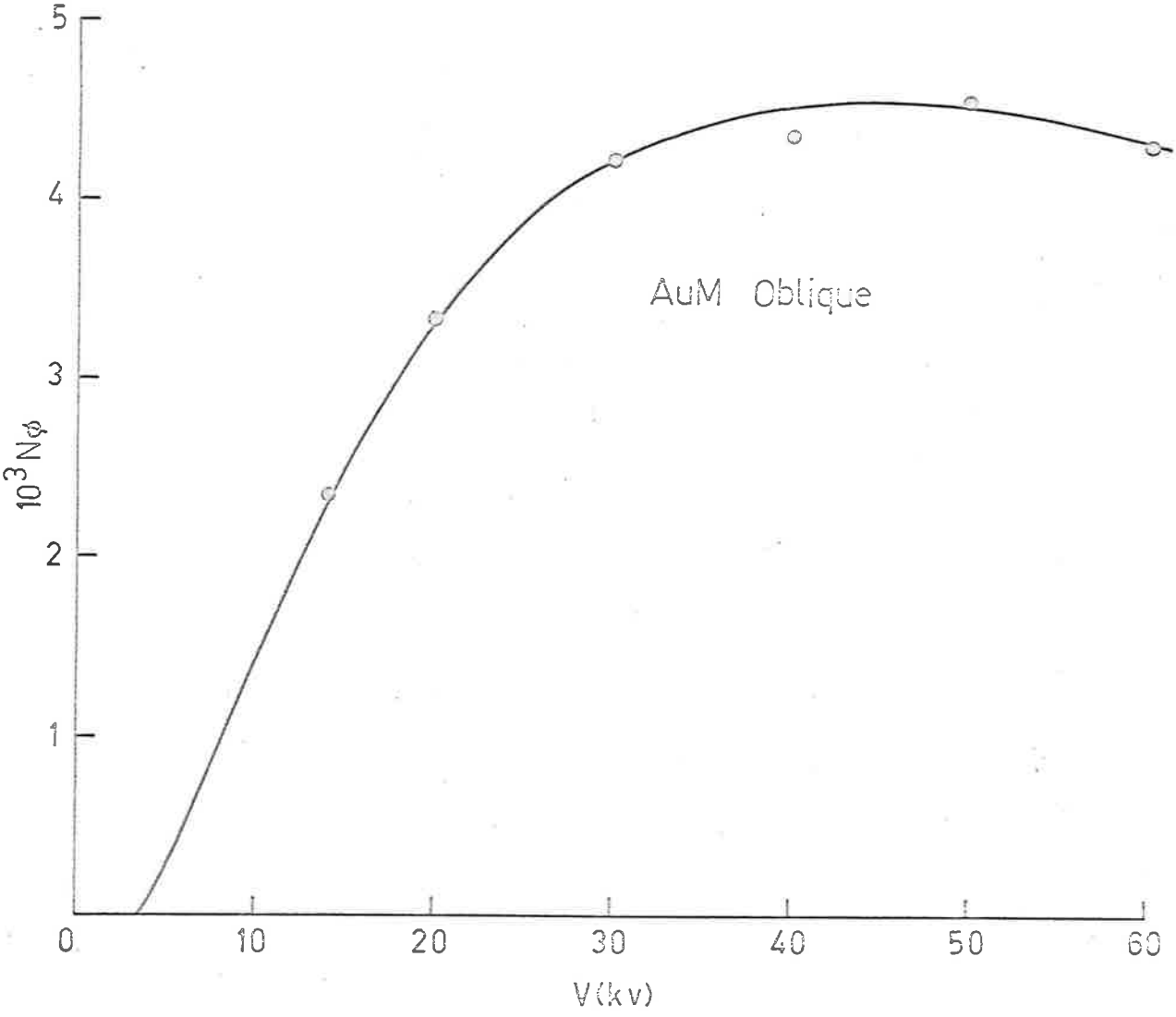

Experimental curve for total AuM radiation intensities.

Figure 4.27

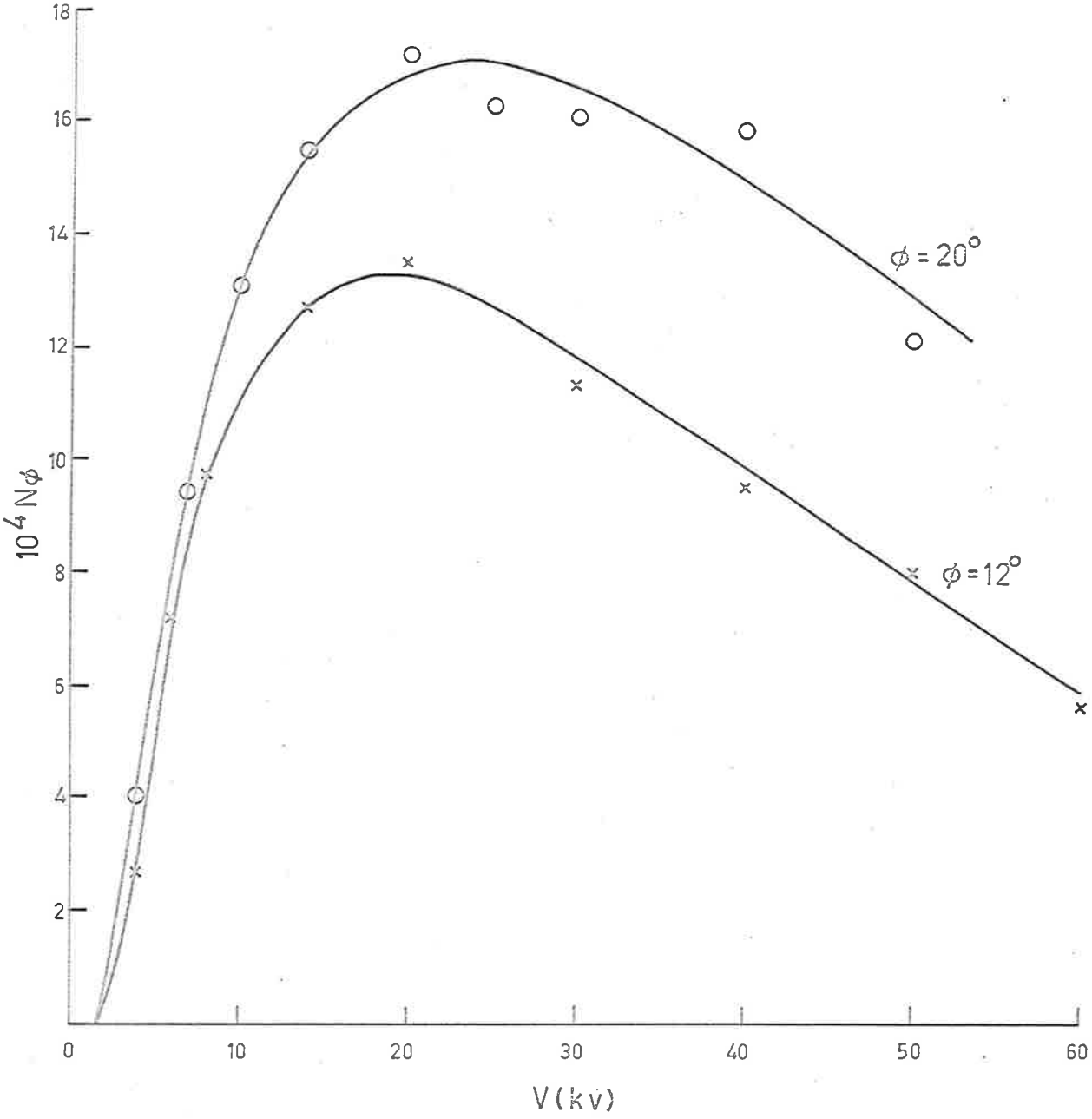

Experimental curves for total WM radiation intensities.

Figure 4.28

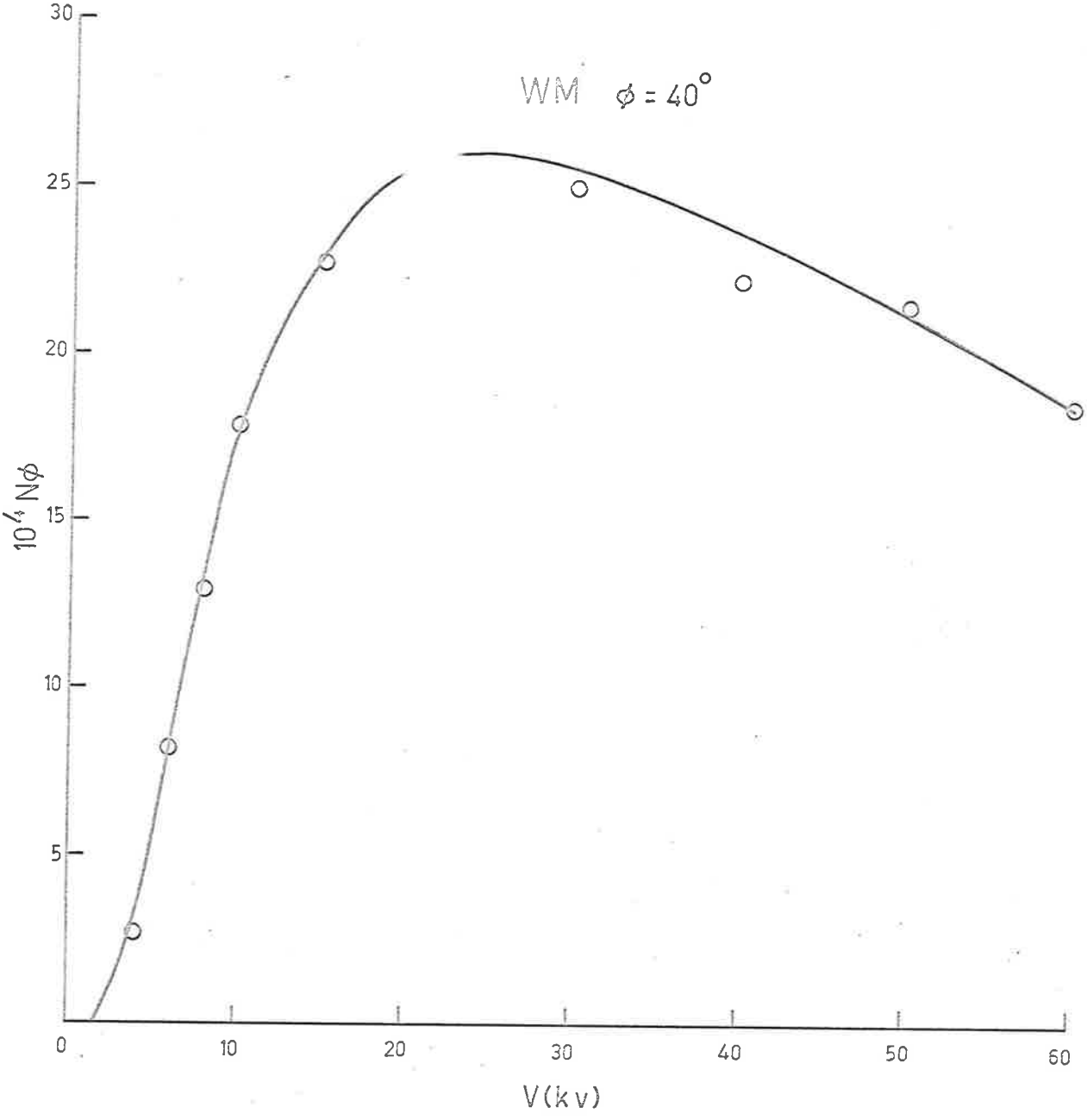

Experimental curve for total WM radiation intensities.

Figure 4.29

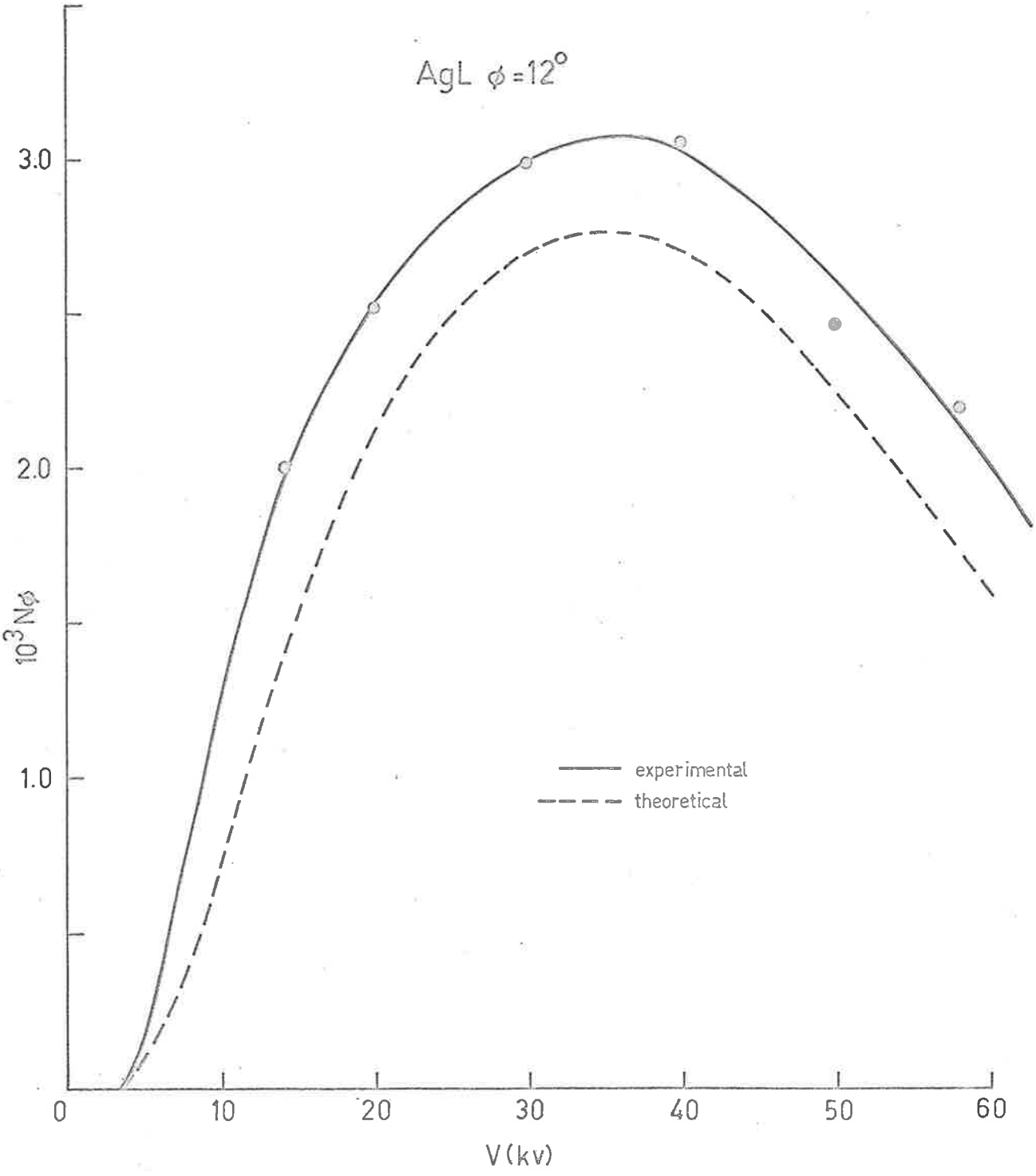

Figure 4.30 Theoretical and experimental curves for total AgL radiation intensities.

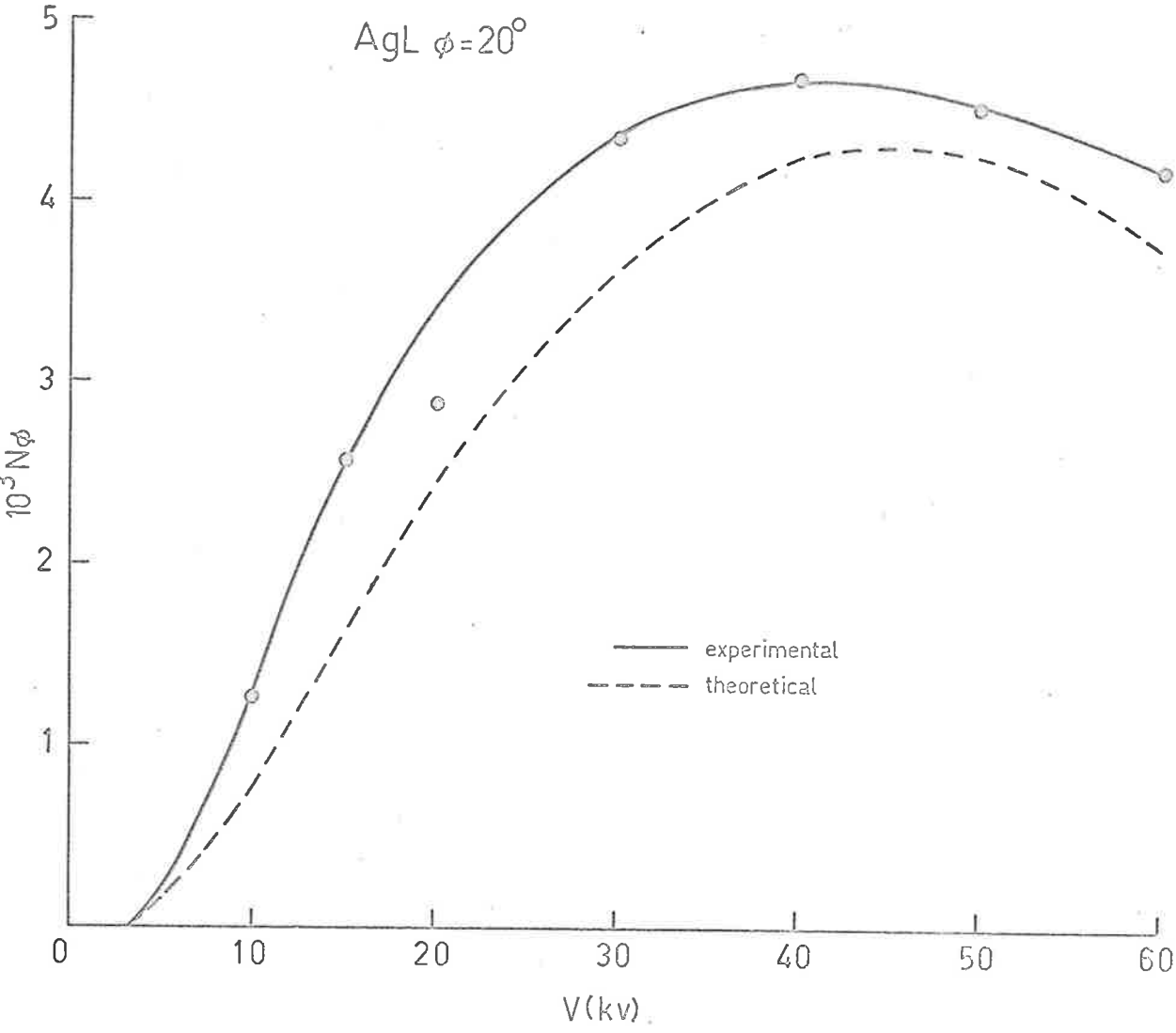

Figure 4.31 Theoretical and experimental curves for total AgL radiation intensities.

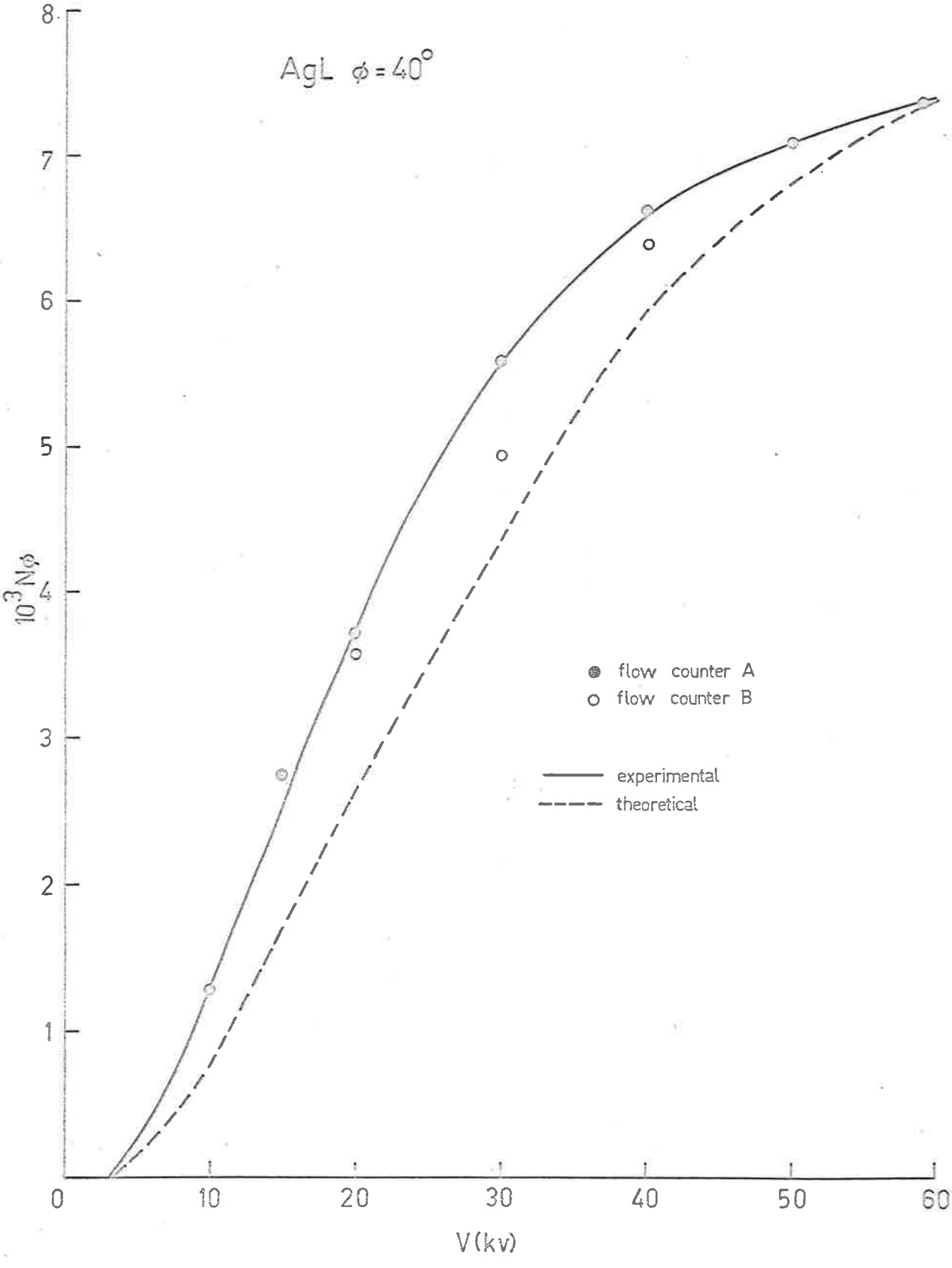

Figure 4.32 Theoretical and experimental curves for total AgL radiation intensities.

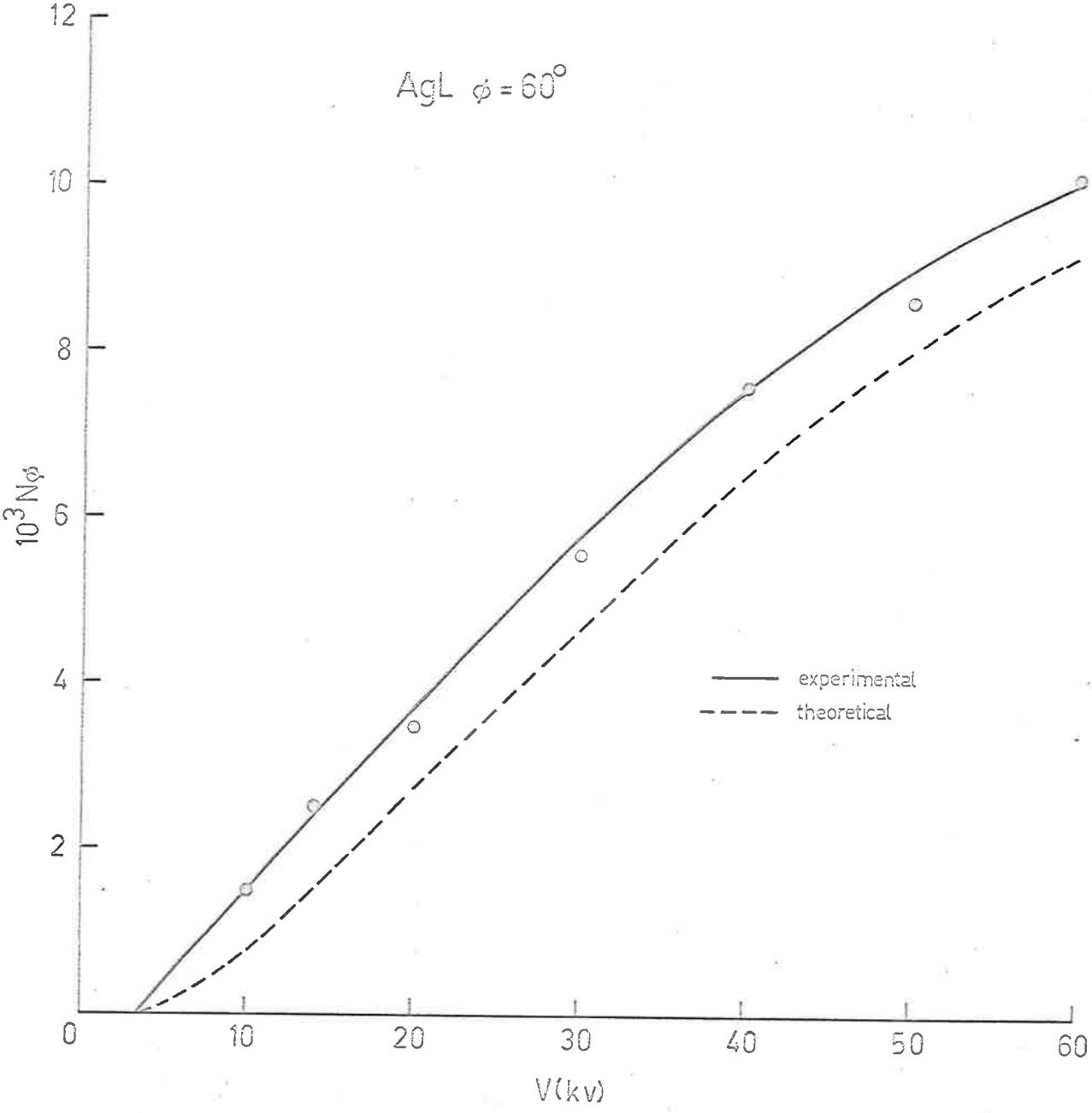

Figure 4.33 Theoretical and experimental curves for total AgL radiation intensities.

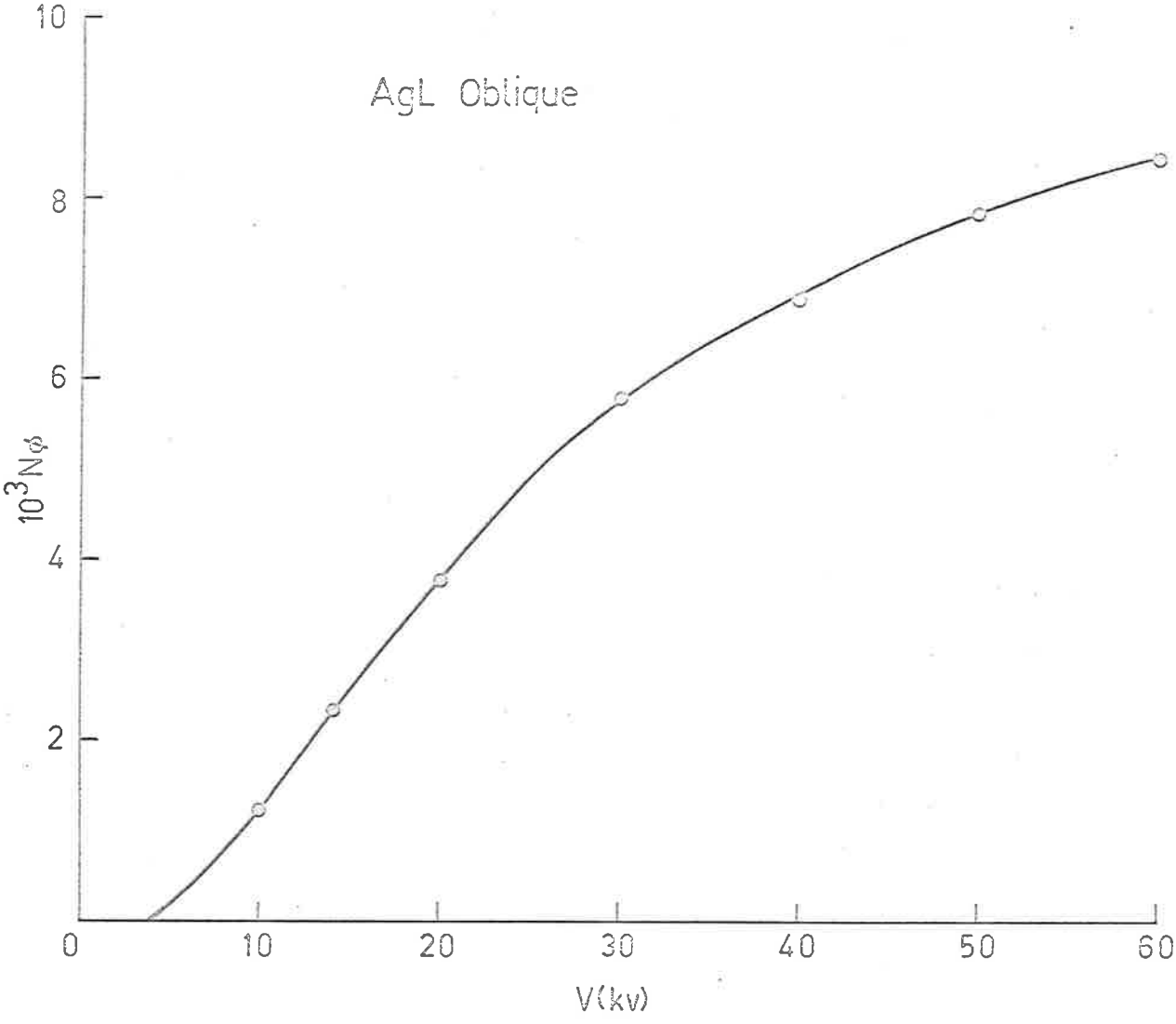

Figure 4.34 Experimental curve for total AgL radiation intensities.

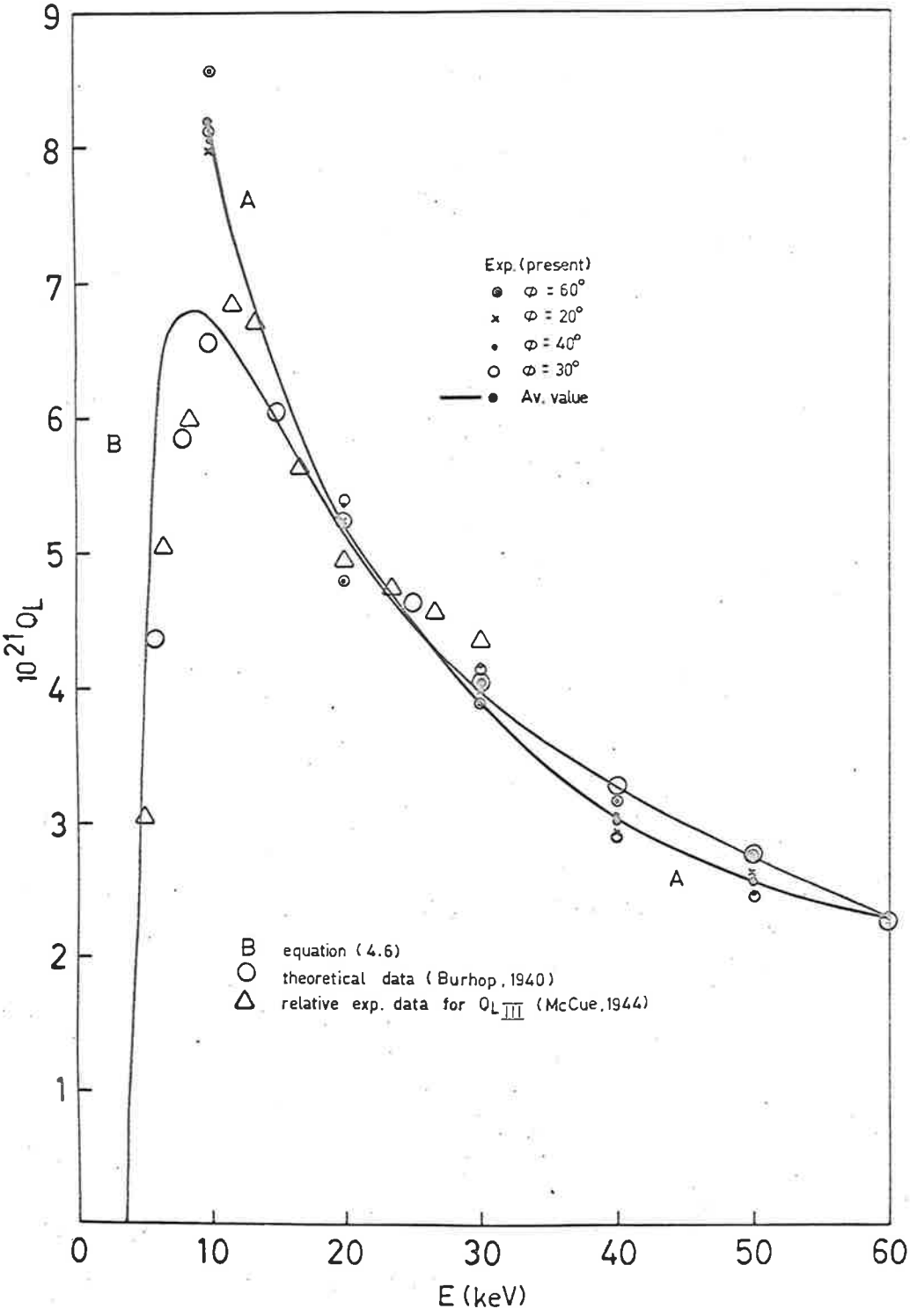

Figure 4.35 Total L ionization cross-sections for Silver.

the only comprehensive source of data for the mass absorption coefficient of the elements for ultra soft radiations. Their semi-empirical formula is only valid for the absorption of radiations of wavelengths up to the L-critical absorption wavelength. The only studies on the L or M ionization cross-sections are those of Burhop (1940) and McCue (1944). Using the Born approximation and neglecting the relativistic effects and the exchange between scattered and ejected electrons, Burhop (1940) calculated the ionization cross-sections of the three L-states of silver and mercury. A relative experimental curve for the ionization cross-section of the L_{III} state of silver was determined by McCue (1944). The theoretical calculations for the AgL intensities are discussed in the next section of this chapter.

4.9 Theoretical calculations of the AgL radiation intensities.

For the intensity calculations, it is desirable to use a less complex expression for the L ionization cross-sections than Burhop's (1940) formula. Owing to the fact that the shape of Burhop's theoretical curve for the AgL cross-sections is similar to that of the curves for the K ionization cross-sections, and that good agreement exists between the semi-empirical formula of Worthington and Tomlin (1956) (equations 2.1 and 2.2) and equation (2.4) for the K cross-sections (section 2.2), an attempt has been made to modify Worthington and Tomlin's expression to suit the L cross-sections. It was found that the following expression for the total L ionization cross-sections, Q_L, agrees closely with

Burhop's (1940) theoretical results,

$$Q_L = \frac{2\pi e^4}{T\,T_L}\ 1.05\ \ln(4T/B) \qquad \ldots(4.6)$$

Where T_L is the L excitation energy and B is given by equation (2.2). The only modification to equation (2.1) necessary was the value of the constant b. The resultant curve (curve B) together with Burhop's (1940) theoretical results are shown in figure (4.35). The L cross-sections for each sub atomic state were given by Burhop. Burhop's results, shown in figure (4.35), were obtained by adding weighted values of the cross-sections of each sub-state. The weights were adjusted according to the number of electrons in each state, i.e.

$$Q_L = 2Q_{L_I} + 2Q_{L_{II}} + 4Q_{L_{III}}$$

The peak of the curve B derived from equation (4.6) appears at a lower energy than that of Burhop's results (figure 4.35). This situation is similar to that encountered in the comparison of the two corresponding formulae for the K cross-sections (section 2.2). McCue's (1944) relative experimental data for $Q_{L_{III}}$ have been included in figure (4.35). These data are fitted with Burhop's result at 10 keV electron energy. As in the case of the K cross-sections, there is a slightly better agreement between the experimental results with Burhop's formula than with equation (4.6). The trend of McCue's relative data indicates that the theoretical cross-sections are underestimated at high energies.

Using Tomlin's (1964) formula, the correction factor for the backscattered electrons was computed for 40 keV electrons incident normally on a silver target. For AgL radiations emitted at 20° to the target surface, the value obtained was the same as Tomlin's correction factor for AgK radiations at 40 keV electron energy. This is reasonable, as Tomlin's formula for R, the correction factor, indicates that the difference in the values for R for K and L radiations of the same element is mainly caused by the difference in shape of the experimental intensity curves for the two radiations. Up to 40 keV there is little difference in shape between the intensity curves for the K and L radiations of silver. For these reasons, Tomlin's correction factors were used for the present AgL calculations. There is some error in this procedure for calculating the intensities at low angles of emission, where the shape of the intensity curve for AgL differs from that of AgK at high energies. As Tomlin's results for K radiations indicate that the variation of R with both the electron energy and the angle of emission is small, it is unlikely that the error is serious.

Several experimental mean fluorescence yield values, $\bar{\omega}_L$, were compiled by Fink et al (1966) for the AgL radiations. These vary from 0.029 (Bertolini et al, 1954) to 0.1 (Lay, 1934), the average being approximately 0.05, which is similar to the value of Bertrand et al (1959). In spite of the fact that Lay used fluorescent excitation to obtain his result and that $\bar{\omega}_L$ depends on the mode of excitation

(Burhop, 1952). Using equation (4.6) for Q_L there is good agreement between the present experimental results and the theoretical intensities derived from an equation similar to the intensity formula (2.12) if Lay's (1934) value of 0.1 is used. Figures (4.30) to (4.33) indicate that the theoretical intensities are lower than the corresponding experimental results by about 15%.

In the theoretical calculations only those L ionizations directl caused by incident electrons have been considered. There is a probability of vacancies being created in the L shells following an ionization of the K shell. However this effect on the resultant intensities must be relatively small as Q_L is about two orders of magnitude higher than Q_K for silver and the average fluorescence yield for this process is small (Fink et al, 1966).

4.10 Approximate Method for deriving ionization cross sections from thick target experimental intensity data.

Owing to the lack of experimental data for ionization cross-sections for L and M electrons, an approximate method has been devised for deriving the cross-sections from a combination of the intensity formula (2.12) and the experimental intensity results. The validity of the intensity formula (2.12) has been shown for the K radiations. In section (2.8), it was shown that $Q_K \frac{ds}{dt}$ is approximately constant and equal to its value at To, for electron energies several times that of the excitation energy. For L and M radiations, for which the excitation energies are low, except for those elements of high atomic numbers,

it is expected that the above assumption holds good for these radiations over most of the energy range up to 60 keV.

From equation (2.12), and assuming

$$Q_L \frac{ds}{dT} = \text{constant} \qquad \ldots(4.7)$$

and is equal to its value at T = To

$$N_\phi = kN\left(Q_L \frac{ds}{dT}\right)_{To} \int_{T_o}^{T_L} e^{-\mu \rho\langle x\rangle \operatorname{cosec}\phi \cos\theta} \, dT$$

where Q_L, T_L are the total L ionization cross-section and the L excitation energy respectively and μ is the mass absorption coefficient of the element for its own L radiations.

$$(Q_L)_{To} = \frac{N_\phi}{kN\left(\frac{ds}{dT}\right)_{To} \int_{T_o}^{T_L} e^{-\mu \rho\langle x\rangle \operatorname{cosec}\phi \cos\theta} \, dT} \qquad \ldots(4.8)$$

Experimental results may be used for N_ϕ. The effect of any error in the theoretical target absorption correction term may be reduced by considering the intensities corresponding to high angles of emission only, where the target absorption is not so important.

The total L ionization cross-sections for silver derived from equation (4.8) are included in figure (4.35). A value of 0.1 was used for ω_L (discussed in section (4.9)). Calculations were made using experimental intensity data for $\phi = 20^\circ$, 30°, 40°, and 60° for normal electron beam incidence. The scatter in the values for Q_L derived from

experimental intensity data obtained under different emission conditions is small. Curve (A) is the curve drawn through the average values obtained. Figure (4.35) shows that there is good agreement between the cross-sections derived from the experimental intensities and the curve calculated from equation (4.6) (curve (B)) and also with Burhop's (1940) theoretical results for electron energies exceeding 15 keV. The discrepancies at low electron energies are mainly caused by the breakdown of the assumption (4.7) at these energies.

To evaluate (4.8), the values for both the fluorescence yield and the mass absorption coefficient of the target element for its own L or M radiations must be known. Calculation of the L and M ionization cross-sections for elements other than silver is not possible as both these quantities are either uncertain or unknown.

Conclusion.

In the calculations of characteristic K intensities excited in light elements, there is uncertainty in the data available for the atomic fluorescence yield. For K radiations excited in elements of moderate atomic numbers, for which the various component terms of the theoretical emission formula are better known, comparison of the theoretical intensities with the experimental results indicates that the Tomlin formula as represented by equation (2.12) is a satisfactory expression for the quantum yield. The approximations in its derivation are second order effects. The assumption that the target medium is infinite in extent in the derivation of $\langle x \rangle$, the average depth of electron penetration, has little effect on the theoretical intensity results except for the softer radiations, for which the target absorption factor is more important. The generally good agreement between the calculated and observed intensity results indicates that the resulting overestimation of the calculated intensities by the assumption mentioned above is counter-balanced by the underestimation of the intensities through the use of $\langle x \rangle$ in the target absorption term instead of a true distribution in x, the depth of electron penetration.

There is no available data for the K fluorescence yield for carbon. The value obtained from a comparison of the theoretical and experimental intensities for CK radiations is approximately 50% higher than Burhop's (1952) theoretical value.

The validity of the simple Tomlin-Worthington formula for the K ionization cross-section extends to light elements. However, comparison with experimental data, indicates that the more complete expression, equation (2.2), is more accurate at higher energies.

As the only available experimental data for the K cross-sections for light elements are those of helium, more measured results are needed for testing the validity of the expressions currently used. There is a similar need for experimental investigations on the atomic fluorescence yield for light elements.

The approximate formula derived in section (2.8) has been shown to be quite accurate for K radiation excited in light elements. This simple expression is of use for rapid calculations of the radiation intensities.

For the L and M intensity calculations, information in the atomic fluorescence yield, the ionization cross-section and the mass absorption coefficient of the element for its own characteristic radiations is limited. It has only been possible to calculate the theoretical AgL radiation intensities. It has been found that an approximate formula, similar to the K cross-section formula of Worthington and Tomlin (1956), may be used for the AgL cross-sections. The procedure in estimating the cross-sections from thick target intensity results has been shown to be satisfactory for the AgL cross-sections.

Extension to the

studies on the emission intensities to cover L and M characteristic radiations would require further studies on the atomic fluorescence yield, the ionization cross-section, and in particular, the mass absorption coefficient of the elements for its own characteristic radiations, for which only that for the AgL radiations is known.

***

PART B

Absolute Intensities of Characteristic Radiations excited by Protons

PLATE B1

Apparatus for the Emission Intensity Studies of Characteristic Radiations excited by Protons.

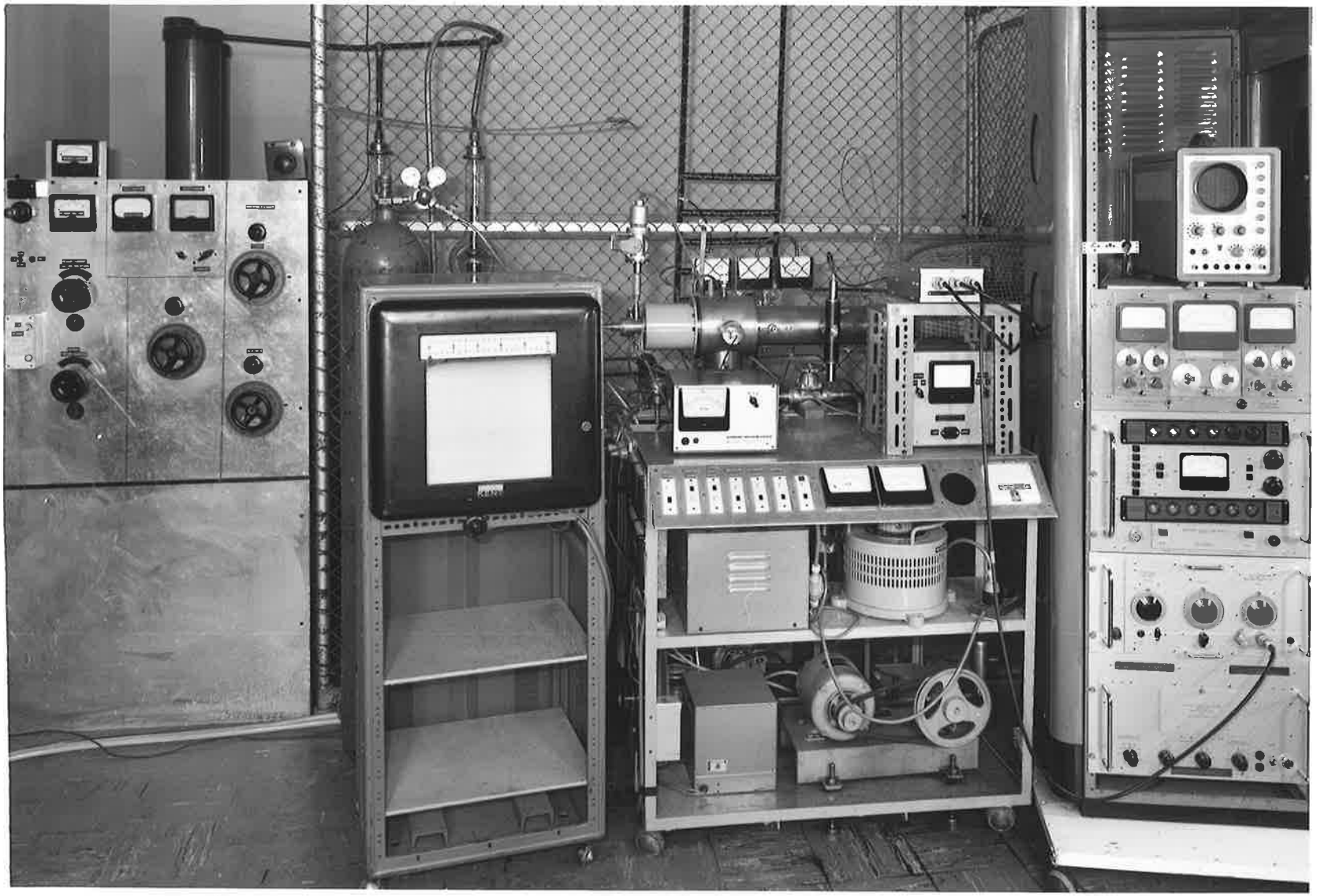

CHAPTER I Introduction

1.1 Review of Literature.

The detection of characteristic radiations excited by positive ions was first reported by Bothe and Franz (1929). Gerthsen and Reusse (1933) extended the investigation to proton excitation. They were able to show that the relationship between the excitation function and the incident particle energy was in qualitative agreement with the results of Bothe and Franz (1929). Similar work was carried out by Peter (1936), whose single absolute yield measurement was given as 1.6×10^5 proton per AlK photon at 132 keV proton energy. The functional form of the variation of his excitation function with energy was found to be consistent with the theoretical considerations of Henneberg (1933), whose analysis showed to a first approximation the intensity varying as the 4th power of the incident energy. In both of these experiments the detector was placed behind a thin target to receive the emitted radiations. The purity of the characteristic beam was established solely on the basis of a comparison between the experimental attenuation factor, obtained by interposing an aluminium foil in the beam, and its calculated value.

Most studies in this field were carried out in the MeV range of energies. These include the relative intensity measurements of Livingston et al (1937), Simane and Urbanec (1955), and the absolute yield studies of Lewis et al (1953) and Bevington and Bernstein (1956).

Their results were reviewed by Merzbacher and Lewis (1958), who also discussed the theoretical aspect of this subject and traced its development from the early classical solution to the more recent quantum mechanical approach. They confined their discussion to an incident particle energy range between 100 keV and 5 MeV and for target elements of atomic number exceeding 10.

Mathematical complexity involved in the numerical solutions required a number of approximations. Using the Born approximation and hydrogenic wave functions and neglecting all atomic screening effects, they obtained an approximate solution for the total K ionization cross-section. The resultant cross-section was found to be directly proportional to the 4th power of the particle energy and inversely proportional to the 12th power of the atomic number of the emitter element. The result was identical with the first term of Henneberg's (1933) series solution. A more complete mathematical solution was also given but it still contained the approximations used in the preliminary theory, except that the work of Slater (1930) was used to describe the screening effect by the inner orbital electrons. The theoretical results were found to be consistent with the existing experimental data.

With the advent of more accurate radiation detectors, absolute measurements were extended to proton energies of an order of a hundred keV (Messelt, 1958; Singh, 1957; Jopson, Mark, and Swift, 1962; Khan and Potter, 1964). Messelt (1958) indicated that the use of the Born approximation, in which plane waves were used to describe the incident

and the scattered particle, resulted in an overestimation of the ionization cross-section, Q_K, at low energies. He derived an empirical formula for Q_K which was shown to be in good agreement with his data for FeK, CuK, MoK and AgK down to 140 keV incident proton energies, at which energy, the K radiation yield emitted from a copper target was given as 1.3×10^{-9} photon per proton. His work suggested that Q_K varied as $E^{4.5}$, where E is the incident proton energy.

Messelt's (1958) observation concerning the validity of the Born approximation was supported by Jopson, Mark, and Swift (1962), who investigated K and L emissions under proton excitation within the incident energy range between 100 keV and 500 keV. They found that their results and those of Messelt (1958) were in better agreement with the theory of Bang and Hansteen (1959), in which the coulomb deflection of the incident particle by the nuclear field was considered.

Studies on the L and M radiation emission intensities were reported by Khan, Potter, and Worley (1964a, 1964b). The quantum yields for the CuL radiations were several orders of magnitude higher than the corresponding values for the CuK radiations.

Recently, experimental investigations on the K characteristic radiations excited by protons of energies less than 50 keV were made. These include the relative AlK and MgK measurements of Brandt, Laubert, and Sellin (1966) and the absolute CK, MgK, and AlK results of Khan, Potter, and Worley (1965), whose measurements extend to 25 keV proton energy.

Intensity studies on the K characteristic radiations excited by low energy protons are limited. The lowest proton energy at which the CuK radiation intensities were determined was 140 keV (Messelt, 1958), and for AlK radiations, 25 keV (Khan, Potter, and Worley, 1965).

1.2 Preliminary calculation of the CuK Quantum Yield.

The object of this part of the project is to make preliminary measurements of the absolute intensities of characteristic radiations excited by protons of energies less than 50 keV in metal elements. Past experimental studies at higher proton energies (e.g. Messelt, 1958; Khan and Potter, 1964) indicated that the characteristic intensities excited by protons are several orders of magnitude lower than the intensities obtained under electron excitation. For this reason, it is first necessary to make an approximate calculation to estimate the beam current required for a successful investigation.

To a first approximation, Merzbacher and Lewis (1958) arrived at the result,

$$Q_K \quad \alpha \quad \frac{E_o^4}{Z^{12}} \qquad \ldots(B1.1)$$

where Q_K is the K ionization cross-section, E_o is the incident proton energy and Z is the atomic number of the target element.

It is desired to calculate the thick target yield of CuK radiations excited by 50 keV protons. The proportionality (B1.1) and the discussion of Merzbachen and Lewis (1958) indicate that if it is

possible to detect CuK radiations excited by 50 keV protons, then it is possible to detect the K radiations excited in target elements of atomic number less than that of copper (Z = 29) and also the L radiations.

Whaling (1958) gave the mean range of 100 keV protons in copper as 0.552 mg/cm^2 or 6.2 x 10^{-5} cm. The mean range of 50 keV protons in copper would be so small that the target absorption of the characteristic radiations could be neglected.

Following the intensity formula for electron excitation (equation 1.1, Part A) and neglecting the target absorption correction term,

$$N_{\phi} = k \int_{E_o}^{E_K} N Q_K \frac{dx}{dE} \, dE \qquad \ldots(B1.2)$$

where E_K and E_o are the K excitation energy and the incident proton energy respectively, and $\frac{dE}{dx}$ is the stopping power of copper for protons. Owing to the uncertainty in the theoretical expressions for Q_K and $\frac{dx}{dE}$ at low proton energies, empirical expressions are employed. For protons of energies of the order of several hundreds of keV, Messelt (1958) found that Q_K for copper obeyed the following proportionality,

$$Q_K \quad \alpha \quad E^{4.5} \qquad \ldots(B1.3)$$

Assuming that the validity of this relationship extends to the energies defined by the limits of the integral (B1.2) and using Messelt's (1958) result for CuK yield at 140 keV,

$$Q_K = 3.72 \times 10^3 \; E^{4.5} \qquad \ldots(B1.4)$$

where E is the proton energy in ergs and Q_K is the K cross-section in cm^2.

Whaling (1958) tabulated values of the atomic stopping cross-sections ε for protons in copper. Values for ε were given at 50 keV and 75 keV proton energies. As ε did not vary much with the proton energy for these energies, it was assumed that ε varied linearly with E for proton energies less than 50 keV. The values for ε at 50 keV and 75 keV were used for evaluating the constants of the linear relationship between ε and E. The following equation was obtained,

$$\varepsilon = 8 \times 10^{-21} E + 2.72 \times 10^{-26} \qquad \ldots(B1.5)$$

where E is the proton energy in ergs and ε is the atomic stopping cross-section in erg-cm^2.

$$\text{Now,} \qquad \varepsilon = -\frac{1}{N}\frac{dE}{dx}$$

$$\text{or,} \qquad \frac{dE}{dx} = -N\varepsilon \qquad \ldots(B1.6)$$

Substituting equations (B1.4) and (B1.6) in (B1.2) and integrating numerically, a value of 2×10^{-11} k photons/proton was obtained for the quantum yield at 50 keV incident proton energy. Assuming the value of the k factor to be approximately the same as that for electron excitation, a value of 1×10^{-11} CuK photon/proton was obtained at 50 keV incident proton energy.

For a milliamp proton beam current and assuming that the detector window subtends a solid angle of 10^{-3} ster-radians at the target, the

number of counts per second registered by a detector, whose QCE is 0.5 for CuK radiations, would be 5. This would give a signal-to-noise ratio of 3. If need be, the solid angle subtended by the counter window at the target could always be enlarged. In any case, past studies (e.g. Merzbacher and Lewis, 1958) have suggested that the characteristic quantum yield increases rapidly with a decrease in atomic number of the emitter element and that the L characteristic yields are several orders of magnitude higher than the corresponding K yields.

The approximate calculation given above indicates that provided the incident proton current is of the order of a milliamp, it shall be possible to detect the K characteristic intensities excited in metal elements of atomic number $\leq$ 29. A description of the proton source which supplies a current of this magnitude is given in the following chapter.

CHAPTER 2 . Description of Apparatus.

2.1 Introduction.

The design for the proton source was adopted from Abele and Meckbach (1959). The author is grateful to them for sending him two articles (Abele and Meckbach, 1959a, 1959b) which give detailed descriptions of the operation of the source and the ion beam analysis. Owing to a lack of suitable power supplies, it was necessary to leave the proton source at earth potential and lower the target assembly to a negative potential. This arrangement was not ideal, but the experiment was intended only as a preliminary one. The effect of the secondary electrons emitted at the target assembly and the precaution taken are discussed in section (3.4). This arrangement also caused difficulty in analyzing the ion beam with a mass spectrometer. Due to a lack of time, mass analysis of the ion beam was not carried out. The results of Abele and Meckbach (1959b) were used.

As there was no blue-print available, it was not possible to reproduce exactly the design of Abele and Meckbach (1959). The actual constructional details remained the work of the author.

2.2 The Proton Source Assembly.

The protons were produced by the electron excitation of hydrogen gas. To increase the excitation probability, the electrons were made to spiral forwards and backwards along an arc chamber containing

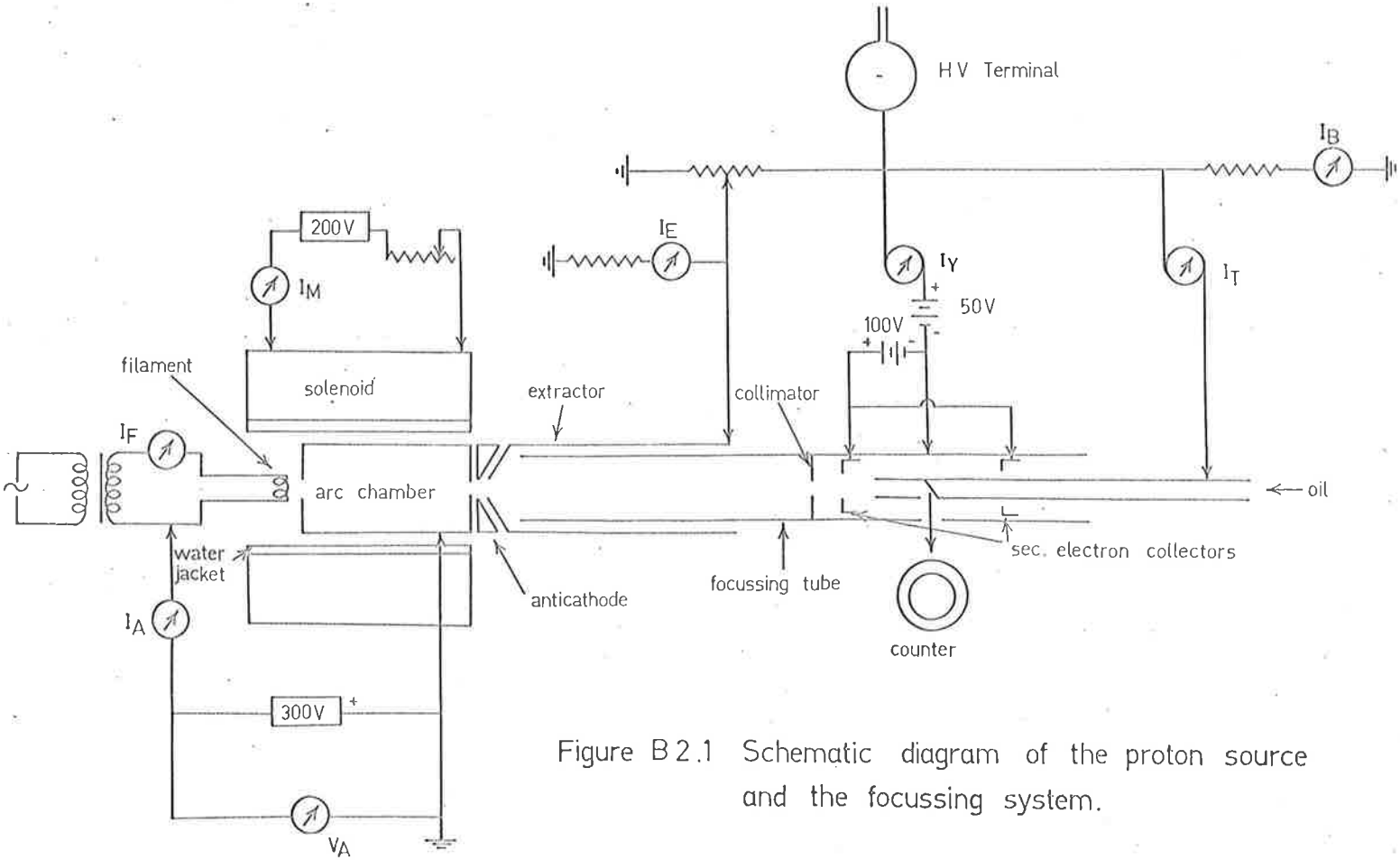

Figure B 2.1 Schematic diagram of the proton source and the focussing system.

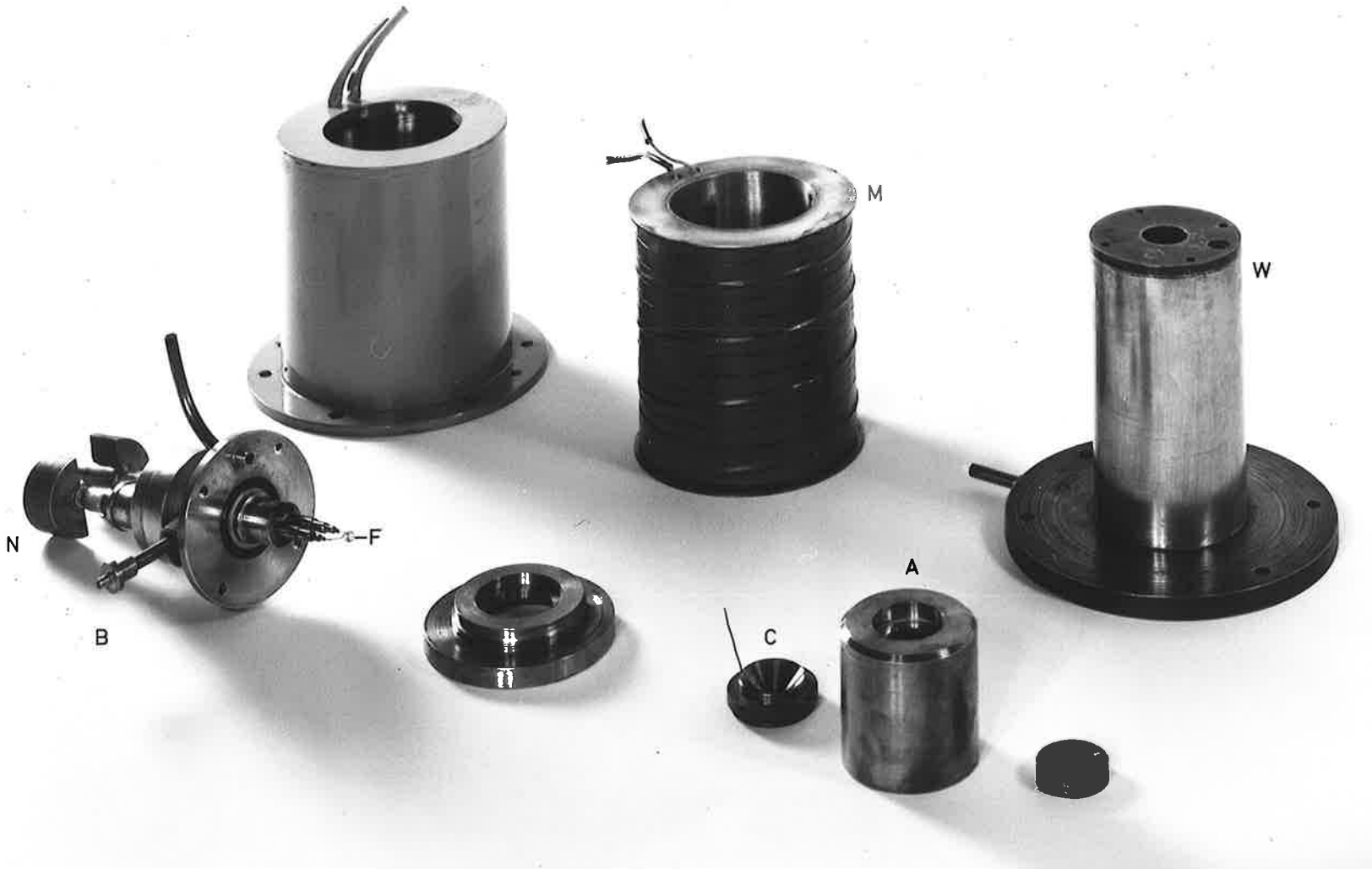

Plate B 2 Components of the proton source.

the gas. A schematic diagram of the proton source is included in figure (B2.1). Plate (B2) shows the actual components.

The electron source consisted of a $\frac{1}{2}$ mm tungsten filament F connected to a variable low voltage power supply. The filament was lowered to a negative potential with respect to the earthed arc chamber A by a continuously variable stabilized DC power supply. The emitted electrons drawn into the arc chamber were confined near the axis of the chamber by a collimator and an axial magnetic field produced by a solenoid M wound round the arc chamber. Power for the solenoid was derived from a 200 volt DC supply. Variation of the solenoid current was achieved by means of a rheostat connected in series with the power supply. The anticathode C, which consisted of a conical conductor with a 3 mm hole in its centre, was insulated from the body of the apparatus. The potential built up on it acted as a retarding potential for the electrons.

The filament assembly B was an easily detachable unit. The tungsten filament was set in steel holders which were in turn attached to brass rods leading to electrical connections outside the vacuum system via glass-to-metal seals. The steel holders maintained a sufficient thermal gradient along the conducting rods to the filament such that the filament current required was not excessive. Heat conducted back along the connecting rods was dissipated in fan-cooled copper fins N in order to protect the glass-to-metal seals.

The hydrogen gas dried over a P_2O_5 desiccator was leaked into

the arc chamber by means of a needle valve. The gas supply lines were evacuated before introducing the hydrogen into the arc chamber.

The arc chamber was cooled by means of a water jacket W.

2.3 The Focussing System.

The proton beam was focussed by an electrostatic lens system whose focussing properties were described by Abdie and Meckbach (1959b). The electrostatic lens system is included schematically in figure (B2.1) and the actual components are shown in Plate (B3). The protons were drawn out of the arc chamber by an extractor tube E and the beam was focussed by the focussing tube FT. The extractor was located concentrically in the earthed cylindrical body of the apparatus and insulated from it by means of perspex fins. The focussing tube was supported concentrically inside the extractor by three glass insulators G which passed through holes in the extractor and were attached to vacuum seals S connected to the body of the apparatus. The length of the glass supports could be adjusted to alter the position of the focussing tube with respect to the axis of the extractor. This enabled the proton beam to be focussed centrally on the target. As the relatively short glass insulators had to withstand a potential difference of up to 50 kV, it was necessary to shape them in such a way as to increase their surface leakage path. One of these is shown in plate (B3). To avoid electrical discharging effects, it was found necessary to keep the metal components of the focussing system highly polished and their insulating

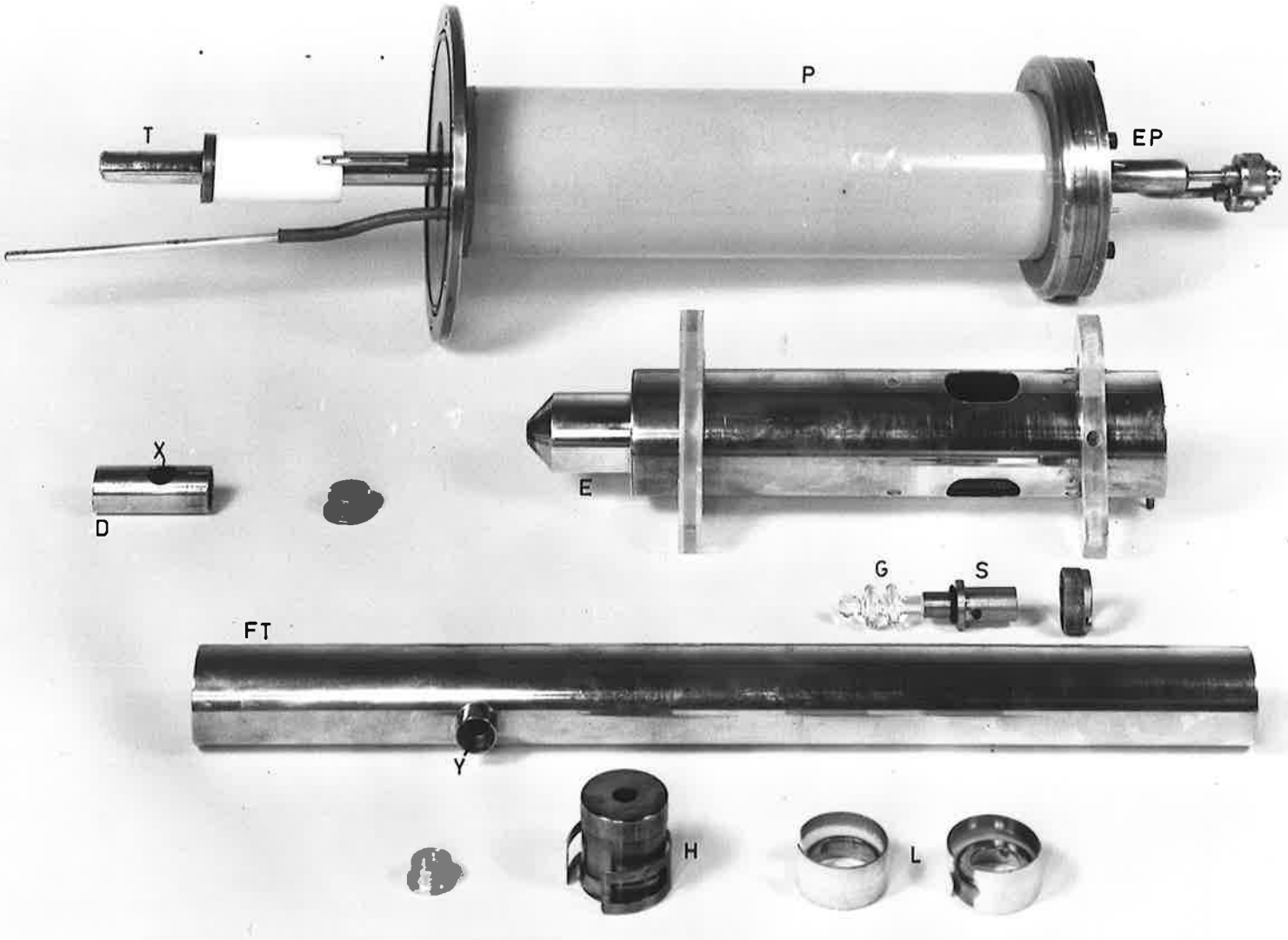

Plate B 3 Components of the focussing system and the target assembly.

supports scrupulously clean.

The potentials for the extractor and the focussing tube came from the same HV supply. Potential for the extractor was obtained by means of a high resistance chain connected to the HV supply. Part of the potential drop across the chain was applied to the extractor tube. Variation of the extractor potential was achieved by tapping the resistance chain at various points. The circuit diagram for the focussing system is included in figure (B2.1).

2.4 The Target Assembly.

The target assembly is shown schematically in figure (B2.2) and the actual components are included in Plate (B3). The incident proton beam was collimated by a collimator H fitted inside the focussing tube. The target holder consisted of a copper plate slotted to accommodate the target material. This facilitated changing of the target. The target was inclined at 45° to both the proton beam and the normal to the detector window. It was necessary to cool the target and this was done by a closed circuit oil cooling system using a heat exchanger.

A Faraday Cage D consisting of a brass tube slid over the target. The focussing tube was supported by and insulated from the target tube by an annular piece of PTFE, the front of which was protected from any stray ions by metal shields to prevent any undesirable heating of the insulator. Electrical connections to the focussing tube and to the secondary electron collectors L were made via brass rods attached

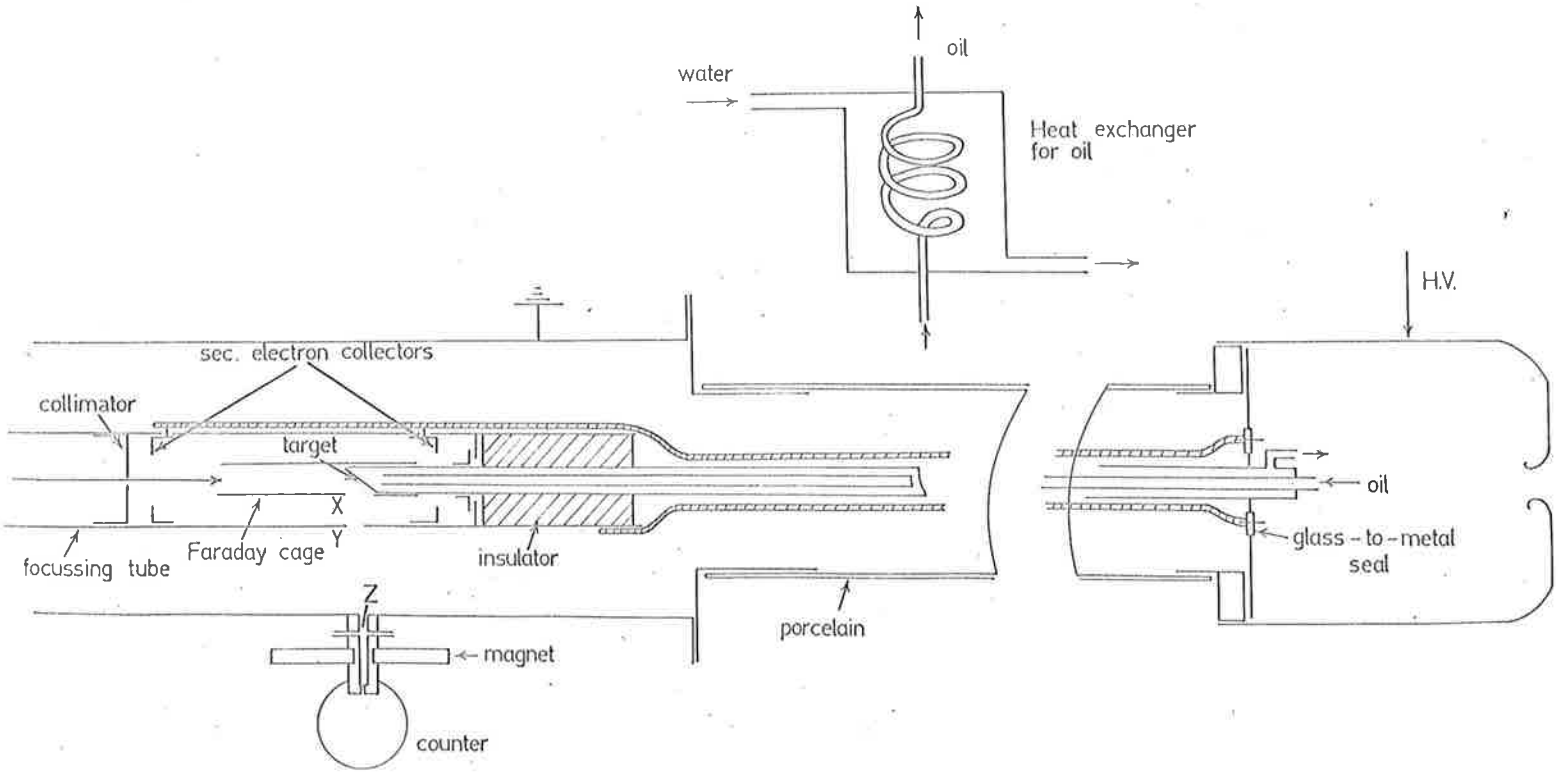

Figure B 2.2 The target assembly

to glass-to-metal seals soldered to the end plate EP, the whole of which was raised to a high negative potential. A smooth metal cover was fitted over the end plate to prevent corona discharges. The end plate was insulated from the earthed body of the apparatus by a glazed porcelain tube P.

Owing to the strong light emitted by the tungsten filament and the heating effect caused by the incident ion beam, it was impractical to study the quality of the focal spot by means of a fluorescent screen. It was found that the size of the focal spot could be estimated by inserting a piece of white cardboard in the path of the ion beam. By momentarily switching on the beam, a charred mark appeared on the paper, the degree of charring being dependent on the intensity of the beam. The focal spot estimated in this way was about 2 mm in diameter. Provided the tube voltage was above 20 kV, there appeared to be very little divergence in the beam over a fair length of its path. There was a noticeable penumbra effect, but this was reduced by the collimator which defined the incident beam so that it struck the target over a total circular area of approximately 4 mm in diameter.

The incidence of ions on the target caused the emission of secondary electrons. As the target meter reading, I_T (figure B2.1), caused by the escape of negative charges from the target was indistinguishable from the proton current reading. It was necessary to suppress the emission of secondary electrons by placing a positive potential of about 50 volts on the target with respect to the focussing tube. Secondary

electrons produced at the collimator and the focussing tube were prevented from being attracted to the target by means of secondary electron collectors placed as shown in the focussing tube (figure B2.2). These have a positive potential of 100 volts with respect to the focussing tube. The bias potentials for the target and the secondary electron collectors were supplied by dry cells. The circuit diagram is included in figure (B2.1).

The opening X in the Faraday cage was covered with either a piece of aluminized mylar or an aluminium foil depending on the wavelength of the characteristic radiations investigated. As there was a potential difference equal to the full tube voltage between the target assembly and the counter window, the opening Y in the focussing tube was covered with a piece of aluminized mylar to reduce the number of secondaries attracted to the counter window.

2.5 The vacuum pumps.

The system was evacuated by a 4" oil diffusion pump backed by a mechanical pump. Backstreaming of oil into the vacuum chamber was minimized by a water-cooled baffle valve. There was a number of safety features included in the vacuum apparatus. In the event of a power failure, the baffle valve and a magnetic isolation valve were automatically closed thus isolating the vacuum chamber and the oil diffusion pump from the atmosphere and from each other, and the air admittance valve was opened to the atmosphere to stabilize the pressure in the

backing pump. A thermal safety device attached to the diffusion pump cut off the heater power supply in the event of overheating of the pump. The electrical switches for the various components of the vacuum system were interlocked so that they could only be energized in a given sequence. The pressure in the vacuum chamber after several hours of pumping was about 5×10^{-6} mm of mercury. With the hydrogen gas supply turned on, the pumping speed was sufficient to maintain a pressure difference of two orders of magnitude between the arc chamber and the chamber containing the focussing system. For normal operations, the arc chamber pressure was about 3×10^{-3} mm Hg and the pressure on the other side of the anticathode was about 3×10^{-5} mm Hg, which was sufficient to maintain the high potentials used on the electrodes.

2.6 The Radiation Detection System.

The detector and associated electronic apparatus were identical to those used in the detection of radiations excited by electrons (Chapter 3, Part A). The gas flow proportional counter B was attached directly to the body of the apparatus as indicated by figure (B2.2). In order to ensure that the detected radiation intensities were sufficiently high, a 5mm diameter counter window, which subtended a solid angle of 1.97×10^{-3} ster-radians at the target, was used.

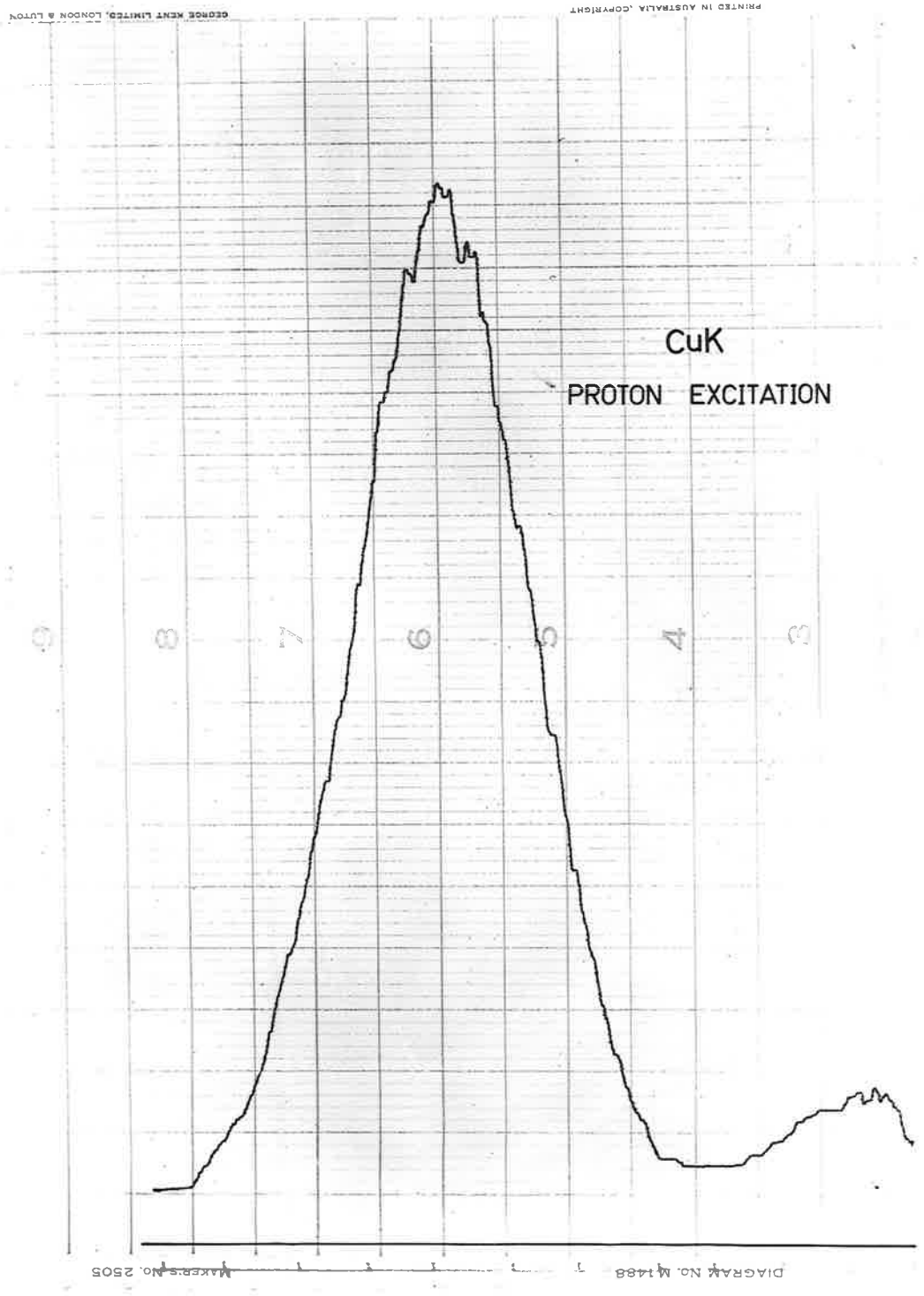

Figure B 3.1 Pulse height distribution from CuK radiations.

CHAPTER 3 Experimental Results.

3.1 Method of measurements.

The method of measuring characteristic intensities excited by protons is similar to that discussed in section (4.1) of part A. It was assumed that the radiations produced were entirely due to proton excitation. The studies of Singh (1957) and of Brandt, Laubert, and Sellin (1966) indicated that the probability of excitation of characteristic radiations by positive ions decreased rapidly with an increase in mass of the incident particle.

A striking feature of the pulse height distribution from radiations excited by protons was that there was a very low bremmstrahlung component. The pulse height distribution from CuK radiations is shown in figure (B3.1).

Merzbacher and Lewis (1958) indicated that the probability of bremmstrahlung production by protons was reduced by a factor $(m/M)^2$ as compared with electron excitation, where m is the mass of the electron and M is the proton mass. This was due to the fact that "a heavy particle has to have a much smaller impact parameter than a light particle of the same charge in order to be deflected by the same amount."

3.2 The Ratio of the Proton Current to the Total Ion Current.

In addition to protons, there is a large percentage of H_2^+,

H_3^+, and O_{16}^+ ions in the incident beam. Abele and Meckbach (1959) analyzed the beam from his ion source and gave the ratio of the proton current to the total hydrogen ion current as 33.8%. No mention was made of the O_{16}^+ ion in the beam. A more complete account of the magnetic analysis of the ion beam was given by Abele and Meckbach (1959b). The effects of the arc voltage, the field strength of the collimating magnet, the extractor potential and the arc chamber gas pressure on the ratios of the various ion currents in the beam were given. Their experimental studies indicated that provided a certain minimum value was exceeded for each of the above mentioned parameters, the ration of the proton current to the total ion current remained fairly independent of the operating parameters.

It was hoped that by satisfying the above condition, the ratio of the proton current to the total ion current in the present proton source would remain independent of the operating parameters and equal in value to that given by Abele and Meckbach (1959b). This is a reasonable assumption, as both ion sources are basically similar in design and in principle of operation.

The various operating parameters of the present proton source are given below:

filament wire diameter	= 0.5 mm
diameter of the anticathode aperture	= 3 mm
filament current, I_F	= 21 amp
arc voltage, V_A	= 250 volts
arc current, I_A	= 0.7 amp
solenoid current, I_M	= 2.3 amp
arc chamber pressure	= 3×10^{-3} mm Hg
vacuum chamber pressure	= 3×10^{-5} mm Hg

The magnetic field strength of the arc chamber was measured with a gauss-meter. It was found that a magnetizing current of 2.3 amp was sufficient to produce an axial magnetic field exceeding 700 gauss, the value used by Abele and Meckbach (1959).

There is some uncertainty in the value to be used for the ratio of the proton current to the total beam current. In figure II.15 of Abele and Meckbach (1959b) and figure (5) of Abele and Meckbach (1959), the percentage of proton current to the total hydrogen ion current was given as 33.8%. This figure was indicated by Abele and Meckbach (1959b) to be the maximum percentage of proton current to the total hydrogen ion current. In the later analysis of Abele and Meckbach (1959b) on the variation of the proportion of various ions in the beam with the source parameters, the proportion of the proton current to the total hydrogen ion current was about 20% and the proportion of O_{16}^{+} ion current to the total hydrogen ion current varied from 10% to 20%. The above figures

referred to the proportion of ions in the beam obtained under conditions where the proportions of various hydrogen ions to the total hydrogen ions were independent of the working parameters.

In the present calculations, it was assumed that the ratio of the proton current to the total ion current was 20%. Although the exact proportion of protons in the ion beam could only be determined by a magnetic analysis of the beam, the use of the estimated percentage quoted could not have been so much in error as to prevent the formation of some conclusions on the preliminary results obtained.

3.3 The Effect of Target Contamination.

The targets were treated in the way described in section (4.1) of part A. Owing to the low penetration of protons into matter (Whaling, 1958), contamination of the target surface would pose a serious problem. As the target was surrounded by the focussing tube and the extractor tube, and was situated well away from the throat of the diffusion pump, contamination of the target by oil vapour was reduced.

After an operating time of an hour, it was found that the region on the target corresponding to the focal spot was quite clean, whereas the surrounding area of the target surface corresponding to the penumbra region was discoloured. It appeared that the ion beam itself, by a combination of local heating and sputtering effect acted as a cleaning agent. The beam intensity in the penumbra region was not sufficient to prevent the deposition of carbonaceous matter by sputtering.

The variation of the radiation yield with the time-length of exposure of the target to the ion beam was found to be negligible over a period of an hour's exposure. Brand, Laubert, and Sellin (1966) observed that provided the temperature of the target exceeded 100°C, contamination of the target by carbonaceous matter was negligible. Khan, Potter and Worley (1965) used a sputtering technique to clean their targets.

3.4 Discussion of Results.

The intensities of AlK and CuK radiations excited by protons of energies up to about 45 keV were measured. The results are shown in figures (B3.2) and (B3.3) respectively. The only previous measurements corresponding to the above range of proton energies are the AlK results of Khan, Potter, and Worley (1965). Their results, which are included in figure (B3.2) are significantly lower than the present measurements; there is a discrepancy of a factor of 100 at 25 keV proton energy, the lower energy limit of their measurements, and a factor of 3 at 45 keV energy, the upper energy limit of the present measurements.

There are no CuK results available for comparison. The magnitude of the present CuK yields corresponds to that of Messelt (1958) at about 200 keV proton energy. Using the proportionality (B1.3), the values obtained by the extrapolation of Messelt's (1958) results are

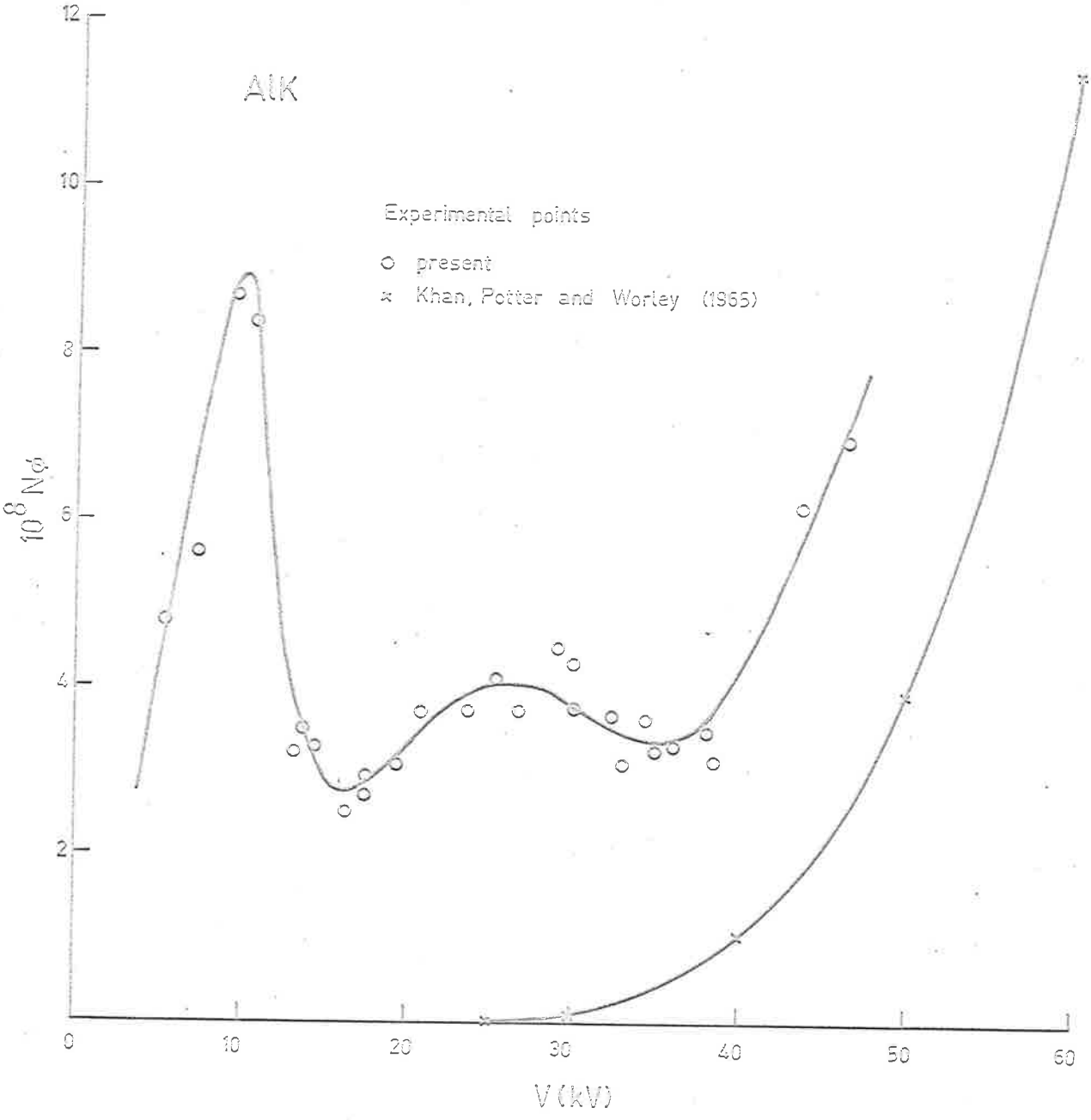

Figure B 3.2 Experimental results for AlK radiation intensities.

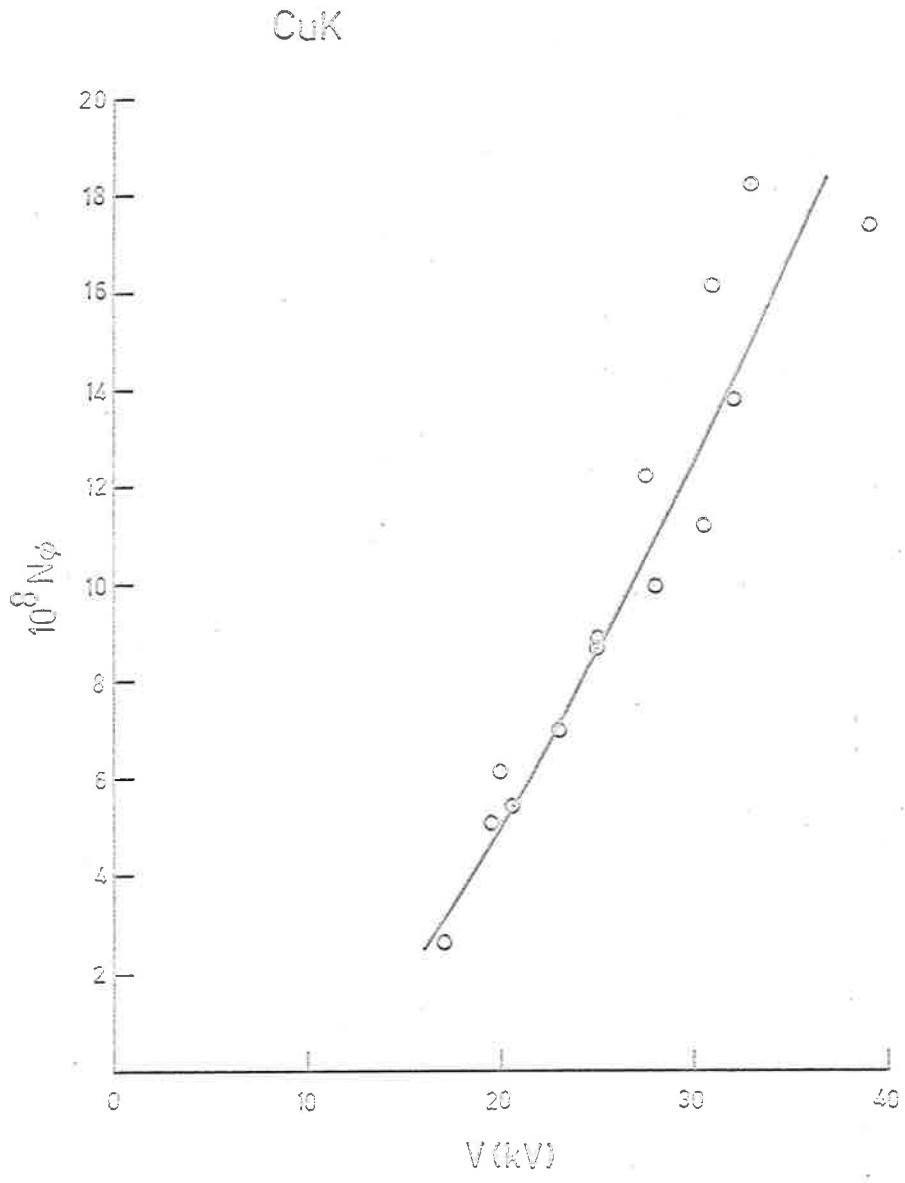

Figure B 3.3 Experimental results for CuK radiation intensities.

less than the present CuK measurements by a factor of about 1000. There is a similar discrepancy between the present AlK results and the extrapolated values of Khan, Potter, and Worley (1965) for proton energies less than 25 keV.

The detector and the detection technique were identical to those used in the measuring of radiations excited by electrons, consequently the intensity measurements may be accepted with confidence.

In the determination of stray counts, only the hydrogen gas supply to the arc chamber was shut off. The remainder of the apparatus was left running. The signal-to-noise ratio was about 1%.

There remained three sources of errors which could result in an overestimation of the intensity measurements,

(1) the detection of spurious radiations excited by secondary electrons;

(2) an underestimation in the measurement of the proton current;

(3) the proportion of protons in the incident ion beam was underestimated.

Secondary electrons were produced by the incidence of protons at the various negative electrodes. Massey and Burhop (1952) indicated that the number produced may be considerable. Even though the proton beam was enclosed by the focussing tube and the target assembly in the vicinity of the detector, and the opening Y in the focussing tube was

sealed with a piece of aluminized mylar (figure B2.2), a large number of secondary electrons were attracted across to the earthed walls of the apparatus with the full tube. These electrons probably originated in the negative electrodes closer to the proton source. Owing to the larger counter window used, it was not possible to collimate the incident radiations to such an extent that only the target was seen by the counter. As the probability of excitation of radiations by electrons was much higher than that of proton excitation, the detection of the spurious radiations excited by secondary electrons at the various earthed components of the apparatus would have seriously affected the measurements. The components of the apparatus were constructed of brass and copper. If proper precautions were not taken, spurious characteristic radiations produced would have seriously affected the CuK measurements.

Secondary electrons magnetically deflected from the counter window onto the brass walls Z of the joint connecting the counter to the apparatus (figure B2.2) had a similar undesirable effect. This source of spurious radiations was particularly serious owing to its proximity to the counter. In the measurements of the CuK radiations, owing to the relatively high penetration of these radiations, it was possible to place before the connecting joint Z an aluminium foil of sufficient thickness to absorb all the secondaries incident on it.

For the AlK intensity measurements, the walls Z were lined with carbon. Direct CK radiations would not have affected the AlK measurements due to pulse height discrimination. In any case, most

would have been absorbed by the mylar counter window. The shape of the pulse height distribution from the bremmstrahlung radiations excited in the carbon by the secondaries would have been distinguishable from that of the AlK characteristic radiations. The low electron backscatter ratio for carbon (section 2.4.1, part A) minimized the spurious effects arising from the incidence of secondaries on the counter due to multiple scattering of the secondaries within Z. Direct incidence of electrons on the window was prevented by the deflecting magnet.

There was no significant difference between the AlK measurements determined with an aluminized mylar counter window and those determined with a plain mylar window.

Measurements of the CuK radiation intensities were repeated using only the carbon lining in Z to minimize the effect of the secondaries incident on Z. There was no significant differenee between these results and those obtained when an aluminium foil was used to absorb all the secondaries entering Z.

The total effect on the radiation intensity measurements by spurious radiations excited by secondary electrons incident on the other earthed components of the apparatus as well as in Z was investigated by replacing the aluminized mylar foil in the opening Y of the focussing tube (figure B2.2) with a lead disc. The counting rate was reduced to a negligible quantity. This indicated that the radiations detected, when the mylar was in position in Y, came from within the opening in the focussing tube. The number of secondary electrons repelled from the

high negative electrodes should not have been affected by replacing the aluminized mylar with a lead disc in the opening Y.

Although the probability of secondary electrons, produced by the incidence of protons on the target, having sufficient energy to excite characteristic radiations at the inner wall of the brass Faraday Cage and at the edges of the opening Y in the focussing tube was probably negligible, precuations were taken to eliminate any such effect in the CuK radiation measurements. The inner walls of the Faraday Cage were lined with aluminium foil and an aluminium insert was placed in the recess at the opening Y of the focussing tube.

The effect of secondary electrons falling directly on the aluminized counter window was investigated by closing the opening Y with a lead plug and removing the deflecting magnet before the counter. A very large counting rate was registered. A pulse height analysis of the detected pulses indicated that there was no discernible peak in the pulse height distribution corresponding to a characteristic line, and that the energy of most of the ionizing radiations or particles detected exceeded the energy of the CuK radiations. These pulses were probably caused by bremmstrahlung radiations excited in the mylar window by secondary electrons or by energetic electrons penetrating the thin counter window. On replacing the deflecting magnet, the counting rate dropped to practically zero. This indicated that the combination of the magnetic deflecting system and the carbon lining in Z was necessary and effective in preventing any spurious effects in the

measurements arising from the incidence of secondaries on the counter window or in the surroundings Z leading to the counter window.

The above series of experiments indicated that the radiations detected originated in the target.

The incidence of positive ions on the target gave rise to a number of processes which could have affected the current reading. Detail description of these processes was given by Massey and Burhop (1952). It was necessary to suppress the emission of secondary electrons and negative ions, as their escape from the Faraday Cage would have been recorded on the target meter as a proton current. In the case of 50 keV protons incident on copper, approximately 4 secondaries were released per proton (Massey and Burhop, 1952). Almost all of these secondaries had energies less than 50 eV. The function of the Faraday Cage and the positive potential of 50 volts on the target with respect to the focussing tube was to prevent their escape. In any case the escape of any negatively charged particles would only tend to underestimate the radiation intensities. The principle concern was to investigate any defect in the experimental technique which might have caused an overestimation of the intensity results by three orders of magnitude.

There was a high probability for positive ions to be backscattered from the target. Massey and Burhop (1952) indicated that the reflection coefficient increased linearly with ion energy up to 1400 eV. The value given for the reflection coefficient of 1400 eV He^+ ions

incident on nickel was 0.8. However there was no available data for ions of higher energies. If the loss of ions from the Faraday Cage were the reason for the overestimation in the radiation intensities, then only a small fraction of 1% of the incident ions was absorbed. As the target current reading I_T (figure B2.1) was about $\frac{1}{4}$ milliamp, this would have meant that the actual ion current had to be several hundred milliamps. The sum total of the current readings I_E, I_y, and I_T (figure B2.1) amounted to about 3 milliamps. This was an estimate of the total ion current entering the extractor tube. Owing to the geometry of the ion collection system formed, and the fact that there were various components at earth potential situated close to the inlet of the extractor tube, the system was an effective ion collector. The earthed components near the inlet of the extractor tube provided a high retarding potential to any protons backscattered. As there was a high probability of secondaries escaping from the ion collector system, it seemed fairly certain that the value obtained for the total ion current was overestimated. This meant that any overestimation of the radiation intensities due to backscattered protons was only by a factor of several times. Abele and Meckbach (1959) using a similar size aperture for the anticathode obtained a total ion current of 18 milliamps, a higher value than the present current. It must be remembered that the two sources were not identical (section 2.1). One difference was in the values of the potential on the anticathode; the value of Abele and Meckbach (1959) was about 200 volts, whereas the present

value was less than 100 volts.

As there was a positive potential of 50 volts on the target with respect to the focussing tube (figure B2.1), there was a possibility of those secondaries, formed at the focussing tube and at the collimator, being attracted to it. This would have underestimated the ion current reading. The function of the secondary electron collectors was to reduce this effect. The potential on these collectors was 50 volts positive with respect to the target. There was a possibility of secondaries produced in the target being attracted across to the collector thus overestimating the target current reading.

By removing the bias potential on the target (i.e. the target and the focussing tube were at the same potential), it was possible to investigate the effect on I_T, of the attraction across to the secondary electron collector, of the secondaries produced at the target. It was found that I_T was increased by only 5% when the positive potential on the secondary electron collectors was increased from 0 to 100 volts. A potential of +100 volts on the secondary electron collectors was probably sufficient as practically all of the secondaries had energies less than 50 eV (Massey and Burhop, 1952).

The target bias potential had two simultaneous opposing effects on the current reading I_T. An increase in the positive bias potential on the target would have been more effective in suppressing the escape of secondaries formed in it, but at the same time, it would have attracted more secondaries produced in its surroundings.

	bias potential on secondary electron collectors	bias potential on target	I_T (milliamp)
(a)	+100	0	.4
(b)	+100	+50	.2
(c)	+100	+100	.1

TABLE (3.1)

Table (3.1) shows the effect of varying the bias potential on the target current I_T with a constant secondary electron collector potential of +100 volts. The values given in Table (3.1) refer to the potentials in volts with respect to the focussing tube. A copper target was used. The arrangement (b) of Table (3.1) was used in the present measurements.

When the arrangement (b) was used in the measurements and assuming the secondary electron collectors were efficient, by reference to Table (3.1), one can estimate the maximum effect, the secondaries had in underestimating I_T, thus overestimating the radiation intensities. As the arrangement (a) of Table (3.1) could have resulted in two effects which overestimated I_T, namely, the escape of secondaries from the target, and to a lesser extent the attraction by the secondary electron collectors of the secondaries produced at the target, the most pessimistic underestimation of I_T through the use of the arrangement (b) is by a factor of two.

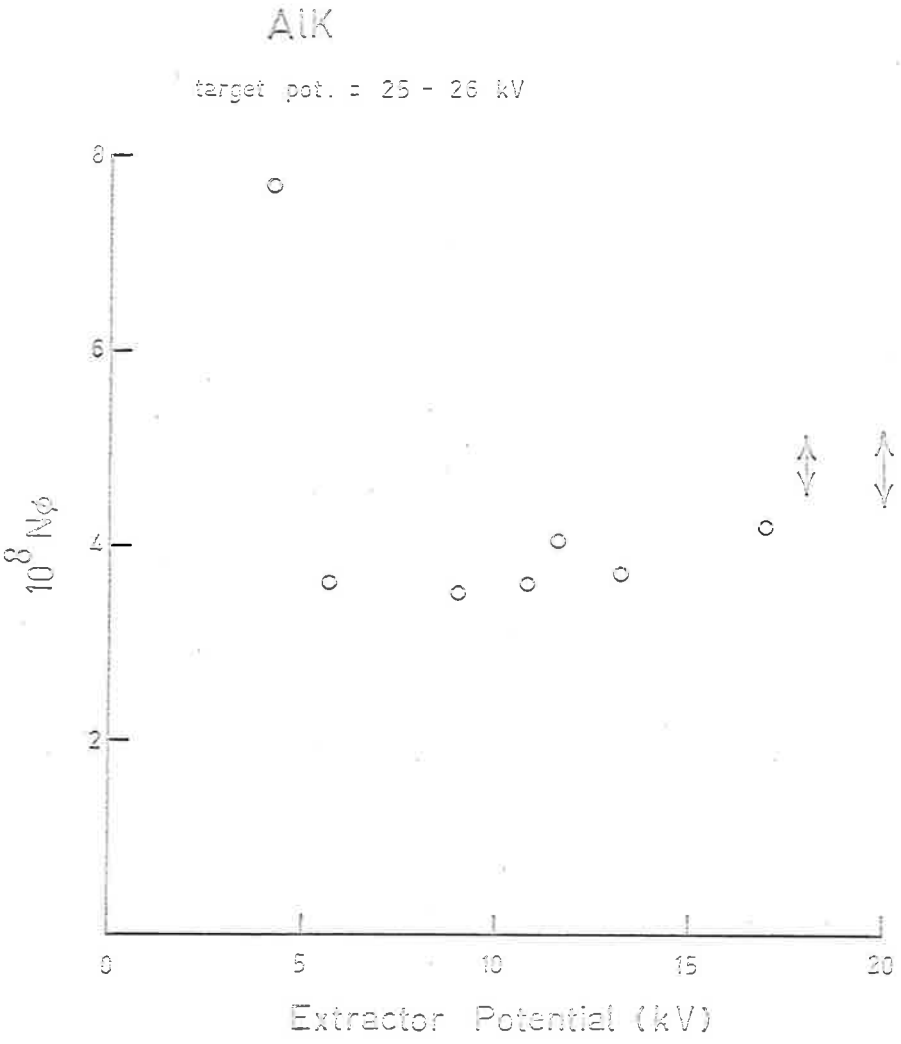

Figure B3.4 Variation of Nø with the extractor potential for a constant target potential.

The third source of discrepancy was in the estimation of the proportion of protons in the ion beam. Even if it were assumed that only protons were present in the beam, the measured intensity results would only have been reduced by a factor of 5.

As a result of the above investigations, it appeared that the measured intensities could only have been overestimated by one order of magnitude. This would not explain the high values obtained for the CuK radiation intensities nor for the AlK intensities at the lower energies.

Not only was there disagreement in magnitude, but also in the variation of the quantum yield with the incident proton energy, between the present results and others (Brandt, Laubert, and Sellin, 1966; Khan, Potter, and Worley, 1965).

A striking feature of figure (B3.2) for the AlK radiation intensities is the appearance of anomalous peaks; a large one occurs at about 10 keV proton energy and a smaller one at 25 keV energy. To ensure that there was no variation in the proportion of protons in the beam with the extractor potential, the extractor potential was kept constant at 10 keV for all incident energies $\geq$ 10 keV. Figure (B3.4) shows that for a constant target potential, the AlK radiation yields are nearly independent of the extractor potential down to 5 keV.

The position of these peaks was nearly independent of the excitation energy of the characteristic radiations. A large anomalous peak was also observed for the CuK radiation intensities (not shown) at about 12 keV proton energy.

It is interesting to note that a similar effect was observed in the Lyman$_\alpha$ production in proton-rare gas collisions (Pretzer, Van Zyl, and Geballe, 1963). But it must be remembered that the excitation energy of the Lyman$_\alpha$ line is much less than the K X-ray line.

Conclusion.

The preliminary investigation on the possibility of detection of characteristic AlK and CuK radiations excited by protons of energies less than 50 keV has been successful within its limitations. However, three questions remain unanswered. Firstly, the measured characteristic emission intensities far exceeded those predicted from existing theories, and also those of the extrapolated values from previous experimental studies. Although the experimental arrangement was not ideal, with the precautions taken, the most pessimistic overestimation of the results has been shown to be about an order of magnitude. This would have explained the discrepancies between the present AlK results and those of Khan, Potter, and Worley (1965) for proton energies exceeding 35 keV but not the AlK results at lower energies. No other experimental CuK data for this voltage range were available for comparison.

Secondly, the relative magnitudes of the AlK yield and the CuK yield at corresponding proton energies were inconsistent with the theoretical prediction of the proportionality (B1.1).

Thirdly, the anomalous peaks which occurred in the curve relating the radiation yield to the incident proton energy was not explained by any existing theory.

For more precise measurements of the characteristic intensities, further investigations on the ion current measuring technique and a

mass analysis of the ion beam are required. Although a mass spectrometer system has been constructed, its use would have involved some modification to the existing apparatus; it would have been necessary to have the target at earth potential. Lack of time prevented the author from further investigations. A grounded target would also be advantageous in removing the spurious effects arising from the secondaries attracted across to the earthed components of the apparatus.

The preliminary observations on the radiation yields at low proton energies, and in particular the anomalous peaks, indicated that certain aspects of the proton excitation phenomenon at low energies were yet to be accounted for theoretically. These certainly would deserve further investigations. However it must be pointed out that the authenticity of these peaks is not conclusive. The experimental arrangement was not ideal; there could have been resonance effects caused by a combination of the effects of the backscattered protons and the secondary electrons on the target current reading.

***

APPENDIX (1)

Pulse height Distributions from AlK and AgL radiations.

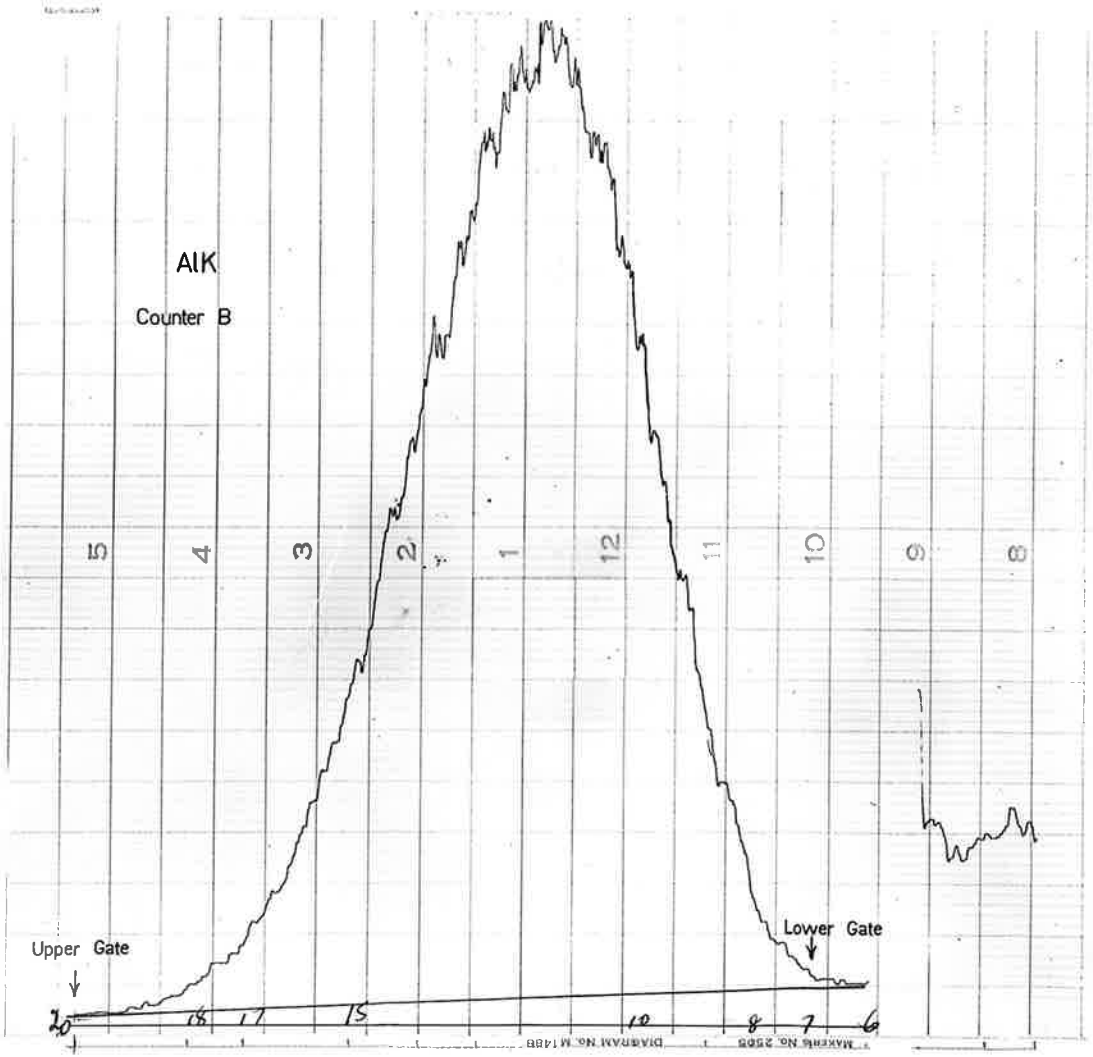

Pulse height distribution from AlK radiations.

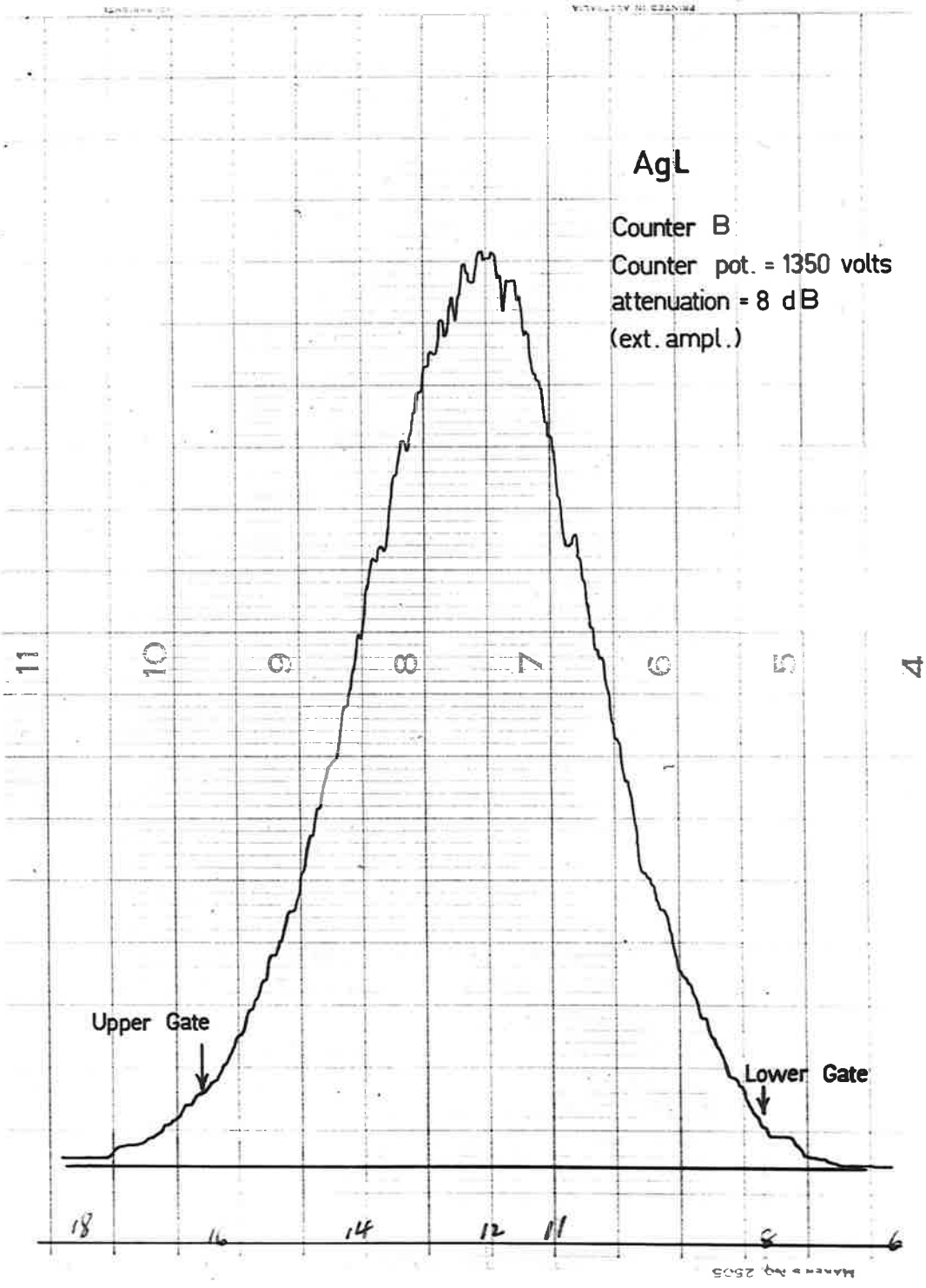

Pulse height distribution from AgL radiations.

APPENDIX (2)

Experimental TiK radiation intensities.

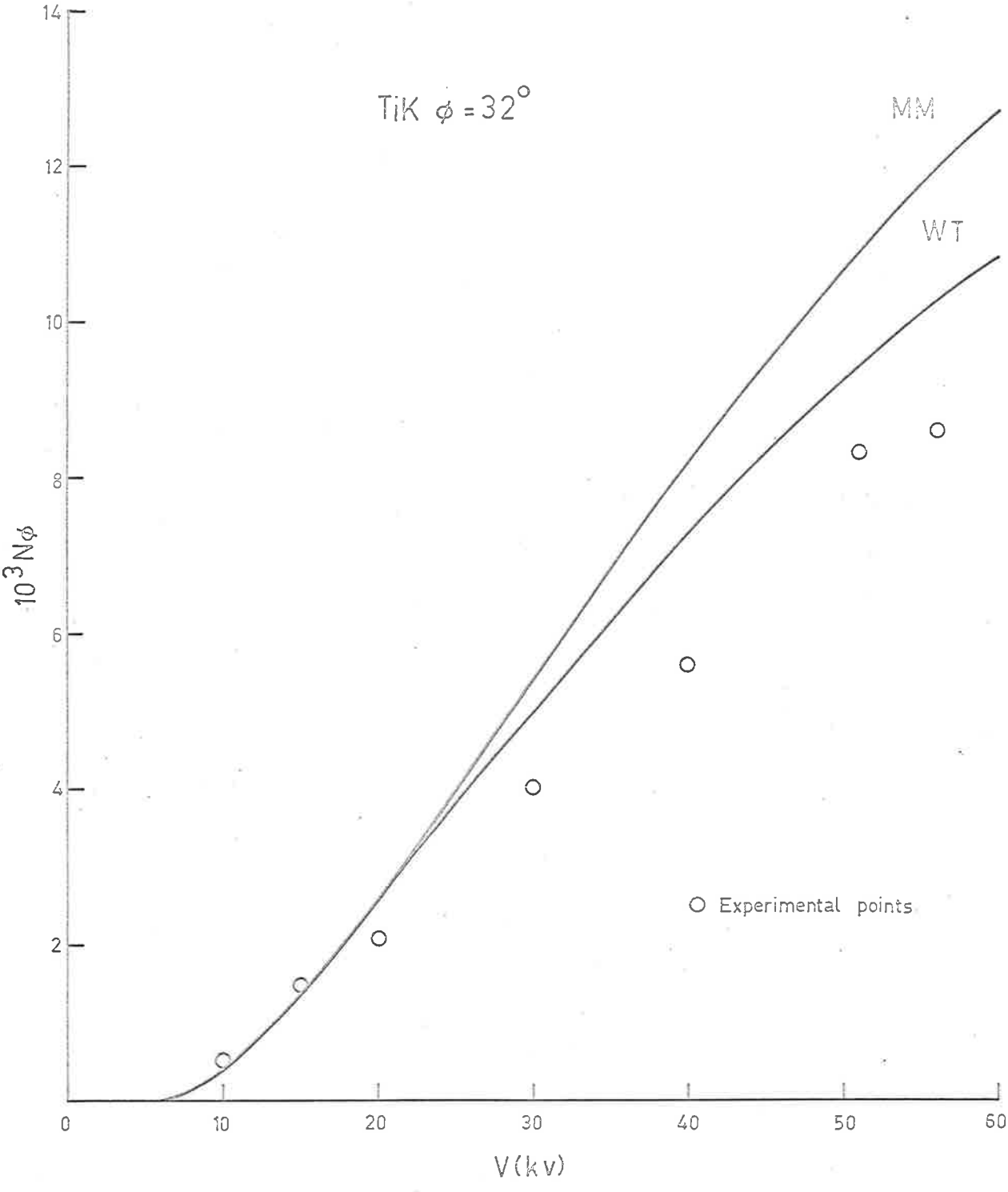

Experimental points and theoretical results for TiK radiation intensities.

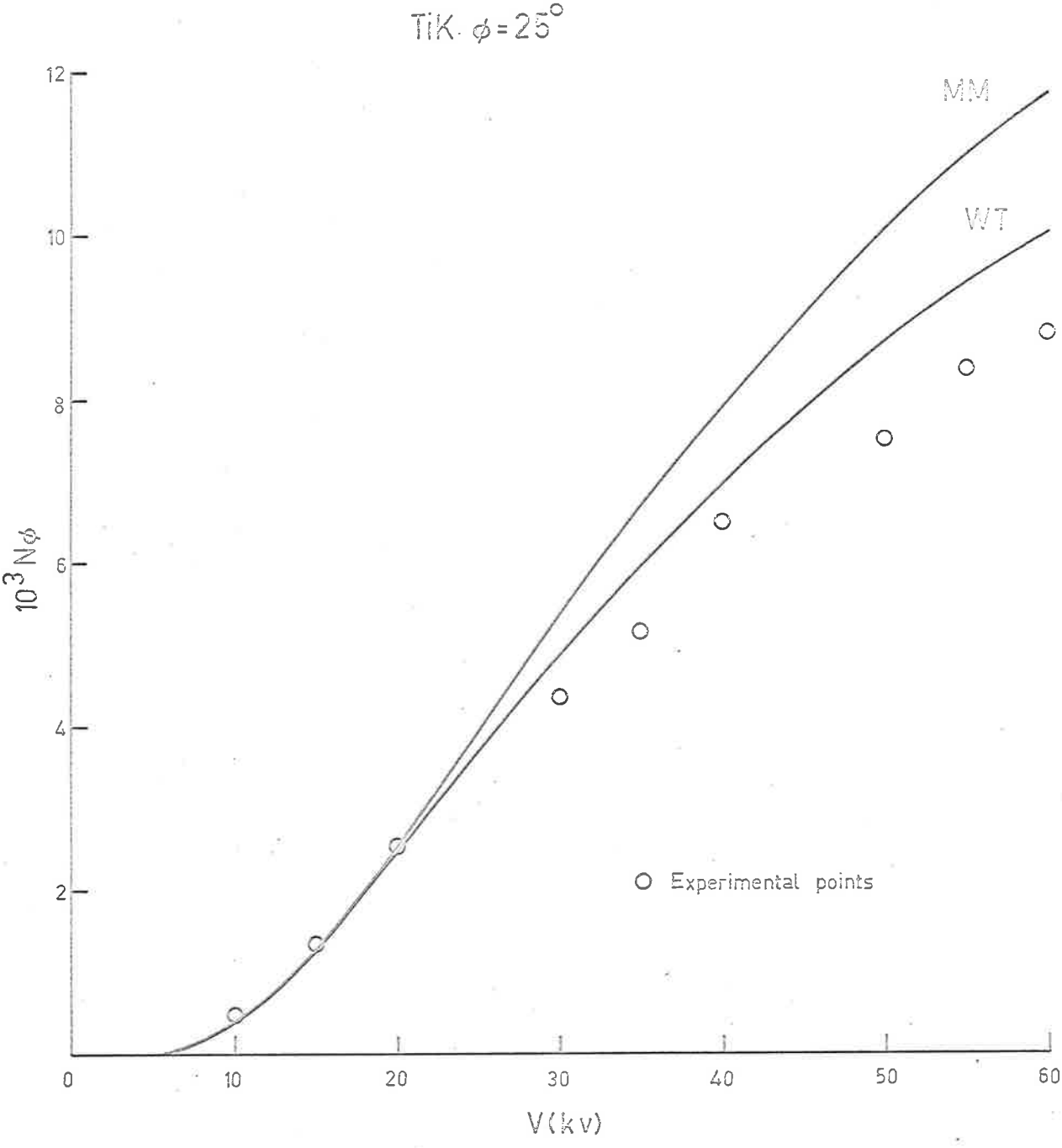

Experimental points and theoretical results for TiK radiation intensities.

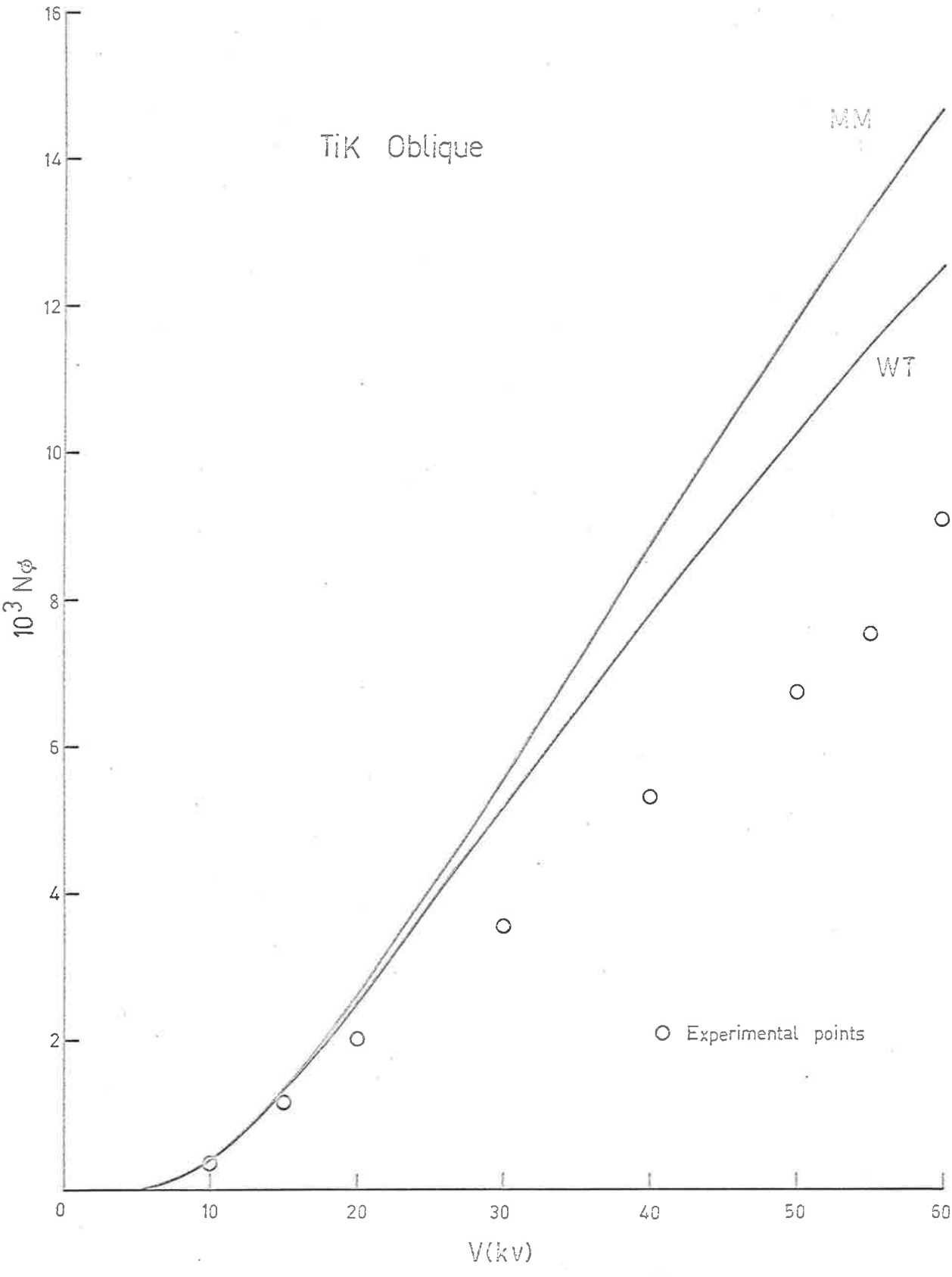

Experimental points and theoretical results for TiK radiation intensities.

APPENDIX (3)

Experimental L and M radiation intensities.

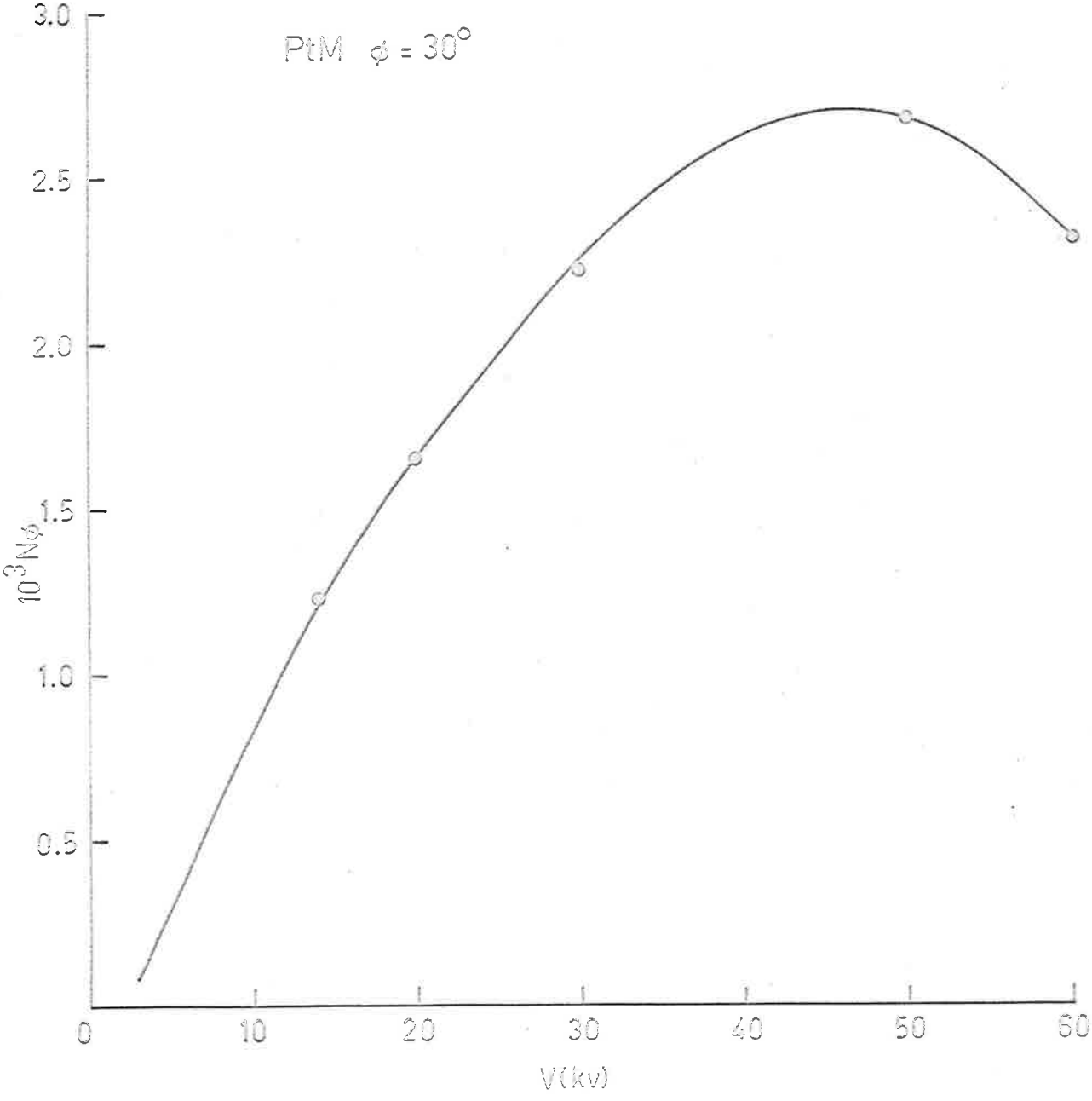

Experimental curve for total PtM radiation intensities.

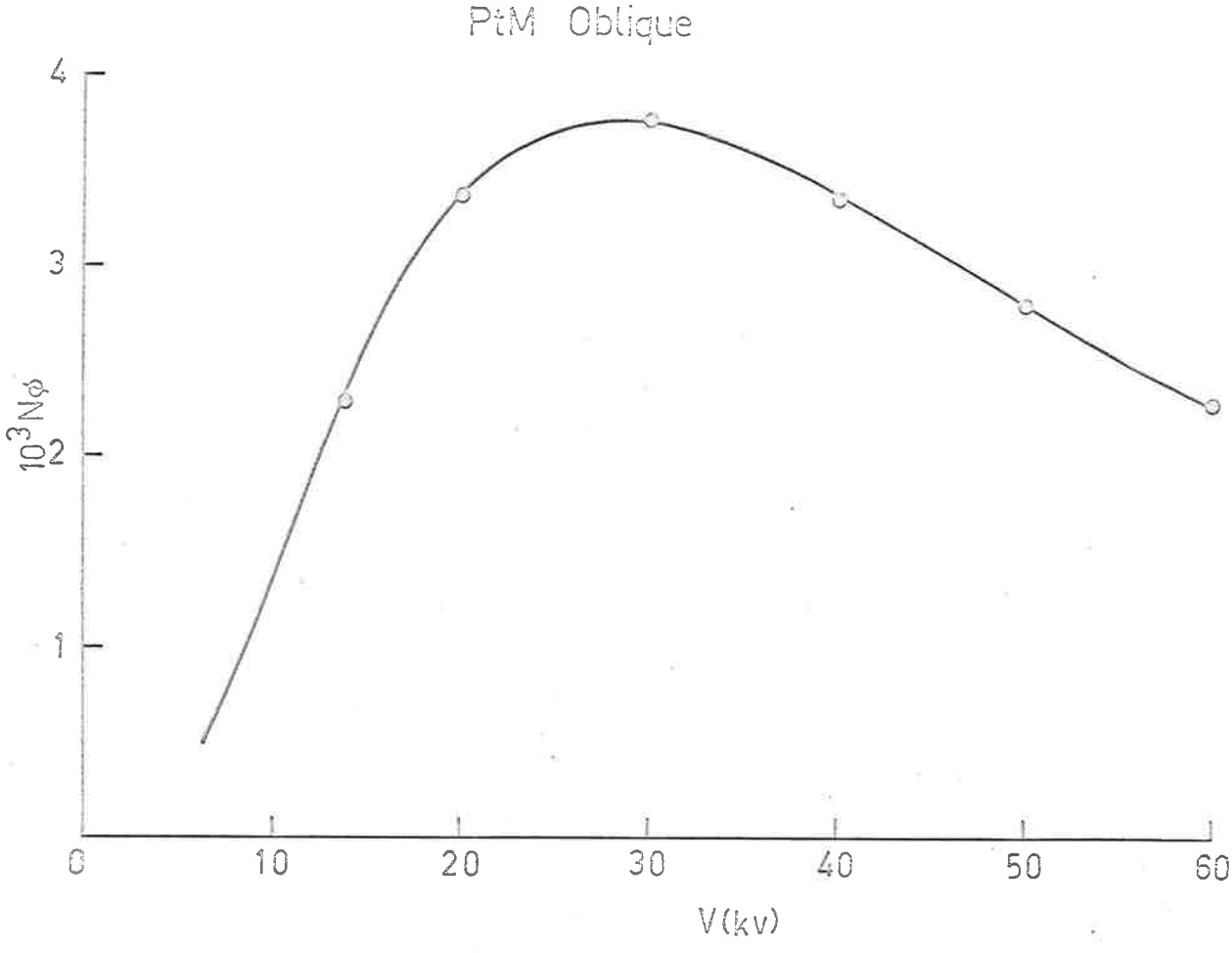

Experimental curve for total PtM radiation intensities.

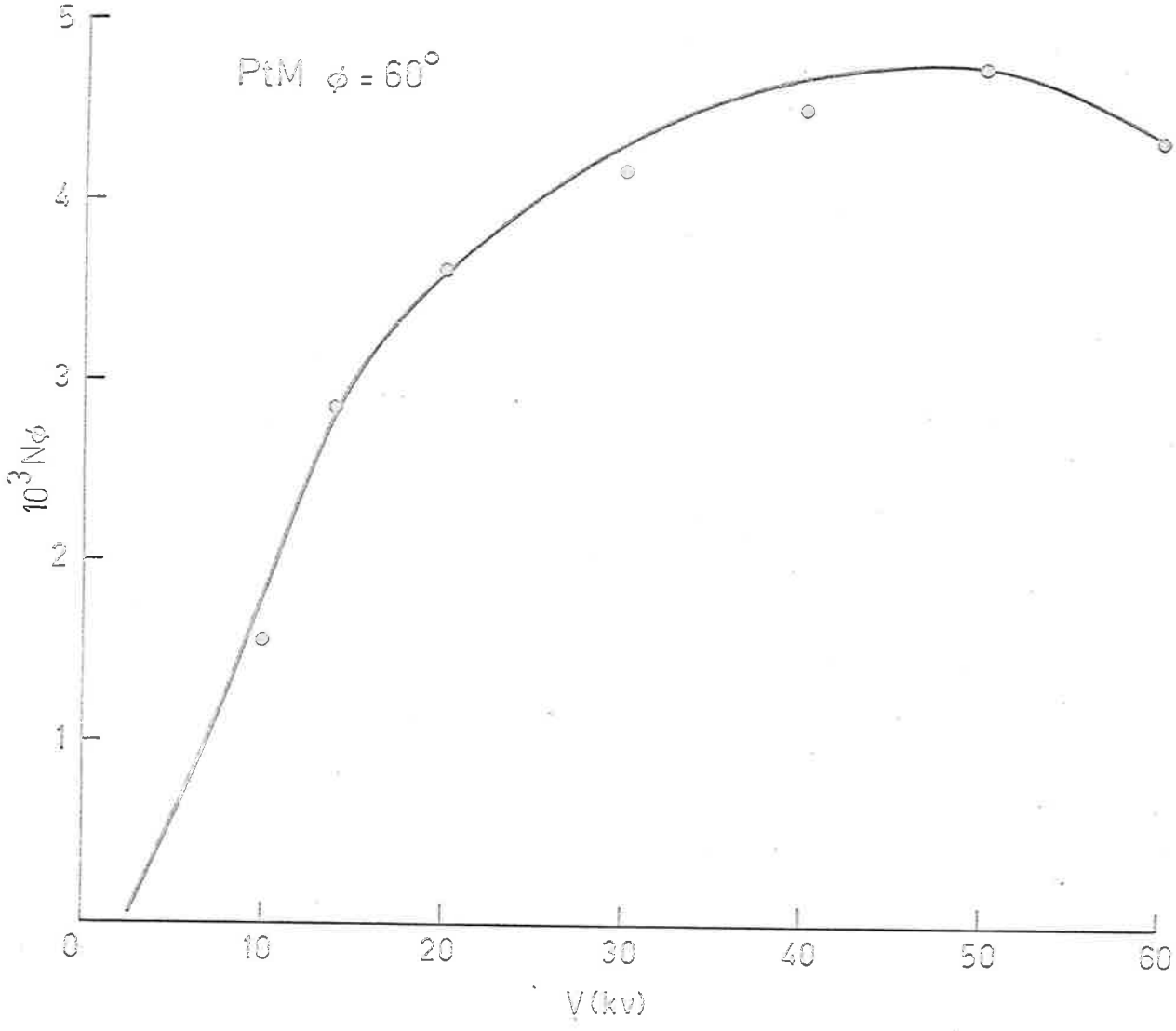

Experimental curve for total PtM radiation intensities.

BIBLIOGRAPHY

Abele, M., and Meckbach, W., Rev.Sci.Instr., 30, 335 (1959).

Abele, M., and Meckbach, W., Publicaciones de la Comision Nacional de Energia Atomica, No. 7 (1959a); Ibid., No. 8 (1959b).

Alexander, L., Kummer, E., and Klug, H.P., J.Appl.Phys., 20, 735 (1949).

Allen, S.J.M., Handbook of Chemistry and Physics (Chemical Rubber Publishing Co. : Cleveland, Ohio.), (1947).

Allison and Armstrong, Phys.Rev., 26, 701 (1925).

Archard, G.D., Proc. 2nd. Inst. Symp. of X-ray Microscopy and X-ray Microanalysis (Amsterdam : Elsevier), 331 (1960).

Archard, G.D., J.Appl.Phys., 32, 1505 (1961).

Archard, G.D., and Mulvey, T., Brit.J.Appl.Phys., 14, 626 (1963).

Bakker, C.J., and Segre, E., Phys.Rev., 81, 489 (1951).

Bang, J., and Hansteen, J.M., Kgl.Danke Nidenskal. Selskab, Mat. Fys. Medd., 31, No. 13 (1959).

Becker, A., Ann. Phys., 78, 253 (1925).

Bertolini, G., Bisi, A., Lazarrini, and Zappa, L., Nuovo Cimento, 11, 539 (1954).

Bertrand, F., Charpak, G., and Suzor, F., J.Phys.Rad., 20, 956 (1959); 20, 462 (1959).

Bethe, H.A., Ann.Phys., 5, 325 (1930).

Bethe, H.A., Ann.Phys.,5, 325 (1940).

Bevington, P.R., and Bernstein, E.M., Bull.Amer.Phys.Soc., 1, 198 (1956).

Binks, W., Reports on Prog. in Phys., 3, 347 (1936).

Birks, L.S., Seebold, R.E. Batt, A.P., and Grosso, J.S., J. of Appl.Phys., 35, 2578 (1964).

Birks, L.S., Seebold, R.E., Grant, B.K., and Grosso, J.S., J. of Appl. Phys., 36, 699 (1965).

Bishop, H.E., Proc.Phys.Soc., 85, 855 (1965).

Bothe, W., and Franz, H., Z.Physik, 52, 466 (1929).

Bothe, W., Ann.Phys., 6, 44 (1949).

Brand, J.O., Ann.Phys., 26, 609 (1936).

Brandt, W., Laubert, R., and Sellin, I., Phys.Rev., 151, 56 (1966).

Braxton, W.L., Baez, A.V., and Kirkpatrick, P., Phys.Rev., 68, 106 (1945).

Brown, D.B., and Ogilvie, R.E., J. of Appl.Phys., 32, 1505 (1964).

Broyes, C., Thomas, D., and Haynes, S., Phys.Rev., 89, 715 (1953).

Burhop, E.H.S., Proc.Camb.Phil.Soc., 36, 43 (1940).

Burhop, E.H.S., The Auger Effect and Other Radiationless Transitions (Cambridge University Press, Cambridge, England) (1952).

Burhop, E.H.S., J.Phys.Rad., 16, 625 (1955).

Burkhalter, P.G., Bureau of Mines Rep. of Investigation, United States Dept. of the Interior, Rep. 6681, (1965).

Burkhalter, P.G., Brown, J.D., and Myklebust, R.L., Rev.Sci.Instr., 37, 1267 (1966).

Callan, E.J., (1963) (See Fink et al (1966)).

Campbell, A.J., Proc.Roy.Soc., A274, 319 (1963).

Castaing, R., Advances in Electronics and Electron Physics, 13, 317 (1960).

Castaing, R., and Descamps, J., J.Phys.Rad., 16, 304 (1955).

Clark, J.C., Phys.Rev., 48, 30 (1935).

Cockroft, A.C., and Curran, S.C., Rev.Sci.Intr., 22, 37 (1951).

Compton, A.H., and Allison, S.K., X-Rays in Theory and Experiment (New York : Van Nostrand), (1935).

Cosslett, V.E., Proc.Phys.Soc.Lond., 78, 1206 (1961).

Cosslett, V.E., Brit.J.Appl.Phys., 15, 107 (1964).

Cosslett, V.E., and Thomas, R.N., Brit.J.Appl.Phys., 15, 883 (1964a); ibid, 1283 (1964b).

Dolby, R., Brit.J.Appl.Phys., 11, 64 (1960).

Dowling, P.H., Hendee, C.F., Kohler, T.R., and Parrish, W., Philips Tech.Rev., 18, 262 (1956).

Duane and Stenström, Proc.Nat.Acad.Sci., 6, 477 (1920).

Duncumb, P., and Shields, P.K., Brit.J.Appl.Phys., 14, 617 (1963).

Dyson, N.A., Brit.J.Appl.Phys., 10, 505 (1959).

Ennos, A.E., Brit.J.Appl.Phys., 4, 101 (1953).

Everhart, T.E., J.of Appl.Phys., 31, 1483 (1960).

Feller, W., An Introd. to Prob. Theory and its Applications, 2nd. ed., Vol. 1, 403 (1957) (New York : Wiley).

Fink, R.W., Jopson, R.C., Mark, H., and Swift, C.D., Rev.Mod.Phys., 38, 513 (1966).

Fuchs, R., and Kulenkampff, H., Z.Phys., 137, 583 (1954).

Fulbright, H.W., Handbuch der Physik, Vol. XLV, 1 (1958).

Gerthsen, C., and Reusse, W., Phys.Z., 34, 478 (1933).

Green, M., and Cosslett, V.E., Proc.Phys.Soc., 78, 1206 (1961).

Green, M., Proc. 3rd. Int. Symp. on X-Ray Optics and X-Ray Microanalysis, Stanford (New York : Acad. press), (1962).

Green, M., Proc. Phys. Soc., 82, 204 (1963).

Hanna, G.C., Kirkwood, D.H.W., and Portecorvo, B., Phys.Rev., 75, 985 (1949).

Henke, B.L., White, R., and Lundberg, B., J. of Appl.Phys., 28, 98 (1957)

Henneberg, W., Z. Phys., 86, 592 (1933).

Hicks, Phys. Rev., 36, 1273 (1930); ibid, 38, 572 (1931).

Holliday, J.E., and Sternglass, E.J., J. of Appl. Phys., 28, 1189 (1957).

Jönson, Zeits. f. Phys., 36, 426 (1926).

Jopson, R.C., Mark, H., and Swift, C.D., Phys.Rev., 127, 1612 (1962).

Kanter, H., Ann.Phys., 20, 144 (1957).

Khan, J.M., and Potter, D.L., Phys. Rev., 133, A890 (1964).

Khan, J.M., Potter, D.L., and Worley, R.D., Phys. Rev., 134, A320 (1964a); ibid, 135, A511 (1964b); ibid, 139, A1735 (1965).

Kieffer, L.J., and Dunn, H., Rev. Mod. Phys., 38, 1 (1966).

Kirkpatrick, P., and Baez, A.V., Phys. Rev., 71, 521 (1947).

Kulenkampff, Ann. Phys., 69, 548 (1922).

Laberrique-Frolow, J., and Radvanyi, P., J. Phys. Rad., 17, 944 (1956).

Lang, A.R., J. Sci. Instr., 33, 96 (1956).

Lay, H., Z. Phys., 91, 533 (1934).

Lewis, H.W., Phys. Rev., 78, 526 (1950).

Lewis, H.W., Simmons, B.E., and Merzbacher, E., Phys. Rev., 91, 943 (1953).

Listengarten, M.A., Bull. Acad. Sci. USSR, Phys., Columbia Tech. Transl., 26, 182 (1962); ibid, 25, 803 (1961).

Livingstone, M.S., and Bethe, H.A., Rev. Mod. Phys., 9, 263 (1937).

Livingstone, M.S., Genevese, F., and Konopinski, E.J., Phys. Rev., 51, 835 (1937).

Lonsdale, K., Acta Cryst., 1, 12 (1948).

Makhov, A.F., Soviet Phys. - Solid State 2, pt. 3, 1934, 1942, 1945 (1960).

Massey and Mohr, Proc. Roy. Soc. A, 140, 613 (1933).

Massey, H.S.W., and Burhop, E.H.S., Electronic and Ionic Impact Phenomena, (Oxford : Clarendon Press), (1952).

Matskevich, Soviet Phys. - Tech. Phys., 2, 255 (1957).

Merzbacher, E., and Lewis, H.W., Handbuch der Physik, Vol. XXXIV, 166 (1958) (Edited by S. Flugge).

Messelt, S., Nuclear Phys., 5, 435 (1958).

Metchnik, V., Thesis for Ph.D., University of Adelaide (1961).

Metchnik, V., and Tomlin, S.G., Proc. Phys. Soc., 81, 956 (1963).

Meyer, Wissenchaftliche Veroffentlichungen Aus dem Siemmens-Konzern, 7, 108 (1929).

Mott, N.F., and Massey, H.S.W., The Theory of Atomic Collisions (Oxford : Clarendon Press), (1949); ibid, 3rd. ed., (1965).

Mulvey, T., and Campbell, A.J., Brit. J. of Appl. Phys., 9, 406 (1958).

Mulvey, T., and Alford, N., unpublished, (1959) (see Archard, G.D., (1960)).

McCue, J.J.G., Phys. Rev., 65, 168 (1944).

Palluel, P., Compt. Rendu, 224, 1492 (1947).

Parrish, W., Philips Tech. Rev., 17, 206 (1956).

Perlman, H.S., Proc. Phys. Soc., 76, 623 (1960).

Peter, O., Ann. Phys., 27, 299 (1936).

Pockman, L.T., Webster, D.L., Kirkpatrick, P., and Harworth, K., Phys. Rev., 71, 330 (1947).

Pretzer, D., Van Zyl, B., and Geballe, R., Phys. Rev. Letters, 10, 340 (1963).

Price, J.W., Nuclear Radiation Detection, 2nd ed. (McGraw-Hill), (1964).

Rubinstein, R.A., and Snyder, J.N., Phys. Rev., 97, 1653 (1955).

Schonland, B.F.J., Proc. Roy. Soc. Lond., 108, 187 (1925).

Short, M.A., Rev. Sci. Instr., 31, 618 (1960).

Simane, C., and Urbanec, J., Czech. J. Phys., 5, 40 (1955).

Singh, B., Phys. Rev., 107, 711 (1957).

Slater, Phys. Rev., 36, 57 (1930).

Smick, A.E., and Kirkpatrick, P., Phys. Rev., 67, 153 (1945).

Snell, A.H., Nuclear Instr. and their Uses, Vol. 1 (Wiley), (1962).

Snyder, H.S., Phys. Rev., 72, 181 (1947).

Stehberger, K.H., Ann. Phys., 86, 825 (1928).

Stephenson, R.J., Phys. Rev., 51, 637 (1937).

Sternglass, E.J., Phys. Rev., 95, 345 (1954).

Suoninen, E.J., Physica, A.VI.166, 1 (1964).

Taylor, J.G.V., and Merritt, Proc. Conf. Atomic Electrons in Nuclear Transformations, Warsaw, Poland, Vol. III, 465 (1963).

Tomlin, S.G., Proc. Phys. Soc., 82, 465 (1963); ibid, 89, 805 (1966).

Tomlin, S.G., Aust. J. Phys., 17, 452 (1964).

Wagner, P.B., Phys. Rev., 35, 98 (1930).

Webster, D.L., Proc. Nat. Acad. Sci., 14, 337 (1928).

Webster, D.L. Clark, H., and Hansen, W.W., Phys. Rev., 37, 115 (1931).

Webster, D.L., Hansen, W.W., and Duveneck, F.B., Phys. Rev., 43, 839 (1933a); ibid, 44, 258 (1933b).

Whaling, W., Handbuch der Physik, Vol. XXXIV, 193 (1958) (Edited by S. Flugge).

Williams, E.J., Proc. Roy. Soc., A130, 310 (1931).

Williams, J.H., Phys. Rev., 44, 146 (1933).

Wilson, R., Beghian, L., Collie, C.H., Halban, H., and Bishop, C.R., Rev. Sci. Instr., 21, 699 (1950).

Wisshak, F., Ann. Phys., 5, 507 (1930).

Woo, Phys. Rev. (2), 48, 427 (1926).

Worthington, C.R., and Tomlin, S.G., Proc. Phys. Soc. Lond., 69, 401 (1956).

Wyckoff, R.W.G., and Davidson, F.D., J. of Appl. Phys., 36, 1883 (1965).

Zacek and Sieghahn, Ann. Phys., 71, 187 (1923).

***